ROCKGLACIER KINEMATICS IN A HIGH MOUNTAIN GEOSYSTEM

Dissertation

zur

Erlangung des Doktorgrades (Dr. rer. nat.)

der

Mathematisch-Naturwissenschaftlichen Fakultät

der

Rheinischen Friedrich-Wilhelms-Universität Bonn

vorgelegt von

Isabelle Roer

aus

Bonn

Bonn, Februar 2005

Angefertigt mit Genehmigung der Mathematisch -Naturwissenschaftlichen Fakultät der Rheinischen Friedrich-Wilhelms-Universität Bonn

1. Referent: Prof. Dr. R. Dikau
2. Referent: PD Dr. A. Kääb

Tag der Promotion: 03.06.2005

I dedicate this in loving memory to my father

and with warm thanks to my mother.

View into the Rothorn-cirque (Hungerlitälli), Brunegghorn (3833 m a.s.l.) and Bishorn (4134 m a.s.l.) in the back.

SUMMARY

The study presents a regional approach for the quantification of rockglacier creep in a high mountain geosystem (Turtmann valley, Swiss Alps).

By a combination of different methods, rockglacier movements were analysed qualitatively and quantitatively on various spatial and temporal scales. The application of digital photogrammetry and terrestrial geodetic survey enabled the quantification of horizontal velocities and vertical changes. The photogrammetric results demonstrate that small-scale aerial photographs are highly useful to measure changes in rockglacier geometry. Also the combination with high resolution imagery (from HRSC-A), which was applied for the first time in rockglacier studies, has been successful. Thus, displacements were investigated in a large area (meso-scale) and over a time span of 26 years (1975 – 2001). Against that, terrestrial geodetic survey enabled the annual quantification of block displacements on two rockglaciers between 2001 and 2004. The first-time application of dendrogeomorphic techniques for the determination of permafrost creep provided preliminary results for two rockglaciers.

The applied techniques and especially the combination of geomorphic mapping and digital photogrammetry allowed the reliable assessment of the state of activity for 45 rockglaciers. Horizontal and vertical surface changes were analysed on 34 rockglaciers and a clear activity was revealed on 18 of them. Most of the permafrost bodies indicated above-average horizontal velocities compared to other rockglaciers in the Alps. In addition, conspicuous spatio-temporal variations in horizontal velocities and vertical changes were observed. Regarding the temporal variations, a distinct increase in horizontal velocity – probably from the beginning of the 1990s – was ascertained for all investigated active rockglaciers.

The described findings were discussed by consideration of probable controls, such as terrain parameters and climatic influences. Although the data on decisive forcing factors and the knowledge on rockglacier dynamics is limited, it is assumed that the observed speed-up is linked to climatic changes and an increase in ground temperatures, respectively. Thus, the investigated kinematics supports the role of rockglaciers as sensitive indicators for changes in the high mountain geosystem.

ZUSAMMENFASSUNG

Im Zentrum der hier vorgestellten Studie steht die regionale Analyse der Blockgletscherbewegung in einem hochalpinen Geosystem (Turtmanntal, Schweizer Alpen).

Mit Hilfe mehrerer Methoden wurde die Blockgletscherkinematik auf unterschiedlichen Raum- und Zeitskalen sowohl qualitativ als auch quantitativ untersucht. Die Anwendung der digitalen Photogrammetrie und der terrestrischen Vermessung ermöglichte die Messung von horizontalen Geschwindigkeiten und vertikalen Veränderungen. Dabei zeigten die Ergebnisse der Photogrammetrie, dass analoge hochgeflogene Luftbilder für die Analyse von Veränderungen der Blockgletschergeometrie durchaus geeignet sind. Auch die Kombination mit digitalen hochauflösenden Daten (der High Resolution Stereo Camera – Airborne; HRSC-A), die erstmalig in der Blockgletscherforschung eingesetzt wurden, war erfolgreich. Dadurch konnten Blockgletscherbewegungen auf großer räumlicher Skale (Mesoskale) und über einen Zeitraum von 26 Jahren (1975 – 2001) quantifiziert werden. Die Anwendung der terrestrischen Vermessung ermöglichte zusätzlich die jährliche Quantifizierung von Bewegungen zwischen 2001 und 2004 auf zwei ausgewählten Blockgletschern. Dendrogeomorphologische bzw. holzanatomische Techniken wurden erstmalig für die Bestimmung der Blockgletscherkinematik eingesetzt und lieferten für zwei Untersuchungsobjekte vorläufige Ergebnisse.

Mit den verwendeten Methoden und besonders durch die Kombination von geomorphologischer Kartierung und digitaler Photogrammetrie konnte der Aktivitätsgrad von 45 Blockgletschern abgeschätzt werden. Horizontale und vertikale Bewegungen wurden dann für die 34 intakten Blockgletscher quantifiziert, von denen 18 eine eindeutige Aktivität zeigten. Viele der untersuchten Permafrostkörper wiesen, im Vergleich zu anderen Blockgletschern der Alpen, überdurchschnittliche horizontale Geschwindigkeiten auf. Außerdem zeigten sowohl die horizontalen als auch die vertikalen Bewegungen deutliche raum-zeitliche Variationen. Bezüglich der zeitlichen Variationen wurde für alle aktiven Blockgletscher eine eindeutige Zunahme der horizontalen Geschwindigkeit – vermutlich ab den 1990er Jahren – bestimmt.

Die geschilderten Ergebnisse wurden unter Einbezug möglicher Kontrollgrössen, wie Relief- und Klimaparametern, diskutiert. Obwohl die Datenlage zu entscheidenden Einflussgrößen und das Wissen über Blockgletscherdynamik limitiert ist, wurde die beobachtete Beschleunigung den klimatischen Veränderungen und dem damit verbundenen Anstieg der Oberflächentemperatur zugewiesen. Folglich stützen die Ergebnisse die Rolle von Blockgletschern als sensitive Indikatoren für Veränderungen im hochalpinen Geosystem.

CONTENTS

APPENDICES

LIST OF FIGURES

CHAPTER 1

CHAPTER 2

CHAPTER 3

CHAPTER 6

LIST OF TABLES

ACRONYMS

a.s.l.	above sea level
ATR	Automatic Target Recognition system
BTS	Bottom Temperature of the winter Snow cover
CCD	Charge Coupled Devices
CIAS	Correlation Image Analysis
DInSAR	Differential Interferometric Synthetic Aperture Radar
DLR	Deutsches Zentrum für Luft- und Raumfahrt / German Aerospace Center
DTM	Digital Terrain Model
EDM	Electronic Distance Meter
GCP	Ground Control Point
GIS	Geographical Information System
GPS	Global Positioning System
HRSC-A	High Resolution Stereo Camera – Airborne
IDL	Interactive Data Language
INS	Inertial Navigation System
LIA	Little Ice Age
MAAT	Mean Annual Air Temperature
MAGST	Mean Annual Ground Surface Temperature
RMS	Root Mean Square error
SMA	Schweizer Meteorologische Anstalt
UTL	Universal Temperature Logger

1 INTRODUCTION

> *Geomorphology will achieve its fullest development only when the forms and processes are related in terms of dynamic systems and the transformations of mass and energy are considered as functions of time.* (Strahler 1952: 935)

This quotation unites in one sentence both foundation and objective of the current geomorphological research. It gives a clear definition of 'geomorphology' within the context of the systems approach building the conceptual and methodological basis. In addition to that it aims at the heart of the here presented study: the analysis of dynamic systems by determination of mass and energy fluxes. Regarding the focus of this study, the high mountain geosystem which is characterised by an extensive transfer of mass and energy, it is also well reflected in this statement.

1.1 Motivation

The increasing interest in recent climatic change and its impact on geosystems confirms the significance of high-mountain environments as sensitive key areas, and not only since the events during the hot summer of 2003. Global environmental change is the result of interactions and feedbacks among the earth's different subsystems at a wide range of spatial and temporal scales. General circulation models predict the major temperature changes in high latitudes (polar region) and high altitudes (high mountains) since horizontal and vertical gradients of the atmospheric variables are more extensive and thus small changes in environmental conditions are noted earlier (Slaymaker & Spencer 1998). This is confirmed for example by a temperature increase, which occurred more intensely in the Alps than elsewhere (e.g., Böhm 2003).

Within the high mountain system, landforms (e.g., glaciers) or ecological boundaries (e.g., lower boundary of permafrost occurrence, tree line) are monitored systematically and act as important indicators for environmental changes (e.g., IPCC 2001a, b). While the sensitivity of periglacial landscapes (in high latitudes as well as in high altitudes) was often considered (e.g., Lachenbruch & Marshall 1986; Anisimov & Nelson 1996), the indicative role of rockglaciers in this context was emphasised only recently (e.g., Harris & Haeberli 2003).

1.2 Objectives

In the 80-year history of rockglacier research, movements were often described and quantified (see appendix 1), but the processes behind and thus the dynamics of the permafrost bodies are still not known in detail. Apart from the measurements at the rockglacier surface (e.g., Kääb et al. 2003), borehole studies (e.g., Hoelzle et al. 1998; Arenson et al. 2002) and laboratory tests (e.g.,

Davies et al. 2001) improved the knowledge during the last decade. But, these investigations are often concentrated on single rockglaciers, due to methodological and financial limitations.
For further investigations of rockglacier creep, several research needs and objectives arise:

- High accuracy techniques and data with high spatial and temporal resolution are required for the quantification of rockglacier movement.
- Long monitoring series on rockglacier kinematics are demanded on large spatial scales (several neighbouring rockglaciers) to analyse spatio-temporal variations reliably.
- In order to deepen the knowledge on rockglacier dynamics, influencing parameters (e.g., temperature, snow cover characteristics, debris supply, etc.) need to be included in the analysis of spatial and temporal variations.
- The sensitivity of rockglaciers has to be determined in order to use these landforms as indicators for changing environmental conditions in high mountain geosystems

The high density of rockglaciers in the Turtmann valley (Swiss Alps) and the existing data on their characteristics and distribution (Nyenhuis 2001; Roer 2001) suggested the area-wide quantification of rockglacier creep for the characterisation of this high mountain geosystem. Some data on rockglacier movements already existed for the study site (Elverfeldt 2002), but they were not sufficient for the analysis of spatial and temporal variations. Therefore, rockglacier kinematics, which is defined as the quantification of movement without considering the forcing factors (in contrast to dynamics), is investigated by the application of different methods.
From the given objectives and in view of the current state of the art (cf., chapter 2), the following research questions are compiled for the here presented study:

- Are the applied methods and the available data suited to the quantification of rockglacier creep in high mountain environments? Which advantages, limitations, resolutions and accuracies are revealed by the different methods?
- Do the applied techniques allow the reliable assessment of the state of activity?
- What are the mean and maximum values of horizontal as well as vertical displacements; also in comparison to other rockglaciers in the Alps?
- Do the movements reflect spatio-temporal variations? Is it possible to distinguish seasonal and interannual variations from longterm trends?
- To what extent are the horizontal velocities and vertical changes conditional upon terrain parameters or climatic influences?
- Is it possible to assess the sensitivity of rockglaciers and thus evaluate their geomorphic and environmental significance in the high mountain geosystem?

1.3 Conceptional background

As part of the Research Training Group 'Landform – a structured and variable boundary layer' (Graduiertenkolleg 437) the focus of the study is given on landforms, their characteristics and spatial distribution as well as their changes in time. In general, landform is characterised by

certain structures or patterns, since it is not distributed arbitrarily in space. Penck (1894) was the first who designed a hierarchy of landforms which was later modified by Kugler (1974) who introduced the term 'complexity' in this context and by Büdel (1977) who considered nested hierarchies. For a review of these classical concepts in geomorphology as well as the parameterization of landform, it is referred to Rasemann (2004).

In the study presented here, landform is considered as a boundary layer or interface, respectively, between the atmosphere/hydrosphere/cryosphere and the pedosphere/lithosphere and thus represents both control factor and result (form, shape) of processes, acting on different spatial and temporal scales. The boundary layer or landform is regarded as a 2-dimensional object in the 4-dimensional space with certain geometrical characteristics, which can be considered in a geomorphodynamic context (Dikau & Schmidt 1999). Here, focus is given on one specific landform (rockglacier), its distribution in space, its activity, its temporal changes in geometry as well as the probable reasons for its change. The repeated measurement of the object geometry allows the quantification of corresponding process rates. Thus, the temporal scale is explicitly included. By consulting the model of the boundary condition (cf., chapter 2.3.5.4) a quasi - 4D-consideration of the rockglaciers is enabled.

Related to the phenomena such as permafrost and rockglacier creep, landform is of significance on various scales. Permafrost is a thermally controlled phenomenon, which can be considered on macro or meso-scale with parameters like mean annual air temperature (MAAT) or solar radiation. But on the micro-scale, different parameters such as latent heat fluxes, snowcover or properties of the substratum are of major importance (cf., chapter 2.2.2). Thus, the scale of consideration influences the determination of relevant parameters decisively. The interconnexion of different scales can be resolved by upscaling- and downscaling techniques. This multiscale approach is based on the consideration of systems in a hierarchical configuration: a system is part of a larger system and can itself be composed of several smaller systems. The systems theory found application in geomorphology by the contributions of Strahler (1952), Hack (1960) and Chorley (1962) and developed into a unifying concept in physical geography by the book: *Physical geography: a systems approach* (Chorley & Kennedy 1971).

Regarding the four system types stated by Chorley & Kennedy (1971) the here presented study depicts a **simple process-response system**, "*which is formed by the intersection of morphological and cascading systems and involving emphasis upon processes and the resulting forms*" (Gregory 2000: 88). This is based on an empirical as well as on a conceptional dynamic model. It is part of the more comprehensive cascading system which is considered in the Turtmann valley to describe the sediment budget of a high mountain geosystem (Nyenhuis 2005).

Different scales are considered in this study, depending on the relevant scale of the phenomenon and the available data. According to the classification by Dikau (1989), the landform 'rockglacier' analysed in this study belongs to the microrelief and is thus regarded on the micro-scale (Figure 1.1). But, due to the applied techniques, the rockglacier kinematics is quantified by the repeated measurement of single blocks at the rockglacier surface. Therefore, the data scale is established in the **nanorelief-level**, whereas results and conclusions are aggregated and compiled on a **micro-**

to mesorelief level (scale of phenomenon). Regarding the **temporal scale**, the data scale is restricted to a period of 29 years by the application of different methods with diverse resolutions. Against that, the scale of the phenomenon (permafrost creep) is referred to the entire Holocene, as the rockglaciers formed during that period and thus depict complex archives of climatic history. Since for rockglaciers reaction times to climatic changes are far from known, the interpretations refer to the last century including the warming after the little ice age (LIA). Thus the temporal scale of the data and the one of the interpretation are not identical and therefore conclusions on relevant forcing factors are probably limited.

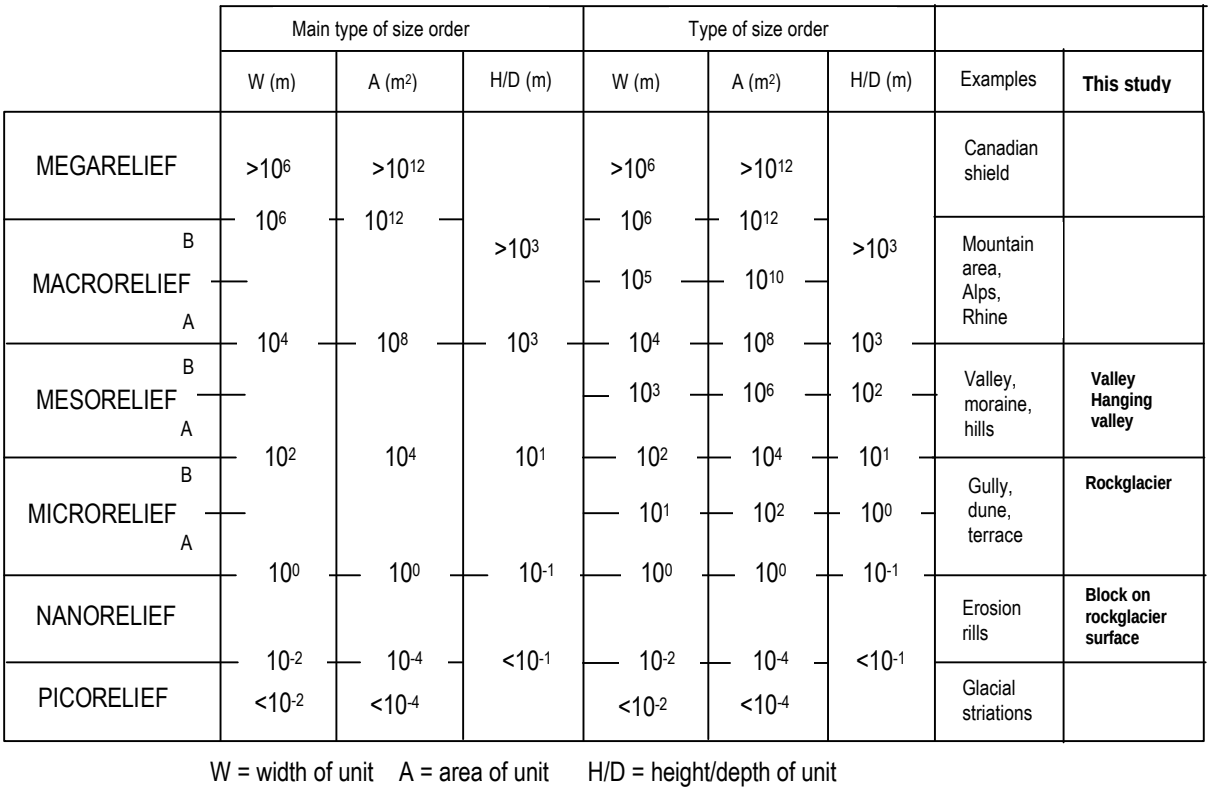

Figure 1.1: Hierarchical level and size of relief units (modified, after Dikau 1989). Bold face indicates relief units considered in this study.

The presented study outlines the scientific background of permafrost and rockglacier research in high mountain geosystems and focuses on the recent developments (**chapter 2**); it gives a thorough compilation of published data on rockglacier kinematics (**appendix 1**); it presents the advantages and limitations of the applied methods and the corresponding spatial and temporal resolution of the data (**chapter 3**); it introduces the study area (**chapter 4**); presents the results and interpretation of rockglacier kinematics (**chapter 5**); gives a discussion on the findings including rheological considerations (**chapter 6**) and ends with conclusions and perspectives (**chapter 7, 8**).

2 SCIENTIFIC BACKGROUND

2.1 High mountain geosystems

2.1.1 Definition & characteristics

The description of mountain environments had its beginning in the documentation by Alexander von Humboldt and Aimé Bonpland who described altitudinal belts in a cross-section of the Andes linking physical parameters with biological observations (Humboldt 1807; Messerli & Ives 1997). Later, most classifications applied single geomorphological parameters such as altitude or steepness of slope to describe high mountains in a quantitative way (Penck 1894; Passarge 1921). But, comparing mountains all over the world, the approaches were inadequate for a unifying definition. Thus, combinations of several parameters were suggested in order to represent high mountain characteristics; Rathjens (1982), Gerrard (1990), Bishop & Shroder (2004), as well as Owens & Slaymaker (2004) provide useful reviews of these classifications. Barsch & Caine (1984) proposed four criteria to determine mountain terrain:

- elevation,
- steep gradients,
- rocky terrain and
- the presence of snow and ice.

Additionally, they depicted a relative relief (i.e., the difference between the maximum elevation of a peak and the elevation of the surrounding terrain) of 500 m/km^2 as a criterion of high mountain systems (Barsch & Caine 1984: 288).

Parallel to these morphological approaches, Troll (1941, 1966, 1973) and Höllermann (1973) followed the geoecological attempt of Humboldt and compiled a comprehensive description of high mountain nature. Troll studied various mountain ranges in order to find characteristics which are applicable all over the world. Finally, he described a high mountain ecosystem as one which extends above:

- the Pleistocene snowline (indicating the variety of glacial landforms),
- the lower boundary of recent periglacial dynamics (lower limit of solifluction, conditioned upon freeze and thaw cycles) and
- the upper timberline.

These 'lines' are more or less close to each other and build up a transition belt that marks the lower margin of the high mountain area. Following this concept, "*high-mountains are mountains which reach such altitudes that they offer landforms, plant cover, soil processes, and landscape character which in the classical region of mountain geography in the Alps is generally perceived as high-alpine*" (Troll 1972, in Höllermann 1973).

Based on this definition, Troll (1966, 1973) documented an additional subdivision of high mountains into three characteristic subbelts:

- a lower subbelt with a close plant cover and with hampered solifluction,
- a middle subbelt of debris cover with a scanty pioneer vegetation and free solifluction, and
- the nival belt above the climatic snow line.

Recently, more holistic descriptions of mountain environments are formulated, e.g. by Messerli & Ives (1997) who integrate and emphasise the role of human beings within this system: *"Mountains, obviously, are regions of accentuated relief and altitude, which influence climate, soil fertility, vegetation, slope instability, and accessibility."*.

As it is apparent from the literature, a rigorous and representative description of high mountains is hard to define, since morphological, climatic as well as biological parameters interact in a complex system and thus lead to a great variability in shape and structure of mountain geosystems. Hence, although this study is concentrated on landforms, the consideration of high mountain geosystems in a pure geomorphological context would be restrictive. Thus, the approach of Troll is emphasised in this investigation. Especially the second 'line' described by Troll directly refers to the purpose of this study; i.e., the measurement of rockglacier kinematics as part of the periglacial dynamics. These landforms are considered as significant indicators for changes at the lower limit of high mountain geosystems. In general, the sensitivity and thus the significance of these systems need to be considered. Regarding mountain geomorphology, Barsch & Caine (1984) stated that it deserves special attention within geomorphology, since due to criteria like steep gradients, environmental changes may occur on shorter time-scales and with lasting consequences. Thus, in spite of a great complexity and variability these changes need to be monitored and sensitivities as well as thresholds need to be identified. They are of great importance if geomorphology is to be useful in prediction.

2.1.2 High mountain geomorphology

High mountain geomorphology is characterised by steep rock walls (> 60°) and steep slopes (35-60°), forming a high-energy environment (Barsch & Caine 1984). Thus, a strong correlation exists between erosion rate and relief (Gerrard 1990). Low relief can only be found on mountain plateaus or on the floor of valleys, since they are filled with sediment of glacial, periglacial and fluvial processes.

In most high mountain areas the topography is dominated by glacigenetic bedrock forms (nunataks, cirques, glacial troughs), as evidence of former (Pleistocene) glacial activity (**glacial erosion**). These macro- to mesorelief-forms are superimposed by meso- to microrelief-forms (moraines, solifluction-lobes, talus cones, fans), which are due to diverse process-domains (glacial, periglacial, gravitational) acting more recently (cf. Anderson & Burt 1981) (**postglacial accumulation**) (Figure 2.1). This apparent disparity between present landforms and

contemporary processes seems to be especially evident in high mountain areas (Barsch & Caine 1984).

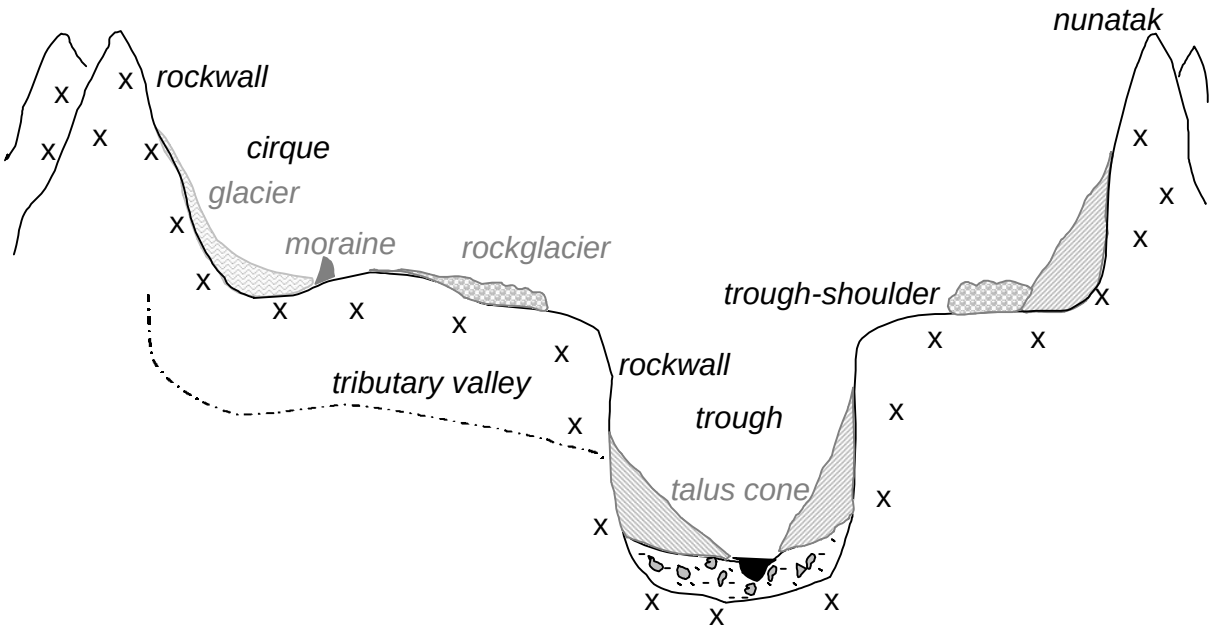

Figure 2.1: Some basic elements of high mountain landforms (modified, after Barsch & Caine 1984). Black lines and type: glacial erosive forms; grey lines and type: postglacial accumulative forms.

Another characteristic is the hypsometric sequence of typical landforms (Lautensach 1952). These are due to process domains (Thornes 1979) resulting from particular environmental parameters, e.g. slope, aspect, climatic conditions. Together with other phenomena such as vegetation, these sequences enable a subdivision in mountain belts: montane, subalpine, alpine, nival. The alpine belt, for example, is defined by the occurrence of solifluction (cf., Rathjens 1982). Concerning the processes operating and their significance as sediment transport systems, rate and intensity at which the processes operate need to be considered and discussed in the context of magnitude and frequency (Wolman & Miller 1960; Gerrard 1990).

2.2 Periglacial & Permafrost

2.2.1 Definition & characteristics

In general, the periglacial belt in mountains as well as in subpolar zones is characterised by freeze and thaw processes (cf., French 1996). Within high mountains it was defined by Troll (1973) as the area between the upper timberline and the snow line. Concerning a definition of the lower periglacial limit, the geomorphologic effectiveness of the cryogenic processes needs to be considered (cf., Hagedorn 1980). This was detailed by Troll, who subdivided the belt in two subbelts of different periglacial dynamics:

- "*a lower subbelt beyond the timberline, where a close carpet of vegetation … exists and where the frost action and the cryoturbation is hampered by and in competition with the growing plant cover…*" (hampered or bound solifluction (cf., Büdel 1948; Höllermann 1985))
- "*an upper substage … with bare scree- and debris-soils and a very scanty pioneer vegetation …*" (free or unbound solifluction (cf., Höllermann 1985)).

In the Alps, a wide area above the timberline is influenced by the occurrence of permafrost, which is defined as lithospheric material with temperatures < 0° C during at least one year (e.g., Haeberli 1975). Thus, the phenomenon permafrost is closely related to the periglacial belt. But, as it is the same in subpolar regions, there is no obligatory overlap between periglacial and permafrost areas. The occurrence of permafrost is an indicator for periglacial conditions but it is not an essential attribute of the periglacial (Karte 1979; Thorn 1992).

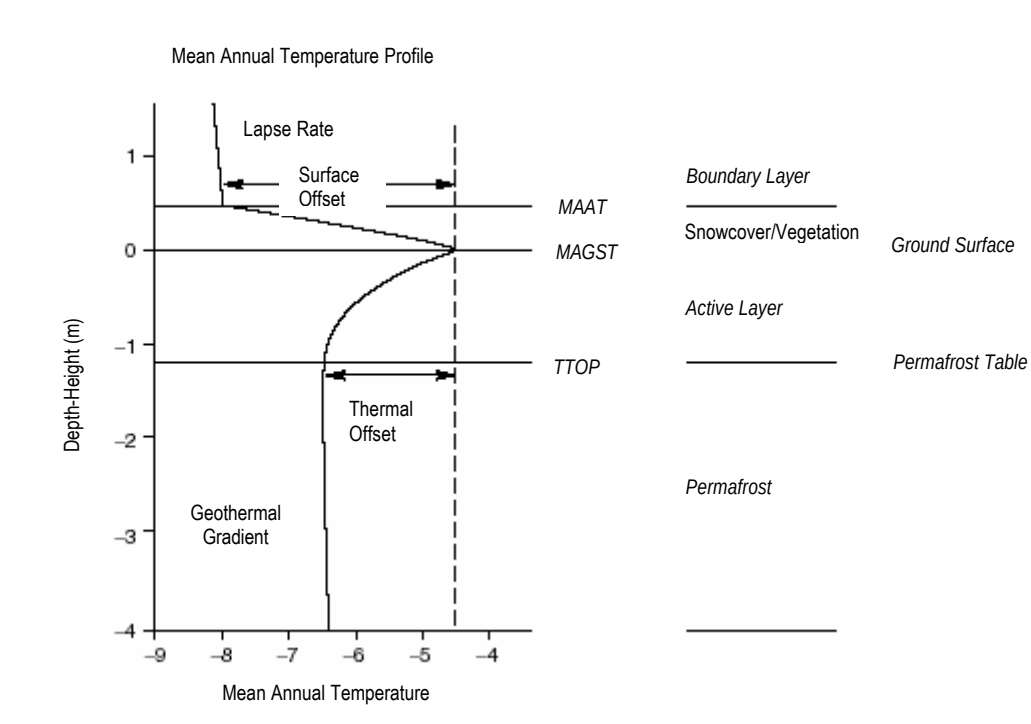

Figure 2.2: Schematic mean annual temperature profile through the surface boundary layer, showing the relation between air temperature and permafrost temperature (modified, after Smith & Riseborough 2002: 5). MAAT = Mean Annual Air Temperature; MAGST = Mean Annual Ground Surface Temperature; TTOP = mean annual Temperature at the Top Of Permafrost.

2.2.2 Influencing factors

As defined, the occurrence of permafrost is characterised by temperature and time and is primarily a function of direct solar radiation, air temperature, as well as the characteristics of soil, vegetation- and snowcover (Haeberli 1990). A typical temperature profile through the surface boundary layer of a permanently frozen ground is depicted in figure 2.2. In order to get a better understanding of the processes within, a lot of recent investigations deal with monitoring and modelling of vertical energy fluxes between permafrost body, active layer, ground surface and

atmosphere (e.g., Humlum 1998c; Stocker-Mittaz et al. 2002). The energy balance at the ground surface is expressed quantitatively in the following equation (Hoelzle et al. 1993; Hoelzle 1994):

$$Q_r \pm Q_h \pm Q_{le} \pm Q_g \pm Q_m = 0$$

Where Q_r is the radiation balance, Q_h the sensible and Q_{le} the latent heat flux, Q_g the conduction of heat into the ground and Q_m the heat of fusion of the ice (Hoelzle 1994). These components discussed in Hoelzle (1994) and Mittaz (1998) in more detail, are variable in space and time since they are influenced by climatic and topographic parameters (Hoelzle et al. 1993). Therefore, the permafrost occurrence is very complex - especially in high mountains, where the permafrost distribution varies strongly due to varying topography. Here, the radiation seems to be the dominating factor (e.g., Hoelzle 1992; Funk & Hoelzle 1992; Hoelzle 1994; Schrott 1994; Krummenacher et al. 1998). Additionally, also the thickness, redistribution and duration of the snowcover (e.g., Hoelzle 1992; Keller 1994; Krummenacher et al. 1998; Harris 2001; Mittaz et al. 2002; Hanson & Hoelzle 2004; Luetschg et al. 2004) as well as the characteristics of the surface material (Humlum 1998a; Herz et al. 2003; Hanson & Hoelzle 2004) play an important role. The knowledge on interrelationships of temperatures and permafrost occurrence on the local scale needs then to be applied to sophisticated models of permafrost distribution on a more regional scale (see below).

2.2.3 Prospecting methods

In order to get to know if permafrost is present in the ground or not, the best method is the direct measurement of temperatures in the ground (e.g., in boreholes) (e.g., Vonder Mühll 1993; Isaksen et al. 2001). Since this is a very expensive prospecting method, indirect means such as geophysical soundings (refraction seismics and DC-resistivity) are used for the determination of permafrost and its distribution (e.g., Dikau 1978; Haeberli & Epifani 1986; Barsch & King 1989; Vonder Mühll 1993; Vonder Mühll et al. 2001; Hauck 2001; Kneisel 2004). Additionally, in the seventies, the significance of the Bottom Temperature of the Snow cover (BTS) was detected as a reliable indicator for permafrost conditions (Haeberli 1973, 1975). Later, the development of miniature data loggers allowed longterm and continuous temperature measurements and improved the data dramatically (Hoelzle 1992; Hoelzle et al. 1993; Hoelzle et al. 1999; Imhof et al. 2000). Best interpretation is enabled by the combined application of different techniques.

2.2.4 Permafrost distribution, modelling & sensitivity

The permafrost distribution in the Alps is controlled by the spatial distribution of energy balance factors (see above) and is thus a function of topographic and climatic parameters (Hoelzle et al. 1993; Keller 1994). In view of these parameters and by considering the rules of thumb for permafrost distribution (Haeberli 1975) which build an important empirical basis, the probability of permafrost occurrence can be calculated using empirical-statistical or process-oriented models (Funk & Hoelzle 1992; Keller 1992; Hoelzle 1994; Imhof 1996; King 1996; Frauenfelder 1998; Gruber & Hoelzle 2001; Hoelzle et al. 2001; Stocker-Mittaz et al. 2002; Guglielmin et al. 2003). Concerning permafrost distribution models, the following spatial scales have been proposed

within the PACE project: a micro or patch scale with a spatial resolution of 25 m, a meso scale with a resolution of 25 to 200 m and a macro scale with a resolution > 250 m (Hoelzle et al. 2001: 55). Depending on the methodology applied and thus on the spatial and temporal scale considered, processes and the relative importance of influencing parameters are variable (e.g., De Boer 1992; Thorn 2003). E.g., on a local scale the permafrost distribution is influenced by snow distribution, vegetation cover, etc. while on a wider scale Mean Annual Air Temperature (MAAT) and solar radiation are consulted as the relevant factors. In this context, it is generally accepted that a MAAT of -2° C indicates discontinuous permafrost whereas a MAAT below -6° C shows continuous permafrost. In areas with mean annual air temperatures warmer than -2° C permafrost occurs only sporadically.

The increase in temperature within the last century has major consequences for the glacial and periglacial belt. The so far observed changes are mostly obvious reactions of the alpine environment on changing climate conditions (Haeberli 1992a, b; Haeberli 1995) and thus are important environmental indications. Additionally to the signal function, the resulting changes in mountain permafrost lead to problems in slope stability of rock and unconsolidated material (moraines, talus cones) (e.g., Haeberli et al. 1997; Nötzli et al. 2003). As a consequence, more data is demanded in order to deepen the knowledge on the ongoing processes and the reaction times of the system. Then, more sophisticated models can be developed to quantify mass fluxes and thus enable assessments on possible natural hazards (e.g., Kääb & Haeberli 1996).

The 'system' permafrost reacts dynamically to environmental changes, whereas the reaction time of permafrost bodies is relevant for the understanding of the system (Haeberli 1990; Hoelzle 1994; Humlum 1998b; Frauenfelder & Kääb 2000). Although the response of permafrost to climatic changes is not known in detail, one can consider that permafrost is very sensitive; even if it shows a delayed reaction to changes in the energy balance. The response time of permafrost depends primarily on the thickness of the permafrost body, the thermal conductivity, the ice content as well as on the amount of unfrozen water (e.g., Haeberli et al. 1993; Osterkamp 1983; Osterkamp & Romanovsky 1999). Direct and delayed reactions and adjustments can be distinguished, since direct response occurs at the permafrost table and results in the increasing thickness of the active layer. Against that, the delayed reaction affects the permafrost base and induces the thinning of the permafrost body. Concerning the relatively warm discontinuous permafrost in the Alps, a response time of several decades to centuries is assumed (cf., Haeberli 1990; Osterkamp & Romanovsky 1999). Haeberli (2000) stated that the permafrost thickness is presently not in equilibrium with the actual - in general warmer - ground surface temperatures. Thus it is assumed, that the actual permafrost occurrence reflects the climatic conditions of the Little Ice Age (LIA) (Etzelmüller & Hoelzle 2001).

The problems in permafrost research arise from the fact that the weighting of single factors (aspect, slope, snow cover, substrate, vegetation, etc.) and their significance within the energy balance is not sufficiently known. Therefore, actual permafrost studies concentrate on the filling of this gap. E.g., in order to get a better understanding of the relation between temperatures and the ground surface, the knowledge on rock temperatures, which show direct reactions since no

'buffer' layers (snow, vegetation, debris or talus) are present, is of major importance (Gruber et al. 2003; Gruber et al. 2004). Further improvements are claimed by the modelling of the former permafrost distribution (palaeopermafrost and palaeoclimate) (e.g., Frauenfelder & Kääb 2000) and possible developments in the future.

2.3 Rockglaciers

2.3.1 History of rockglacier research

In the beginning of the twentieth century so-called "*Rock Glaciers*" were described for the Rocky Mountains (Howe 1909) as well as for Alaska (Capps 1910) (from Pillewizer 1957). In Europe, Emil Chaix (1918; from Eugster 1973) was the first to call attention to these peculiar landforms he observed in the Swiss National Park. He started geomorphological investigations which were continued by André Chaix. By measuring stone lines on the rockglaciers Val Sassa and Val dell' Acqua, André Chaix (1923) delivered the first evidence on the movement of these features. Later, Heinrich Jäckli (1957) was concerned with the rockglaciers in this area. By 1920, in Austria E. de Martonne was the first to report on "*Blockgletscher*" in the Doisental (from Pillewizer 1957). In 1938, Pillewizer started investigations on rockglacier movement by means of terrestrial photogrammetry. The measurements were interrupted by the Second World War, but in the fifties he continued with detailed studies on the Hochebenkar rockglacier which until now provides the longest series on rockglacier movement (Pillewizer 1957; Vietoris 1972; Haeberli & Patzelt 1982). In recent times, rockglaciers are monitored in many places and by diverse methods (see Matsuoka & Humlum 2003 for summary).

2.3.2 Rockglacier origin & nomenclature

Since the second half of the twentieth century, rockglaciers were studied in diverse regions all over the world. At the same time, a wide discussion on the origin of these landforms started and two main positions evolved. One position focused on the glacial origin of rockglaciers (e.g., Outcalt & Benedict 1965; Potter 1972; Whalley 1974; Humlum 1982, 1988, 1996; Evans 1993; Whalley et al. 1994; Hamilton & Whalley 1995) while the others argued with a general periglacial origin (e.g., Wahrhaftig & Cox 1959; Haeberli 1985; Barsch 1977, 1988, 1992). Even some claim a polygenetic formation of rockglaciers as combination of periglacial, glacial and catastrophic mass movement processes (cf., Whalley & Martin 1992). Thus, rockglaciers may reflect geomorphic equifinality. Detailed discussions on rockglacier origin and nomenclature are given in several publications (e.g., Johnson 1983; Haeberli 1985; Corte 1987; Martin & Whalley 1987; Barsch 1987a, 1987b, 1992, 1996; Humlum 1988, 1996, 2000; Whalley & Martin 1992; Hamilton & Whalley 1995; Clark et al. 1998). The view that most rockglaciers are of periglacial origin has remained dominant since the comprehensive study on rockglaciers in Alaska by Wahrhaftig and Cox (1959).

The existing study follows the reasoning of Barsch and Haeberli. But, the influence of glaciers may not be denied in individual cases (see chapter 5.1.6). In general the terminology of the phenomenon (rockglacier) is a mistake, since the nomenclature implicitly relates to classical

glaciers. But, the latter belong to the hydrosphere, whereas rockglaciers with their debris-ice mixture are subordinated to the lithosphere. In order to emphasise the autonomy of the phenomenon, the term 'rockglacier' is written in one word according to Barsch (1988).

2.3.3 Rockglacier definition

Today, rockglaciers as well as ice-cored moraines are considered as morphological indicators for the presence of permafrost in high mountains (e.g., Haeberli 1985; Barsch 1996; Humlum 2000). In order to indicate the recent occurrence of permafrost, the considered rockglaciers need to be in an active status. Following Barsch (1992, p.176), "*active rockglaciers are lobate or tongue-shaped bodies of perennially frozen unconsolidated material supersaturated with interstitial ice and ice lenses that move downslope or downvalley by creep as a consequence of the deformation of ice contained in them and which are, thus, features of cohesive flow*". Haeberli (1985) focused on the process and described the phenomenon as "*visible expression of steady-state creep of ice-supersaturated mountain permafrost bodies in unconsolidated materials. They display the whole spectrum of forms created by cohesive flow*" (from Barsch 1992). The existing definitions give fundamental information on form, material and process, although the knowledge on the ongoing processes is still limited. A multiplicity of influencing parameters exists, but the interrelationships are often not known in detail.

2.3.4 Rockglacier distribution, morphology & stratigraphy

Detailed information on rockglacier occurrence, distribution and environmental conditions is given in Höllermann (1983), Haeberli (1985), Barsch (1992, 1996), and Humlum 2000. Large scale climatological boundary conditions can be compiled with mean annual air temperatures (MAAT) below -1°C to -2°C and annual precipitation of less than 2500 mm (Haeberli 1985), but on a local scale, the topographic and meteorological controls on rockglacier initiation and growth are still not known in detail (Humlum 1998b, 2000). Kirkbride & Brazier (1995) discussed rockglacier formation on a regional scale using qualitative conceptual models and concluded, that the timing of the formation more likely follows the rules of deterministic chaos than corresponds to climatic cooling.

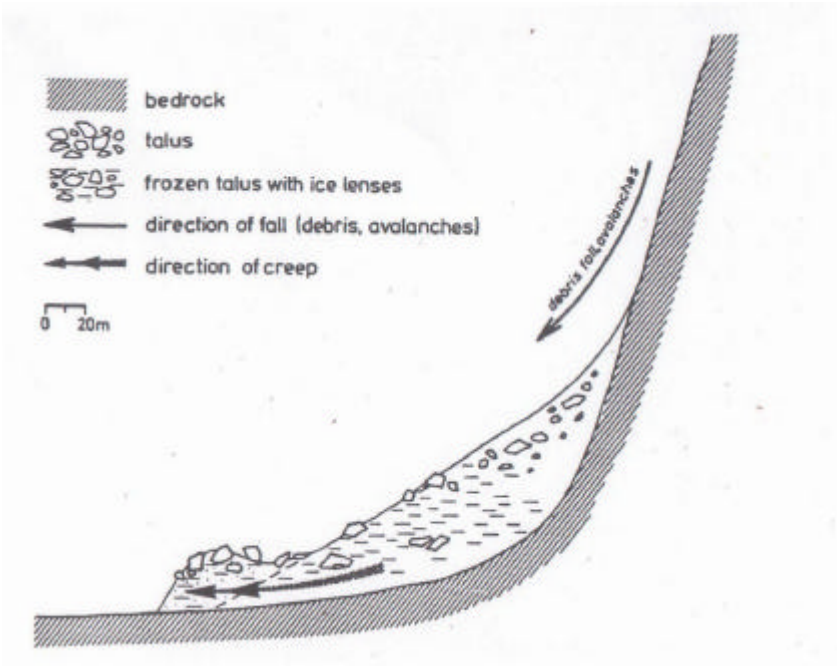

Figure 2.3: Model of the development of talus rockglaciers (below mountain talus slopes) in discontinuous mountain permafrost environments (from Barsch 1996: 186).

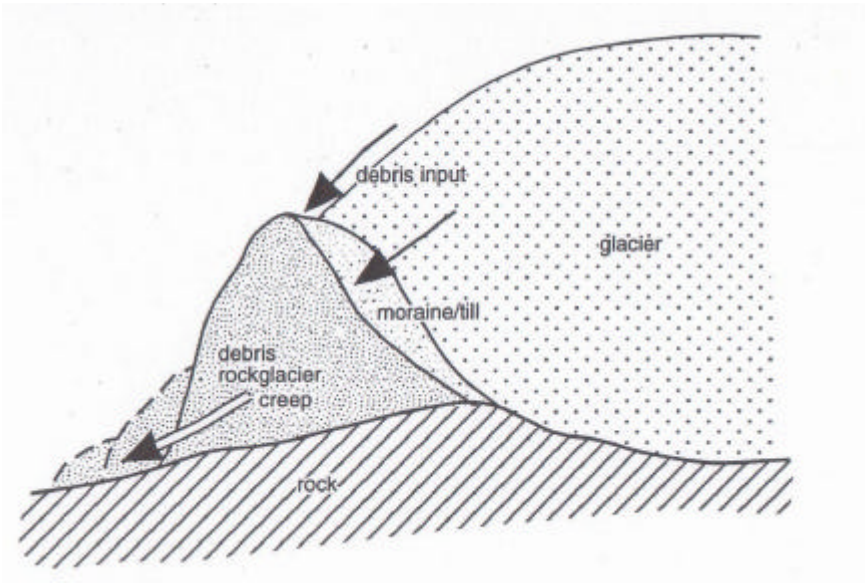

Figure 2.4: Model of the development of a debris rockglacier in mountain permafrost environments (from Barsch 1996: 187).

Rockglaciers are typically situated at the foot of free rock faces (talus rockglacier, figures 2.3, 2.8, 2.10) or below moraines (debris rockglacier, figures 2.4, 2.9) and form tongue- or lobe-shaped bodies with a typical length of 200 – 800 m (Barsch 1996). Normally they are 20-100 m thick; direct means such as coring or indirect means such as geophysical soundings delivered a typical rockglacier thickness of about 50 m (cf., Humlum 2000). A special characteristic are steep lateral and frontal slopes standing at the angle of repose with an apron of coarse blocks at the foot of the slope built by the rockglacier creep (Haeberli 1985). Often, several lobes are superimposed on

each other building a complex topography from different rockglacier generations. These types are called polymorphic bodies, while monomorphic rockglaciers are features without marked surface relief (cf., Frauenfelder et al. 2004).

The rockglacier stratigraphy is described by several authors (e.g., Haeberli 1985; Barsch 1992, 1996; Burger et al. 1999; Humlum 2000; Ikeda & Matsuoka 2002) as a sequence of three main layers: the uppermost 1-5 meters consist of big boulders and are riding on an ice-rich permafrost layer - with 50-70 % of ice and about 30 % of finer-grained material (Barsch 1996) - which is creeping downslope. Below, the third layer consists again of larger rocks, which were deposited at the rockglacier front and subsequently overrun by the other layers. This characteristic sorting of the rockglacier material becomes visible at the rockglacier front. More detailed studies on stratigraphy are delivered by indirect means such as geophysical soundings (e.g., Vonder Mühll 1993; Hauck et al. 2001; Vonder Mühll et al. 2001) or by direct observation in borehole-cores (e. g., Vonder Mühll & Haeberli 1990; Haeberli et al. 1998; Arenson et al. 2002). Burger et al. (1999: 108-109) compiled a comprehensive reference-list of locations, where the internal structure of rockglaciers was investigated.

As derived from four boreholes drilled in 1999, figure 2.5 shows the complex internal structure of the Muragl rockglacier (Arenson et al. 2002). Despite this valuable data, one needs to take into account, that this depicts only local information! The variable distribution of ice layers all over the rockglacier remains speculation.

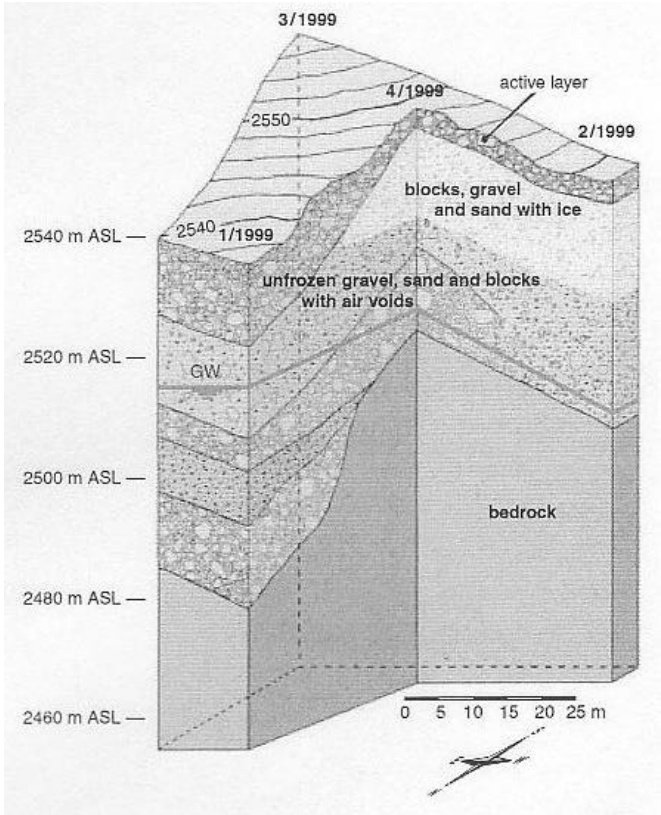

Figure 2.5: Internal structure of the Muragl rockglacier (from Arenson et al. 2002: 122).

The top layer of the permafrost body is typically composed of coarse (0.2 – 5 m) rock fragments (cf., Humlum 1998a) and builds a "*surface relief*" (Humlum 1982) of ridges and furrows which are related to the flow processes, thus, indicating the complex history of rockglacier deformation (Haeberli 1985; Johnson 1992). A detailed description of 'microrelief on rock glaciers' is given in Wahrhaftig & Cox (1959). Field measurements and laboratory tests on the development of transverse ridges are discussed in Kääb & Weber (2004). In general, it is supposed that transverse ridges and furrows result from compression flow (e.g., Haeberli 1985; Kääb et al. 1998). According to Wahrhaftig & Cox (1959) and Barsch (1977), also variations in material supply may lead to the formation of a complex surface topography. Below the furrows subsurface running water is often audible during summer (cf., Elconin & LaChapelle 1997). Other striking but currently not explicable features are small-scale bumps of fine material, probably related to the rockglacier movement.
Additionally, some rockglaciers depict crevasse-like features perpendicular to the flow direction; probably resulting from fast movement such as in steep terrain (e.g., Haeberli & Patzelt 1982). Wahrhaftig & Cox (1959) described these features as tension cracks built by the lateral spreading of the moving mass.

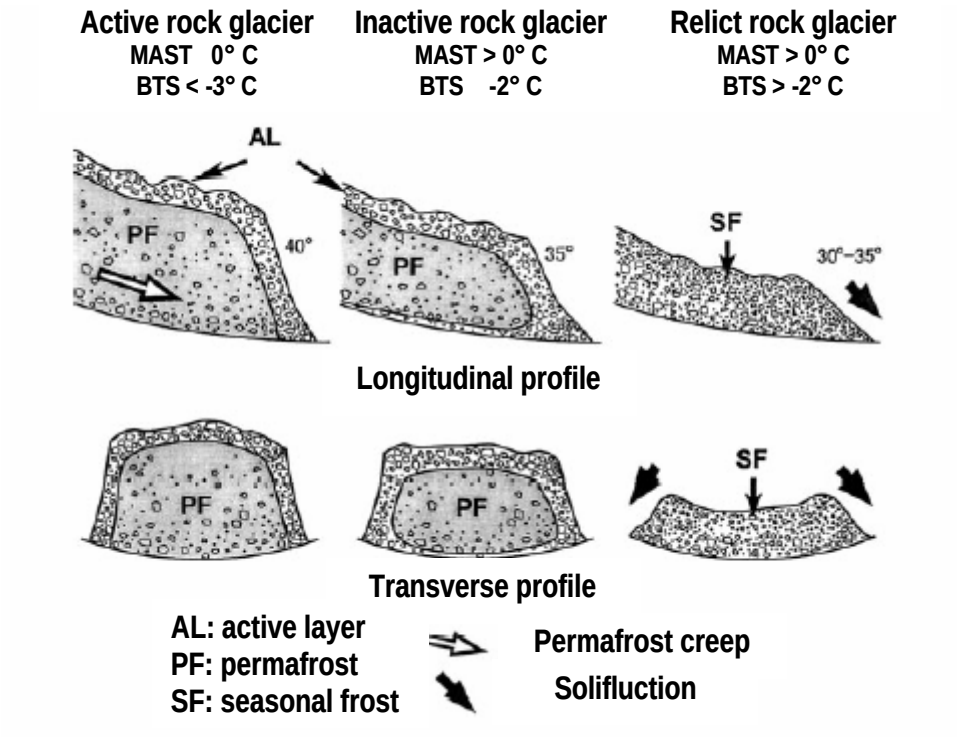

Figure 2.6: Schematic profiles of active, inactive and relict rock glaciers (from Ikeda & Matsuoka 2002: 158).

Due to their ice content and flow behaviour, rockglaciers are classified into the following types: active, inactive and relict. Often they are situated one over the other, forming a sequence of active rockglaciers in higher altitudes to relict rockglaciers in lower altitudes (cf., figure 2.11). A

comparison of morphology, structure and thermal conditions for active, inactive and relict rockglaciers is given in figure 2.6 by Ikeda & Matsuoka (2002). In a strict sense, the activity of rockglaciers is determined e.g., by geodetic survey or photogrammetry, which gives information on their movement. But, in several studies the state of activity has been assessed by morphological characteristics (cf., Wahrhaftig & Cox 1959; Haeberli 1985; Krummenacher et al. 1998; Barsch 1996; Burger et al. 1999; Ikeda & Matsuoka 2002; Nyenhuis et al. in press). Thus, a steep terminal front (> 35°) with loose boulders and without vegetation indicates the activity of the feature, whereas inactive rockglaciers, which still contain ice but actually do not move, have a gentler front with stable boulders and partial or full vegetation. Because of their ice content, active and inactive rockglaciers are grouped together as 'intact' rockglaciers (cf., Haeberli 1985). In addition to the morphological approach, the BTS (Bottom Temperature of the winter Snow cover) method is used for the determination of intact rockglaciers and consequently the occurrence of permafrost (Hoelzle 1992; Hoelzle et al. 1999; see chapter 3.5).

Regarding the inactivity of rockglaciers, Barsch (1996) emphasised two causes for inactivation, depending on thermal and mechanical factors (figure 2.7). On one hand the climatic induced inactivity, which is characterised by a thickening of the active layer due to melting of the frozen core and therefore is related to the lower limit of the discontinuous permafrost belt (cf., Ikeda & Matsuoka 2002). In comparison to that, the dynamic induced inactivity results from a reduction in shear stress due to a reduced incorporation of debris and ice or a downslope decrease in slope gradient (Barsch 1996). This kind of inactivation was related only to rockglaciers in continuous permafrost, although a change in debris- and ice-input may occur also in discontinuous permafrost. Olyphant (1987, from Ikeda et al. 2003) made a numerical simulation and confirmed that a decrease in debris input leads to a deceleration of rockglacier advance.

Relict rockglaciers show a collapsed surface due to the melting of the ice. The furrows and ridges are still visible, but the front has a lower angle and the rockglacier surface depicts a dense vegetation cover – at least in areas with fine material (Roer 2001). Relict rockglaciers are valuable indicators for the former permafrost distribution and therefore they are consulted for paleoclimatic reconstructions (cf., Kerschner 1985; Tatenhove & Dikau 1990; Konrad et al. 1999; Frauenfelder & Kääb 2000; Frauenfelder et al. 2001). In addition to reconstructions from landform characteristics, different attempts had been made to date rockglaciers with absolute and relative age-determination methods (e.g., Barsch & King 1975; Kirkbride & Brazier 1995; Humlum 1996; Frauenfelder & Kääb 2000; Haeberli et al. 2003; Frauenfelder et al. 2004).

Generally, the ecological significance of rockglaciers is reflected in their influence on the water cycle (cf. Haeberli 1985; Krainer & Mostler 2002) as well as in their contribution to sediment transport (cf., Höllermann 1983; Barsch 1996). Barsch (1977) stated that about 20 % of all alpine mass wasting is done by rockglaciers. Additionally, due to their thermal dependency, they depict sensitive indicators for environmental changes.

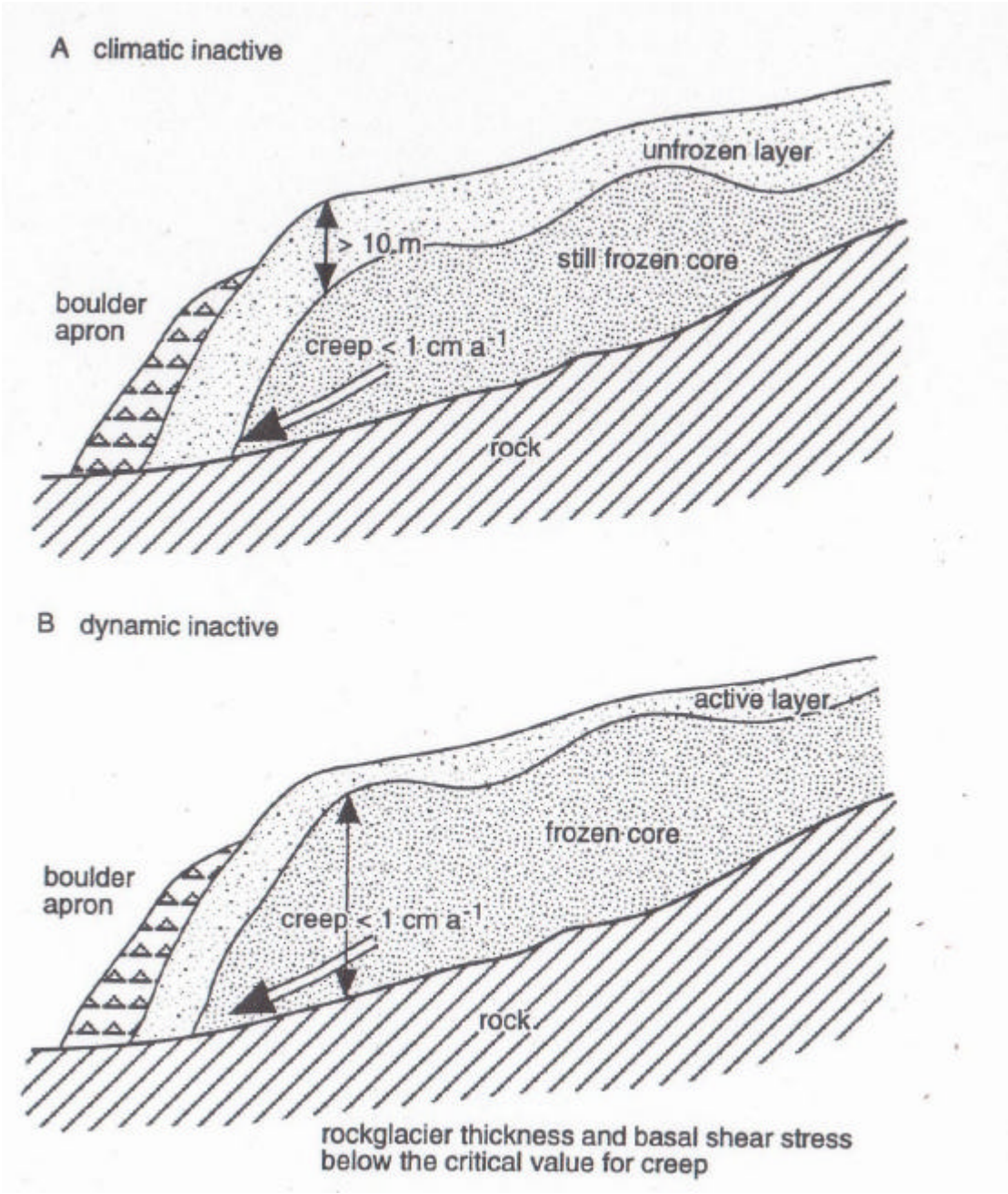

Figure 2.7: Model of inactive rockglaciers. A: Model of a climatic inactive rockglacier. B: Model of a dynamic inactive rockglacier (from Barsch 1996: 193).

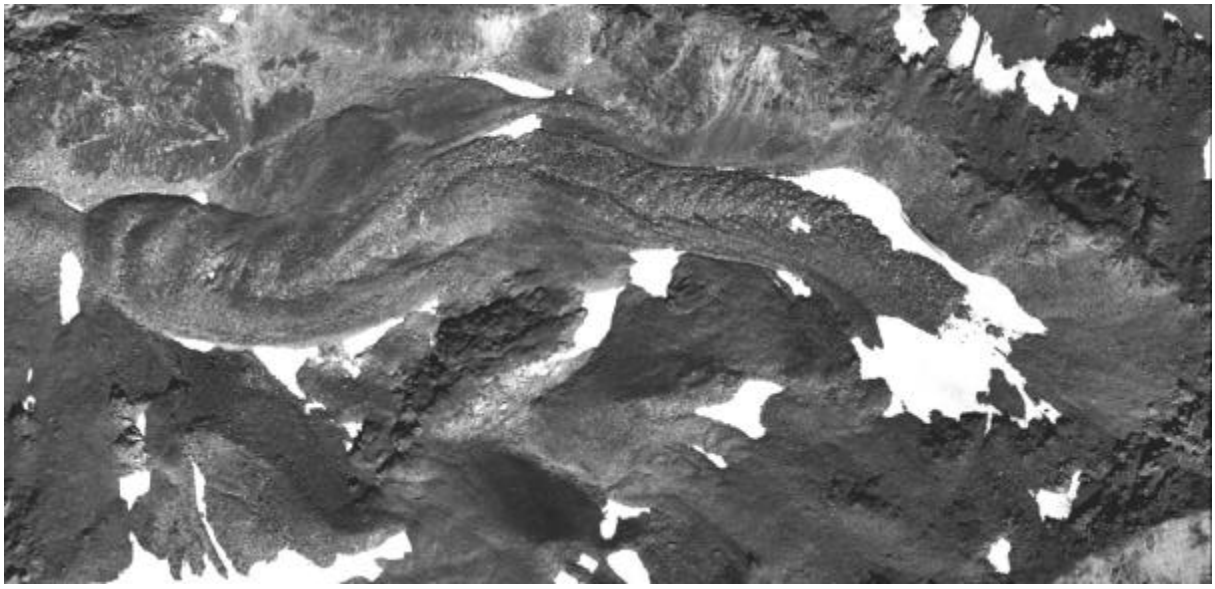

Figure 2.8: Talus rockglacier in discontinuous permafrost at Grüeobtälli (Turtmann valley, Switzerland). Underlying orthophoto of 20.08.1993 (flight-line 16, aerial photographs taken by Swisstopo). Plait-like ridge and furrow topography in the upper part of the rockglacier seems to result from sediment input of two different source areas.

Figure 2.9: Debris rockglacier in discontinuous permafrost at Pipjitälli (Turtmann valley, Switzerland). Underlying orthophoto of 20.08.1975 (flight-line 22, aerial photographs taken by Swisstopo). Former lateral moraines form the margins of the rockglacier.

Figure 2.10: Talus rockglacier in continuous permafrost at Templet (western Svalbard Archipelago, Norway). Photograph taken in September 2004.

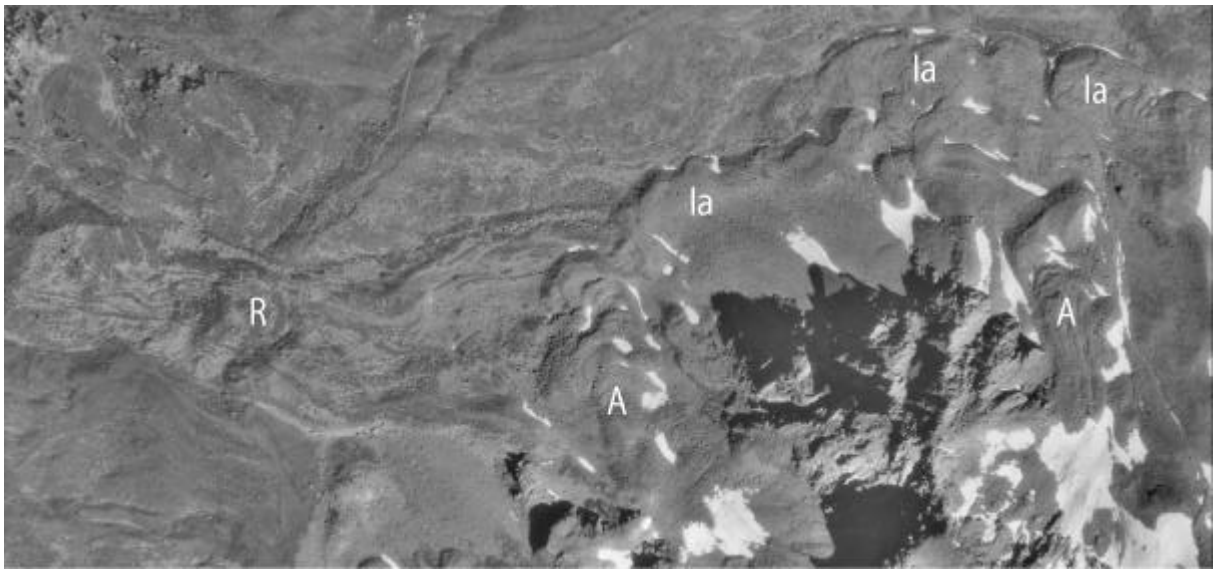

Figure 2.11: Rockglacier sequence in the Hungerlitälli (Turtmann valley, Switzerland); A = active, Ia = inactive and R = relict. Underlying orthophoto of 20.08.1975 (flight-line 22, aerial photographs taken by Swisstopo).

2.3.5 Rockglacier kinematics

Kinematics [greek: kínema = movement] is defined as the quantification of movement (velocity, acceleration) without considering the forcing factors (in contrast to dynamics). The velocity is generally described as a vector in a four-dimensional field $v = (v_x, v_y, v_z)^T$, where x and y represent the coordinates and z depicts the altitude. The horizontal components at the surface are determined by $Äx/Ät = v_x^s$ and $Äy/Ät = v_y^s$. Thus, the velocity includes temporal aspects (velocity between the times of the measurements) as well as spatial aspects (velocity between the corresponding points) (Kääb 1996). Against that, **dynamics** [greek: dýnamis = force] involves forces and their interactions as well as the resulting changes in physical systems (based on the second axiom of Newton).

2.3.5.1 Rockglacier movement

For the quantification of rockglacier movement which results from permafrost creep, in general three different components are considered: horizontal velocities, vertical changes and the front advance. Regarding horizontal displacements, rockglaciers move from a few centimetres to one meter per year (Haeberli 1985), generally well below one meter (Whalley & Martin 1992), i.e. at a considerably slower rate than normal glaciers. Barsch (1996) described horizontal velocities between 1-2 cm (minimum) and 100-200 cm (maximum). Higher movements are rare and mostly result from specific topographic conditions (extremely steep gradients). A comprehensive review of published data on rockglacier kinematics (horizontal velocities, vertical velocities and front advance) is given in the appendix 1. In general, the velocities are within the spectrum given by Barsch (see above). Exceptionally fast-moving rockglaciers with velocities of up to 100 m/a are reported from the Andes (Corte 1987) and from Asia (Gorbunov et al. 1992). In the Alps, the highest horizontal velocities (almost 7 m/a) were documented by Chesi et al. (1999) and Krainer & Mostler (2000) for the rockglacier Inneres Reichenkar (Austria). Also the rockglacier Äusseres Hochebenkar (Austria) showed maximum velocities of 5-6 m/a (Vietoris 1972; Schneider 2001). In Switzerland, mean velocities of 2 m/a were measured on Val da l' Aqua rockglacier (Chaix 1943; Jäckli 1978, from Barsch 1992) in Grisons. Highest mean velocities in the Valais are described by Krummenacher et al. (1998) for the Furggentälti rockglacier (1.35 m/a) and by Strozzi et al. (2004) for the Gruben rockglacier (2 m/a).

Vertical movements may result from diverse processes like 3-dimensional straining (compression, extension), input of debris, formation of ice from snow or water, climatic influences or the advance of individual lobes (for summary see Kääb et al. 2003). All these influences are reflected in the thickening or thinning, respectively, at the rockglacier surface (see chapter 2.3.5.4). The rates are mostly very low and thus often below the level of significance (cf., reference-list in appendix 1). A typical vertical movement of -0.06 m/a was measured by Barsch & Hell (1975) on Murtèl rockglacier (Grison) by means of photogrammetry.

The front advance of rockglaciers is many times lower than the horizontal movement, due to the vertical velocity profile which is indicated by the boulder apron in front of the terminus. Velocities between 0.01 m/a (Murtèl), 0.05 m/a (Muragl) and 0.15 m/a (Gruben) were

monitored by Kääb (1996, 1997) (cf., reference-list in appendix 1). Thus, the values are around 10 % of the corresponding horizontal velocity.
Comparisons of rockglaciers in the European Alps and the polar regions show clear differences in horizontal and vertical velocities as well as front advance, which result from the differences in ground thermal conditions (Kääb et al. 2002, 2003).

2.3.5.2 Spatial variation of movement (surface & depth)

The spatial variation of horizontal velocities mostly reveals highest horizontal velocities in the central flowline while to the borders of the rockglacier the displacement often decreases abruptly (e.g., Barsch 1992, 1996; Roer et al. 2005). Regarding the root zone, it is suggested that the velocities are lower due to a smaller thickness of the deforming layer (Kääb et al. 2003). At the other margins, this phenomenon is due to increased friction which leads to compressing flow (Haeberli 1985). The latter is reflected in the small-scale topography (cf., figure 2.18). In parts where horizontal creep compression takes place, the velocities are in general lower than in parts with extensive flow. Due to mass balance effects horizontal compressive flow is accompanied by vertical extension, which becomes visible in ogive-like transverse ridges. Their downslope movement approximately equals that of the creeping mass (Kääb et al. 1998). In areas of horizontal extension, vertical compression takes place (e.g., Gorbunov et al. 1992). Thus, a close correlation between spatial variations of horizontal and vertical movement exists. Apart from these flow effects, losses and gains of material may influence the mass balance. Kääb et al. (1998) documented changes in rockglacier surface elevation with distinct losses on perennial ice banks and gains in areas with debris accumulation. Due to topographic reasons, these gains and losses are mostly concentrated in the upper part of the rockglacier.
Beside the mass balance effects, the vertical movement is regarded in different ways. On one hand the flow component due to movement parallel to the surface, which amounts to 10-60 % of the horizontal displacement (Haeberli 1985: 87). On the other hand the profile of the movement in depth, where velocity varies according to a parabolic function (Burger et al. 1999). Within the profile, highest velocities occur at the rockglacier surface, thus indicating the cumulative movement of the whole body. But, about 2/3 of the movement is concentrated in a thin - a few metres thick - layer in a certain depth, while the remaining deformation is distributed regularly in the matrix above. This phenomenon is well investigated by borehole deformation measurements (e.g., Vonder Mühll & Haeberli 1990; Wagner 1992; Arenson et al. 2002). Deformation profiles of different rockglaciers are given in figure 2.12.

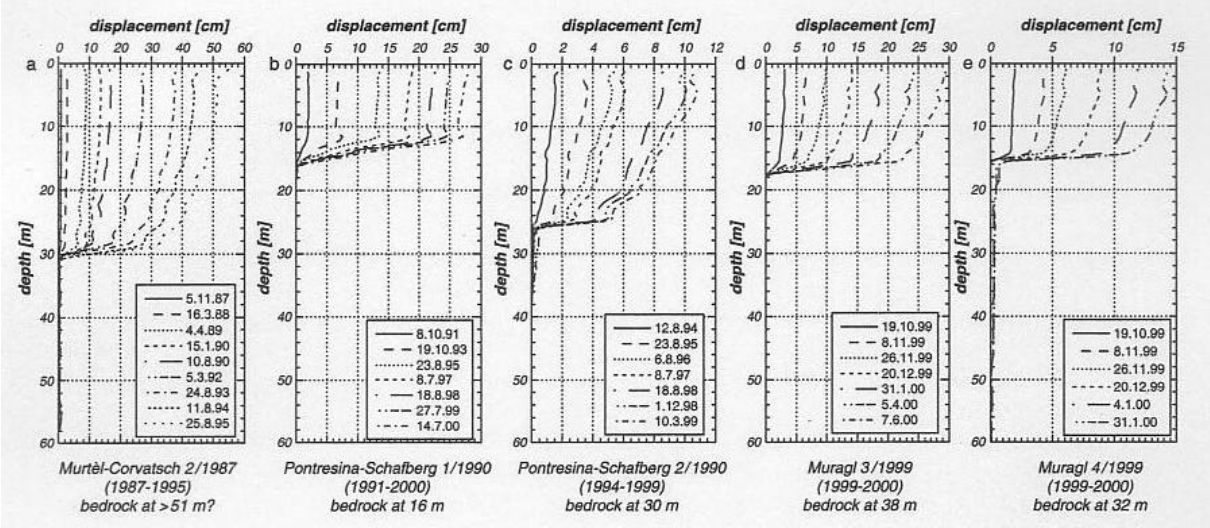

Figure 2.12: Horizontal downslope borehole deformation. a) Mutèl-Corvatsch, borehole 2/1987: 1987-1995; b,c) Pontresina-Schafberg, boreholes 1/1990 and 2/1990: 1991-2000, 1994-1999; d, e) Muragl, boreholes 3/1999 and 4/1999: 1999-2000 (from Arenson et al. 2002: 124).

On complex rockglaciers where several lobes in different states of activity are situated one over the other, also the surface movement appears complex. In some cases, actively creeping lobes can be distinguished from passively moving lobes (influenced by active lobes on top or at the side) by looking at the orientation of the horizontal flow vectors. Normally, they indicate the direction of the flowing mass following the general slope (Haeberli 1985: 88). Due to overriding or pushing by other lobes, they may be oriented in other directions or reveal a non-uniform pattern.
Another structure of surface velocities is given in situations where rockglaciers flow over a terrain threshold onto a steep slope. In this case highest velocities are found in the frontal part of the tongue, sometimes accompanied by transverse crevasses resulting from increased stress (Barsch 1992, 1996). Vietoris (1972) described this flow behaviour for the Hochebenkar rockglacier.

2.3.5.3 Temporal variation of movement (surface & depth)

In most publications, rockglaciers are suggested to show steady-state flow behaviour with stable velocities and therefore temporal variations are rarely discussed in the context of rockglacier kinematics. Nevertheless, it is mostly suggested that changes in deformation rates are related to changes in climatic parameters (Kääb et al. 1997; Kääb & Frauenfelder 2001). Since these relations are still not known in detail and appropriate data are mostly lacking, different assumptions and specifications were made. Concerning an increase in temperature and its impact on rockglaciers, Barsch (1996: 258) summarised four possible consequences: first the increase in thickness of the active layer, second the increase in thickness of the unfrozen layer at the rockglacier front, third the penetration of heat into the rockglacier by circulating meltwater and last the variations of creep rates.
Temporal variations were first mentioned by White (1971, from Haeberli 1985) and later discussed by Barsch & Hell (1975), who described seasonal changes in horizontal and vertical

velocities on the rockglaciers Murtèl and Muragl (Grisons, Switzerland). The same phenomenon was monitored by Haeberli (1985) also on Muragl rockglacier and on Gruben rockglacier (Valais, Switzerland). Recent geodetic measurements on Muragl showed seasonal variations between 0.01 and 1 m/a with maximum velocities in late autumn and minimum values in spring and early summer (Kääb & Vollmer 2000). Different phases of movement were also investigated on the rockglacier Macun I (Zick 1996). Beside the seasonal changes, longterm degradation of rockglaciers was observed. Barsch (1988) reported on a decrease from 1 m/a around 1920 (measured by Chaix 1923) to nearly zero today at Val Sassa rockglacier (Grisons, Swiss Alps). Gorbunov et al. (1992) documented on rockglaciers in the Karakorum with a distinct decrease in velocity (e.g., from 7.75 to 1.28 m/a) and others with increased velocities over a 15 year period (Whalley & Azizi 1994). In the recent past, some authors presented data on rockglacier acceleration in the Alps which seem to be linked to changes in climatic conditions (e.g., Zick 1996; Schneider & Schneider 2001; Ikeda et al. 2003; Lambiel & Delaloye 2004). Schneider & Schneider (2001) discussed rockglacier surface velocities in relation to morphological and climatic parameters on the Äusseres Hochebenkar rockglacier and concluded a direct influence of Mean Annual Air Temperatures (MAAT) on surface velocities. The same conclusion was already drawn from borehole data at the rockglacier Pontresina-Schafberg (Grisons, Switzerland), where Hoelzle et al. (1998) depicted a connection between surface velocities and annual temperatures. Ikeda et al. (2003) compared information on rockglacier deformation with temperature data and DC resistivity soundings and observed an increased horizontal surface velocity with rising Mean Annual Surface Temperature (MAST) and low resistivities. They concluded a permafrost situation close to the melting point with high sensitivity to changes in ground temperatures. Recently, Lambiel & Delaloye (2004) reported on the horizontal acceleration (10-50 %) between 2000 and 2003 on rockglaciers in the western Swiss Alps. Regarding probable reasons, also they refer to the general temperature increase without giving details on reaction times. Finally, Arenson et al. (2002) described changes in horizontal deformation rates within several boreholes in Switzerland. They measured seasonal changes (with clearly higher deformation rates during the winter months) in shallow shear zones, while greater depths are more affected by long-term variations (cf., Kääb et al. 2003). Regarding probable controls, they described an ongoing warming at greater depth of Murtèl rockglacier, resulting in higher deformations rates. Thus, also they concluded degrading permafrost, represented by temperatures very close to the melting point and fast movements in shallow shear zones. The same signal was revealed by Kääb et al. (2002), who emphasised rockglaciers with thermal and spatial proximity to melting conditions as sensitive indicators for spatio-temporal changes of boundary conditions. Thus, a direct link between changing permafrost temperatures and changing deformation rates appears probable from different studies. But, in most observations one critical fact exists: "*no correlation could be seen between changes of one rock glacier and corresponding changes of a nearby rock glacier during the same period*" (Haeberli 1985: 95).

Therefore, in order to relate such local observations to overall climatic trends, investigations of creep variations are required on a more regional scale and long monitoring series are needed to

depict interannual variations and long-term trends (e.g., Barsch & Zick 1991). In order to find out driving forces for the prevailing behaviour, Barsch (1996) demands to discuss short- and long-term variations separately.

Temporal variation in vertical movement is strongly connected to the horizontal velocities and their variations due to a mass balance effect. Thus, increased horizontal velocities may result in areas with a thinning of the rockglacier body, whereas in other parts a thickening occurs. Vertical losses can also reflect the melting of ice.

2.3.5.4 Rockglacier rheology

Measurements of rockglacier kinematics mostly demonstrate changes in surface geometry and do not reveal direct information on internal deformation processes (Arenson et al. 2002). But, since the surface velocity (v^s) reflects the internal deformation of the permafrost body (v^d), the sliding on shear horizons (v^g) and the deformation at the rockglacier base (v^u) (figure 2.13), processes below the surface are to be considered, e.g. in statistical, empirical and process-oriented models (Kääb 1996).

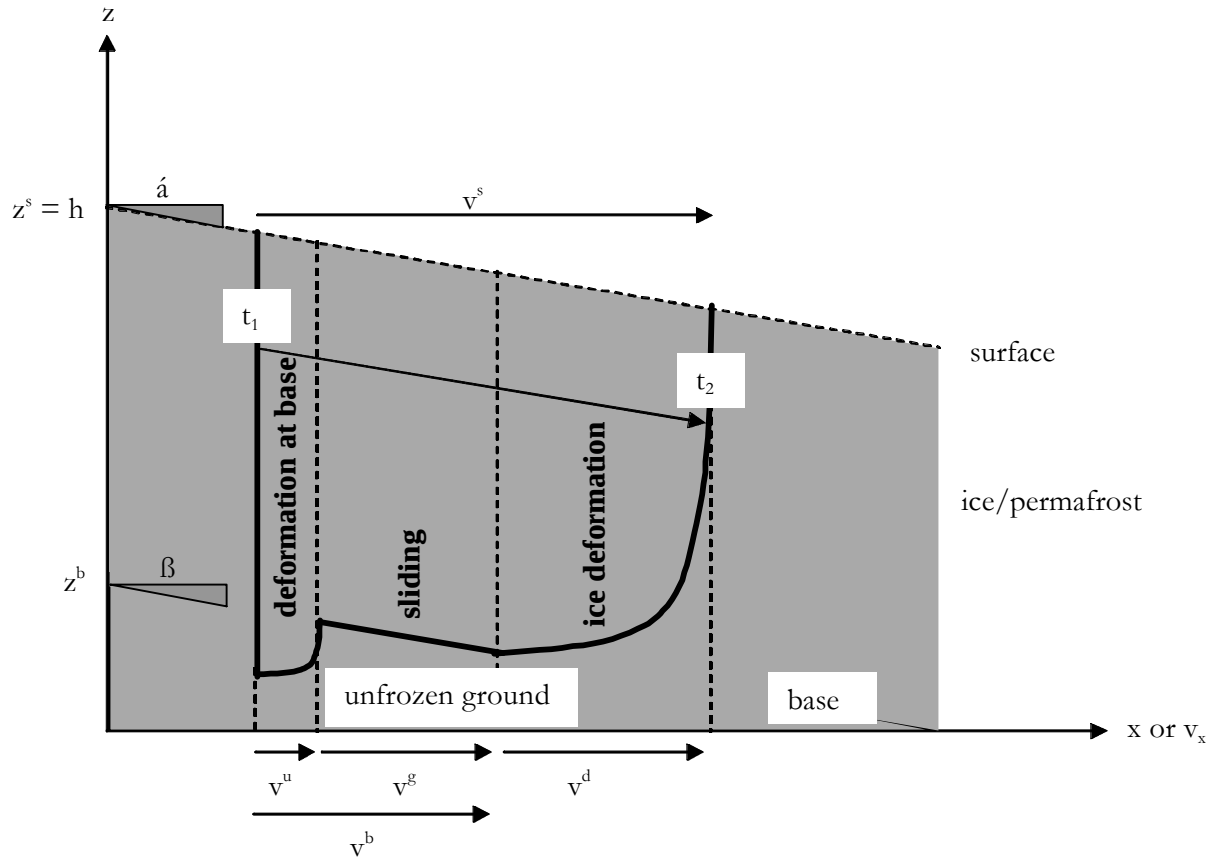

Figure 2.13: Components of rockglacier movement: internal deformation (v^d), sliding (v^g) and deformation at the base (v^u), which are reflected in the surface velocity (v^s) (from Kääb 1996: 65). Sliding and deformation at the base are subsumed into basal velocity (v^b).

In order to make conclusive interpretations of surface movements and their variations and thus deal with dynamic considerations, knowledge on the rheological behaviour of permafrost bodies is required.
In a simple conceptual model, Barsch (1996) summarised the parameters influencing rockglacier deformation (figure 2.14). From that, it becomes clear how many data are needed to calculate shear stress and strain for a rock/ice-mixture and model the ongoing processes.

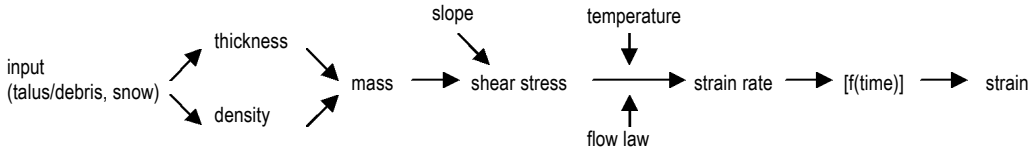

Figure 2.14: Conceptual model of the parameters affecting the deformation of ice-supersaturated mountain permafrost bodies (from Barsch 1996: 169).

Detailed investigations, reviews and discussions on rockglacier rheology are given in Wahrhaftig & Cox (1959), Haeberli (1985), Whalley & Martin (1992) and Barsch (1996). But, since the internal composition is mostly unknown and the thermal regime is poorly understood, no appropriate rheological model for rockglaciers exists up to now (Whalley & Azizi 1994). At first, flow laws for uniform materials like ice (Glen's flow law) and rocks (Coulomb equation) were suggested to study rockglacier creep (e.g., Whalley & Azizi 1994). In general it is assumed, that rockglacier movement follows the creep law for pure ice formulated by Glen (1952, cf. Wahrhaftig & Cox 1959; Haeberli 1985; Barsch 1996). His flow law describes the relation between shear strain rate $\dot{\varepsilon}_{xy}$ and shear stress τ_{xy} :

$$\dot{\varepsilon}_{xy} = A\tau_{xy}^{n},$$

where n is a constant but A depends on ice temperature, crystal orientation, impurity content and other factors (Paterson 1994: 85). Transferred to rockglaciers, which consist of a rock/ice - mixture, the deformation rate under the same stress is smaller than that of a pure ice body (e.g., Barsch 1992).
Based on Wahrhaftig & Cox (1959), Haeberli (1985: 118) calculated the rockglacier basal shear stress τ from:

$$\tau = f\rho_p \cdot g h_p \cdot \sin\alpha ,$$

where f is a shape factor, ρ_p is the average density, g is the acceleration due to gravity, h_p is the thickness of the permafrost body and α is the surface slope (cf., Whalley & Azizi 1994).
In summary, rockglaciers show long term steady state (secondary) creep behaviour under constant temperatures, stresses and strain rates (Haeberli 1985: 113). It is supposed, that the flow results from the plastic deformation of the ice inside the supersaturated permafrost body in

response to gravity and is controlled mainly by the internal structure (e.g., Barsch 1977, 1992). Sliding in shear horizons may play an additional role; this can be supposed since measurements in the Murtèl borehole showed that 75% of the movement takes place in a thin layer between 28 and 30 m depth (shear planes) where reduction in viscosity enabled the higher deformation (Wagner 1992). In creep models this component is neglected so far (Whalley & Azizi 1994; Barsch 1996).

Currently, investigations concentrate on laboratory or in situ tests of mechanical properties (shear strength and creep susceptibility of rockglacier material), and thus improve the models on temperature dependent soil behaviour (Davies et al. 2001; Arenson et al. 2003a, b). Davies et al. (2001) showed in several laboratory tests that temperature is an important parameter in the strength of ice/rock-mixtures. They proved, that a rise in temperature leads to reduction in shear capacity of ice-bonded discontinuities and thus may lead to slope failure. Arenson et al. (2003a, b) combined in situ pressuremeter tests with laboratory test and concluded, that due to the extremely heterogeneous content of ice, unfrozen water and air, as well as different grain sizes, unique frozen soil properties were hard to determine (Arenson et al. 2003b).

Regarding rockglacier dynamics, Kääb et al. (2002) discussed potential controls of deformation. By applying different values for the factor A in Glen's flow law, they described non-linear effects of ice temperature on the deformation rate factor of massive ice, which is also expected for ice-rock mixtures. They concluded that temperature has an influence on rockglacier deformation, but other factors like ice-content, etc. should not be excluded.

Additionally to rheological characteristics, considerations of mass balances support decisively the interpretation of multitemporal information on rockglacier movement. In order to calculate rockglacier mass balances, the model of the 'kinematic boundary condition at the surface' can be applied (Paterson 1994; Kääb 1996, 2004; Kääb & Funk 1999; Kääb et al. 1998). Thus, information on surface kinematics is used to get two- or three-dimensional information on the permafrost body, since in dynamic systems a change in surface geometry is always related to mass gains/losses or internal shifting of mass.

2-dimensional:

The two-dimensional case is expressed as:

$$\frac{\partial h}{\partial t} = b - \frac{\partial q}{\partial x} \qquad [1]$$

where $\frac{\partial h}{\partial t}$ is the change in surface elevation with time, b is the mass balance at the surface and $\frac{\partial q}{\partial x}$ is the divergence in horizontal flow q.

The equation is valid for any surface point and indicates that any change in surface elevation results from changes in mass balance (e.g., gains and losses of snow and debris) (figure 2.15 A) and/or flow balance (change in horizontal flow) (figure 2.15 B). One restriction of this model results from the assumption that the density of the material is constant.

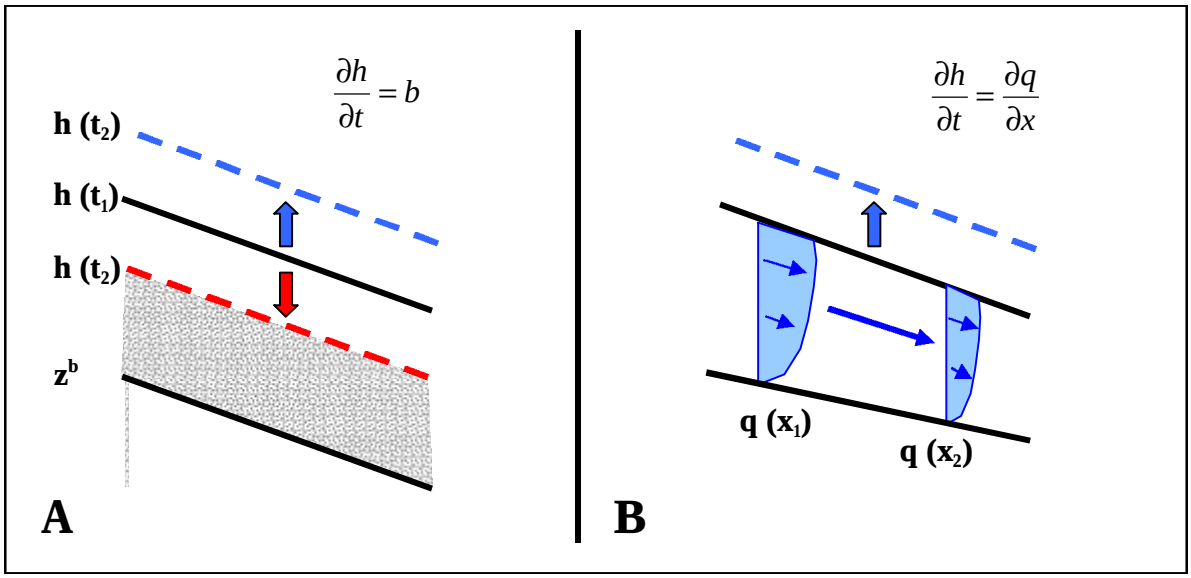

Figure 2.15: Change in surface elevation: A) resulting from a change in mass balance; divergence of flow = 0. B) resulting from a change in flow balance; mass balance = 0. (from: http://www.geo.unizh.ch/~kaeaeb/e&mhtml/kinbed.html).

The flow balance is described by the difference of in- and outcoming mass within a vertical column or as the change in flow into flow direction x. Thus, a reduction in flow leads to a rise (figure 2.15 B) while the increase in flow leads to a lowering of the surface. The divergence in flow may result from a change in cross-section or from a change in flow velocity in direction of the flow. The first case is depicted in figure 2.16, where a narrowed cross-section causes an increase of mass within a vertical column by constant flow velocity. The influence of a change in cross-section can be determined by the surface slope in flow direction $\frac{\partial h}{\partial x}$ and the local horizontal flow velocity v_x^s, as well as from the basal slope of the moving mass $\frac{\partial z^b}{\partial x}$ and the local horizontal velocity v_x^b (see [2]) (http://www.geo.unizh.ch/~kaeaeb/e&mhtml/kinbed.html).

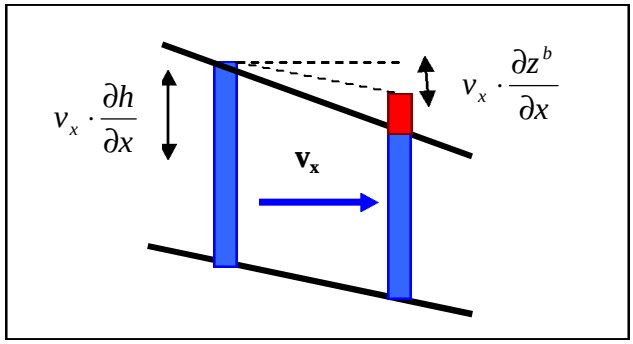

Figure 2.16: Influence of a narrowed cross-section on the divergence of the flow and a change in surface elevation (from http://www.geo.unizh.ch/~kaeaeb/e&mhtml/kinbed.html).

The second case is displayed in figure 2.17 where a decrease in velocity in flow direction causes a rise in surface elevation, due to compression of the mass. Extension of the mass would result from an increase in flow velocity. Assuming, that the mass is incompressible, an extension or a compression of the mass directly affects the geometry: $\frac{\partial q}{\partial x} = \frac{\partial q}{\partial z} = \frac{\partial h}{\partial t}$. In order to determine the total flow balance, the velocity change in flow direction $\frac{\partial v_x}{\partial x}$ for the whole thickness of the moving mass (from z^b to h) needs to be considered (see [2]).
By integrating both cases, the divergence in flow is described in the following equation:

$$\frac{\partial q}{\partial x} = v_x^s \frac{\partial h}{\partial x} - v_x^b \frac{\partial z^b}{\partial x} - \int_{z^b}^{h} \frac{\partial v_x}{\partial x} dz \qquad [2]$$

If the mass is incompressible the following is valid for the two-dimensional case: $\frac{\partial v_x}{\partial x} = \frac{\partial v_z}{\partial z}$.
The last two terms of equation [2] describe the vertical velocity of a particle in the moving mass at or near the surface (v_z^s):

$$v_z^s = v_x^b \frac{\partial z^b}{\partial x} + \int_{z^b}^{h} \frac{\partial v_x}{\partial x} dz \qquad [3]$$

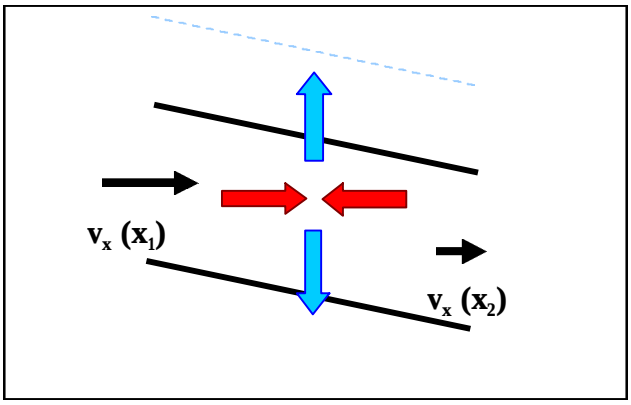

Figure 2.17: Influence of a change in velocity on the divergence of flow and a change in surface elevation (from http://www.geo.unizh.ch/~kaeaeb/e&mhtml/kinbed.html).

3-dimensional:
As compiled by Kääb et al. (1998), for the three-dimensional case the kinematic boundary condition at any surface point is:

$$b = \frac{\partial h}{\partial t} + v_x^s \frac{\partial h}{\partial x} + v_y^s \frac{\partial h}{\partial y} - v_z^s \qquad [4]$$

with mass balance at the surface *b*, surface altitude *h*, change in surface elevation with time $\frac{\partial h}{\partial t}$, the horizontal surface velocity components v_x and v_y of the three-dimensional velocity vector *v* =

$(v_x, v_y, v_z)^T$, the surface slope components $\frac{\partial h}{\partial x}$ and $\frac{\partial h}{\partial y}$ and the vertical velocity at the surface v_z^s (cf., Paterson 1994). Concerning equation [4] Kääb et al. (1998) stated, that all terms on the right hand side, except the vertical velocity at the surface v_z^s, can be determined by photogrammetrical investigations.

The vertical velocity at the surface is:

$$v_z^s = \int_{z^b}^{h} \frac{\partial v_z}{\partial z} dz + v_z^b \qquad [5]$$

with the vertical velocity at the basal layer v_z^b where $v = 0$ for $z < z_b$. Thus, with the vertical strain rate $e_{zz} = \frac{\partial v_z}{\partial z}$, equation [5] can be written as:

$$v_z^s = v_x^b \frac{\partial z^b}{\partial x} + v_y^b \frac{\partial z^b}{\partial y} + \int_{z^b}^{h} e_{zz} dz \qquad [6]$$

Assuming incompressibility of permafrost:

$$e_{xx} + e_{yy} + e_{zz} = 0 \qquad [7]$$

the vertical velocity at surface v_z^s can be written as:

$$v_z^s = v_x^b \frac{\partial z^b}{\partial x} + v_y^b \frac{\partial z^b}{\partial y} - \int_{z^b}^{h} e_{xx} dz - \int_{z^b}^{h} e_{yy} dz \qquad [8]$$

That means that horizontal compression is compensated by vertical extension and vice versa (e.g., Haeberli 1985). Vertical extension indicates a velocity reduction in the surface flow field, while vertical compression reflects horizontal acceleration (cf., chapter 2.3.5.2).

In equation [6] the basal velocities v_x^b and v_y^b, and e_{zz} are estimated or determined by the measurement of ice deformation or basal sliding (Kääb 1996). For the equations [7] and [8] the incompressibility may not be fulfilled when dealing with structured permafrost instead of massive ice or supersaturated permafrost (Kääb et al. 1998).

The mass balance described in equation [4] represents the sum of all mass changes which are reflected in a corresponding change in surface elevation. Thus, internal mass variations without influence on surface elevation or flow regime are not considered by the kinematic boundary condition (Kääb et al. 1998). In general, interpretations on rockglacier mass balances need to be conducted carefully since changes in surface elevation may result from climatic influences (mass/gain of ice and debris) or internal dynamics. Kääb et al. (1998) concluded, that short-term variations of surface elevation are mostly caused by mass balance changes (climatic impact), while spatial variations of $\frac{\partial h}{\partial t}$ are noticeably influenced by spatial variations of the flow regime. Haeberli (1985: 86) stated, that the only possible source of major volume changes result from melting or formation of ice.

For the rockglacier Murtèl (Grisons, Swiss Alps), Kääb et al. (1998) calculated the mass balance b at a well investigated borehole site. Thus, the limited use of the model due to lacking data on the vertical velocity of other rockglaciers becomes apparent. From their investigations on Murtèl they

summarised in a complex figure (2.18) the concluding links between horizontal velocity and small scale topography, which is characterised by furrows and ridges resulting from horizontal compression. Thus, a close correlation between $\frac{\partial h}{\partial t}$ and $v_x^s \frac{\partial h}{\partial x}$ is indicated.

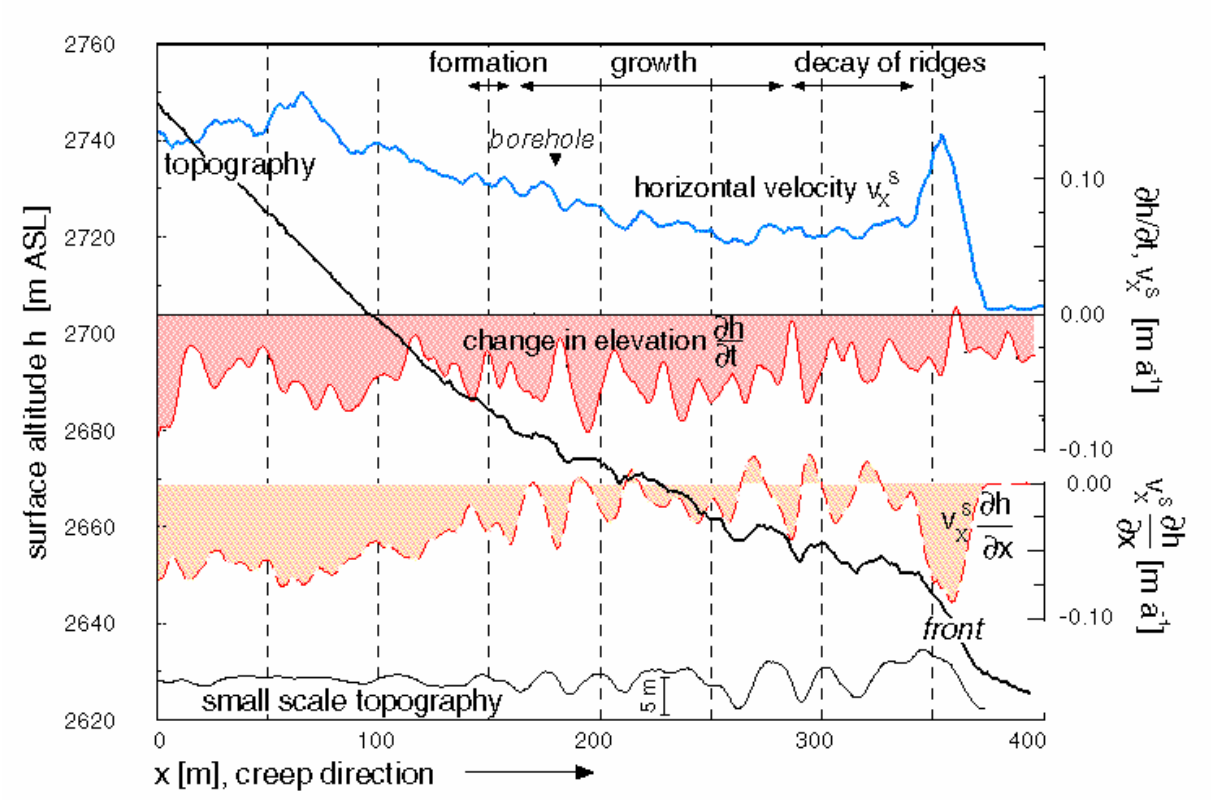

Figure 2.18: Longitudinal profile of rockglacier surface, surface velocities and derived kinematic quantities 1987-1996. The photogrammetric profile measurements have a spatial resolution of 1 m. Surface topography depicted with two times exaggeration. Small scale topography is defined as difference between surface topography at each point and a running average over 200 m (four times exaggeration). (from Kääb et al. 1998: 534).

2.3.5.5 Methods to monitor rockglacier kinematics

In the 80-year history of rockglacier monitoring, first simple methods like remeasurement of painted stone-lines were used to detect rockglacier movements (e.g., Chaix 1923; Pillewizer 1957). Then, geodetic techniques were applied (e.g., Wahrhaftig & Cox 1959; Vietoris 1972; Barsch & Zick 1991; Francou & Reynaud 1992; Lambiel & Delaloye 2004), while later more and more different air- and space-borne remote sensing methods were exploited (e.g., Messerli & Zurbuchen 1968; Barsch & Hell 1975; Kääb & Vollmer 2000; Kaufmann & Ladstädter 2003; Kenyi & Kaufmann 2003a; Strozzi et al. 2004). Corresponding applications of the mentioned techniques in various regions, together with the quantified displacements, are compiled in a detailed list (appendix 1).

Air- and space-borne methods are in particular useful to monitor remote areas that are difficult to access for in situ measurements, and to cover large areas within regional-scale studies. Therefore,

and with increasing spatial and temporal resolution and accuracy, remote sensing techniques offer highly suitable tools for rockglacier studies (Kääb et al. 2003; Kääb 2004). Up to now, these methods were rarely applied for deriving rockglacier movement on a regional scale. Frauenfelder et al. (2004) derived surface velocity fields from repeated aerial photographs for a number of rockglaciers in the Swiss Alps. Strozzi et al. (2004) compared an in situ inventory with airborne and spaceborne remote sensing data to analyse mountain permafrost creep in the Simplon/Saas valley region.

In the study presented here, digital photogrammetry is applied to quantify rockglacier creep for an entire valley (i.e., following a regional approach). Therefore, small-scale aerial photographs are combined for the first time with digital pushbroom imagery from the High Resolution Stereo Camera – Airborne (HRSC-A) (Roer et al. 2005). Such high-resolution digital camera data was adopted in high mountains (Hauber et al. 2000), but not in the context of monitoring rockglacier creep. The analogue processing of conventional photographs is still time consuming unlike the application of digital photogrammetric cameras, which are believed to form the future data acquisition technique in photogrammetry (Hauber et al. 2000; Baltsavias et al. 2001).

On the local scale, the results derived from digital photogrammetry are compared to high-resolution data from terrestrial geodetic survey covering a three - year period (2001 – 2004).

In addition, a new approach was designed by using dendrogeomorphological methods. In permafrost science, and especially in rockglacier studies, dendrogeomorphology was carried out rarely. This results mainly from the position of rockglaciers above the timberline. Since rockglaciers consist of coarse material, the vegetation cover is generally sparse (e.g., Giardino et al. 1984; Roer 2001). Zoltai (1975) was the first to report on reaction wood in different *Picea*-species related to gelifluction in the Subarctic. He took slices from 157 trees and was able to illustrate different phases of activity between 1847 and 1943. Additionally, he tried to correlate the activity phases with climatic parameters. Giardino et al. (1984) studied reaction wood, tree-ring variations and tilting at 283 trees on a rockglacier complex and conducted different periods of movement since the 15th century. Jakob (1995) monitored dwarf-shrubs in the Canadian Arctic, which were run over by gelifluction lobes. He was able to quantify movement rates between 1.9 and 3.5 cm/a. Bachrach et al. (2004) used dendrogeomorphological methods, to document the long-term development of a rockglacier in Alberta, Canada. In this case, trees (*Picea engelmannii* and *Abies lasiocarpa*) were covered by an advancing rockglacier. By the comparison of death-dates of different trees, a front advance of 1.6 cm/a was estimated. Recent studies on cell structures in tree rings ascertained the great potential of wood-anatomical investigations. Regarding geomorphic processes, the analysis of anatomical changes in exposed roots enabled the reconstruction of erosion rates (Gärtner et al. 2001; Gärtner 2003a, b). Annual ring width variations and related growth variations in shrubs due to environmental stress are rarely studied (e.g., Gers et al. 2001). Investigations on wood anatomy of trees or shrubs influenced by rockglaciers do not exist up to now.

Basic principles and measurement design of the applied methods are detailed in chapter 3.

3 METHODS

3.1 Geomorphic mapping

Since geomorphic mapping is the fundamental method in geomorphology, it serves also in this study as an important basis for all following investigations and interpretations. Therefore, mapping was conducted directly in the field and by stereoscopic interpretation of aerial images at the photogrammetric workstation. The latter allowed an easy and area-wide examination and interpretation of landforms in an often inaccessible terrain. Additionally, geomorphometric terrain parameters as well as temporal changes were quantified in a commercial GIS software (ArcGIS) using a high-resolution DTM.

The mapping was concentrated on the geomorphic setting of rockglaciers within their periglacial and glacial environment. Thus, the study focuses on two process regimes, while other landforms and processes are neglected. The geomorphogenesis was indirectly derived from landforms and their distribution in the landscape based on an actualistic approach. That means that a recent or sub-recent consideration, respectively, leads to a genetic interpretation by a 'sorting' of landforms in space and a description of processes-activity in time.

The emphasis of the interpretation was laid on rockglacier distribution and characteristics. They were identified by morphological, sedimentological and biological (vegetation cover) characteristics and with the before mentioned techniques, several parameters (situation, size, slope, surface relief) were compiled for each feature. Finally, the rockglacier activity (active, inactive, relict) was assessed by a combined analysis of geomorphometric and ecological characteristics. Since inactive rockglaciers are transition forms, their definition holds the highest uncertainty. The data are summarised in overview maps and rockglacier parameters are compiled in an inventory list (according to Hoelzle 1989).

Rockglaciers are important indicators for the former and present occurrence of permafrost (e.g., Haeberli 1985) and thus the detailed mapping of these landforms enables the determination of permafrost distribution (cf., Hoelzle 1989; Nyenhuis 2001; Nyenhuis et al. in press). Additionally, rockglaciers are important mass transport systems (e.g., Barsch 1977), connecting talus slopes and glaciers to other systems. These fluxes are only partially discussed in this study. Detailed descriptions of sediment cascades, combined with a comprehensive geomorphic map, are depicted for the study area by Otto & Dikau (2004).

3.2 Digital photogrammetry

3.2.1 Basic principles

The general objective of photogrammetry is based on the fact that for any object point represented in at least two photographs it is possible to calculate the three-dimensional terrain coordinates. With the development from analogue via analytical to digital photogrammetry,

several photogrammetric steps are meanwhile automated and thus, the technique is no more restricted to specialists only.

Concerning the geometric basics in photogrammetry, it is referred to the relevant core literature (e.g., Konecny 1984; Kraus 1996, 1997). The main parameters of aerial photogrammetry (flying height, focal length) and their importance for the image orientation are indicated in figure 3.1 and are detailed in chapter 3.2.3.

Since the quantification of changes in surface geometry is based on the comparison of multitemporal Digital Terrain Models (DTMs) and orthoimages, their generation from stereo aerial photographs is one of the major tasks in digital photogrammetry (e.g., Baltsavias 1996; Chandler 1999). The principle of photogrammetric DTM generation is depicted in figure 3.1.

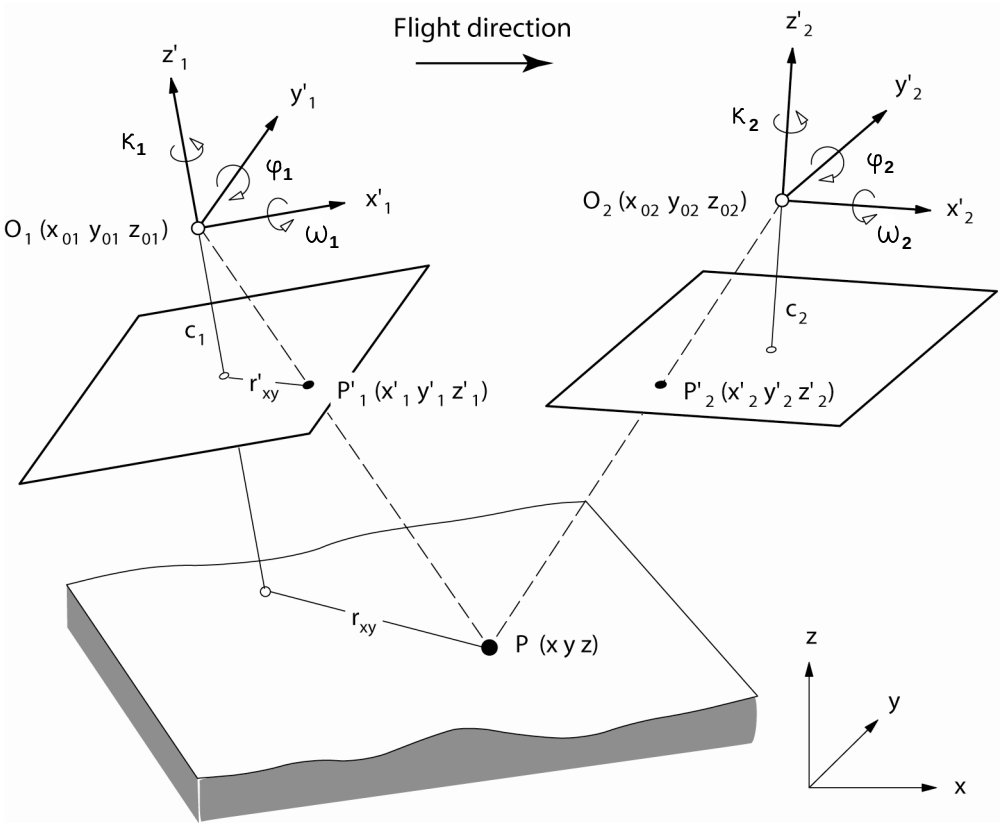

Figure 3.1: Principle of photogrammetric DTM generation from a monotemporal stereo model composed of two overlapping images taken from different positions (from Kääb 2004: 23). c = focal length; r_{xy} = the horizontal (radial) distance of a terrain point from the sensor nadir; r'_{xy} = radial distance between the image centre and the projection of a terrain point into the image. κ, φ and ω are the rotation angles, decisive for the exterior orientation of the images. The terrain point P is determined by the intersection of oriented rays, fixed by the known projection centres (O_1, O_2) and the projections (P'_1, P'_2).

Concerning the monitoring of creeping permafrost, different software packages based on block-matching techniques using multitemporal orthoimages were developed (Vollmer 1999; Kääb & Vollmer 2000; Kaufmann & Ladstädter 2000, 2003). The CIAS-software applied in this study (chapter 3.2.4) enables the calculation of 2D horizontal flow vectors from multitemporal orthoimagery while vertical changes are computed from DTM differences (Vollmer 1999; Kääb & Vollmer 2000). Against that, Kaufmann & Ladstädter (2000, 2003) measure 3D surface flow vectors using 'quasi-orthoimages' (calculated from coarse DTMs) as intermediate products. Both programs track the displacement of greyscale image features on the rockglacier surface within multi-temporal digital images. A comparison of these approaches is detailed in Kääb (2004).

3.2.2 Data

3.2.2.1 Aerial photography

The basic data applied here are small-scale black and white aerial photographs from the Swiss Federal Office of Topography (Swisstopo) with average scales ranging from 1:19,500 – 1:23,000. For the study site, analogue aerial stereo photographs are available for the years 1975, 1981, 1987, 1993. They were taken with a Wild/Leica – Camera type RC 5 / RC 8 (1975), RC 10 (1981, 1987) and RC 30 (1993). The photographs of the years 1975 and 1993 were found to be best suited for the displacement measurement. Only one rockglacier was additionally monitored in 1981 and 1987. Concerning the purpose of this study, the date of recording is a significant fact (table 3.2). The objects of interest are situated at around 2600 – 2800 m a.s.l. and to measure the displacement of single rocks on the rockglacier surface, these areas need to be free of snow.

3.2.2.2 HRSC-A data

To extend the monitoring period for another eight years, the Turtmann valley was covered by an airborne survey with a digital linear array sensor (pushbroom) in September 2001. This system, implemented in the High Resolution Stereo Camera – Airborne (HRSC-A), was developed at the German Aerospace Center (DLR) and was originally designed for the planet Mars exploration. For airborne earth operations the system was moderately changed. The camera records simultaneously with nine CCD (Charge Coupled Devices) line sensors mounted in parallel on the focal plane of the camera (Hoffmann et al. 2000). Four CCD arrays are used for multispectral imagery (colour channels in red, green, blue and infrared) and five CCD arrays for multi-stereo capabilities (providing stereo angles of ± 18.9°, ± 12.8° and high resolution at 0°) (Neukum 1999). The latter are decisive for the photogrammetric processing and the DTM derivation. A software system was developed by the DLR in cooperation with the Technical University of Berlin for the radiometric and geometric correction of the raw data as well as the automatic processing of the DTMs and the orthophotos. In this context, calibration data for camera- and image orientation are needed. Therefore, orientation and position were measured continuously during the flight by means of differential GPS and a strap-down inertial navigation system (INS) (Neukum 1999). For this purpose, a GPS reference station has to be placed in the area of interest, forming the only non-remote step within this procedure.

The photogrammetric accuracy of the scan data amounts to +/-15-20 cm in lateral and vertical direction, with regard to the exterior orientation (Hoffmann 2000). The ground resolution lies within decimetres (10 – 40 cm), depending on the camera height above ground. Details on the general survey realisation and the processing of the photogrammetric data are described in Hoffmann (2000) and Gwinner et al. (1999). Since the camera fulfils the radiometric and geometric requirements of an operational photogrammetric camera system, i.e. precise geometric calibration, high resolution (10 cm/pixel resolution on ground from an altitude of 2500 m) (Neukum 1999), the data are useful for any photogrammetric or remote sensing application.
By order of the Research Training Group (GRK 437), the flight campaign was performed in September 2001. The automated digital photogrammetric processing system delivered a DTM with a horizontal ground resolution of 1 m for the Turtmann valley. Multispectral orthoimages with a resolution of 0.5 m had been derived by orthoprojection using the DTM. In table 3.1 an overview is given on the system characteristics, compared to aerial photography. The main difference consists in the principle of data recording and the degree of automatisation. Obviously, using the HRSC-data there is no possibility for the scientists to control single steps within the automated processing (figure 3.2).

Table 3.1: Sensor parameters of aerial photography and HRSC-A data (modified, after Hoffmann 2000).

	Aerial photographs	**HRSC-A**
Spectral properties	black/white	multispectral
System	passive	passive
Focal length	f ~ 150 mm	f = 175 mm
Aperture angle	75-100°	11,8°
Mode of recording	single photos	image strips (continuous recording)
Image size	23*23cm²	length of strip variable, width of strip depending on flight altitude
Image overlap	60 % along-track, 20-30 % cross-track	9*100% (9 CCD lines), cross-track strip overlap 30-50 %
Spatial resolution	12-32 cm (altitude of flight 2500m), (depending on scan resolution)	10 cm (altitude of flight 2500m)
Exterior orientation	reconstruction of the camera position for the old photographs using ground control and tie points	direct measurement of the camera position using GPS/INS systems
Accuracy x/y	± 5 cm (altitude of flight 2500m)	± 12-15 cm (altitude of flight 2500m)
Accuracy z	± 7,5 cm (altitude of flight 2500m)	± 15-20 cm (altitude of flight 2500m)
Basis for orthophoto generation	DTM	DTM

Table 3.2: Flight parameters and properties of aerial photography and HRSC-A data for the Turtmann valley.

	Aerial photographs	**HRSC-A**
Date of flight	11.8./20.8./1.9. 1993 20.8./6.10. 1975	28.9.2001
Altitude of flight	5500-6000m a.s.l.	6350m a.s.l.
Scale	1:19,500 – 1:23,000	1:22,000
Relative orientation	0.65 pixel RMS	-
Accuracy x/y	~ 4.3 m RMS	~ 0.25 m RMS
Accuracy z	~ 1.5 m RMS	~ 0.20 m RMS

3.2.3 DTM & orthophoto generation

For the photogrammetric analyses the analogue data were scanned with 800 dots per inch (dpi; approximately 30 μm) using a commercial scanner. The use of commercial scanners is considered to be crucial (Kaufmann & Ladstädter 2003), but the quality and resolution of the scan data is sufficient for this purpose, where the relative accuracy between the images is of highest priority (cf. Kääb & Vollmer 2000).

Image orientation, automatic DTM generation and digital orthoprojection were performed within the commercial software SOCET SET (version 4.4.0) by LH-Systems (San Diego, California, USA) at a digital photogrammetric workstation. Firstly, interior orientation was calculated from the fiducial marks given in the image and the camera calibration reports, which are available at the Swiss Federal Office of Topography (Swisstopo). With this information, the software was able to calculate the relation between the camera-internal coordinate system and the pixel coordinate system. Secondly, the relative orientation within the multi-temporal image block was computed from tie-points connecting all overlapping images irrespective of their acquisition data. By that procedure a high relative accuracy between the multi-temporal images is ensured. For measuring changes in geometry relative accuracy is more important than the absolute position of the images (Kääb 2002). In this context it is significant, that the tie-points are set in non-moving areas in order to improve the data for the investigation of changes in permafrost creep. Finally, the entire multi-temporal image block was as a whole transformed into ground coordinates (i.e. absolute orientation) using ground control points (GCPs) from field survey and topographic maps. After setting the ground control points, an automatic tool (residual error report) checked and evaluated the quality of the GCPs and the outer orientation, respectively, in order to detect blunders. Partly, more tie-points or ground control points were added to improve the connection of the images.

Subsequently, the digital terrain models (DTMs) were automatically generated from mono-temporal stereo-models. To eliminate errors, the control by the operator was an important step for deriving high-quality DTMs (Kääb & Vollmer 2000). Finally, the orthophotos were calculated with the resampling-method nearest neighbour (Vollmer 1999). They were saved in GeoTIFF-

format with an additional TFW-file containing the georeferenciation (coordinate of the upper left pixel as well as the pixel resolution). From the 1975 and 1993 digital imagery DTMs with 10 m spacing and orthophotos with 0.5 m ground resolution were generated.

An accuracy assessment was not explicitly performed in this study, since Kääb and Vollmer (2000) made several tests and compared operator-measured and automatically-extracted DTMs. Under favourable conditions, the comparison of the data delivered a standard deviation of approximately ± 0.6m and maximum differences in the range of approximately ± 1.5 m (Kääb & Vollmer 2000). With the subsequent generation of the orthophotos, errors in elevation of the DTMs are transformed into horizontal deviations in pixel location (cf., Kraus 1997; Kääb 1996). Generally, systematic errors have to be expected at the edge of the aerial photographs and image blocks, respectively. Additionally, in areas with steep terrain or low contrast (e.g., due to snow cover), the accuracy is reduced. Therefore, measuring is best suited in the centre of the images and in areas with good contrast. The photogrammetric accuracy for this study is estimated to be roughly three times higher than the values given by Kääb and Vollmer (2000), since they worked with 1:6'000 scale images, whereas about 1:20'000 scale images were used in the study presented here. Thus, the general accuracy of the DTMs derived from small-scale aerial stereo-photography is estimated to lie within the range of two pixels RMS (Root Mean Square Error) (i.e. here: +/-1 m).

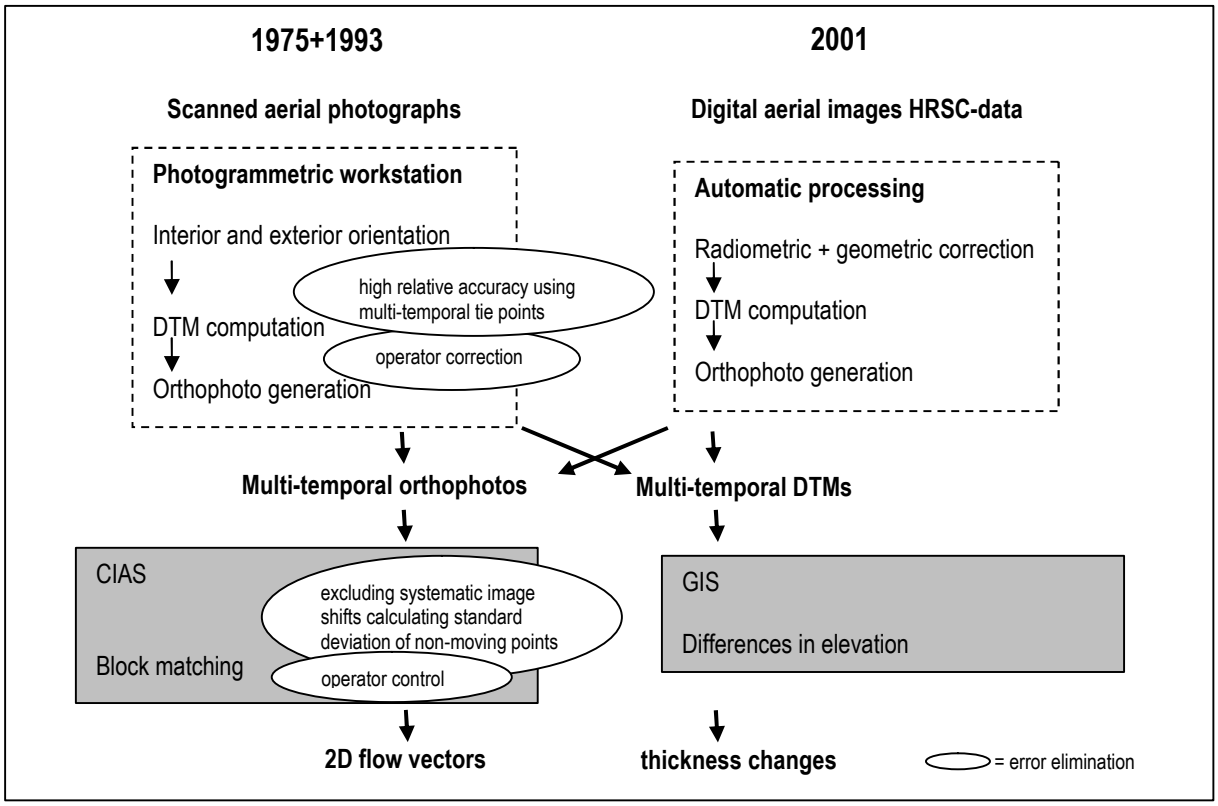

Figure 3.2: Processing schema for digital measurement of rockglacier flow-fields (from Roer et al. 2005). Comparison of different input data, processing steps and resulting output data using analogue aerial photographs and digital aerial images. The ellipses mark steps, where the operator can influence the processing to increase the quality of the output data.

Different input and output data using analogue aerial photographs and digital aerial images are summarised in figure 3.2 together with controlling steps, where the operator can influence the processing in order to increase the quality of the output data. The recording and the processing of the frame imagery and the pushbroom data showed major differences (table 3.1, figure 3.2), but the output data (DTMs and orthophotos) had similar characteristics. For details on the procedures used see Kääb & Vollmer 2000, and Kääb 2002.

3.2.4 Measurement of horizontal velocities

For the analysis of horizontal displacements on rockglaciers, the software CIAS (Correlation Image Analysis) has been used, which was developed at the Department of Geography, University of Zürich by M. Vollmer (1999). It is written in IDL (Interactive Data Language, Research Systems Inc, USA). In order to derive horizontal surface displacements, this software compares multi-temporal digital orthophotos by the identification of corresponding image-blocks.

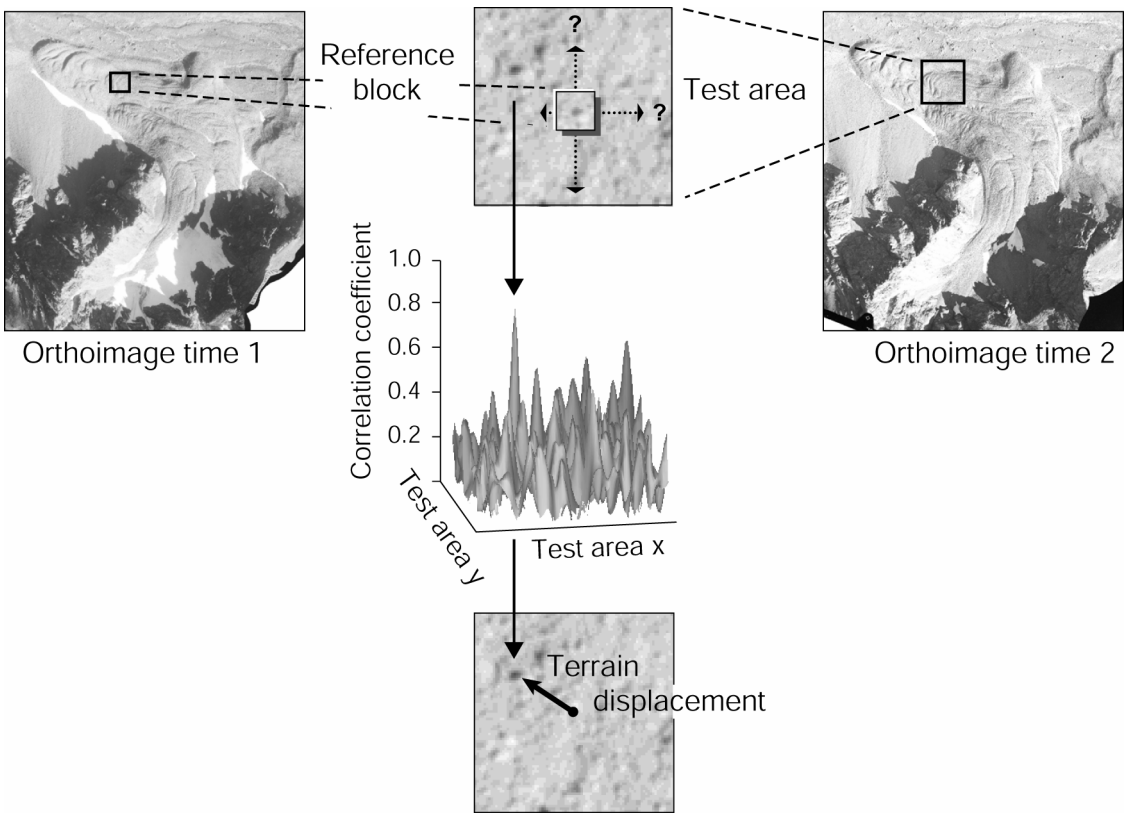

Figure 3.3: Schema of measuring surface displacements from repeated digital orthoimages by block-correlation techniques (from Kääb & Vollmer 2000: 319). A reference block in the orthoimage at time 1 is searched for in a test area in the orthoimage at time 2. The horizontal shift between the reference-block location and corresponding test block gives the surface displacement.

First, the size of the reference and the test block as well as the size of the test area has to be adjusted. The formers depend on surface characteristics, while the latter is estimated by the expected maximum displacement, so that the test block which corresponds with the reference block is included within the test area (Kääb & Vollmer 2000). In this study, the reference block mostly had a size of 16 × 16 pixel and the test area a size of 100 × 100 pixel. Second, some well-distributed points are measured in both images in immobile areas around the rockglaciers to assess systematic errors. With these data, systematic shifts, rotations and scale differences between the multi-temporal images are corrected using a Helmert similarity transform. Finally, the measurement starts with the selection of a sharply contrasting reference block in the orthoimage of time 1 (figure 3.3). The ground coordinates of its central pixel are given by the orthophoto georeference (Kääb & Vollmer 2000). Within the test area determined before, the corresponding test block is then searched in the orthoimage of time 2. The identification of the corresponding image blocks is performed by a double cross-correlation function based on grey values (Kääb & Vollmer 2000):

$$\Phi(i,k) = \frac{\sum_j \sum_l s\left((i+j,k+l) - \left(\frac{T_{test}}{N_{test}}\right)\right) \times m\left((j,l) - \left(\frac{T_{ref}}{N_{ref}}\right)\right)}{\sqrt{\sum_j \sum_l s^2\left((i+j,k+l) - \left(\frac{T_{test}}{N_{test}}\right)\right) \times \sum_j \sum_l m^2\left((j,l) - \left(\frac{T_{ref}}{N_{ref}}\right)\right)}}$$

The equation depicts the coordinates of the test block (i,k) and of the reference block (j,l), respectively. s describes the spatial grey value function of the test block, while s(i,k) is the corresponding grey value at location (i,k). m is the appropriate spatial grey value function of the reference block and m(j,l) the corresponding grey value at location (j,l). T indicates the sum of grey values of the test or reference block, while N denotes the number of pixels of the test or reference block ($N_{ref} = N_{test}$) (Kääb & Vollmer 2000). The value of the double cross-correlation function F (i,k) lies between -1 and +1. If the value is +1, the reference and the test block show total equivalence (Vollmer 1999). The T / N terms in the equation normalise the grey values of the test and reference blocks and ensure that differences in overall grey value do not affect the correlation result (Kääb & Vollmer 2000).

If the measurement is successful, the differences in central pixel coordinates directly reveal the horizontal displacement between time 1 and time 2, indicated by a displacement vector (figure 3.3). The results are stored in a *.dat-file. Then, within a special program (cia2arc) the *.dat-file is transformed into a *.txt-file in order to import the data into a GIS. In this context the difference in time, the correlation coefficient (min), the displacement (min and max) and the azimuth (min and max) is called up. The program outputs the coordinates of the reference block (x,y), the changes in x and y, the velocity, the direction and the correlation coefficient.

From high precision aerial photographs, the measurement of 2D flow vectors can be done automatically, generating a dense scatter-plot. In this study the program operated semi-

automatically. The user directly selects the terrain point of interest and controls the measurement. An experienced user is able to identify measurements, which are obviously mismatches, and is able to delete them directly. That leads to an improvement of the resulting vector field. Nevertheless a large amount of blocks (sometimes up to 1000, depending on rockglacier size) was measured to get a statistical quantity and to display complete flow fields on the rockglacier.

Regarding the accuracy assessment, Kääb and Vollmer (2000) compared the digitally-derived displacements (CIAS) with the velocity field created by an analytical plotter. The average difference in speed was 0.02 m a^{-1} ± 0.03 m a^{-1}. Since the average speed of the investigated rockglacier amounted to 0.2 m a^{-1}, the results represent an error of 10%. Thus, the results depict a similar accuracy as the operator-derived data (estimated error c. 10-15%) (Kääb & Vollmer 2000). Also here, one has to be aware that the tests were made in 1:6'000 scale images whereas this study works with 1:20'000 scale images. Kääb (2002) gives a rule of thumb, that an accuracy (one-sigma level) for photogrammetrically-derived horizontal velocities and thickness changes of about one image pixel size can be expected for favourable conditions in mountain terrain, i.e. in this study 0.5 m.

The application of the before estimated accuracy of two pixels (RMS) for the DTMs and the orthoimages used in this study results in an accuracy of the horizontal velocities of 5.5 cm/a (for 1975-1993) and 12.5 cm/a (for 1993-2001).

For the displacement measurement, snow patches or shadows in the images inhibited the measurement of terrain displacements, as it is visible in figure 3.4. Especially in the 2001 orthoimage, where fresh snow had fallen before the data acquisition, some rockglaciers are at least partially covered by snow. Thus, at some part of the rockglaciers, no results or mismatches were produced by the program, due to poor results of the corresponding grey-value correlation. The same problem is given, when major changes on the rockglacier surface – probably due to a shifting process regime – lead to a loss of coherence. This phenomenon becomes apparent on rockglacier Grueo1 (figure 3.4), where the lower part of the rockglacier is much faster than the upper part, resulting in transverse cracks of several meters depth. Thus, the vectors show a chaotic feature, since the blocks were shifted into the cracks and were superimposed by other blocks. Additionally, snow patches and shadows limit the measurement of displacement vectors in the root zone. Against that a coherent field of velocities around 2 m per year is depicted in the middle part of the rockglacier.

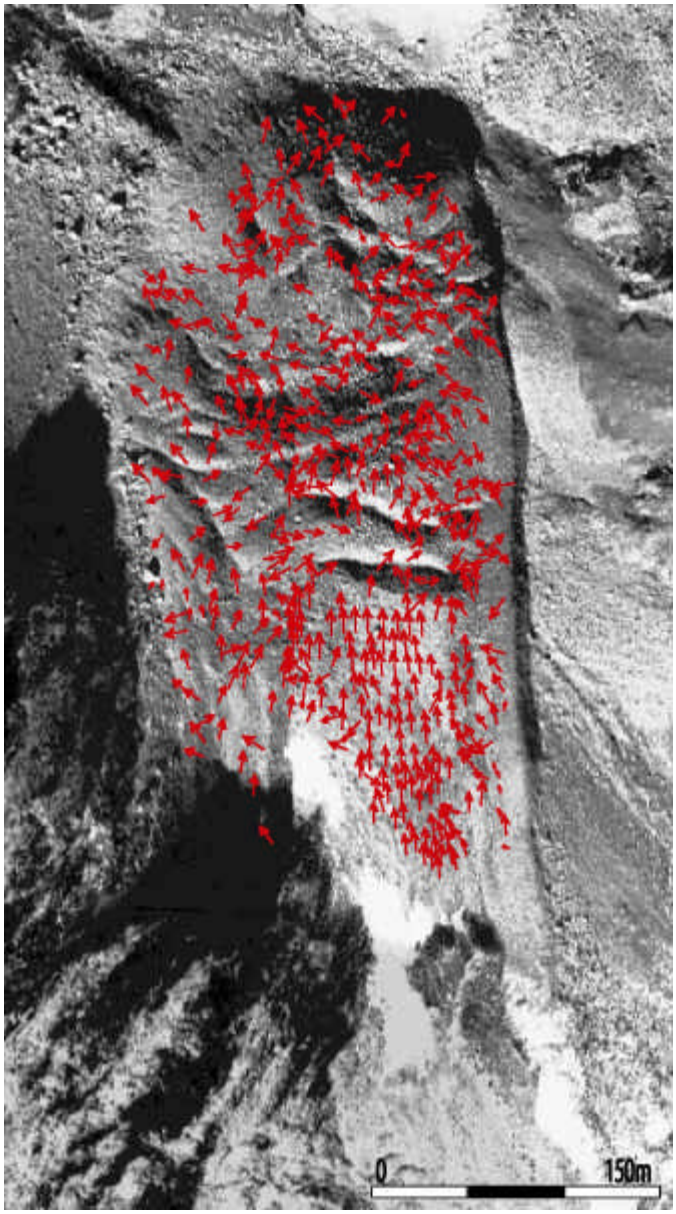

Figure 3.4: Annual horizontal displacements (raw data) on rockglacier Grueo1 between 1993 and 2001 (underlying orthoimage of 2001). Due to major changes on the surface in the lower part of the rockglacier, there is a strong loss of coherence resulting in a chaotic vector field, while snow patches and shadows inhibited the measurement of displacement vectors in the root zone.

3.2.5 Computation of thickness changes

For the quantification of vertical changes in rockglacier geometry, the DTMs were compared using a commercial GIS software (ArcGIS). Cumulative and annual changes in surface elevation are derived by subtraction of the multi-temporal DTMs. Also here, Kääb and Vollmer (2000) made an accuracy assessment by the comparison of operator-measured thickness changes and the automatically-derived ones. The difference in elevation changes amounted to 0.06 m a^{-1} on

average, with a standard deviation of ± 0.13 m a^{-1} and maximum errors of 1 m a^{-1} and more at rockwalls (Kääb & Vollmer 2000).
The before mentioned accuracy of the applied DTMs results in an accuracy of the vertical changes similar to that stated for the horizontal displacements. Thus annual values of 5.5 cm/a (for 1975-1993) and 12.5 cm/a (for 1993-2001) depict the range of uncertainty. In areas with steep walls or snowcover, the errors in the DTMs are often depicted by extraordinary vertical changes.

One objective of the study is to evaluate, to what extent small-scale aerial photographs and digitally acquired airborne data can be used for monitoring and quantification of rockglacier creep. The recording and the processing of the frame imagery and the pushbroom data show differences (table 3.1), but the output data (DTMs and orthoimages) have similar characteristics.
An overview of the main processing steps in digital photogrammetry as well as the further applications (computation of horizontal velocities and thickness changes) is compiled in figure 3.5.

Following page:
Figure 3.5: Main processing steps for the generation of DTMs and orthophotos (A), horizontal velocities (B) and the computation of thickness changes (C) (modified, after Vollmer 1999).

A) DTM and orthophoto generation

aerial photography

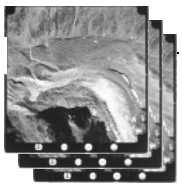

scanner

interior orientation

+ camera calibration files +

fiducial marks

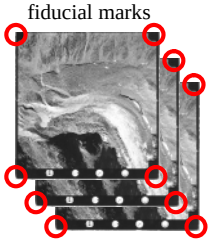

relative orientation

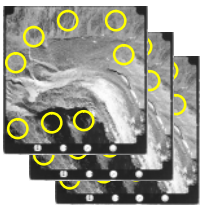

multitemporal image block

absolute orientation

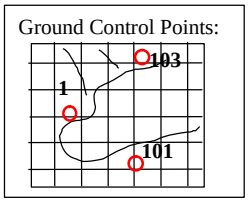

+ multitemporal image block

generation of Digital Terrain Models (DTMs)

computation of orthophotos

B) Horizontal velocities

digital orthophotos: same section, same resolution

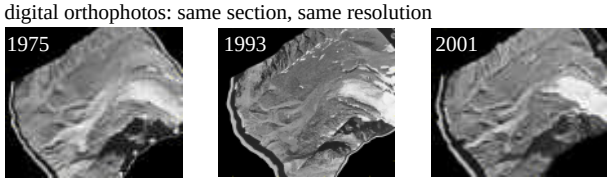

software CIAS → 2 digital orthophotos →

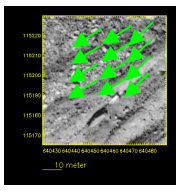

results.txt →

- maps
- tables
- diagrams

C) Thickness change

Geographical Information System (GIS) →

multitemporal Digital Terrain Models (DTMs)

→

- maps
- tables
- diagrams

3.3 Terrestrial geodetic survey

3.3.1 Total-station

With a total-station (tachymeter), which allows high accuracy, selected blocks at the rockglacier surface were repeatedly surveyed. Today's electronic total-stations are characterised by an opto-electronic distance meter (EDM) and electronic angle scanning. Horizontal distances, height differences and coordinates are calculated automatically and all measurements and additional information are recorded (cf., Kahmen 1997). Some instruments are additionally equipped with an automatic target-recognition system (ATR), completely integrated into the telescope. With this function it is sufficient to point the telescope approximately at the reflector; a touch on the corresponding button then automatically triggers the fine pointing and the angle- and distance measurements, and records all of the values (Zeiske 2000). Thus, a fast and easy targeting is combined with a constant measuring accuracy, which is independent of the operator. For the Leica tachymeter (TCA 1800L, Leica Geosystems AG, Heerbrugg, Switzerland) used in this study (figure 3.7), the technical details are summarised in table 3.3. Regarding the physical and mathematical basics of geodetic survey, it is referred to the core literature of geodesy (e.g., Kahmen 1997; Torge 2001).

Table 3.3: Technical details of the Leica tachymeter TCA 1800L (cf., Kahmen 1997).

Range*	1 km
Standard deviation position	2 mm
Standard deviation of measurement in both telescope faces	0.3 mgon
telescope	30x
Shortest range	1.7 m
Tracking	0.3 s
Weight	6.4 kg
Characteristics	dual-axes compensator, ATR (Automatic Target-Recognition)

* circular prism, average atmospheric conditions

One important aspect is the maintenance of the instrument, since this is decisive for the measuring accuracy. Thus, every two years the total-station used in this study was sent to the producer (Leica Geosystems) in order to inspect the mechanics, electronics and optics. Additionally, the instrument errors are checked before every measurement, since the equipment is sensitive against shaking during the transport and is influenced by temperature variations. With the programmable check the following errors are identified and automatically stored.

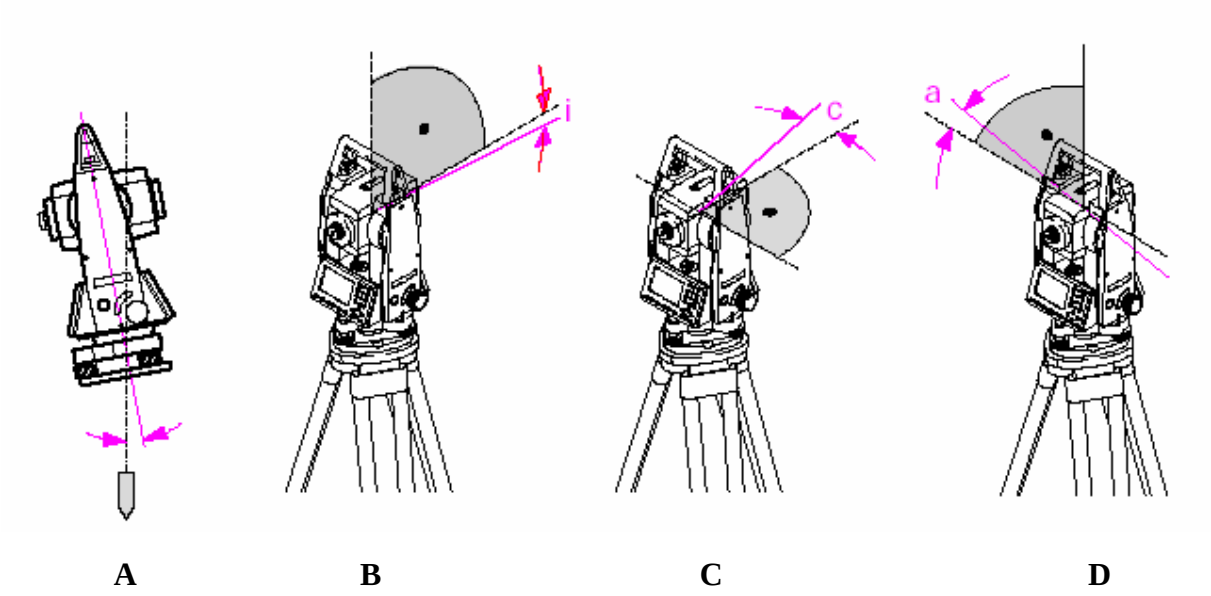

Figure 3.6: Instrument errors of a total-station. A = vertical axis tilt; B = height-index error (i) (V index); C = line-of-sight error (c) (Hz collimation); D = tilting-axis error (a) (from Zeiske 2000: 25).

The vertical axis tilt (figure 3.6 A) depicts the angle between plumb line and vertical axis. This error is not an instrument error; it arises because the instrument has not been adequately levelled up, and measuring in both faces cannot eliminate it. But, its influence on the measurement of the horizontal and vertical angles is automatically corrected by the dual-axes compensator (Zeiske 2000: 24).

The height-index error *i* is the angle between the zenith direction and the zero reading of the vertical circle (figure 3.6 B). By measuring in both faces and then averaging the data, the index error is eliminated; it can also be determined and stored.

The line-of-sight, or collimation error *c* is the deviation from the right angle between the line of sight and the tilting axis (figure 3.6 C), while the tilting-axis error *a* is the deviation from the right angle between the tilting axis and the vertical axis (figure 3.6 D). These errors can be determined and stored. Thus, they are taken into consideration automatically whenever an angle is measured. Additionally these errors are eliminated by taking measurements in both telescope faces.

The instrument errors can actually be indicated as follows:

- **Error of dual-axes compensator:**

last survey (08/2004): alongside: 0.0001°, diagonal -0.0003°

tolerance limit: 0.09°

- **Height-index error (i):**

last check by Leica Geosystems: -0.00009°

last survey (08/2004): 0.0014°

tolerance limit: 0.9°

- **Line-of-sight-error (c):**

last check by Leica Geosystems: -0.00153°
last survey: -0.0011°
tolerance limit: 0.09°

- **Tilting-axis error (a):**

last check by Leica Geosystems:< 0.0018/60 ° in tolerance
last survey (08/2004): 0.0003°
tolerance limit: 0.09°

By determination and storage of all these errors, accuracies of around 1 cm in height and 1 cm in position are calculated for a maximum distance of 600m. The additional measuring in both telescope faces and with the help of the dual-axes compensator, the measurement is practically free of systematic error. Further errors due to positioning of the instrument and the reflectors is limited by the measurement design (see chapter 3.3.2). Thus, in consideration of divergences resulting from the curvature of the earth and from refraction (both not quantified in this study), a maximum range of uncertainty of 2-3 cm was compiled for the velocity vectors. This range is comparable to accuracies given in other studies (cf., Berthling et al. 1998; Ødegard et al. 2003).

3.3.2 Measurement design

A geodetic network was established respectively in 2001 and 2002 for two rockglaciers (figure 3.9), consisting of reference points in non-moving terrain and observation points on the rockglacier surface. Since the terrestrial survey with a total-station was applied to get some high precision data on spatio-temporal changes in rockglacier geometry, high accuracy is one of the main objectives for the application of this method. Therefore, the reference points were selected under the following conditions (cf., Kaufmann & Heiland 1998):

- good visual connection to other reference points and to the observation points on the rockglacier,
- stability of the ground (not affected by gravitational and other processes),
- possibility of a resistant marking.

The observation points were distributed regularly on the rockglacier surface (in some places arranged in profiles) and were fixed on big blocks embedded in the matrix of the active layer, probably reaching the permafrost. Thus, superimposed processes acting on the rockglacier surface (e.g., gelifluction) are excluded and the displacement measured is truly reflecting the creep of the rockglacier mass. The position of the observation points was measured from reference points situated on a latepleistocene moraine and on bedrock. One orientation point to the official geodetic net was established by static measurement using differential GPS (Global Positioning System) in 2000 in the lowermost part of the moraine (cf. Rasemann 2004).

One main problem with terrestrial geodetic measurements is the exact positioning of the target (Haeberli 1985). Thus, in order to re-survey the points with high accuracy, steel dowels - where the prisms can directly be screwed into the threads - were drilled into the boulders and bedrock,

respectively (figure 3.8). Therefore, centring errors are nearly eliminated (cf. Berthling et al. 1998, 2001). Additionally, on some very big boulders two dowels were fixed to measure individual rotations.

Figure 3.7: Total-station on one of the reference points situated on a latepleistocene moraine with an overview of the research object (rockglacier in the background).

Figure 3.8: Steel dowels were drilled into the blocks for high-accuracy re-measurement. The thread, where the prism can directly be screwed into for the measurement, is protected by a plastic screw throughout the year.

For the first installation of the geodetic network, the total-station was set up on a known point in a local coordinate system. Then a second prominent point was selected for the purposes of orientation; after this has been targeted the horizontal circle was set to zero. With this so-called polar method, three-dimensional positions are determined by measuring angles and distances (cf., Kahmen 1997). For following readings in the existing network, the instrument is set up on a known point and the horizontal circle is lined up with a second known point. In order to check the positions of the reference points and therefore exclude their movement, all reference points were measured from two known positions during each survey campaign.

In case of rockglacier HuHH1, the distances between the position of the instrument and the uppermost observation points were too long to require high accuracy data. Thus, free-station survey was applied. With this program, the position of the instrument is calculated from measurements to at least two known points. The advantage of this method is the free selection of favourable positions for the instrument.

During the survey, every reference point was measured repeatedly in both telescope faces of the instrument. Also the observation points on the rockglaciers were measured in both faces in order to check the measurements and to guarantee high accuracy data. The measured distances and angles are then calculated as the average of the repeated readings.

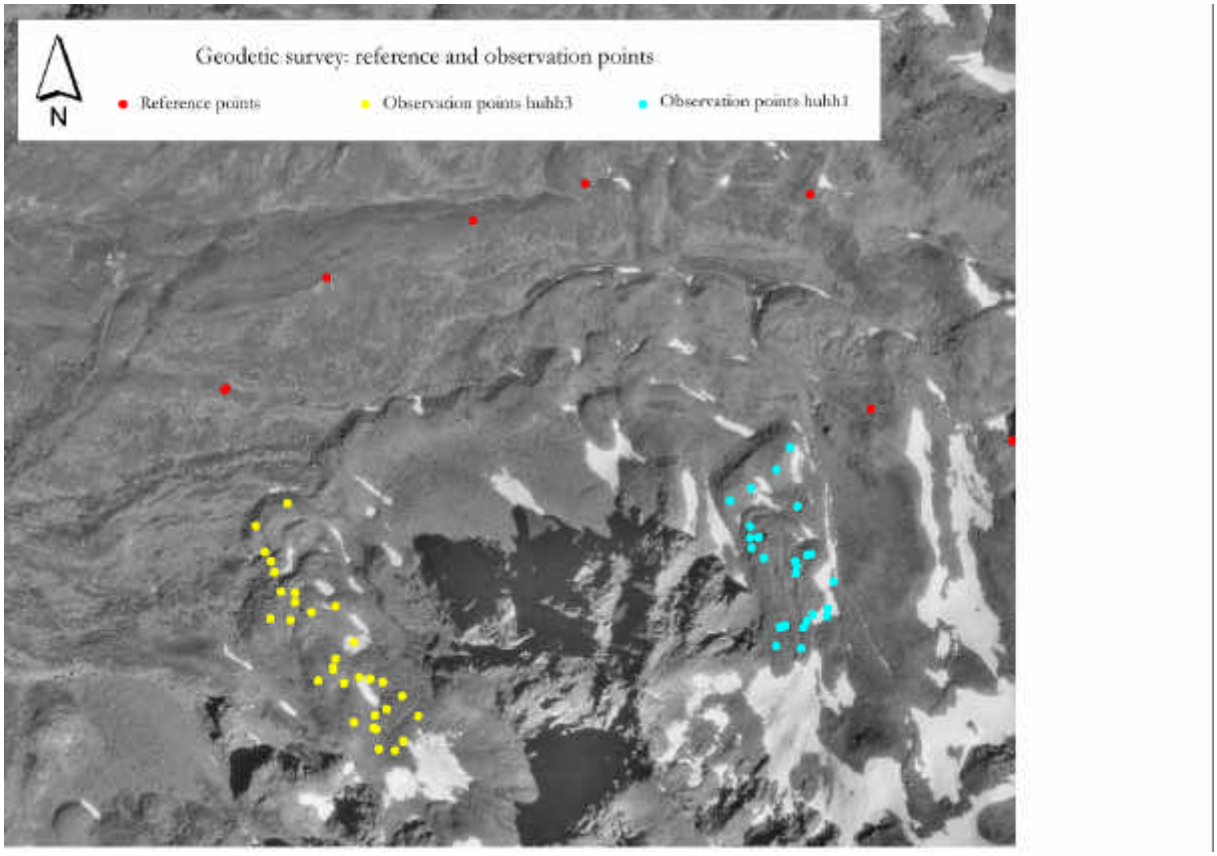

Figure 3.9: Terrestrial geodetic survey in the Hungerlitälli: reference and observation points. Underlying orthoimage of 20.08.1975 (flight-line 22, aerial photographs taken by Swisstopo).

The survey of 15 blocks on rockglacier huhh1 (figure 3.9) was started in September 2001. These blocks were remeasured in June 2002. In August 2002, the network was expanded on huhh1 by another 11 boulders in the upper part and was also installed on rockglacier huhh3 in September 2002. Then, all blocks on both rockglaciers were repeatedly measured in Juli 2003, August 2003 and Juli/August 2004. Due to snow cover and avalanches, measurement in winter, spring and early summer was generally not feasible. Through the two measurement-campaigns conducted at the beginning and end of summer in 2002, it was possible to determine summer displacement-rates in comparison to displacements during the rest of the year (autumn, winter and spring) (Roer 2003).

As stated before, the accuracy of the applied technique is in the range of 2-3 cm at most. Since the investigated rockglaciers are definitely active and show relatively high surface velocities, the recorded data are far beyond the level of uncertainty.

The terrestrial monitoring serves as validation for the results from digital photogrammetry, even if the two methods do not cover the same period. Geodetic survey was carried out in the years 2001 – 2004 and thus expands the length of the overall monitoring series. Regarding the vertical changes, it has to be considered that there are differences between the photogrammetric data and the data from geodetic survey. The DTM-comparison gives area-wide information on changes in elevation and thus allows the interpretation of mass- and flow-balance changes. Against that, the

position of selected blocks is measured by terrestrial geodetic survey. Hence, a decrease in elevation results automatically from the downslope movement of the blocks. This vertical component due to movement parallel to the surface amounts to 10 - 60 % of the horizontal displacement (Haeberli 1985).
Terrestrial survey is a very accurate method to measure geometries, but the application is laborious in terms of rough weather conditions and limited accessibility, in particular in high mountain environments. Nevertheless, since the network was established with numerous orientation-points and well-fixed observation-points it is appropriate for annual measurement over long time scales, at least over the next decade.

3.4 Dendrogeomorphology

3.4.1 Basic principles

Dendrochronology is one of the classical dating methods (e.g., Lang et al. 1999; Schweingruber 1996). The ability of dating (annual) rings in stems of trees is given in areas, where the growth of a tree is annually interrupted by the seasonality of the climate. The boundary between tree rings is depicted in a contrast of flattened cells with thick cell walls in the latewood (build at the end of the vegetation period) and bigger, thin walled cells in the earlywood (build in the beginning of the following vegetation period) (Schweingruber 1983; Bräuning 1995). Thus, the development and history of the tree and the plant, respectively, is reflected in the pattern of tree rings (e.g., variability of ring width) as a chronology. Variations in ring width result from variable environmental conditions influencing the growth.
The application of tree-ring analysis in geomorphology (Dendrogeomorphology, Alestalo 1971) enables the reconstruction and dating of gravitational processes (e.g., Schweingruber 1983, 1996). The basic principle of the 'process-event-response-chain' (cf., Shroder 1978) represents the link between geomorphic processes, their influences on the tree and the corresponding reaction in tree growth. These reactions include not only variations in tree-ring width (e.g., sudden reduction in growth), but also changes in the structure of the cells, like e.g., the development of compression or tension wood (Gärtner et al. 2004; Fantucci & McCord 1995) caused by the tilting of the stem.
In order to analyse the wood, samples need to be taken from the trees. This is done with an increment corer, which enables the extraction of a core (ø 5 mm) from the stem. The outermost tree ring (directly below bark and cambium), taken from a living tree, shows the cells which were build last and thus allow an exact dating. Working with dwarf shrubs, the extraction of cores is in most cases not possible. Thus, a slice of the stem needs to be taken to count and analyse the rings. Since the plant is destroyed by this kind of sampling, the number of samples needs to be limited.
After the preparation of the samples (cores and slices), the tree rings are counted and are compiled and compared in so-called skeleton-plots (Stokes & Smiley 1968; Schweingruber et al. 1990). This visual comparison allows the depiction of sudden growth changes and the evidence of missing tree rings in individual samples. Afterwards, the tree-ring width is measured with an

accuracy of 1/100 mm. The resulting tree-ring-width-curve (chronology) is proved and dated using the crossdating-method (Douglass 1941).
For the analysis of structural changes in wood anatomy, the preparation of micro-sections (thickness ~15 µ) of tree-ring sequences using a sledge-microtome is required. These micro-sections are stained and embedded in Canada balsam. (Schweingruber 1990; Gärtner 2003b). From the resulting slides, digital micro photos are taken and further analysed using image analyses software (cf., Gärtner 2003b).

3.4.2 Measurement design

During different field campaigns, some small trees (*Pinus cembra, Larix decidua*) and dwarf shrubs (*Juniperus nana, Salix helvetica*) were found on rockglaciers in the Turtmann valley (cf., Roer 2001). Several samples (discs or whole plants) were taken from two active rockglaciers (HuHH3, Grueo1). Additionally, trees and shrubs in the surrounding areas, not affected by rockglacier creep, were sampled. With this strategy, climatic signals in the tree rings can be distinguished from indications of geomorphic activity (e.g., movement of the ground). Thus, anatomical variations resulting from mechanical and/or climatic stress conditions are analysed in the samples.
Regarding the analysis of shrubs, reaction wood is hard to investigate due to the lack of a main stem. The single branches of shrubs often show reaction wood caused by individual mechanical stresses. Against that, the root collar and especially the roots of the shrubs are fixed and distributed in the soil. Therefore, and in view of the purpose of this study, they are best suited for the investigation of possible influences of ground movements. Changes in the close environment of the roots lead to stress conditions and result in changes of the (anatomical) structure of their rings (Gärtner 2003a, 2003b; Garcia Gonzales & Eckstein 2003).
In order to study these potential changes, eight *Salix helvetica* shrubs were taken from an active rockglacier lobe (Grueo1) as well as from an adjacent inactive rockglacier. The whole root system of these shrubs was unearthed and taken to the lab (figure 3.10) to analyse anatomical variations in the respective rings.

Figure 3.10: *Salix helvetica* shrub taken from rockglacier Grueo1. White rectangles (1 and 2) indicate the positions of the taken root samples for the analysis of anatomical variations.

In the lab, 20 samples (discs) were taken from the individual roots of the shrubs. The small size of the roots (~1.5 cm) enabled the preparation of micro-sections of whole cross sections using a sledge microtome. These micro-sections were stained with Safranin and Astrablue to distinguish between lignified (Safranin) and not lignified (Astrablue) parts of the rings and to get a better contrast for the ongoing image analysis procedure. For dehydration, the samples were rinsed with alcohol, immersed in Xylol, imbedded in Canada-Balsam and dried at 60° C in the oven for about 24 hours (Gärtner et al. 2001).

The resulting micro slides were then placed under a microscope and digital photos, with 40 times magnification, were taken. Hence, the anatomical structure of the rings is clearly visible (figure 3.11). In addition to the micro-sections, micro scales were photographed using the same magnification to guarantee correct image analysis. The micro photos were than used to analyse the size of vessels and probable variations in the annual rings of stressed (active rockglacier) and unstressed (inactive rockglacier) roots using the image analysis program WinCELL (Regents Instruments, Canada). This program enables automated measuring of the size (length, width, area) of single cells. The setting of special filters allows the separation of vessels from cells of the ground tissue.

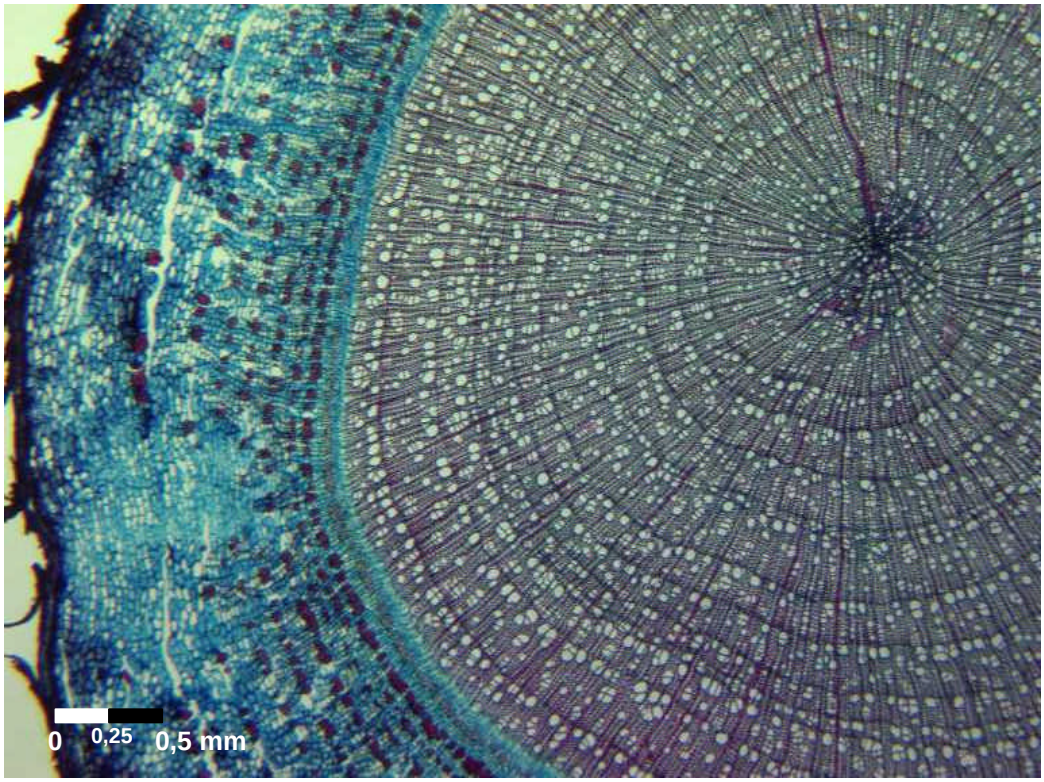

Figure 3.11: Digital micro photo (40x magnification) of a lateral root micro slide showing annual rings and the surrounding bark. Shrub-ID: Isa_W04 (*Salix helvetica*).

3.5 Temperature monitoring

3.5.1 Basic principles

Since permafrost is a thermally defined phenomenon, the determination of ground temperatures is one of the best suited methods for the evidence of its occurrence. Permanently frozen ground is indicated by a Mean Annual Ground Surface Temperature (MAGST) of < 0° C. This temperature corresponds theoretically to the temperature at the Zero Annual Amplitude (ZAA), which is normally described as permafrost temperature (Haeberli 1975). In discontinuous permafrost, this temperature lies between 0°C and -5°C (Haeberli 1992a).

In the 70s, the method of the Bottom Temperature of the winter Snow cover (BTS) was developed by Haeberli (1973) for the Alps and was later transferred to Scandinavia (e.g., King 1983). The precondition for this method is a snow cover of about 0.8 to 1 m thickness, which then isolates the active layer thermally from the atmosphere (cf., Haeberli 1973; Hoelzle 1992, 1994). Thus, the BTS-temperatures are very constant and reflect the thermal state of the ground below. This condition is normally given in spring (February - April). Therefore, BTS-measurements are restricted to this period (cf., Haeberli & Patzelt 1982).

On the basis of well investigated areas, the following limiting values for the occurrence of permafrost were compiled for the Alps and Scandinavia (Haeberli 1973; Hoelzle 1994; Hoelzle et al. 1993, 1999; Keller 1994):

< -3° C:	permafrost probable
between -2° C and -3° C:	permafrost possible
> -2° C:	no permafrost

3.5.2 Measurement design

The temperature monitoring was performed in one hanging valley (Hungerlitälli) over the period 2001-2004. Temperatures were measured continuously over the year at the active layer - surface using Universal Temperature Loggers (UTL) (Krummenacher et al. 1998). These thermistors are characterised by a small and robust body with an integrated temperature sensor. The precision of the instrument is +/- 0.1° C within the operating range of -29° C to +39° C. Due to the memory-resolution of 8 bit, the data are stored with a resolution of 0.27° C only (http://www.utl.ch/geotest.html). The temporal resolution of the measurement is unrestricted. For the study site a measurement-interval of 1 h was selected, which enables the recording of up to 331 days. Then the memory needs to be read out. For this purpose the program BoxCar (Onset Computer Corporation, Version 3.7) was applied. The data-loggers were calibrated before their placement in 2001 and are indirectly calibrated in the following years by the zero curtain in spring (cf., Hanson & Hoelzle 2004).

About 45 thermistors were placed in various situations (on rockglaciers and surrounding terrain) between 2500 and 2780 m a.s.l. Thus, temperatures on and beyond the permafrost bodies can be compared. The resulting data serve to determine the extent of the permafrost occurrence by the calculation of MAGST as well as the interpretation of the BTS-values (cf., Nyenhuis 2005.).

3.6 Summary

The range of methods applied in this study reaches from geomorphic mapping to digital photogrammetry, terrestrial geodetic survey, dendrogeomorphological techniques, and temperature monitoring.

Classical geomorphic mapping in the field and on aerial photographs is used for the selection of the terrain features subsequently investigated. Digital photogrammetry and terrestrial geodetic survey serve to quantify horizontal and vertical displacements at rockglacier surfaces on different temporal and spatial scales. The former combines for the first time small-scale aerial photography and digital airborne pushbroom imagery for the investigation of rockglacier kinematics.

The application of dendrogeomorphology in this context enters new scientific paths. For the first time, anatomical variations in the roots of dwarf shrubs were related to rockglacier movement.

In addition, a temperature monitoring was conducted in one hanging valley in order to determine the local permafrost occurrence and to analyse possible climatic controls on rockglacier kinematics.

4 STUDY SITE

4.1 General characteristics

The Turtmann valley is located in the southern part of Switzerland, in the Canton of Valais, in-between the Matter valley and the Anniviers valley (figure 4.1). The southern tributary of the river Rhone covers a catchment area of 110 km^2 and extends over 15 km from 4506 m a.s.l. at the top of Weisshorn to 620 m a.s.l. in the Rhone valley. The valley head is dominated by the two glaciers Turtmann and Brunnegg. Further down, the morphology of the valley is structured into the glacial trough descending slightly from 2200 m a.s.l. at the glacier tongue to 1800 m a.s.l. and a steep gorge at the outlet to the Rhone valley. Above the shoulders of the trough the valley is subdivided into fourteen east-west and west-east striking hanging valleys, so called Tällis, with several small glaciers and glacierets. The summits of Bella Tola (3025m a.s.l.), Turtmannspitze (3080m a.s.l.) and Les Diablons (3609m a.s.l.) in the west, Signalhorn (2911m a.s.l.), Schwarzhorn (3201m a.s.l.) and Stellihorn (3409m a.s.l.) in the east, as well as the Tête de Milon (3676m a.s.l.), the Bishorn (4135m a.s.l.) and the Brunegghorn (3833m a.s.l.) in the south mark the boundaries of the catchment (figure 4.2). The photographs shown in figure 4.2 give an impression of the Turtmann glacier in the valley head (nr. 5), the hanging valleys (nr. 1-3) and the valley floor (nr. 4).

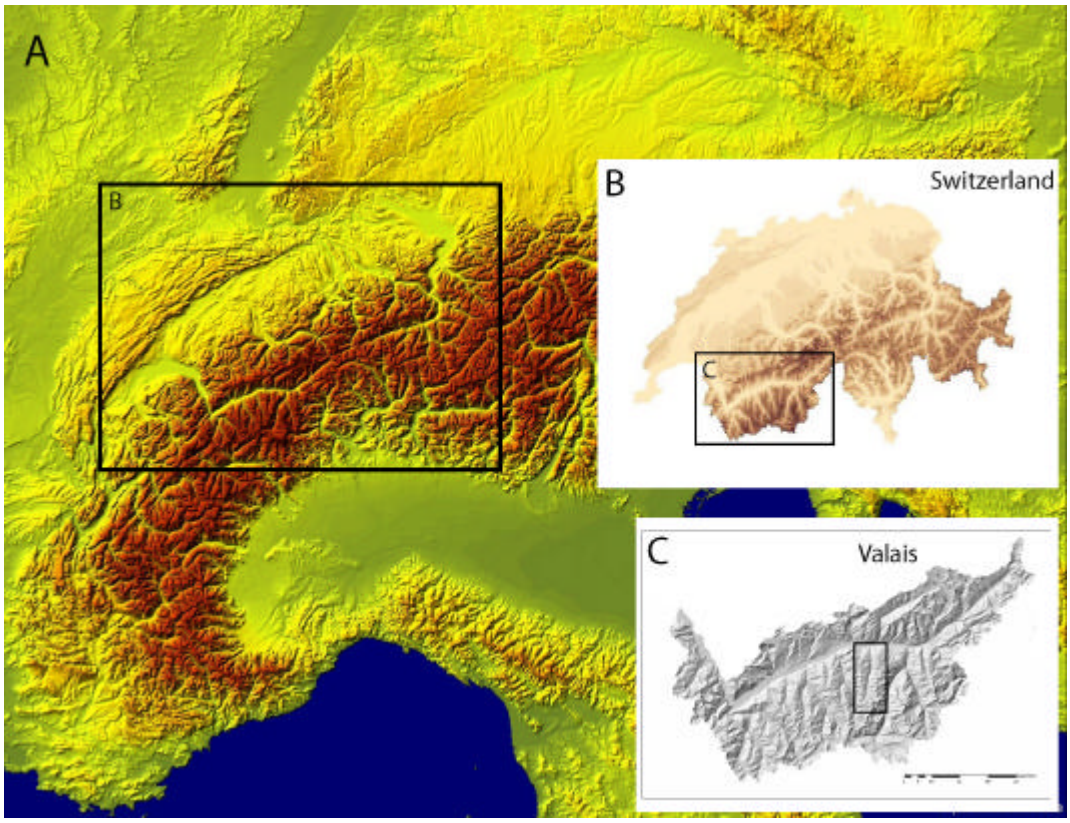

Figure 4.1: Location of the Turtmann valley (square in Figure C) within the Valais (© Luzi Bernhard, WSL), Switzerland and the Alps (http://www.scilands.de).

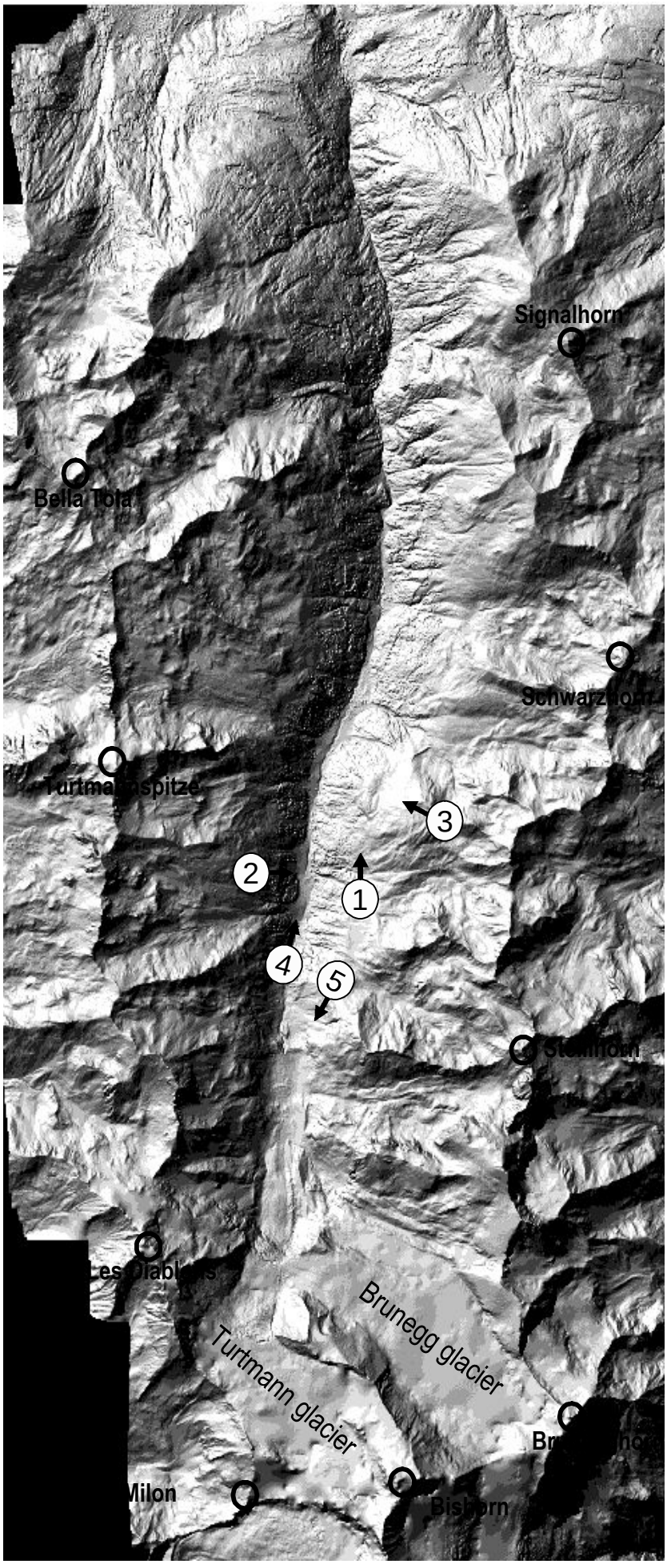
Signalhorn
Bella Tola
Schwarzhorn
Turtmannspitze
1
2
3
4
5
Brunegg glacier
Turtmann glacier
Milon
Bishorn


1
View to the north


2
View to the east (Hungeritälli)


3
View to north-west (Hohtälli)

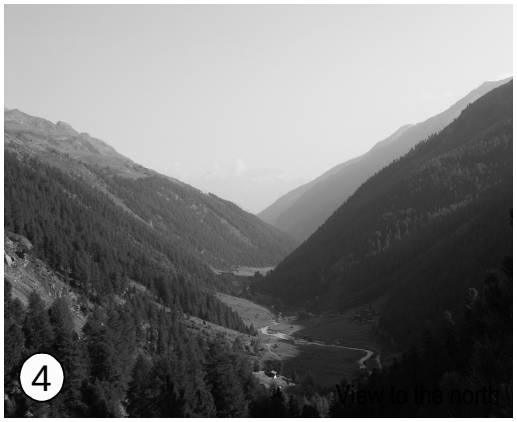
4
View to the north


5
View to south-west (Turtmann glacier)

Previous page:

Figure 4.2: Shaded relief visualisation of the Turtmann valley and impressions of different subsystems. The numbers and arrows in the map mark the corresponding photograph and its direction of sight.

4.2 Geology

The whole area of the southern Valais, in-between the Simplon area, the Rhone valley and the Great St. Bernhard, is formed by the penninic nappes Bernhard and Monte Rosa (Labhart 1998). They consist nearly exclusively of metamorphic rocks, which developed from the crystalline base as well as from sedimentary rocks. The Bernhard nappe depicts different tectonic units, which are arranged in overlapping layers (figure 4.3).

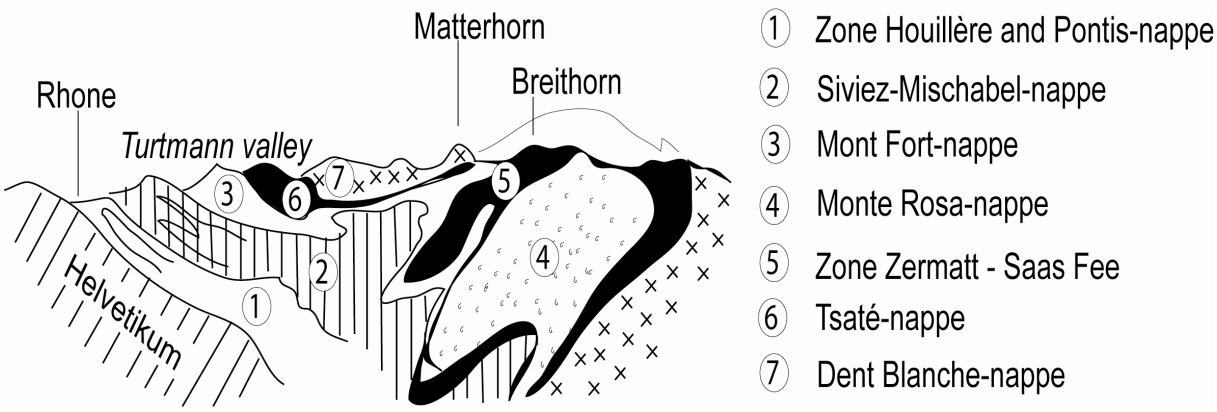

Figure 4.3: Geological profile through the Valais Alps with the position of the study site (Labhart 1998: 94, modified).

The Turtmann valley is characterised by the Siviez-Mischabel-nappe (figure 4.4), where metamorphic rocks such as two-mica gneisses and muscovite phyllades dominate. Additionally, at some places these are superimposed by sedimentary rocks of the Barrhorn-serie, which consist of Mesozoic and Tertiary limes, marbles and sandstones (Bearth 1980). For instance, these rocks form the southern slopes of the Pipjitälli and can clearly be distinguished from the former by bright colors and small-grained weathering. More rarely, quartzites, marbles and dolomites (Perm to Cretaceous) – relicts of the Mont-Fort-nappe - are exposed in the western part of the Turtmann valley (Hsü & Briegel 1991; Sartori 1990). In the south of the valley, rocks of the Dent-Blanche nappe appear in the great summits of Les Diablons, Bishorn and the Weisshorn (Gilliéron 1946).

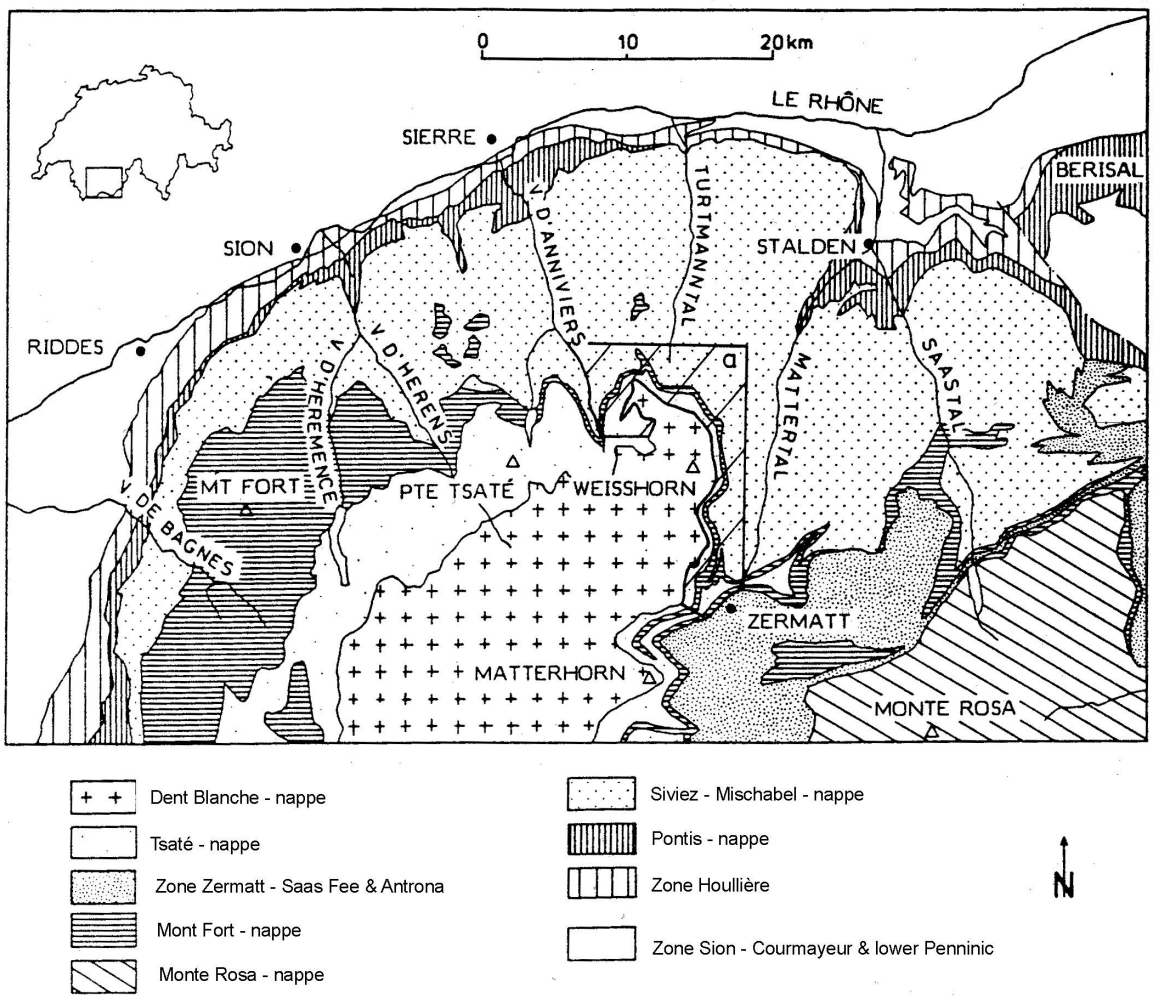

Figure 4.4: Tectonic map of the middle and upper Penninic in the southern Valais (Sartori 1990, modified).

4.3 Climate

The study area is characterised by an inner-alpine continental-type climate. The surrounding topography isolates the valley from precipitation, coming predominantly from the west. Therefore, the Turtmann valley is situated in one of the most arid regions in the Alps (cf., figure 4.5).

Since no meteorological station exists in the area itself, records of neighbouring stations are consulted to assess the climatic conditions (table 4.1). In some places the values – especially the precipitation data – shows distinct differences (e.g., station Grächen). Hypsometric temperature gradients were calculated for the neighbouring Matter valley in the east (Visp – Grächen, Visp – Zermatt) and for the Hérens valley in the west (Sion – Evolène) and were transferred to the Turtmann valley (cf., Elverfeldt 2002; Otto 2001; Roer 2001). The gradient between the stations in Visp (640 m a.s.l.) and Grächen (1617 m a.s.l.) result in a value of 0.37° C / 100 m, while the

gradient between Visp and Zermatt (1638 m a.s.l.) amounts to 0.47° C / 100 m. Between Sion (482 m a.s.l.) and Evolène (1825 m a.s.l.) it reveals 0.36° C / 100 m. In comparison to hypsometric temperature gradients for the whole of Switzerland (0.57° C / 100m) (Ozenda 1988) and for the Valais (0.55° C / 100 m) (Escher 1970, after Pfeffer 2000) there are great differences. The latter was determined between Grächen and the mountain rescue hut at Testa Grigia (3479 m a.s.l.). From these gradients, a mean temperature reduction of 0.49° C / 100 m was calculated for the Matter valley. Furthermore, all the calculated temperature gradients allow a first assumption of the location of the 1° and 2° C annual isotherm in order to determine the lower boundary of the discontinuous permafrost. Transferring the gradients Visp – Grächen and Sion – Evolène to the Turtmann valley reveals the 1° C annual isotherm at 3087 m a.s.l. and 3156 m a.s.l., respectively. This appears to be unlikely, since numerous glacial and periglacial landforms occur in lower altitudes. Probably, the fall in temperature between the valley outlet and a 'middle' station in the valley is lower than the gradient in higher altitudes, resulting in an overestimation of the prevailing location of the isotherm. Taking the gradient for the Valais (0.55° C / 100 m) into account, the 1° C isotherm in the Turtmann valley would be at 2300 m a.s.l., resulting in an underestimation. Therefore, the mean temperature gradient for the southern hanging valleys of the Rhone valley is suspected to lie between 0.36° and 0.55° C / 100 m. Hence, the lower boundary of the discontinuous permafrost in the Turtmann valley is situated between 2498 m and 2854 m a.s.l.

Table 4.1: Elevation, mean annual precipitation and mean annual air temperature for selected stations in the Rhone valley (1-7), the Matter valley (8-11), the Anniviers valley (12, 13) and the Hérens valley (14, 15). Apart from station Evolène, the SMA-values represent mean values of the period 1901 – 1960.

Nr.	Station	Elevation (m)	Precipitation (mm)	Temperature (° C)	Reference
1	Martigny	471	759	9.5	Werner 1994
2	Sitten/Sion	549	592	9.9	Werner 1994
3	Sitten/Sion	482	575	8.5	SMA
4	Siders/Sierre	565	587	9.3	Werner 1994
5	Visp	658	625	8.4	Werner 1994
6	Visp	640	710	8.2	SMA
7	Brig	671	723	9.0	Werner 1994
8	Grächen	1617	512	4.6	Werner 1994
9	Grächen	1617	611	4.6	SMA
10	Zermatt	1638	694	3.9	Werner 1994
11	Zermatt	1638	694	3.5	SMA
12	Vissoie	1260	617	-	Werner 1994
13	Zinal	1678	728	-	Werner 1994
14	Evolène	1378	940	-	Werner 1994
15	Evolène	1825	-	3.6	SMA

The determination of precipitation conditions is even more difficult, since they are more influenced by local effects. Table 4.1 shows, that precipitation rates are low, even in elevations of 1600 m a.s.l.. Tatenhove and Dikau (1990) estimated the annual precipitation in the Turtmann valley at 2000 m a.s.l. to lie between 600 and 900 mm/a. Against that, figure 4.5 depicts the precipitation in the Turtmann valley to lie between 900 and 1600 mm/a. Thus, one can conclude that all these calculations and values remain estimations of the climatic conditions in the Turtmann valley. In future, these uncertainties will be reduced, since an automatic weather station was installed in 2002 in one of the hanging valleys (Hungerlitälli).

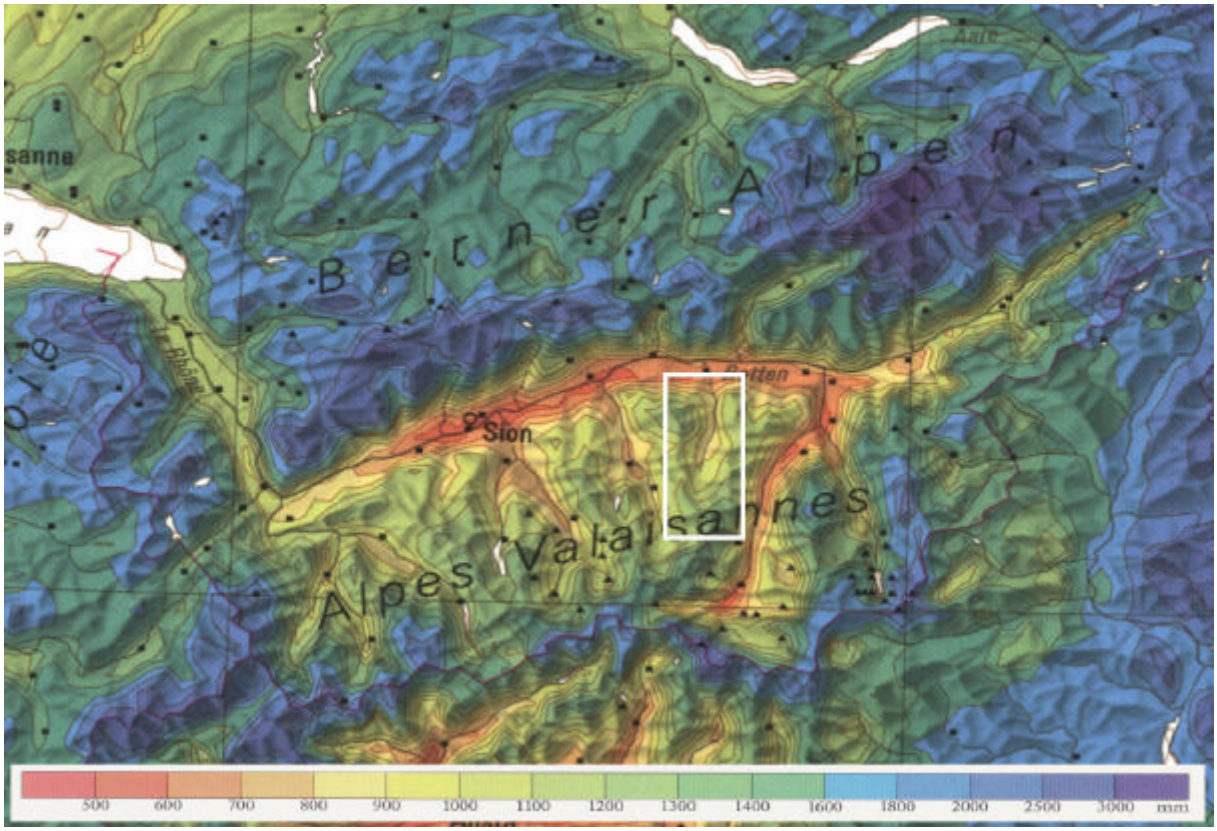

Figure 4.5: Mean annual precipitation values (1971 – 1990, corrected) in the Valais (Hydrologischer Atlas der Schweiz 2001, © Bundesamt für Landestopographie). The white rectangle marks the study area.

4.4 Geomorphology

The glacigenous character of the Turtmann valley becomes visible in the glacial trough, the trough shoulders at about 2400 m a.s.l. as well as the superimposed hanging valleys. The geomorphology of these Tällis (= small valleys) is dominated by glacial and periglacial processes. Therefore they are filled with glacial and periglacial sediments. Several moraine ridges indicate the former glacial activity and enable an approximate explanation of the geomorphogenetic development. Recently, in three hanging valleys on the east side of the Turtmann valley small glaciers exist with equilibrium-line altitudes between 2900 and 3260 m a.s.l. (Tatenhove & Dikau

1990), while the hanging valleys on the west side show no glaciation. Altogether, glaciers cover around 14 % of the valleys area (Otto & Dikau 2004).

The periglacial process domain is – in general - limited by the lower boundary of solifluction (treeline) and the climatic snowline (Rathjens 1982). By transferring this to the Turtmann valley, the periglacial belt extends between 2300 and approximately 3200 m a.s.l. Because of the climatic characteristics, the periglacial belt is very distinct and typical landforms, e.g. rockglaciers, gelifluction lobes, ploughing boulders, are numerous. Approximately 80 rockglaciers in all degrees of activity can be found in the catchment (Nyenhuis 2001). This validates the assumption of Messerli & Zurbuchen (1968) and Barsch (1996) that the Turtmann valley is located in an area of high rockglacier concentration. Typically, they are situated in the hanging valleys, arranged in sequences from active to inactive and relict. The existence of several active rockglaciers coincides well with the regional distribution of discontinuous permafrost with a lower boundary of around 2620 m a.s.l., where MAAT is approximately -1.5° C.

The lower part of the valley is characterised by a steep gorge, which was cut into the bedrock by the creek Turtmänna. By following the creek for approximately four kilometres through the gorge, it passes the 50 m waterfall at the village of Turtmann and reaches the bottom of the Rhone valley.

The geomorphology of the hanging valleys on the east side of the Turtmann valley is detailed in chapter 5.1. For more information on landforms and processes in the Turtmann valley, it is referred to the geomorphic maps by Broccard (1998) and Otto (2001), Otto & Dikau (2004).

5 RESULTS

5.1 Geomorphic mapping

All hanging valleys or so-called 'Tällis' (= little valley) on the orographic right side of the Turtmann valley (figure 5.1) were analysed by direct geomorphological mapping in the field and by interpretation of aerial photographs. Due to the purpose of this study, the mapping was concentrated on glacial and periglacial landforms and related processes allowing a better interpretation of rockglacier occurrence and activity. In the following, the structure of each hanging valley is described shortly. Rockglacier distribution is depicted on aerial images and parameters are detailed in corresponding tables.

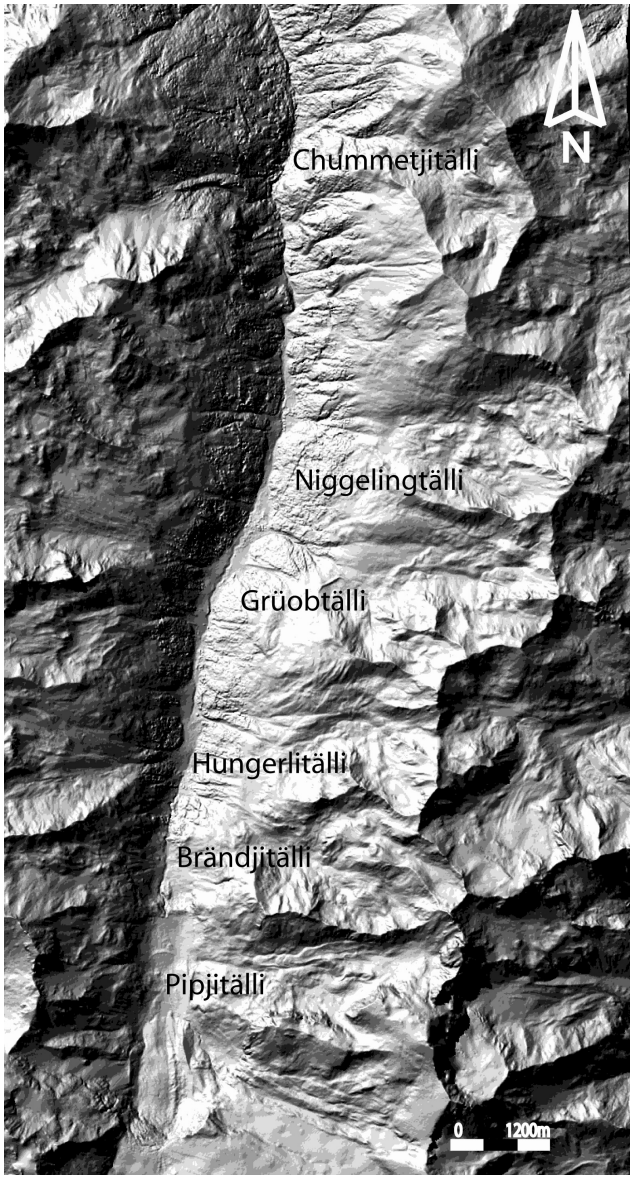

Figure 5.1: Orographic right side of the Turtmann valley with investigated hanging valleys (Tällis). Underlying DTM of 2001.

5.1.1 Hungerlitälli

This hanging valley will be described first, since most data on landforms and processes are available in this area. Similar structures and phenomena can thus be transferred to the other hanging valleys which resemble the Hungerlitälli.

The Hungerlitälli is, as seen from the Turtmann glacier, the third hanging valley on the orographic right side (figure 5.1). It spreads from Jungpass (2990m a.s.l.) over 2.3 km to the shoulder of the glacial trough (at about 2400 m a.s.l.) and over 1.7 km from Gigi-ridge (2850 m a.s.l.) in the north to the ridge between Rothorn (3278 m a.s.l.) and Hungerlihorli (3007 m a.s.l.) in the south (figure 5.2). The landforms within the valley are dominated by moraines and rockglaciers. A big moraine (probably of late glacial origin (Egesen)) extends straight through the valley, embracing three small cirques of the Hungerlihorli / Rothorn-massiv (figure 5.2). The area within this lateglacial moraine is recently covered by a small glacier in the uppermost cirque, some smaller moraines, two talus-cones on the north-exposed flank of the Hungerlihorli and several rockglaciers in different states of activity. Further down, where the lateglacial moraine is lying on the shoulder of the trough, a formerly active rockglacier has broken through the moraine ridge and crept down further for another 500 meters. Moraines of Holocene age are visible as remnants in the valley bottom directly in front of the inactive rockglaciers as well as in the recent glacier forefield (figure 5.2). The last-mentioned can be divided into a north-south directed lateral moraine (probably indicating the maximum size of the little ice age advance (1850)) and a small terminal moraine (probably indicating the glacial position around 1920). But, since the described landform pattern does not agree with the Siegfried map (sheet 500, St. Niklaus (1891)), the argumentation needs to be considered carefully. The map depicts the Rothorn-glacier covering the whole cirque including the area where recently active rockglaciers (nr. 13, 15) are situated. But, a glacial retreat of around 500 meters and the development of a rockglacier of 330 meters length within 100 years is unlikely.

The other half of the Hungerlitälli (south-exposed) shows quite different landforms and processes. It has a lower relief and spreads gentler from the Gigi-ridge to the lateglacial moraine. The surface is covered by block fields, often vegetated, and is structured by two relict rockglaciers, which descended from the north and overflowed the Egesen-moraine. In the north-east, another rockglacier is situated in a cirque below the Furggwanghorn. Additionally in the valley head below the pass, a rockglacier is situated. With two lobes it extends over 400 m and the terminus is also creeping over the lateglacial moraine.

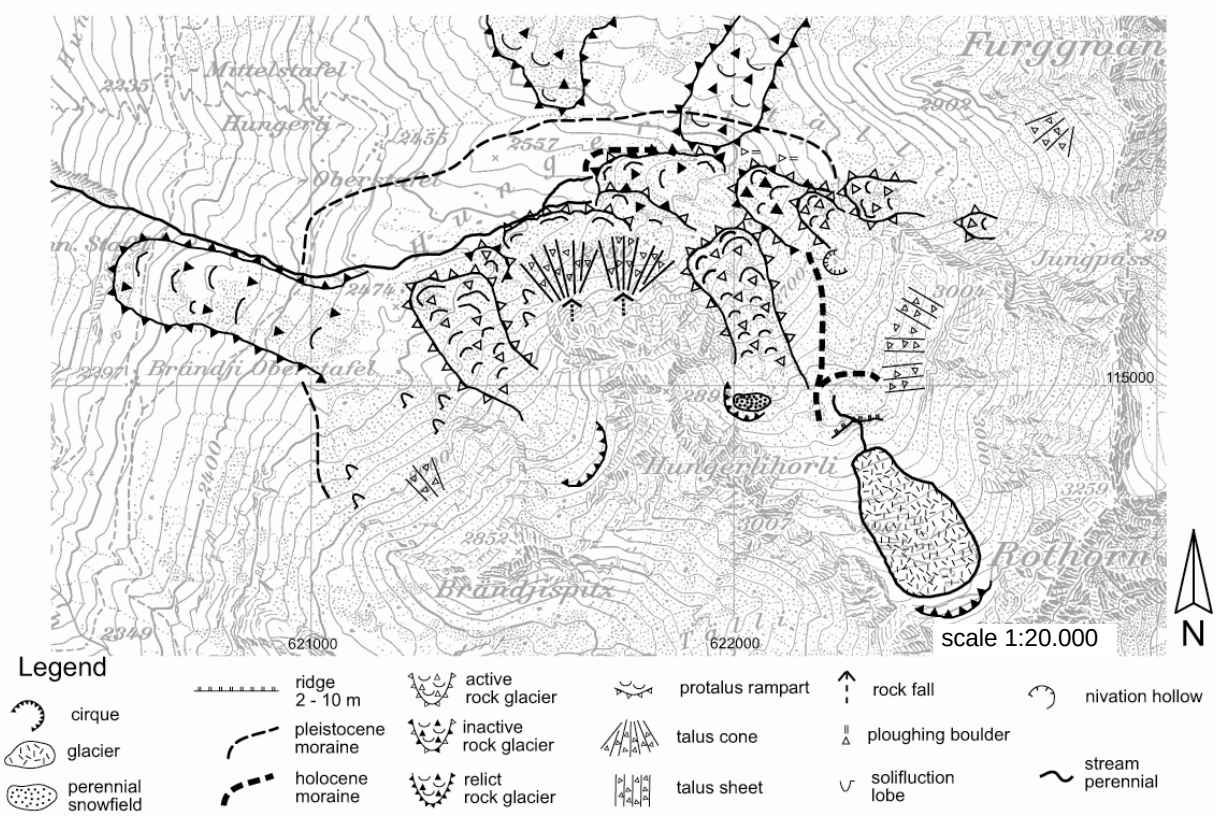

Figure 5.2: Geomorphological map of the Hungerlitälli (from Roer 2003). Legend based on Kneisel et al. (1998). Basic map: Pixelkarte 1:25.000 (© Swiss Federal Office of Topography).

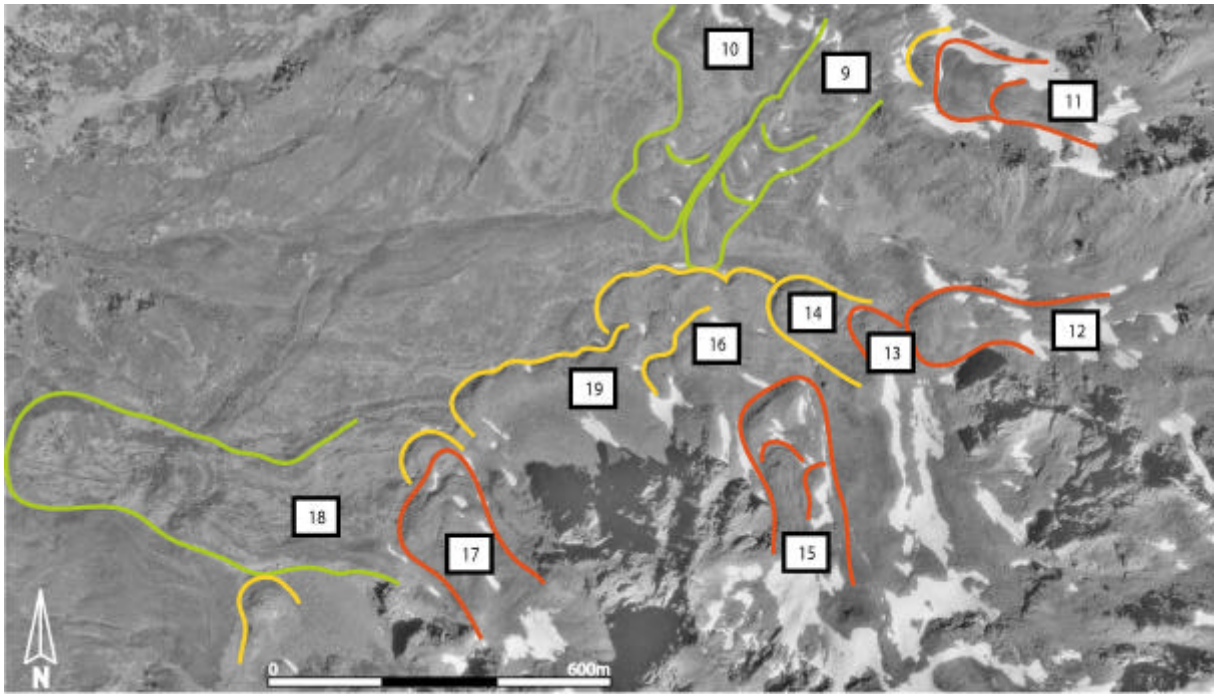

Figure 5.3: Rockglacier occurrence and activity in the Hungerlitälli. Red line = active rockglacier, yellow line = inactive rockglacier, green line = relict rockglacier. Given numbers correspond to the inventory table (table 5.1). Underlying orthophoto of 20.08.1975 (flight-line 22, aerial photographs taken by Swisstopo).

Table 5.1: Rockglacier inventory of the Hungerlitälli.

Nr. inventory	Name of hanging valley	Name of rockglacier, abbreviation	Altitude of rockglacier front (foot) [m a.s.l.]	Altitude of rooting zone [m a.s.l.]	Length (L) [m]	Width (W) [m]	Quotient length/width (L/W)	Average slope [°]	Aspect of front	Aspect of rooting zone	Visible creep structures?	State of activity (mapping result)	Nr. of map sheet (1:25'000)	Aerial photograph: year, nr.
9	Hungerli	Gigigrat 1, Hugg1	2580	2750	530	120	4.42	16	S	W	clear	relict	1308	1975:6222,6223 1993:4321-4323
10	Hungerli	Gigigrat 2, Hugg2	2610	2720	530	220	2.41	14	SW	SW	some	relict	1308	"
11	Hungerli	Furggwang-horn, Hufh	2780	2890	300	100	3	21	W	W	few	active	1308	"
12	Hungerli	Jungpass, Hujp	2680	2850	450	100	4.5	22	W	WSW	few	active	1308	"
13	Hungerli	Rothorn 1, Hurh1	2640	2690	150	80	1.87	20	WNW	W	no	active	1308	"
14	Hungerli	Rothorn 2, Hurh2	2600	-	190	120	1.58	12	NW	NW	some	inactive	1308	"
15	Hungerli	Hungerlihorli 1, Huhh1	2630	2780	330	130	2.54	26	NNW	N	clear	active	1308	"
16	Hungerli	Hungerlihorli 2, Huhh2	2550	-	300	170	1.76	12	W	NW	some	inactive	1308	"
17	Hungerli	Hungerlihorli 3, Huhh3	2515	2650	310	140	2.21	27	NW	NW	clear	active	1308	"
18	Hungerli	Hungerlihorli 4, Huhh4	2270	2490	700	180	3.89	18	W	NW	clear	relict	1308	"
19	Hungerli	Protalus rampart, Hupr	2500	2530	70	350	0.2	15	NW	NW	no	inactive	1308	"

The rockglaciers in the Hungerlitälli reveal different states of activity (figures 5.2, 5.3). While relict rockglaciers are found in lower and in south-exposed situations, the active ones occur in higher altitudes and on north- or north-west exposed slopes. Inactive rockglaciers, which are morphologically not easy to distinguish from active ones, are concentrated in the valley bottom. The inactive feature below the talus cones can be defined as an embryonic rockglacier or protalus rampart (as defined by Haeberli 1985) which did not develop further. Independent of their activity, some rockglaciers show distinct creep structures. Thus, these characteristics simplify the mapping of rockglaciers in general, but they do not allow a thorough differentiation in the state of activity. The active rockglaciers below cirques (nr. 11, 15 and 17) show great similarities in shape and size, even though they are situated in different altitudes. Their surface topography is often characterised by compressive structures on the lower part and by extending flow features in the upper part of the tongue. In the last summers (2002-2004) the occurrence of permafrost was confirmed on rockglacier Huhh1 (nr. 15) by exposed clear ice (probably segretation ice) at an eroded ridge.

The comparison of DTMs of the years 1975 and 2001 allows the interpretation of vertical changes within the Hungerlitälli (figure 5.4). The speckled high values in the middle of the image reflect errors in the DTM resulting from shadows in the aerial photographs (visible in figure 5.3),

but the high values at the lower right margin display the loss in thickness at the Rothorn-glacier. In general, slight losses occur at the slopes, while in other parts like the area between the Egesen moraine and the rockglaciers a gain occurs.

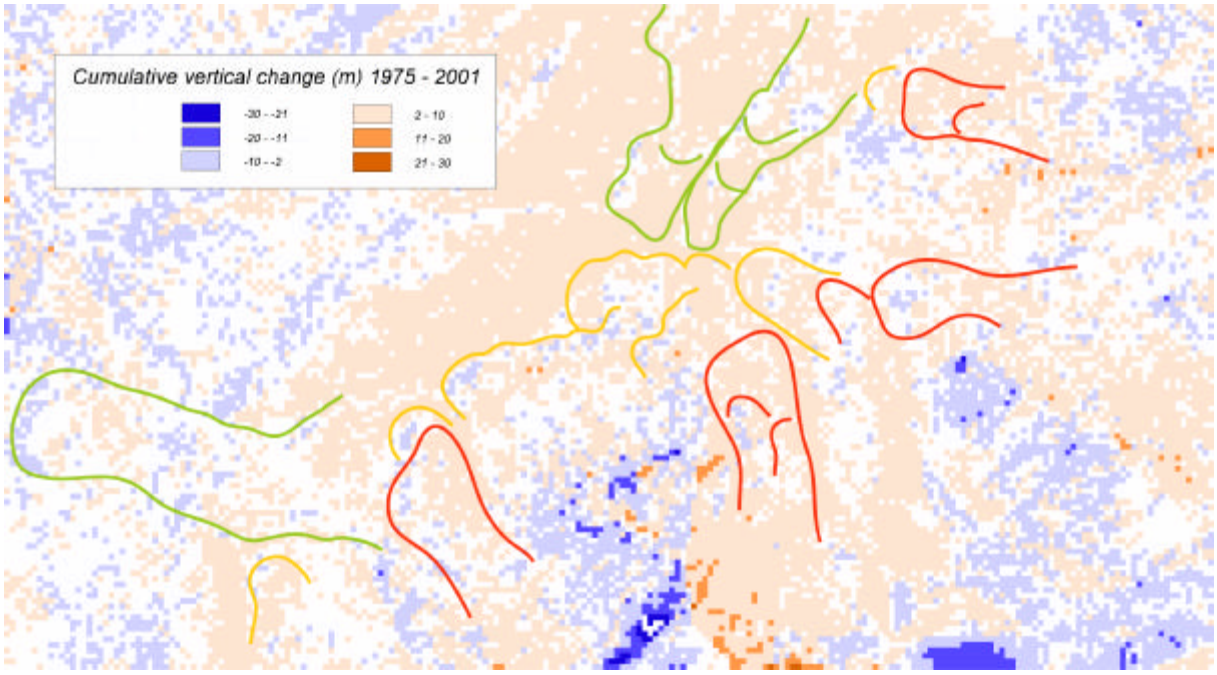

Figure 5.4: Vertical surface changes in the Hungerlitälli between 1975 and 2001 (DTM comparison).

5.1.2 Grüobtälli

The Grüobtälli borders in the north on the Hungerlitälli and spreads over 2.75 km from the Augstbordpass (2894 m a.s.l.) in the east to the trough shoulder of the main valley and over 2 km from Grüob-ridge (at about 2800 m a.s.l.) in the north to the Gigi-ridge in the south. The valley shows a quite similar geomorphology to the Hungerlitälli. Recently it has not been glaciated, but a big moraine situated in the centre of the valley indicates a former glaciation of the north exposed part. Additionally, a small moraine in the north, directly below the Grüob-ridge, reflects a previous glaciation also on this side of the valley. This moraine partially shows creep structures indicating a reactivation by permafrost creep. Recently, this feature seems to be relict (figure 5.5). The valley head and the north-exposed side are dominated by several active and inactive rockglaciers. Some of them (table 5.2, nr. 22, 26) arise from high elevated cirques. The latter (nr. 26) reaches a great length due to overrunning of a step slope. The former (nr. 22) depicts a complex topography with a plait-like pattern. This results from debris supply out of separated rock faces. A different pattern is displayed in the surface topography of rockglacier Grueo7 (nr. 27), which is also of great length. The cascade of lobes (polymorphic body) does not reflect a spatial variation in material input rather than a temporal sequence of active phases. Another striking feature is the relatively thick rockglacier Grueo1 (nr. 21) which showed a smooth surface

topography in 1975 (figure 5.5) and developed deep crevasses until 2001. The inactive features, which are again concentrated on the valley floor, are characterised by lower slope angles and by a lack of surface structures. An exception is Grueo4 (nr. 24), where an active lobe is creeping over an older, inactive generation. The relict rockglaciers (nr. 20, 29) are less striking than in the Hungerlitälli, but their position and extent is comparable. Nr. 29 is either interpreted as a small moraine which started creeping in the form of a small debris rockglacier, or as a protalus rampart comparable to the feature in the Hungerlitälli. The comparison of multitemporal DTMs (figure 5.6) shows a general slight thickening in the valley floor (very homogeneous on the meadows) and a slight loss on the steeper slopes. The high values at the upper and lower margin of the image result from errors in the DTMs. The linear structure at the relict rockglacier (nr. 20) exposes the avalanche dam, which was built in 1997/1998. The mass flux depicted on rockglacier Grueo 1 (nr. 21) is detailed in chapter 5.2.4.1.

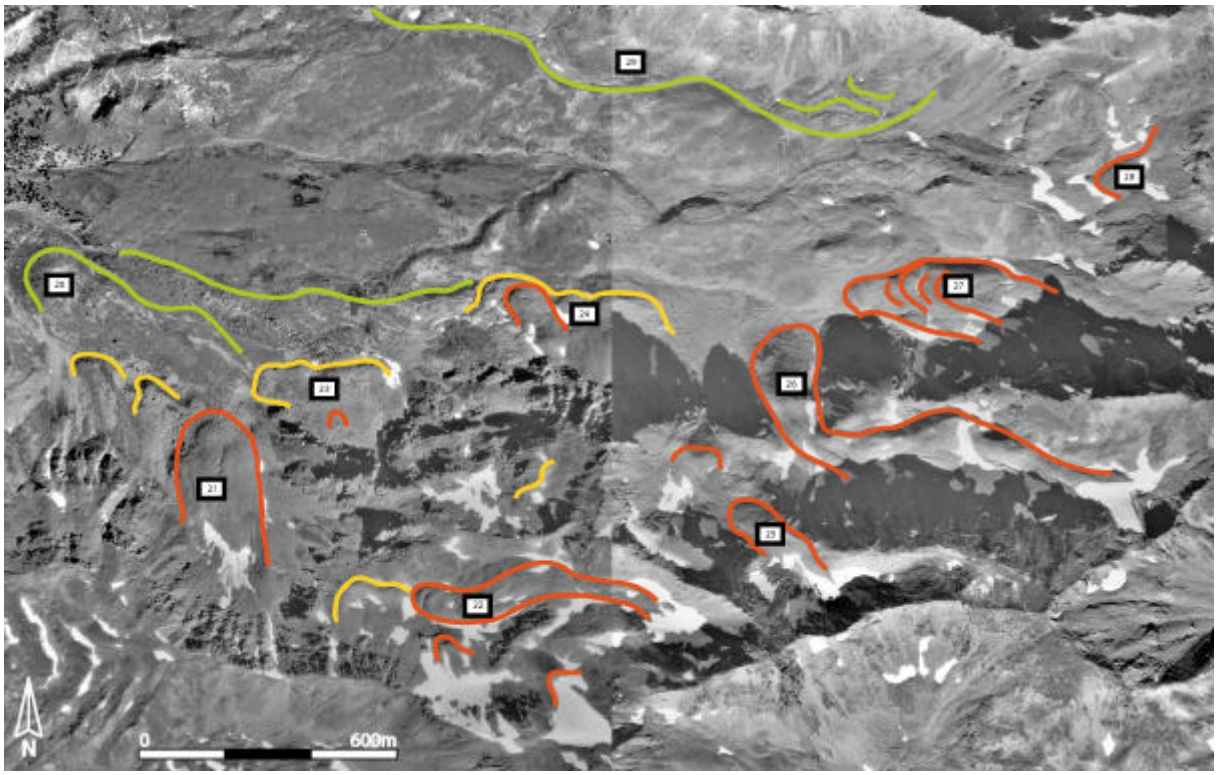

Figure 5.5: Rockglacier occurrence and activity in the Grüobtälli. Red line = active rockglacier, yellow line = inactive rockglacier, green line = relict rockglacier. Given numbers correspond to the inventory table (table 5.2). Underlying orthophoto of 20.08.1975 (left) and 6.10.1975 (right) (flight-line 22 (left), 21 (right); aerial photographs taken by Swisstopo).

Table 5.2: Rockglacier inventory of the Grüobtälli.

Nr. inventory	Name of hanging valley	Name of rockglacier, abbreviation	Alttitude of rockglacier front (foot) [m a.s.l.]	Altitude of rooting zone [m a.s.l.]	Length (L) [m]	Width (W) [m]	Quotient length/width (L/W)	Average slope [°]	Aspect of front	Aspect of rooting zone	Visible creep structures?	State of activity (mapping result)	Nr. of map sheet (1:25´000)	Aerial photograph: year, nr.
20	Grüob	Grueo0	2240	2430	660	200	3.3	12	NW	WNW	few	relict	1308	1975:6220,6221; 6459,6460 1993:4321,4322
21	Grüob	Grueo1	2420 (in 2001!)	2650	500	200	2.5	16	NNW	NNW	few	active	1308	"
22	Grüob	Grueo2	2755	2950	610	90	6.8	21	W	NW	clear	active	1308	"
23	Grüob	Grueo3	2435	2550	220	120	1.83	18	WNW	NNW	few	inactive	1308	"
24	Grüob	Grueo4	2500	2620	340	140	2.43	25	NW	N	few	active	1308	"
25	Grüob	Grueo5	2855	2970	270	90	3	12	NW	WNW	no	active	1308	"
26	Grüob	Grueo6	2585	2930	1100	100	11	14	NNW	WNW	few	active	1308	"
27	Grüob	Grueo7	2630	2930	760	160	4.75	12	W	W	clear	active	1308	"
28	Grüob	Grueo8	2805	2830	150	170	0.88	10	W	W	no	active	1308	"
29	Grüob	Grueo9	2605/2660	2650/2750	150	850	0.18	13	WSW	SW	few	relict	1308	"

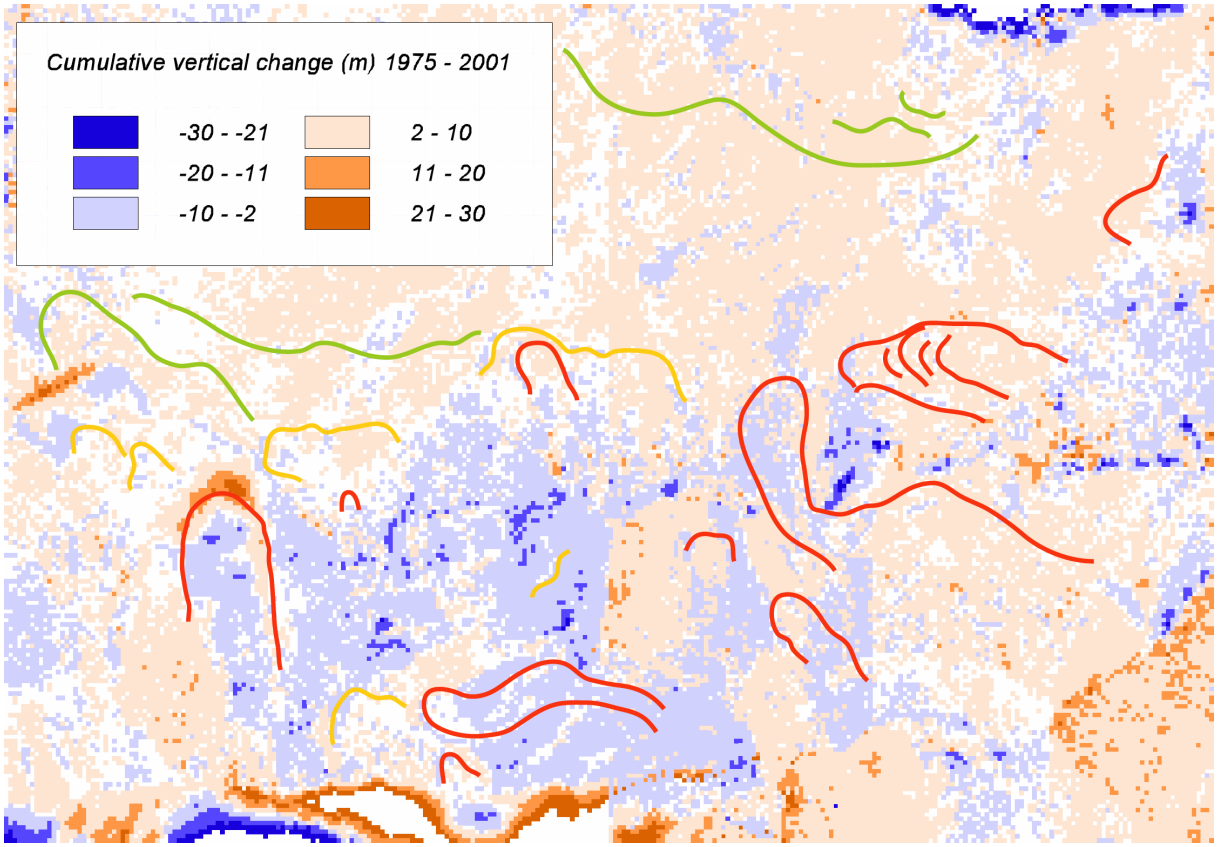

Figure 5.6: Vertical surface changes in the Grüobtälli between 1975 and 2001 (DTM comparison).

5.1.3 Niggelingtälli

This Tälli is again the adjoining hanging valley to the north (cf., figure 5.1). It extends from the Dreizehntenhorn (3052 m a.s.l.) over 2.7 km to the west and over 2 km from the Schwarze Blatte (2975 m a.s.l.) in the north to the Grüob-ridge in the south. In contrast to the before described hanging valleys, the Niggelingtälli shows no clear moraines. But some peculiar landforms exist, which are interpreted as moraines reactivated by permafrost creep and relict at present (nr. 30). A ridge (Roti Ritze) divides the valley into two parts, which are both geomorphologically dominated by rockglaciers. Rockglacier Niggel2 (nr. 32) occurs in a similar position like Grueo7 (nr. 27) and also shows a similar multi-lobe surface structure indicating a complex history (figure 5.7). Above the ridge, a massive but relatively small permafrost body (nr. 35) of the monomorphic type is situated in the south-east. Some rockglaciers (nr. 31, 34) developed in narrow valleys with small root zones. Inactive rockglaciers again lie in the valley bottom (nr. 33, 34) or as protalus rampart below a crest (nr. 36). Relict rockglaciers are identified on the south-exposed slope (nr. 38) and in the lower part of the valley (nr. 30, 39). Their fronts are situated in the same altitude of about 2375 m a.s.l.

The analysis of vertical changes between 1975 and 1993 (figure 5.8) displays again the overall losses on the slopes and gains in the flatter areas. High values in the right side of the image result from shadows in the aerial photographs.

Table 5.3: Rockglacier inventory of the Niggelingtälli.

Nr. inventory	Name of hanging valley	Name of rockglacier, abbreviation	Altitude of rockglacier front (foot) [m a.s.l.]	Altitude of rooting zone [m a.s.l.]	Length (L) [m]	Width (W) [m]	Quotient length/width (L/W)	Average slope [°]	Aspect of front	Aspect of rooting zone	Visible creep structures?	State of activity (mapping result)	Nr. of map sheet (1:25'000)	Aerial photograph: year, nr.
30	Niggeling	Niggel0	2380	-	680	270	2.52	10	NW	WSW	some	relict	1308	1975:6219,6220; 6458,6459 1993:3720,3721
31	Niggeling	Niggel1	2580	2690	260	60	4.3	20	NW	NW	clear	active	1308	"
32	Niggeling	Niggel2	2550	2760	880	170	5.18	15	NW	WNW	clear	active	1308	"
33	Niggeling	Niggel3a	2555	2600	180	380	0.47	10	NW	NW	few	inactive	1308	"
34	Niggeling	Niggel3b	2600	2790	470	110	4.27	24	W	NW	some	inactive	1308	"
35	Niggeling	Niggel4	2750	2840	350	250	1.4	10	NW	NNW	no	active	1308	"
36	Niggeling	Niggel5	2790/2850	2840/ 2870	80	500	0.16	12	W	W	few	inactive	1308	"
37	Niggeling	Niggel6	2650	2740	330	300	1.1	17	SW	SW	few	active	1308	"
38	Niggeling	Niggel7	2600	2670	130	440	0.3	10	SW	S	clear	relict	1308	"
39	Niggeling	Niggel8	2370	2620	670	170	3.94	18	W	SW	some	relict	1308	"

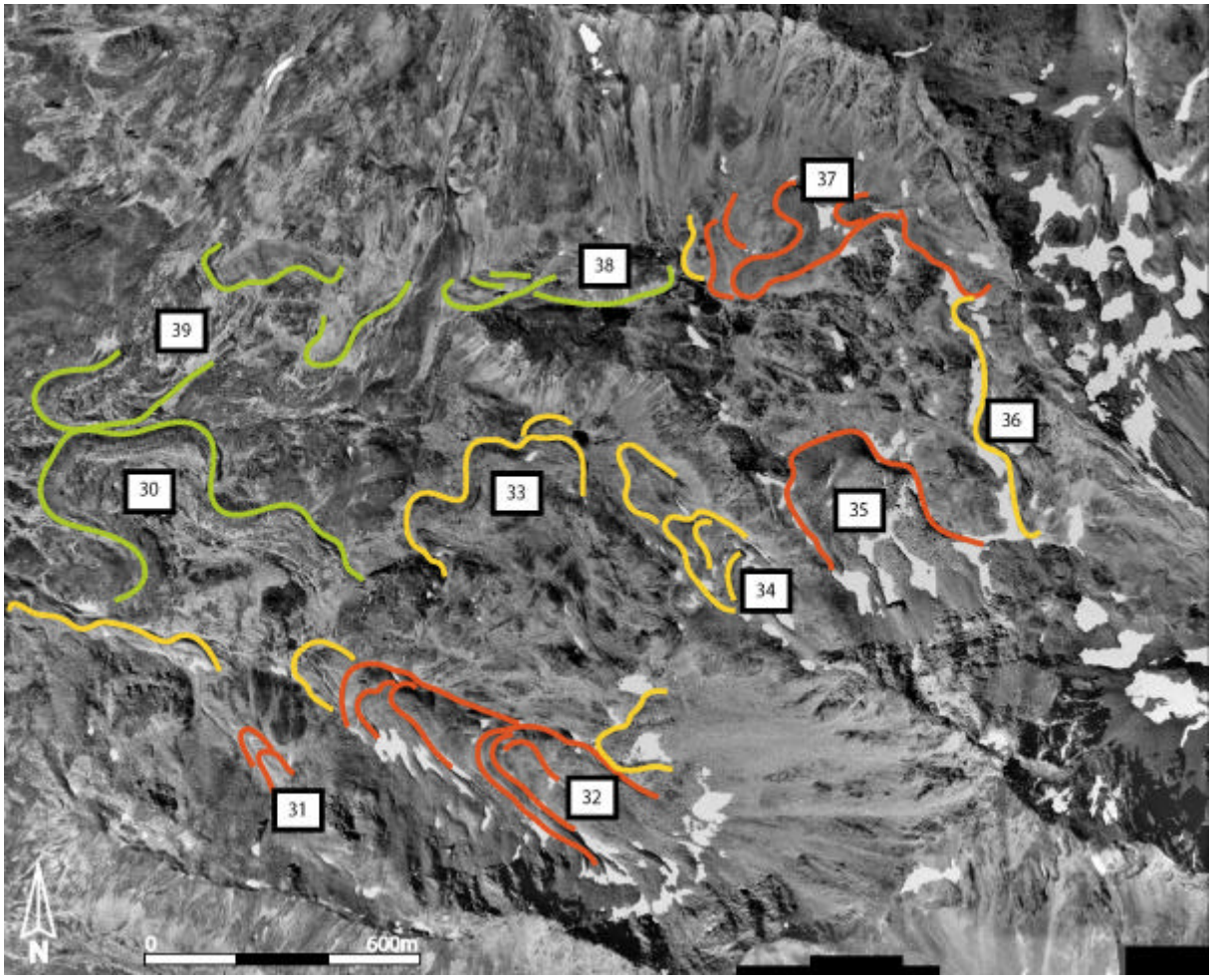

Figure 5.7: Rockglacier occurrence and activity in the Niggelingtälli. Red line = active rockglacier, yellow line = inactive rockglacier, green line = relict rockglacier. Given numbers correspond to the inventory table (table 5.3). Underlying orthophoto of 11.08.1993 (flight-line 20, aerial photographs taken by Swisstopo).

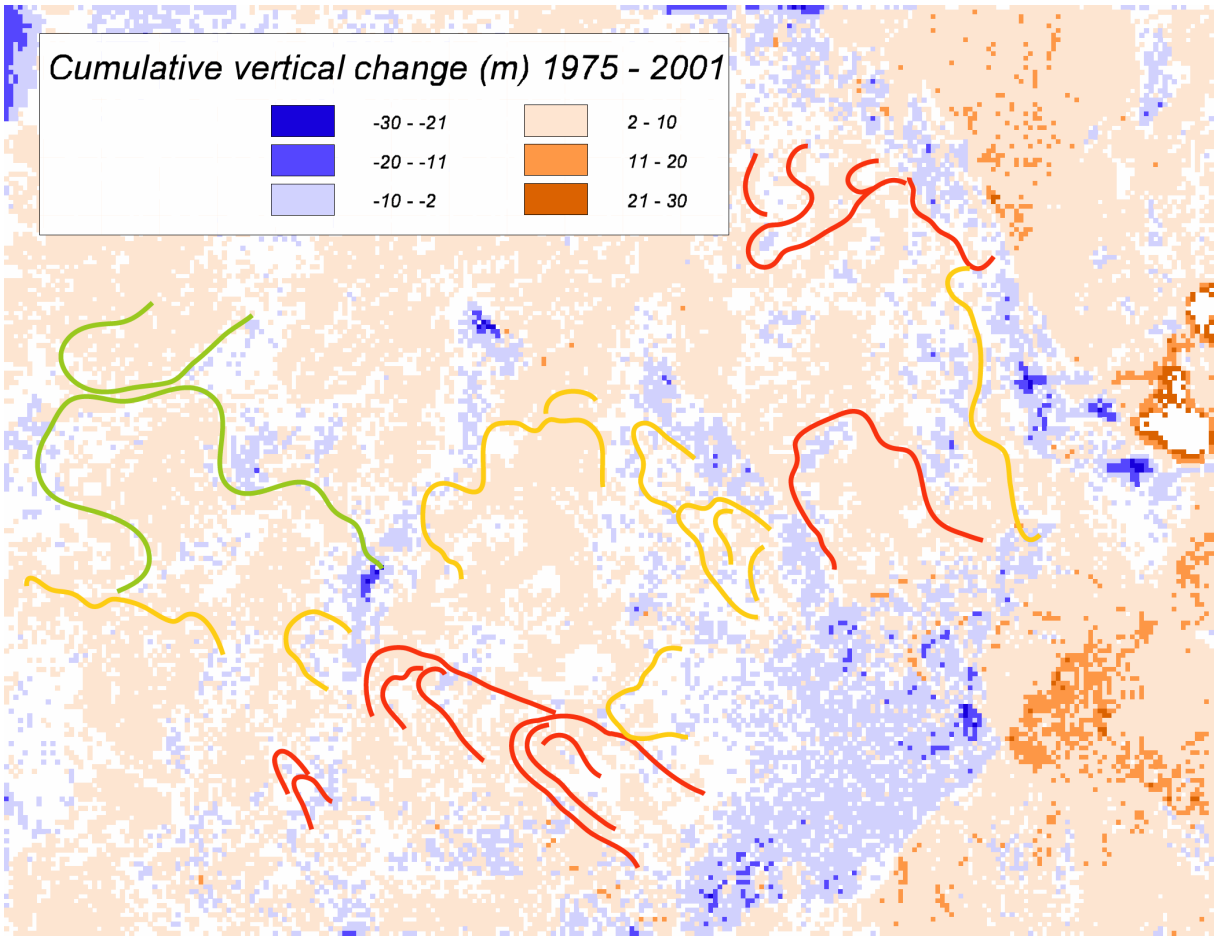

Figure 5.8: Vertical surface changes in the Niggelingtälli between 1975 and 2001 (DTM comparison).

5.1.4 Chummetjitälli

This northernmost hanging valley is not clearly west-east oriented like all the other valleys. With a length of about 2 km and a width of 1.3 km it is also smaller. Prevailing landforms are rockglaciers in the valley bottom and gelifluction lobes on the north-east exposed slope. In some places it was even difficult to distinguish between small rockglaciers and gelifluction lobes. The most striking rockglacier (nr. 40) is situated in the uppermost cirque, which was probably glaciated in former times (figure 5.9). This becomes apparent in the surprisingly fine material and is confirmed by the Siegfried map (sheet 500, St. Niklaus (1891)) which depicts a small glacier on the north exposed slope. Another tongue-shaped rockglacier (nr. 43) occurs directly to the west of the cirque. Due to its vegetation cover it was mapped as inactive. The rockglaciers on the south-west exposed slope are lobate-shaped talus rockglaciers. In the valley bottom which is now densely vegetated, ridges and a front at the valley outlet are interpreted as a relict rockglacier (nr. 44). Additionally, in a position which strictly speaking does not belong to the Chummetjitälli, another rockglacier tongue (nr. 45) is situated below the crest.

The multitemporal comparison of DTMs (figure 5.10) depicts an overall increase in height, beside a few slopes with losses. The high values in the middle of the image and at the front of the

relict rockglacier (nr. 44) are due to shadow-related errors.

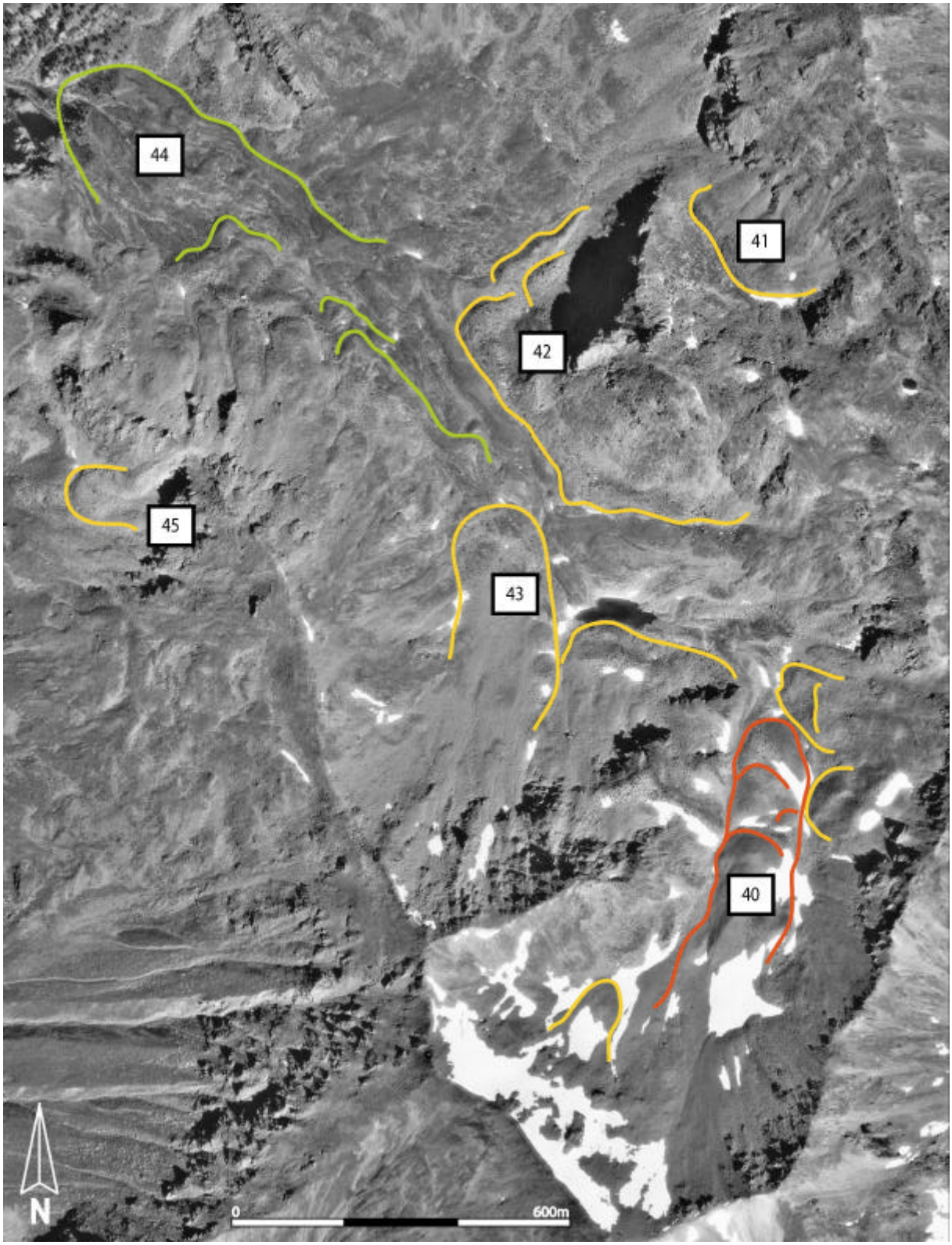

Figure 5.9: Rockglacier occurrence and activity in the Chummetjitälli. Red line = active rockglacier, yellow line = inactive rockglacier, green line = relict rockglacier. Given numbers correspond to the inventory table (table 5.4). Underlying orthophoto of 20.08.1975 (flight-line 22, aerial photographs taken by Swisstopo).

Table 5.4: Rockglacier inventory of the Chummetjitälli.

Nr. inventory	Name of hanging valley	Name of rockglacier, abbreviation	Altitude of rockglacier front (foot) [m a.s.l.]	Altitude of rooting zone [m a.s.l.]	Length (L) [m]	Width (W) [m]	Quotient length/width (L/W)	Average slope [°]	Aspect of front	Aspect of rooting zone	Visible creep structures?	State of activity (mapping result)	Nr. of map sheet (1:25'000)	Aerial photograph: year, nr.
40	Chummetji	Chu1	2650	2780	500	140	3.57	18	N	NE	few	active	1308	1975:6217,6218 1993:3720,3721
41	Chummetji	Chu2	2615	2650	70	230	0.3	16	SW	SW	no	inactive	1288	"
42	Chummetji	Chu3	2470/2540	2500/2570	150	750	0.2	16	WNW /WSW	WNW /WSW	few	inactive	1288	"
43	Chummetji	Chu4	2545	2645	350	170	2.06	22	N	N	few	inactive	1308	"
44	Chummetji	Chu5	2245	2470	750	150	5	12	WNW	NNW	some	relict	1288	"
45	Chummetji	Chu6	2470	2550	150	105	1.43	22	W	W	No	inactive	1308	"

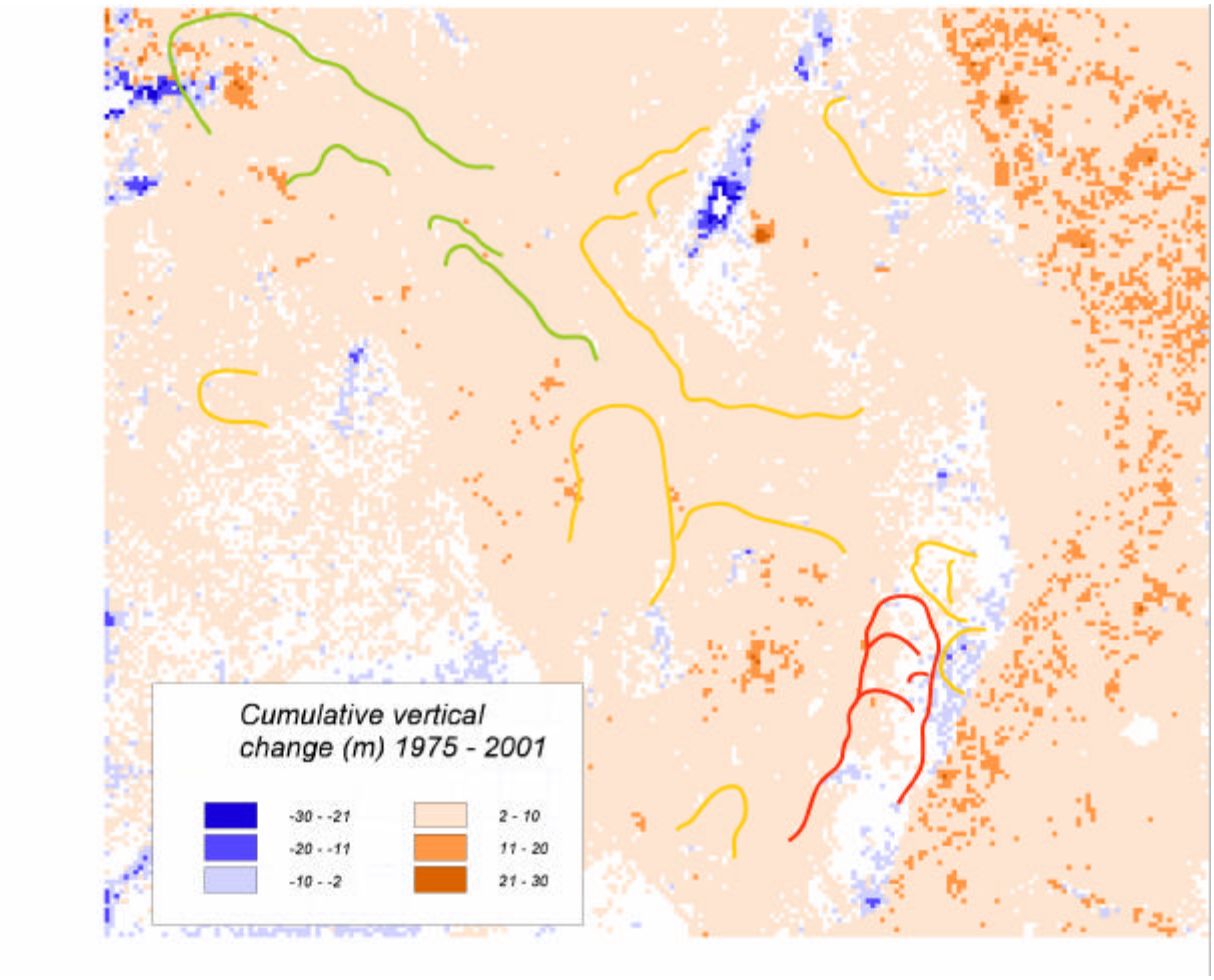

Figure 5.10: Vertical surface changes in the Chummetjitälli between 1975 and 2001 (DTM comparison).

5.1.5 Brändjitälli

The Brändjitälli is situated south of the Hungerlitälli and it spreads over 2.5 km in west-east direction and over 1.7 km from the Hungerlihorli in the north to the Längi Egga in the south. It is divided into the Verlorus Tälli with the Brändji-glacier and the real Brändjitälli. The latter is completely filled by rockglacier sediments, apart from the small Holestei-glacier in the valley head. A spatulate rockglacier (nr. 6) with a distinct ridge-and-furrow topography occurs in the glacier-forefield (figure 5.11). Additionally, a lobate shaped rockglacier (nr. 7) with a relatively flat and unstructured surface built at the orographic left side of the glacier. A former glaciation of this part of the cirque is indicated in the Siegfried map (sheet 500, St. Niklaus (1891)) and is also reflected in the DTM comparison (figure 5.12). The two rockglaciers developed separately due to an outstanding rock in the middle of the valley. Below the front of the spatulate rockglacier, another tongue (nr. 8) is situated, which is rooting in the talus of the north exposed slope. No relict rockglacier was identified in this hanging valley. But since the valley outlet is dammed by a ridge forming a small lake, probable indicators may be covered. Vertical surface changes between 1975 and 2001 are depicted in figure 5.12. The melting of the Brändji-glacier (upper right corner) with up to -40m is most conspicuous. Also the other glaciers show great losses, whereas the forefields reveal slight gains. Some areas on the rockglaciers and in the rockglacier-forefield are very stable. Some high values correspond to shaded areas in the orthophoto and thus reflect errors in the DTMs.

Table 5.5: Rockglacier inventory of the Brändjitälli.

Nr. inventory	Name of hanging valley	Name of rockglacier, abbreviation	Altitude of rockglacier front (foot) [m a.s.l.]	Altitude of rooting zone [m a.s.l.]	Length (L) [m]	Width (W) [m]	Quotient length/width (L/W)	Average slope [°]	Aspect of front	Aspect of rooting zone	Visible creep structures?	State of activity (mapping result)	Nr. of map sheet (1:25'000)	Aerial photograph: year, nr.
6	Brändji	Holestei 1, Brho1	2615	2870	650	170	3.82	22	NW	NW	clear	active	1308	1975:6223,6224 1993:4539-4541
7	Brändji	Holestei 2, Brho2	2820	2870	250	260	0.96	10	NW	WNW	few	active	1308	"
8	Brändji	Längi Egga, Brle	2560	2660	230	75	3.06	13	NW	N	at the front	active	1308	"

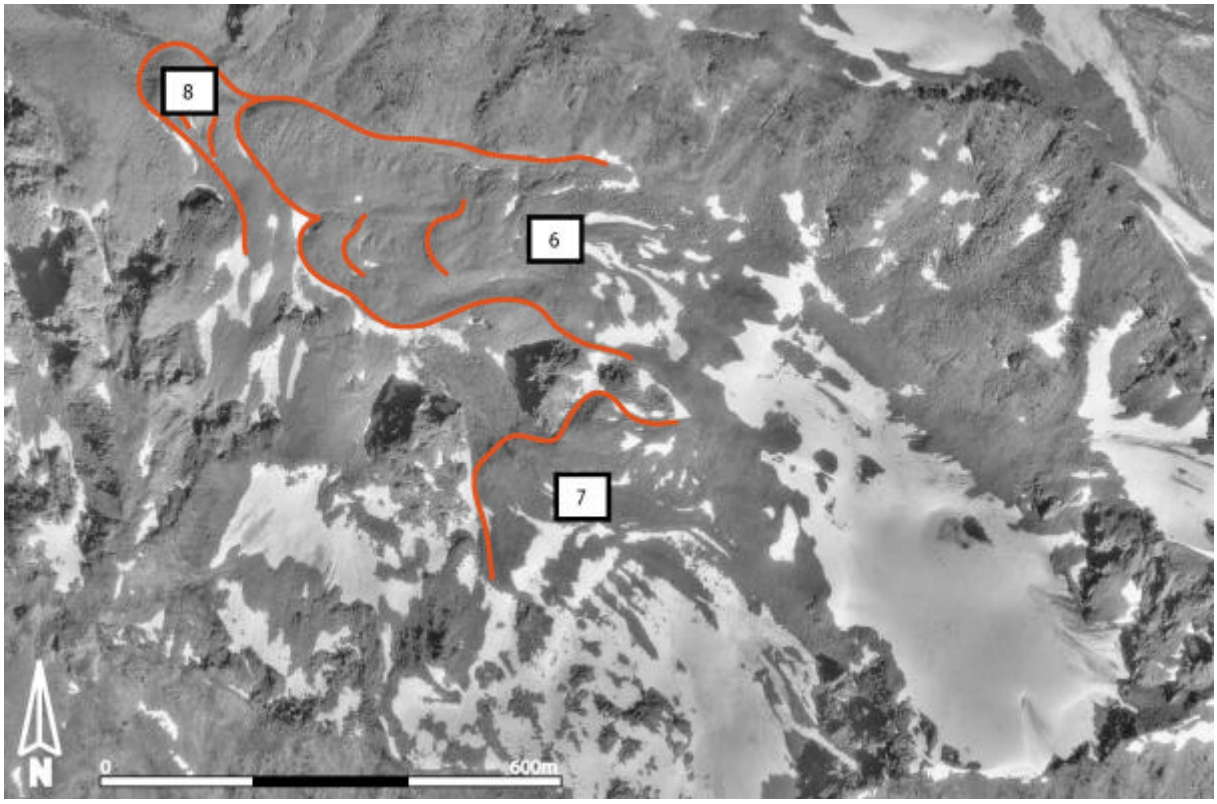

Figure 5.11: Rockglacier occurrence and activity in the Brändjitälli. Red line = active rockglacier. Given numbers correspond to the inventory table (table 5.5). Underlying orthophoto of 20.08.1975 (flight-line 22, aerial photographs taken by Swisstopo).

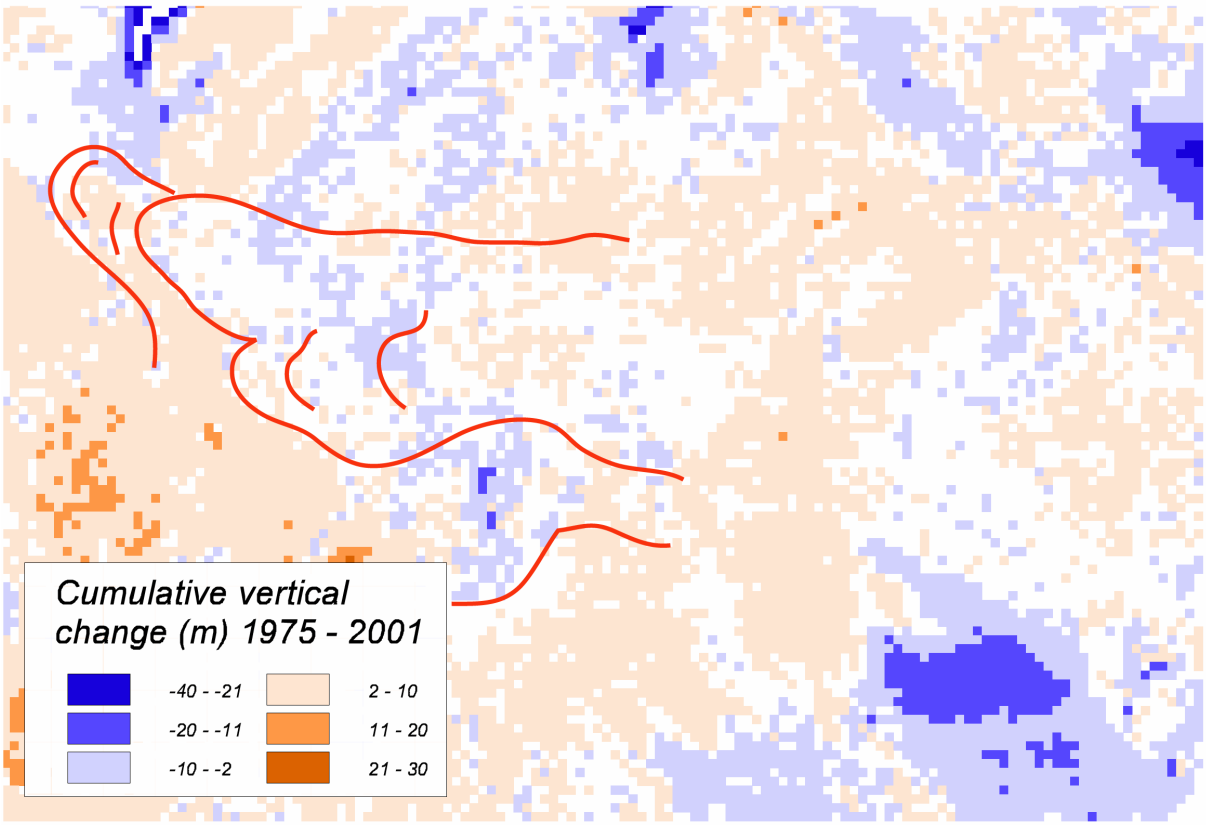

Figure 5.12: Vertical surface changes in the Brändjitälli between 1975 and 2001 (DTM comparison).

5.1.6 Pipjitälli

The Pipjitälli is the southernmost hanging valley and shows a lot of differences compared to the other valleys, which becomes most apparent in the different lithology. While the before mentioned rockglaciers are all composed of the same rock type (gneisses and schists), the landforms in the Pipjitälli consist of marbles and sandstones. The colour of this rock is much lighter and the material is finer grained. The valley extends over 2.5 km from the trough shoulder to the Inneres Stellihorn (3409 m a.s.l.) and over 1 km from the Längi Egga in the north to the Barrwang in the south. The latter is a huge rock face (relief of about 200 m) which casts shadow to the valley. Thus, beside the Pipji-glacier in the east, a debris-covered glacier exists below the rock face in the south. It reveals distinct thermokarst occurrence (figures 5.13, 5.14). Both glaciers are directly connected to rockglaciers filling the valley bottom. The terminal moraine of the Pipji-glacier developed into a polymorphic rockglacier with 3 tongues (nr. 2, 3, 5) indicating different generations. The rooting zone of the rockglacier is hard to determine. The other debris rockglacier (nr. 4) is distinguished from the glacier or dead-ice body by the clear thermokarst depressions. The Barrwang-rockglacier (nr. 1) was identified as a talus rockglacier, but since in the Siegfried map (sheet 500, St. Niklaus (1891)) a glacier was mapped directly at the foot of the rock face, it is also possible that it consists of debris. DTM comparison of the years 1975 and 2001 (figure 5.14) clearly demonstrates the changes within this hanging valley, which refer mainly to the melting of the glacier ice. Due to their mass loss, the extents of the glaciers as well as the thermokarst areas become clearly apparent. The unsorted high values result from errors in the DTMs due to steep slopes or shadows (below the rock face) and margin-effects.

Table 5.6: Rockglacier inventory of the Pipjitälli.

Nr. inventory	Name of hanging valley	Name of rockglacier, abbreviation	Altitude of rockglacier front (foot) [m a.s.l.]	Altitude of rooting zone [m a.s.l.]	Length (L) [m]	Width (W) [m]	Quotient length/width (L/W)	Average slope [°]	Aspect of front	Aspect of rooting zone	Visible creep structures?	State of activity (mapping result)	Nr. of map sheet (1:25'000)	Aerial photograph: year, nr.
1	Pipji	Barrwang, pibw	2650	2760	295	274	1.08	18	NW	N	few	active	1308	1975:6224,6225 1993:4539-4541
2	Pipji	Pipp1	2665	2800	1120	230	4.87	10	W	W	at the front	active	1308	"
3	Pipji	Pipp2	2635	-	97	173	0.56	10	W	-	-	inactive	1308	"
4	Pipji	Pipp3	2650	2700	200	150	1.34	6	NW	N	few	active	1308	"
5	Pipji	Pipp4	2560	-	260	150	1.73	13	W	-	-	inactive	1308	"

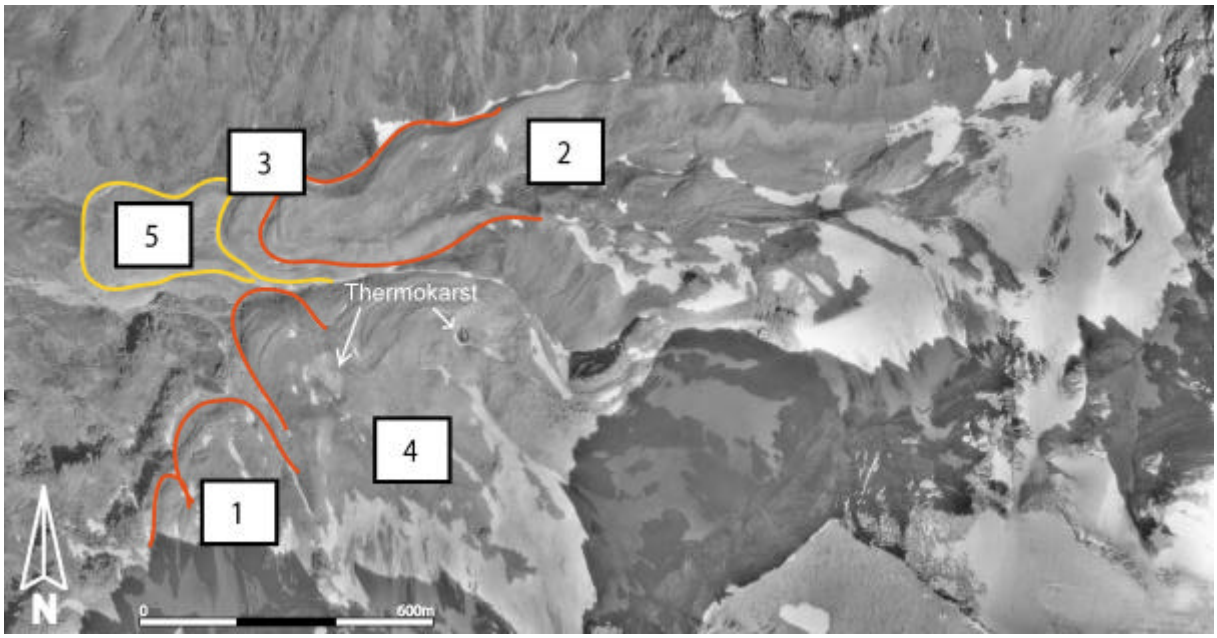

Figure 5.13: Rockglacier occurrence and activity in the Pipjitälli. Red line = active rockglacier, yellow line = inactive rockglacier. Given numbers correspond to the inventory table (table 5.6). Underlying orthophoto of 20.08.1975 (flight line 22, aerial photographs taken by Swisstopo).

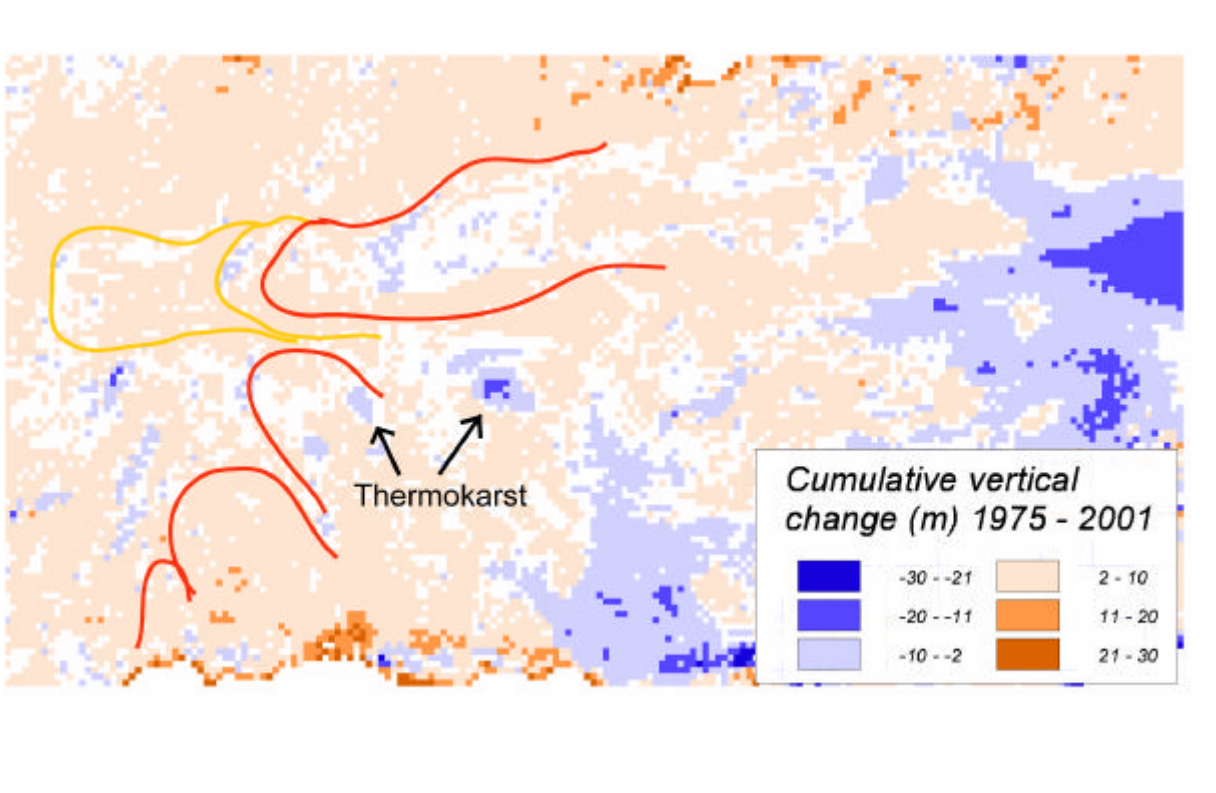

Figure 5.14: Vertical surface changes in the Pipjitälli between 1975 and 2001 (DTM comparison).

5.1.7 Summary

The geomorphic mapping of all hanging valleys (Tällis) on the orographic right side of the Turtmann valley by direct inspection in the field, interpretation of aerial images and the analysis of DTMs, enabled the deduction of rockglacier activity in a geosystematic context.

There is no doubt that rockglaciers are the prevailing landforms; they occur in all Tällis and take up a large part of the area. Considering their activity, 51 % of the rockglaciers are active, 29 % are inactive and 20 % are identified as relict. Although some rockglaciers are mapped with different activities, these values are comparable to the rockglacier mapping of the whole Turtmann valley conducted by Nyenhuis et al. (in press). They classified 46 % of the rockglaciers as active, 29 % as inactive and 25 % as relict. About 55 % of the here investigated rockglaciers occur on north and north-west exposed slope, while 31 % are situated in west exposed and about 13 % in south and south-west facing aspects. Again these data fit very well with the comprehensive inventory by Nyenhuis et al. (in press), who ascertained 53 % of all rockglaciers in north-exposed areas (N, NW, NE), 24 % in southern aspects and 23 % in orientation to the west and the east.

Regarding their spatial distribution, the pattern reflects the difference in radiation which is emphasised by the clear west-east orientation of the hanging valleys. Vertically, the rockglaciers are typically arranged in sequences of different generations. In general, the active rockglaciers are concentrated in altitudes between 2600 and 2800m a.s.l. (front altitude) and on north- and north-west exposed slopes. The rockglaciers Huhh3 (2525m a.s.l.) and Grueo1 (2420m a.s.l.) are the exception. Inactive rockglaciers are often situated off the active ones, with a front altitude below 2600 m a.s.l. Some occur in the base of the hanging valleys (p.e., Hungerlitälli, Grüobtälli), probably due to lower slope-angles or damming landforms like moraines. This kind of inactivity is not controlled by climatic influences or by changes in sediment supply and therefore it is proposed to introduce the new term 'morphologically inactive'. Relict rockglaciers were identified in the northern hanging valleys (Hungerlitälli to Chummetjitälli) and occur in comparable positions. In each of the mentioned valleys, one big rockglacier reached the valley outlet (front altitude between 2240 and 2380m a.s.l.) while others are situated on south exposed slopes (front altitude between 2580 and 2600m a.s.l.). Since no relict rockglacier was mapped in the southern Tällis, this phenomenon seems to be related to the duration of the deglaciation or the ice-free period, respectively. In the Hungerlitälli, where a small glacier is still present, the relict rockglacier (nr. 18), which overruns the Egesen moraine, is more apparent than in the other valleys. Thus, regarding the hanging valleys from north to south, a kind of sequence is visible in the geomorphology: increasing glaciation, decreasing variety and probable age of landforms, etc. A combined consideration of rockglaciers and glaciers allows a temporal organisation of landforms and their genesis, at least in some places. This was detailed for the Hungerlitälli, where the pattern of landforms and their activity depict an asymmetry of the valley, which give rise to the assumption that the Pleistocene glaciation was confined to the north exposed side of the hanging valley. Beside the difference in radiation, this phenomenon may also result from a greater humidity in this area, e.g., due to snow drift.

Regarding the recent vertical changes in the hanging valleys over a period of 26 years (1975 –

2001), the glaciers indicate a conspicuous loss in thickness, whereas changes in the remaining area were much lower, apart from rockglacier Grueo1 (nr. 21). Considering the landforms described above in the context of the sediment budget, all sediments (except solution) seem to be stored in the hanging valleys for several hundreds or thousands of years (cf., Höllermann 1983; Barsch & Caine 1984).

5.2 Digital photogrammetry

Based on the rockglacier inventory (chapter 5.1) all features mapped as inactive or active are investigated by digital photogrammetry. Thus the multitemporal DTMs and orthoimages derived from stereo-imagery are used to determine horizontal velocities as well as vertical changes. First of all, horizontal displacements were quantified over the whole measurement period (1975 – 2001) in order to prove whether the rockglacier is active or not. On the features which are confirmed to be active, horizontal and vertical changes are then measured for both periods (1975 – 1993 and 1993 – 2001) in order to describe spatio-temporal variations. On rockglaciers with high surface velocities often more blocks were matched in the shorter periods than for the entire period, which is probably influenced by the chosen size of the test area in the CIAS-program.
Regarding the illustration of horizontal changes in this chapter, on each rockglacier every single matched block is depicted by a velocity vector indicating the magnitude as well as the direction of the displacement. The magnitude is given by the length of the vector as well as by its colour. Depending on maximum values, the vectors are divided into 3 – 6 classes. The intervals of the classes are normally identical in order to compare velocityfields of different rockglaciers. Since the estimated accuracy of the horizontal velocities lies in the range of 0.06 m/a (for 1975 – 1993) and 0.13 m/a (for 1993 – 2001), the first class (0 – 0.15 m) reflects the range of uncertainty. The second (0.15 – 0.3 m) and the third class (0.3 – 0.5) represent magnitudes which are often measured on rockglaciers (cf., appendix 1) while velocities around 1.0 m and more are rarely quantified.

5.2.1 Pipjitälli

5.2.1.1 Rockglacier Pipp1

Horizontal velocities

The displacement of about 1000 blocks was quantified on rockglacier Pipp1 (nr. 2 of the inventory) in both measurement periods (figures 5.15, 5.16). Between 1975 and 1993 small but uniform velocities of about 0.06 – 0.1 m/a are depicted in the glacier forefield as well as in the central part of the rockglacier. Against that, velocities of 0.3 – 0.6 m/a are measured on the orographic right side of the rockglacier respectively the lateral moraine. Here the vectors are directed to the central flowline of the rockglacier, and - with decreasing slope – the displacements become smaller again. Closer to the front, the velocities increase again showing a gradient from 0.08 – 0.14 – 0.23 m/a and depict highest velocities (0.35 – 0.7 m/a) in the centre of the lobe, directly above the front. In the second period (1993 – 2001) Pipp1 shows a similar pattern of velocityfields, but the values are slightly higher, especially in the lower part of the rockglacier (figure 5.16). Due to snow cover in the 2001 orthoimage and the corresponding loss in coherence, measurements were inhibited in the upper orographic left part of the rockglacier. On the opposite slope, i.e. on the lateral moraine, high velocities (1.0 – 2.0 m/a) are quantified in the upper part near the current glacier tongue. Further down (to the west) velocities become smaller (at about 0.1 m/a) and the vectors are clearly directed to the glacier. With changing orientation of the vectors (in direction to the rockglacier front) the velocities increase again (0.22 – 0.34 m/a)

and display a small area with values up to 0.6 m/a. In the lower part of the rockglacier a gradient from 0.26 – 0.5 – 1.0 m/a is measured in the central flowline, while to the margins the velocities are below 0.1 m/a. At the front, values are quite high with velocities between 0.45 and 0.7 m/a.

Vertical changes

On rockglacier Pipp1 the cumulative vertical change, quantified by comparison of multitemporal DTMs, shows different patterns in the two investigated periods. Between 1975 and 1993 a thinning of -2 - -5 m, i. e. of -0.1 - -0.3 m/a, is depicted on the orographic right side of the rockglacier (figure 5.17). The lower part of the tongue reveals no significant vertical changes. Against that, a widespread thickening (2 – 5 m; 0.25 – 0.6 m/a) occurred between 1993 and 2001 (figure 5.18), apart from the middle part of the rockglacier tongue, where horizontal velocities showed the highest values.

The debris rockglacier Pipp1 depicts a very interesting and unique feature in the study area. It is clearly an active rockglacier, which shows increased velocities in the second period. The combined analysis of horizontal and vertical displacements indicates a shifting of mass in the lower part of the rockglacier resulting from changes in flow balance (cf., chapter 2.3.5).

A differentiation between the rockglacier area and the glacier forefield is not clearly indicated in the velocityfield. Thus, the root zone of the rockglacier is hard to define and seems to be represented in a transition zone. Probably the 'real' rockglacier occurs only in the lower part of the investigated object. Hence the movements on the orographic right lateral moraine either reflect permafrost creep probably not connected to the rockglacier mass or another continuous process (e.g. landsliding).

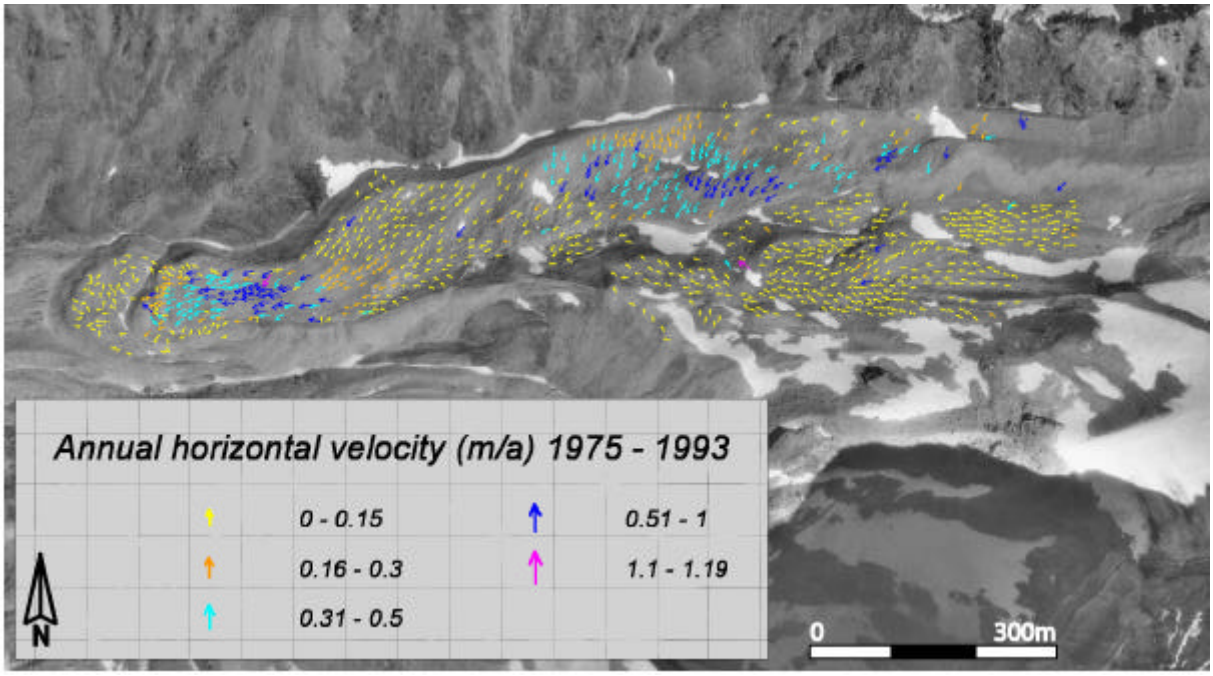

Figure 5.15: Mean annual surface velocities between 1975 and 1993 on the rockglaciers Pipp1 and Pipp2. Underlying orthoimage of 20.08.1975 (flight line 22, aerial photographs taken by Swisstopo).

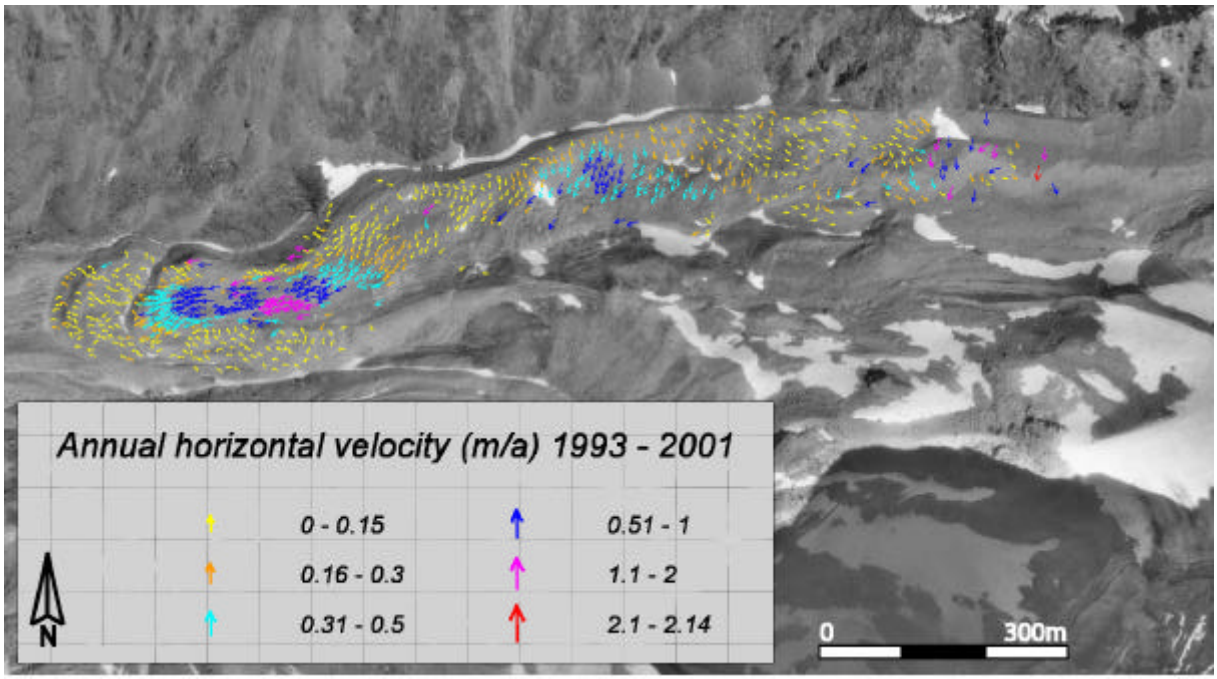

Figure 5.16: Mean annual surface velocities between 1993 and 2001 on the rockglaciers Pipp1 and Pipp2. Underlying orthoimage of 20.08.1975 (flight line 22, aerial photographs taken by Swisstopo).

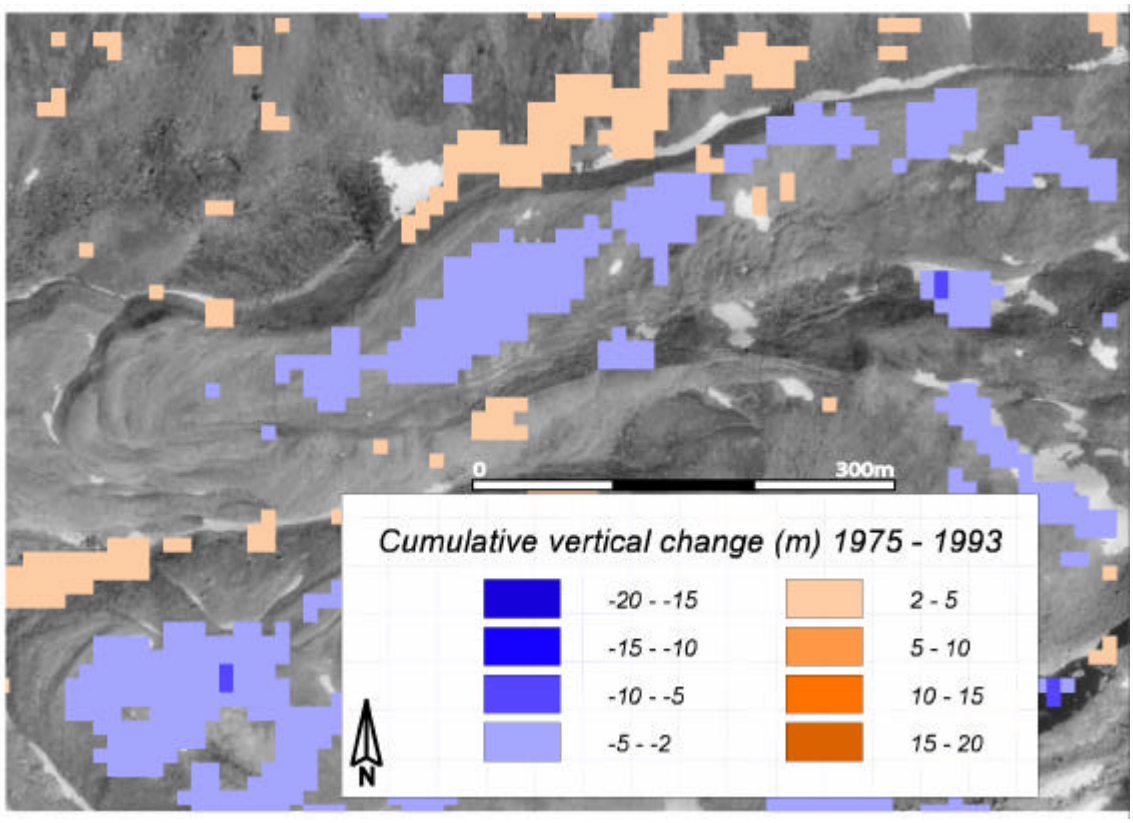

Figure 5.17: Cumulative vertical change on rockglacier Pipp1 between 1975 and 1993 (smoothed by a median-filter, window size 3x3). Underlying orthoimage of 20.08.1975 (flight line 22, aerial photographs taken by Swisstopo).

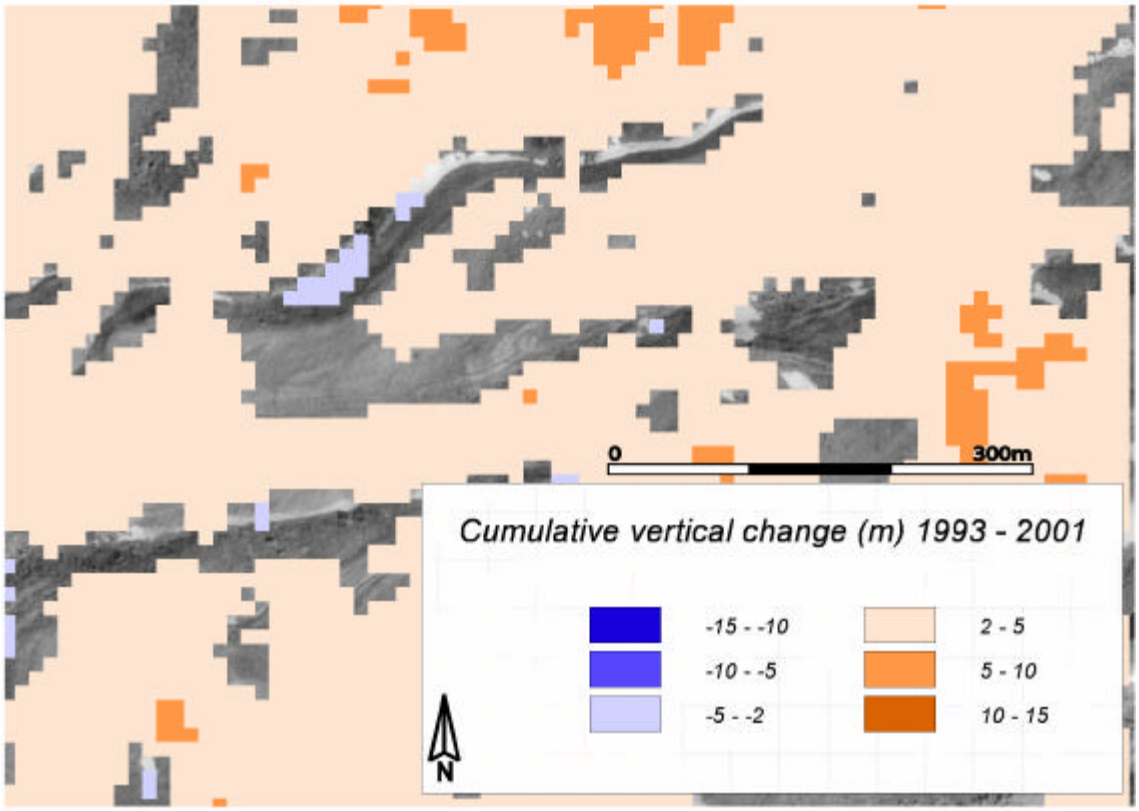

Figure 5.18: Cumulative vertical change on rockglacier Pipp1 between 1993 and 2001 (smoothed by a median-filter, window size 3x3). Underlying orthoimage of 20.08.1975 (flight line 22, aerial photographs taken by Swisstopo).

5.2.1.2 Rockglacier Pipp2

Horizontal velocities

Rockglacier Pipp2 (nr. 3 of the inventory) is situated off rockglacier Pipp1 and is therefore integrated in the figures 5.15 and 5.16. In spite of the small size of the feature, about 50 blocks were matched at its surface in each measurement period. In both periods most vectors depict uniform velocities below 0.1 m/a. Between 1993 and 2001 single blocks moved with slightly higher velocities. More distinct differences are indicated in the orientation of the vectors. While in the first period (1975 – 1993) they are often arranged in a whirl and thus underline the inactivity of the feature, they show a clear downslope orientation in the second period (1993 – 2001).

Vertical changes

Regarding the vertical component, rockglacier Pipp2 depicts no changes in the first period (1975 – 1993), whereas a widespread thickening (2 - 5 m; 0.25 – 0.6 m/a) is indicated between 1993 and 2001 (figures 5.17, 5.18).

Rockglacier Pipp2, which was mapped as inactive, shows no clear behaviour in the investigated period. Generally an inactive state seems to be appropriate due to the low velocities, which are at least in the second period below the level of significance (0.13 m/a). But, a possible 'activation' is indicated between 1993 and 2001. Probably this 'activation' results from the increased velocities on rockglacier Pipp1. Thus, the lobe is pushed by the other rockglacier and a passive movement is reflected in the horizontal displacements as well as in the vertical thickening.

5.2.1.3 Rockglacier Pipp3

Rockglacier Pipp3 (nr. 5 of the inventory) is situated below the before described rockglaciers and like the lobe of Pipp2 it represents an older generation of Pipp1. A simple comparison of orthoimages (by flickering of the images 1975 and 2001) revealed no movements on this feature. Thus, the inactivity of the rockglacier was confirmed and the block-matching program (CIAS) as well as the DTM comparison was not applied.

5.2.1.4 Rockglacier Pipp4

Horizontal velocities

Also on this rockglacier (nr. 4 of the inventory), which was mapped as an active one, the comparison of orthoimages by flickering showed no significant displacements. Apart from that, surface changes occur in the thermokarst areas and movements are revealed in the root zone which is probably affected by a glacier. Therefore, CIAS was applied to quantify these movements over the entire period 1975 – 2001. Due to shadows and snow cover, especially in the orthoimage of 2001, only a few blocks were matched by the program. The vectors depicted in figure 5.19 show very diverse magnitudes and directions. In the centre of the vectorfield some blocks depict a flowline with creep rates between 0.17 and 0.29 m/a and thus indicate activity.

Vertical changes

Regarding the vertical changes between 1975 and 2001, great losses (up to 20 m; 0.8 m/a) are depicted in figure 5.14, which result from thermokarst occurrence and the melting glacier in the root zone.

Since a clear differentiation of the rockglacier and the glacial affected area is not possible, the measured horizontal velocities in the root zone are not included in the activity assessment of Pipp4. Probably, the small terminal lobe depicts the only part affected by permafrost creep. Since this lobe revealed no significant horizontal displacements and only small vertical changes it seems to be inactive.

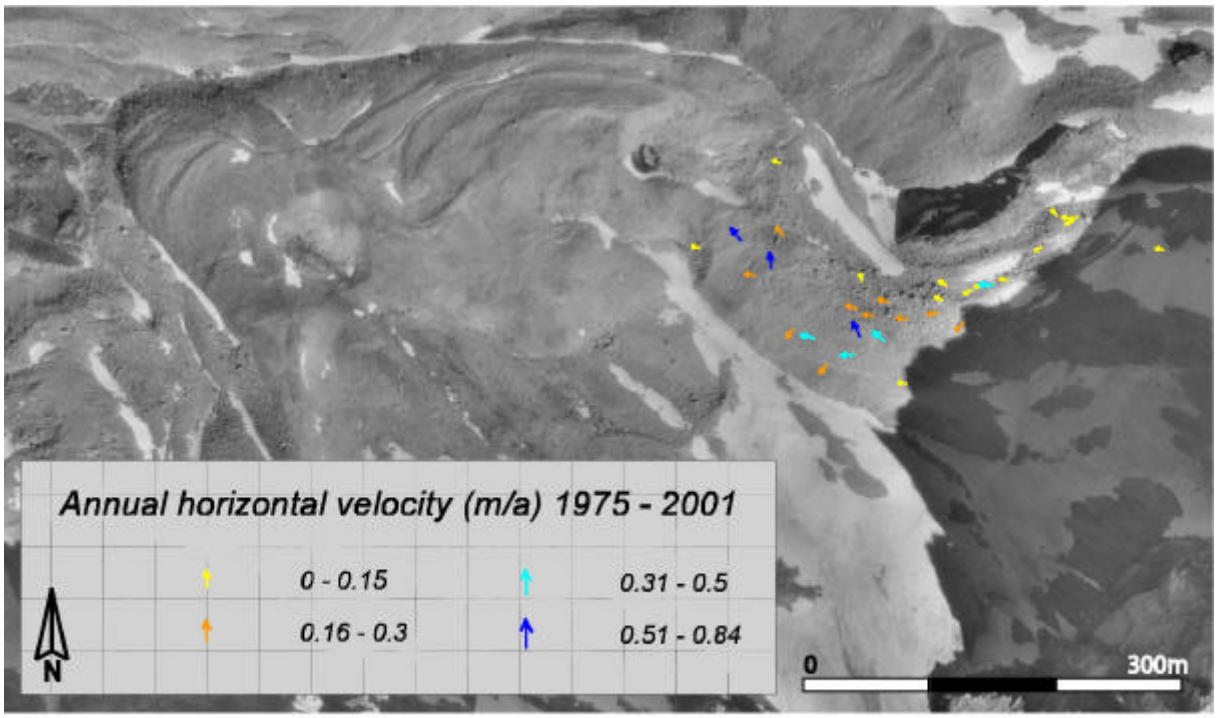

Figure 5.19: Mean annual surface velocities 1975 – 2001 on the rockglacier Pipp4. Underlying orthoimage of 20.08.1975 (flight line 22, aerial photographs taken by Swisstopo).

5.2.1.5 Rockglacier Pibw

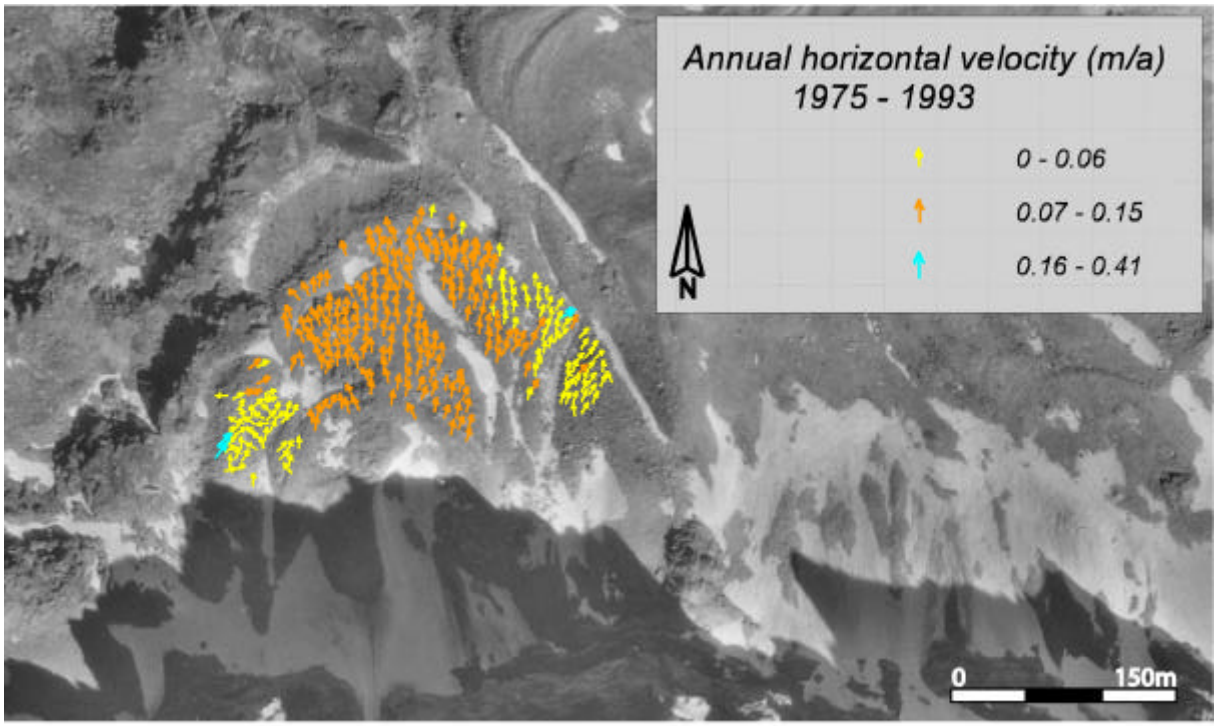

Figure 5.20: Mean annual surface velocities 1975 – 1993 on the rockglacier Pibw. Underlying orthoimage of 20.08.1975 (flight line 22, aerial photographs taken by Swisstopo).

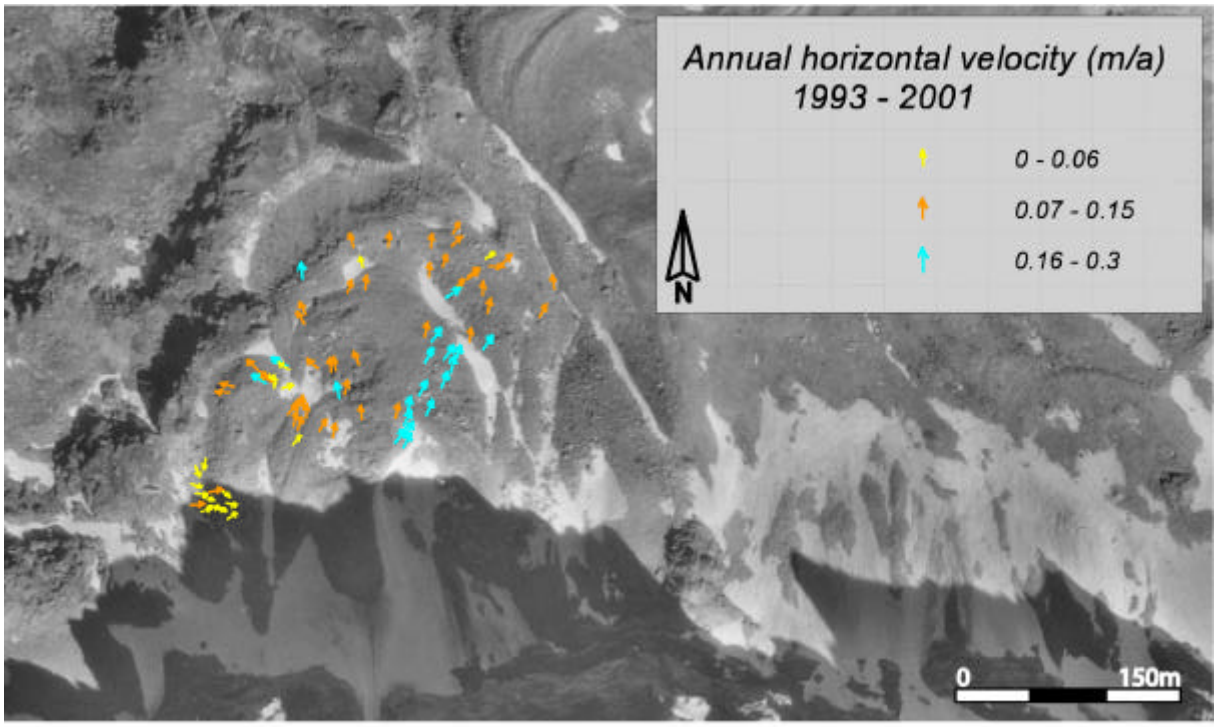

Figure 5.21: Mean annual surface velocities 1993 – 2001 on the rockglacier Pibw. Underlying orthoimage of 20.08.1975 (flight line 22, aerial photographs taken by Swisstopo).

Horizontal velocities

Over the first investigated period (1975 – 1993) a lot of blocks were matched on the surface of rockglacier Pibw (nr. 1 of the inventory) apart from the root zone which is situated in the shadow of the Barrwang-wall in the south. The vectors present a uniform flowfield (figure 5.20). At the margins of the rockglacier (orographic left and right parts) the velocities are in the range of uncertainty (up to 0.06 m/a), whereas they amount to 0.15 m/a in the central part.

Against that, only a few blocks were matched between 1993 and 2001 (figure 5.21) due to snow in the orthoimage of 2001. The middle part of the lobe reveals velocities between 0.06 and 0.15 m/a with up to 0.3 m/a in a central flowline. At the orographic left margin small displacements (< 0.06 m/a) with an upslope orientation are depicted, probably indicating the inactivity of this part.

Vertical changes

The cumulative vertical changes on Pibw between 1975 and 1993 show a slight thickening at the front and a slight thinning on the orographic right side, while the major part of the rockglacier depicts no significant changes (figure 5.22). Due to errors of the DTMs in shaded and snow-covered areas, the root zone of the rockglacier is not included in the interpretation. This is also valid for the second period (1993 – 2001), where the whole permafrost body shows an increase in thickness between 2 and 5 m (0.25 – 0.6 m/a) and up to 10 m (1.25 m/a) in the central part (figure 5.23).

The lobe-shaped rockglacier Pibw is a clearly active feature, which reveals increased velocities in the second period. The vertical change shows a distinct gain in mass between 1993 and 2001 probably resulting from debris input out of the steep wall above the root zone.

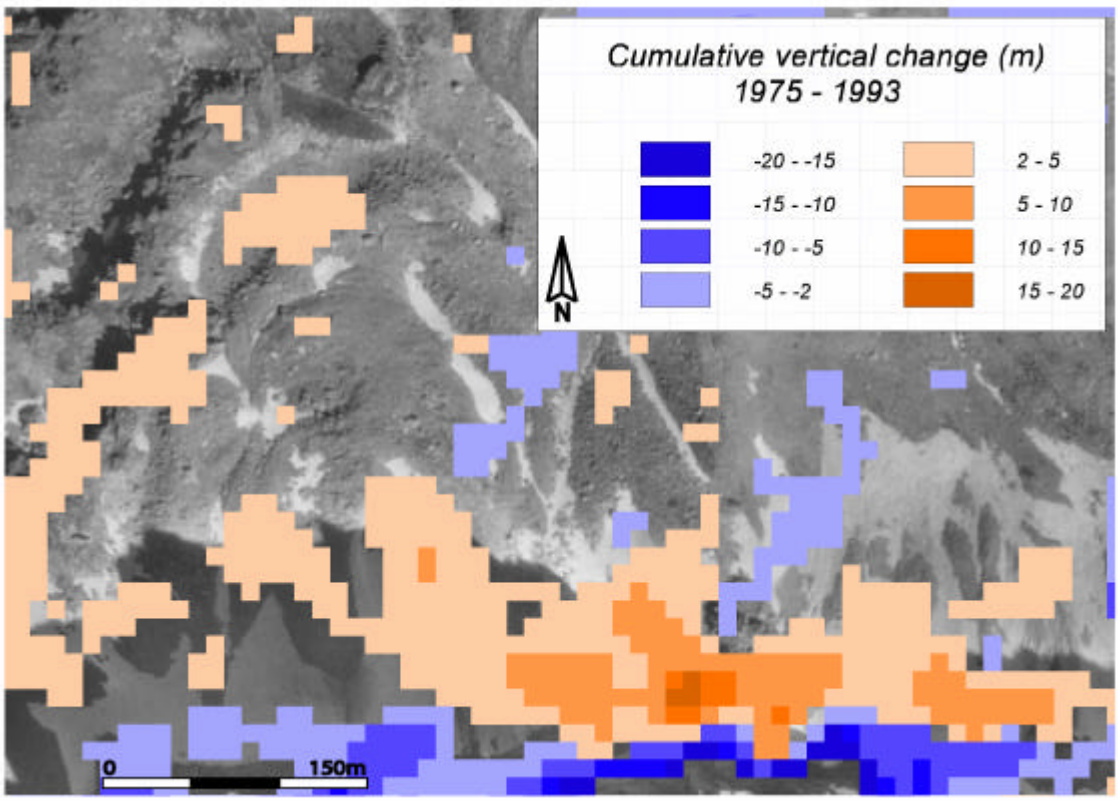

Figure 5.22: Cumulative vertical change on rockglacier Pibw between 1975 and 1993 (smoothed by a median-filter, window size 3x3). Underlying orthoimage of 20.08.1975 (flight line 22, aerial photographs taken by Swisstopo).

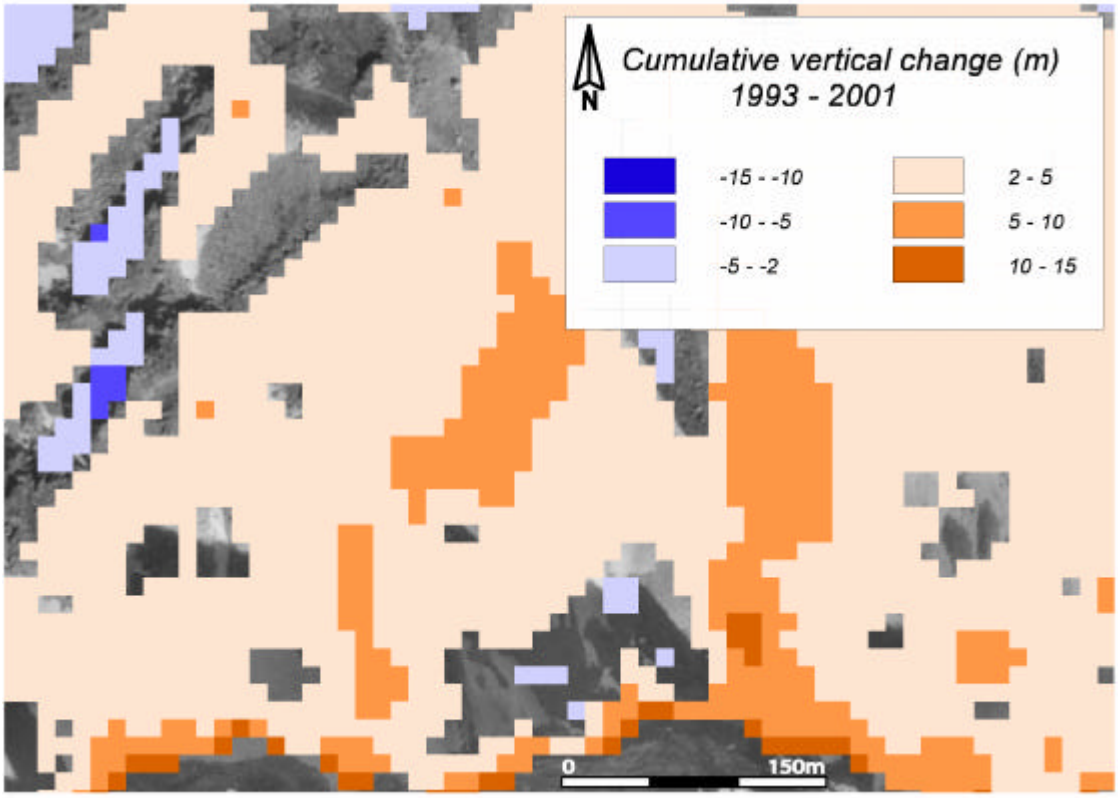

Figure 5.23: Cumulative vertical change on rockglacier Pibw between 1993 and 2001 (smoothed by a median-filter, window size 3x3). Underlying orthoimage of 20.08.1975 (flight line 22, aerial photographs taken by Swisstopo).

5.2.2 Brändjitälli

5.2.2.1 Rockglacier Brho1

Horizontal velocities

On rockglacier Brho1 (nr. 6 of the inventory) the displacement of more than 1000 blocks was quantified in both investigated periods (figures 5.24, 5.25). Due to snowpatches in the root zone the data are limited in this area. In the first period (1975 – 1993) a large part of the rockglacier depicts small movement rates. In the lower part, on both lobes of the divided tongue, the velocities are below 0.06 m/a and thus in the range of uncertainty. Additionally, the vectors are oriented in diverse directions and in some places are arranged in a whirl. Therefore, inactivity is assumed for the lower part of rockglacier Brho1. Against that, the upper part shows clear activity indicated in uniform velocityfields including a distinct direction of the creeping mass. At the margins the velocities are low (0.08 – 0.12 m/a) but outside the range of uncertainty. To the centre of the rockglacier the rates increase significantly in concentric fields with highest values between 0.5 and 0.6 m/a. A second high-velocityfield (0.6 – 1.0 m/a) is depicted at the orographic left part of the upper front while the right part shows rates of about 0.2 m/a.
In the second investigated period (1993 – 2001) some differences are depicted in the velocityfields (figure 5.25). Again, the lower part of the rockglacier mostly shows movement rates below 0.15 m/a (range of uncertainty) and diverse directions. But, at the lowermost front a uniform field with higher rates (between 0.18 and 0.32 m/a) occurs. In the upper part, velocities are significantly higher than in the first period. The central flowline shows values at about 1.0 m/a while the upper front (orographic left) reveals maximum velocities of 2.0 m/a.

Vertical changes

By comparison of multitemporal DTMs, vertical changes are quantified on rockglacier Brho1 between 1975 and 2001. In the first period (1975 – 1993) a cumulative thinning of -2 - -5 m (-0.1 - -0.3 m/a) is indicated in the orographic right part of the lower lobe (figure 5.26). A comparable thinning is also depicted on the orographic left side directly at the upper front while further down an increase in elevation is revealed. Thus, the advance of the clearly active front is shown in the vertical changes. Between 1993 and 2001 (figure 5.27) again a decrease in elevation (-2 - -5 m; -0.25 - -0.6 m/a) is quantified at the upper front on the orographic left side and in a small area on orographic right side of the lower lobe. The rest of the rockglacier surface reveals nearly no changes. In the 'reactivated' area at the lowermost front a slight thinning is indicated, probably resulting from a change in flow balance.

Brho1 is a very complex and interesting rockglacier. The flat lower part depicts inactivity, apart from the lowermost front showing a reactivation between 1993 and 2001. Regarding the vertical changes, the surface is very stable and shows only partial thinning, which may result from mass balance changes. Against that, the upper lobe is clearly active and reveals a distinct speed-up in the second period. Thus, the vertical changes at the upper front emphasise the change in flow balance, at least in the first period.

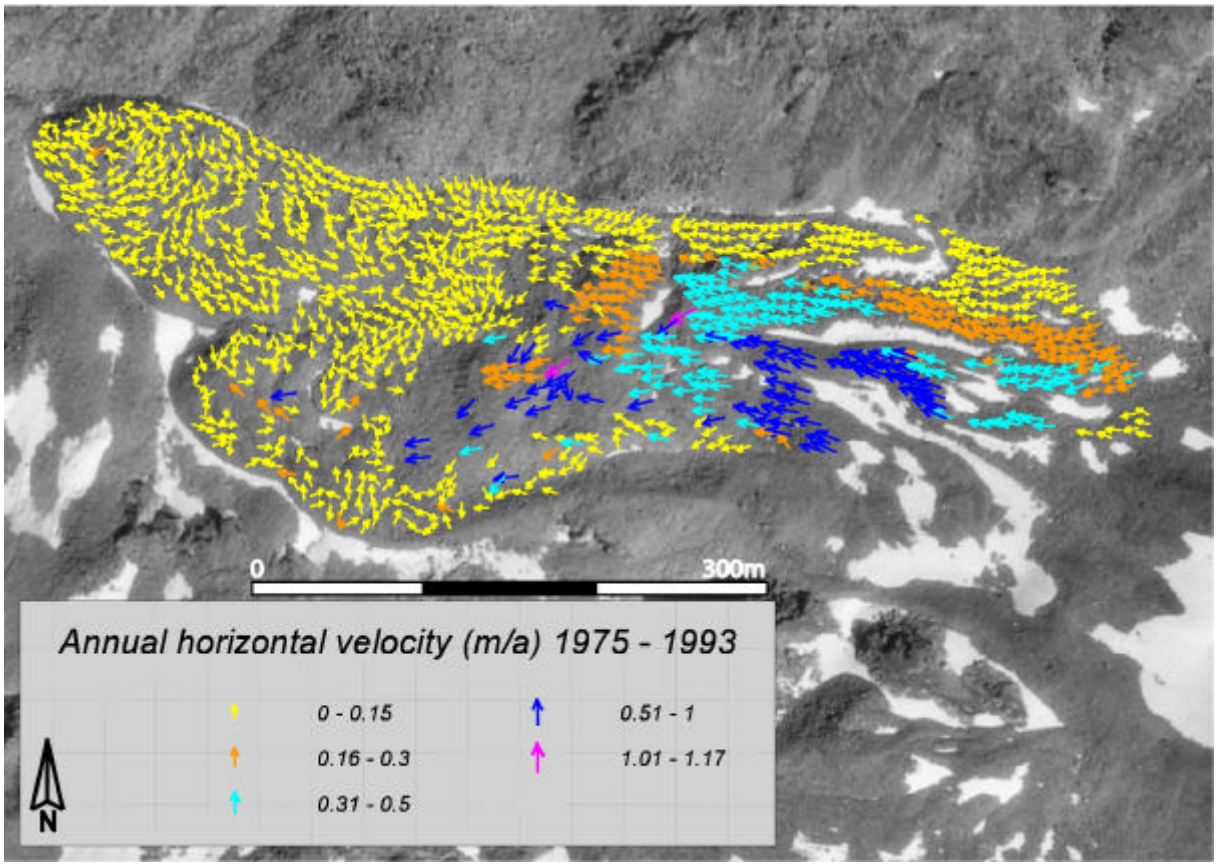

Figure 5.24: Mean annual surface velocities 1975 – 1993 on the rockglacier Brho1. Underlying orthoimage of 20.08.1975 (flight line 22, aerial photographs taken by Swisstopo).

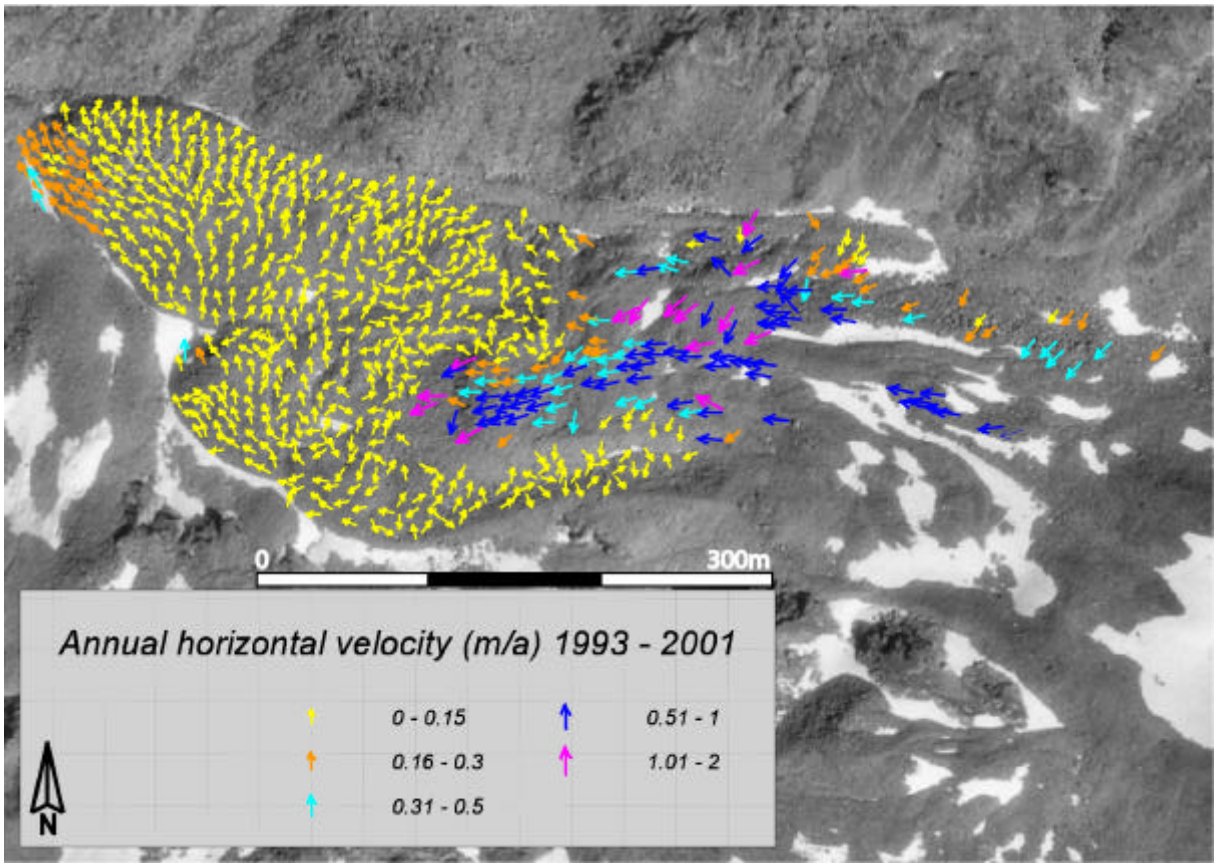

Figure 5.25: Mean annual surface velocities 1993 – 2001 on the rockglacier Brho1. Underlying orthoimage of 20.08.1975 (flight line 22, aerial photographs taken by Swisstopo).

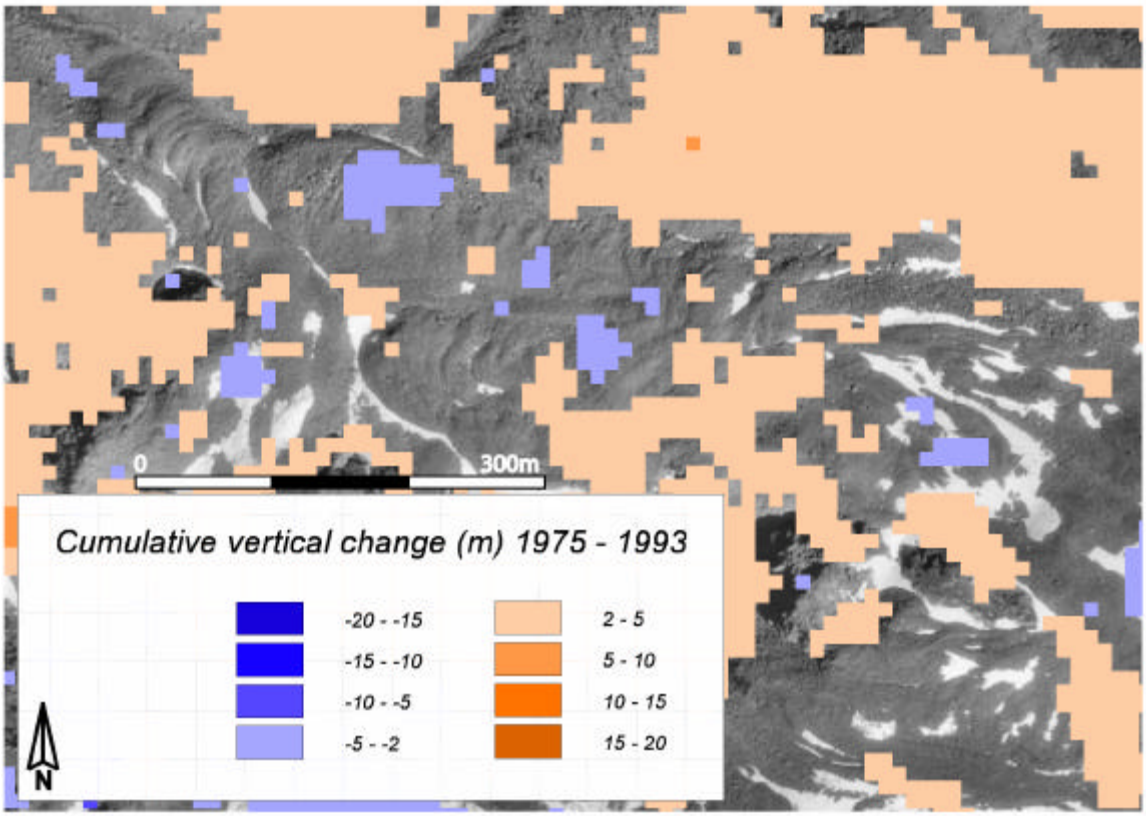

Figure 5.26: Cumulative vertical change on the rockglaciers Brho1 and Brle between 1975 and 1993 (smoothed by a median-filter, window size 3x3). Underlying orthoimage of 20.08.1975 (flight line 22, aerial photographs taken by Swisstopo).

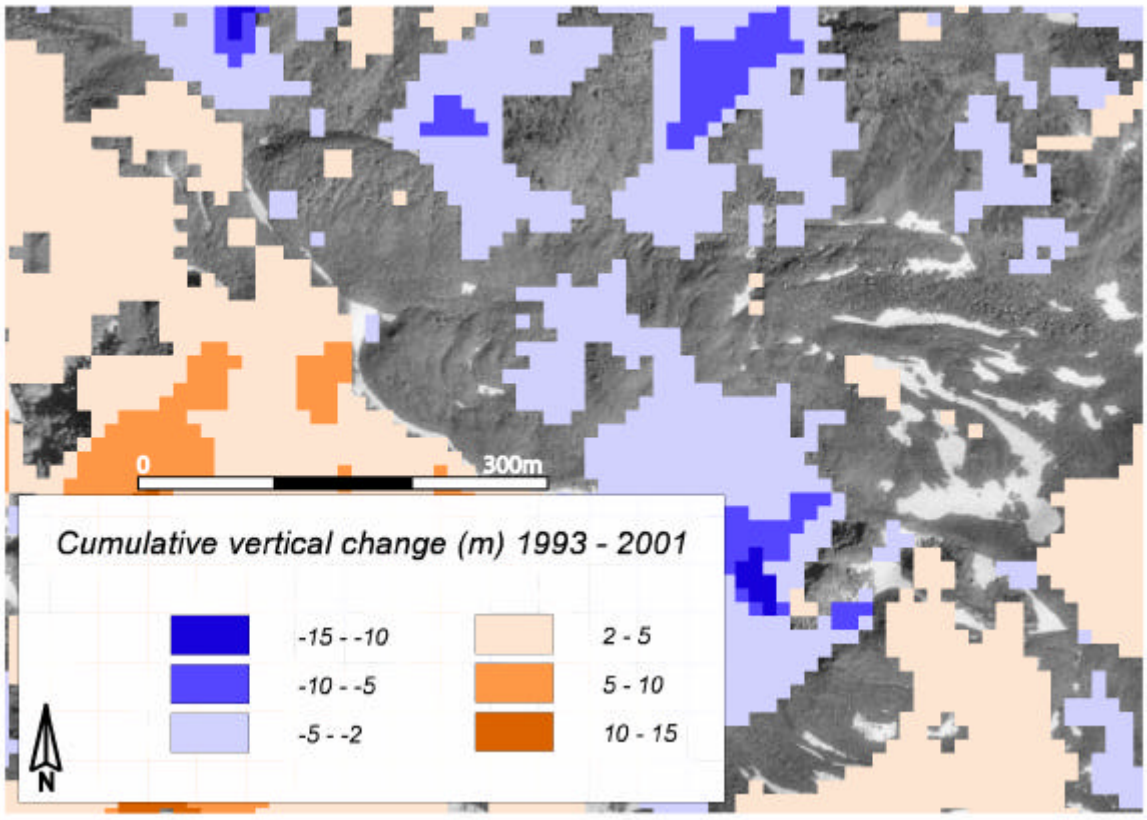

Figure 5.27: Cumulative vertical change on the rockglaciers Brho1 and Brle between 1993 and 2001 (smoothed by a median-filter, window size 3x3). Underlying orthoimage of 20.08.1975 (flight line 22, aerial photographs taken by Swisstopo).

5.2.2.2 Rockglacier Brho2

Horizontal velocities

The rockglacier Brho2 (nr. 7 of the inventory) displayed only small movements in the comparison of orthoimages (flickering). Therefore, velocities were quantified over the entire period (1993 – 2001), but due to poor coherence (snow on the orthoimage of 2001) only a few blocks were matched by the program. They indicate velocities between 0.3 and 0.45 m/a at the front and values between 0.05 and 0.15 m/a in the upper part. Since the range of uncertainty is determined to lie below 0.04 m/a for the entire period, the velocities confirm the activity of the feature.

Vertical changes

Vertical changes on Brho2 are displayed in figure 5.12 for the entire period 1975 - 2001. While the upper part of the rockglacier is influenced by melting of glacier ice (-2 – 10 m; -0.08 - -0.4 m/a), the lower part depicts a cumulative increase of the surface (2 – 10 m; 0.08 – 0.4 m/a).

5.2.2.3 Rockglacier Brle

Horizontal velocities

On rockglacier Brle (nr. 8 of the inventory) creep rates were quantified for both measurement periods (figures 5.28, 5.29). In the first period (1975 – 1993) velocities in the lowermost part are below 0.05 m/a and are arranged irregularly. Further up they show rates between 0.1 and 0.16 m/a combined with a uniform orientation. Single blocks depict higher velocities.

Between 1993 and 2001 velocities increased significantly in the middle part of the rockglacier and show a uniform vectorfield of about 0.3 m/a. In the steep upper part rates between 0.12 and 0.15 m/a are depicted. At the front the displacements are in the range of uncertainty, but in comparison to the first investigated period they show a clear direction.

Vertical changes

Between 1975 and 1993 cumulative vertical changes are very scattered (figure 5.26). A small field in the middle part of the rockglacier indicates a slight thickening (2 – 5 m; 0.1 – 0.3 m/a). Against that, a distinct increase in thickness (in some places up to 10 m; 1.25 m/a) is depicted in great parts of the rockglacier in the second period (1993 - 2001) (figure 5.27).

Concerning the horizontal velocities, a distinct speed-up is monitored on rockglacier Brle in the second period. This coincides well with the reactivation at the front of Brho1, which is directly adjoining. The displacements show very similar magnitudes and directions and therefore seem to build one creeping mass. Thus, even if the two permafrost bodies are separated at the surface by the steep front of rockglacier Brho1, they are probably connected in depth. The vertical changes reveal a distinct thickening between 1993 and 2001. In this pattern probably different processes are revealed. While the upper part shows mass gains (e.g., by debris input), changes in flow balance are likely to occur in the lower part.

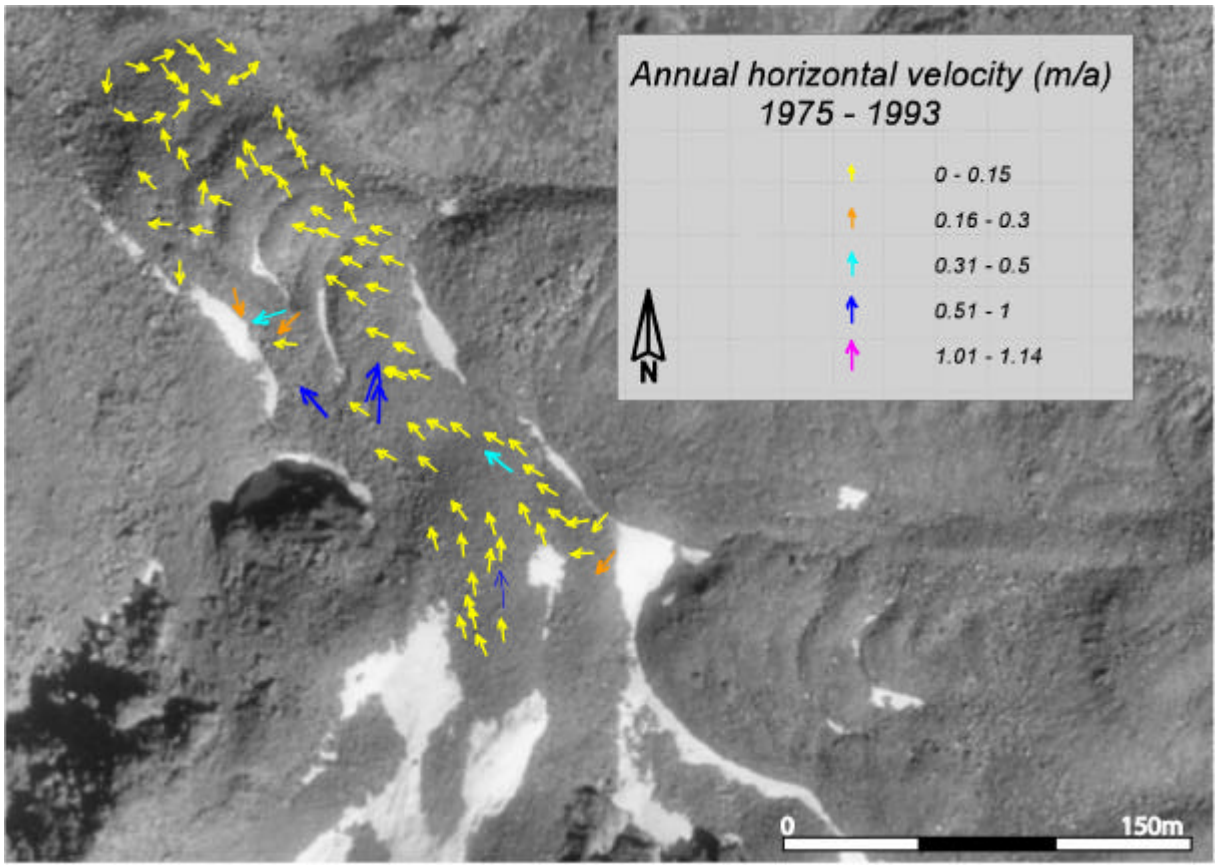

Figure 5.28: Mean annual surface velocities 1975 – 1993 on the rockglacier Brle. Underlying orthoimage of 20.08.1975 (flight line 22, aerial photographs taken by Swisstopo).

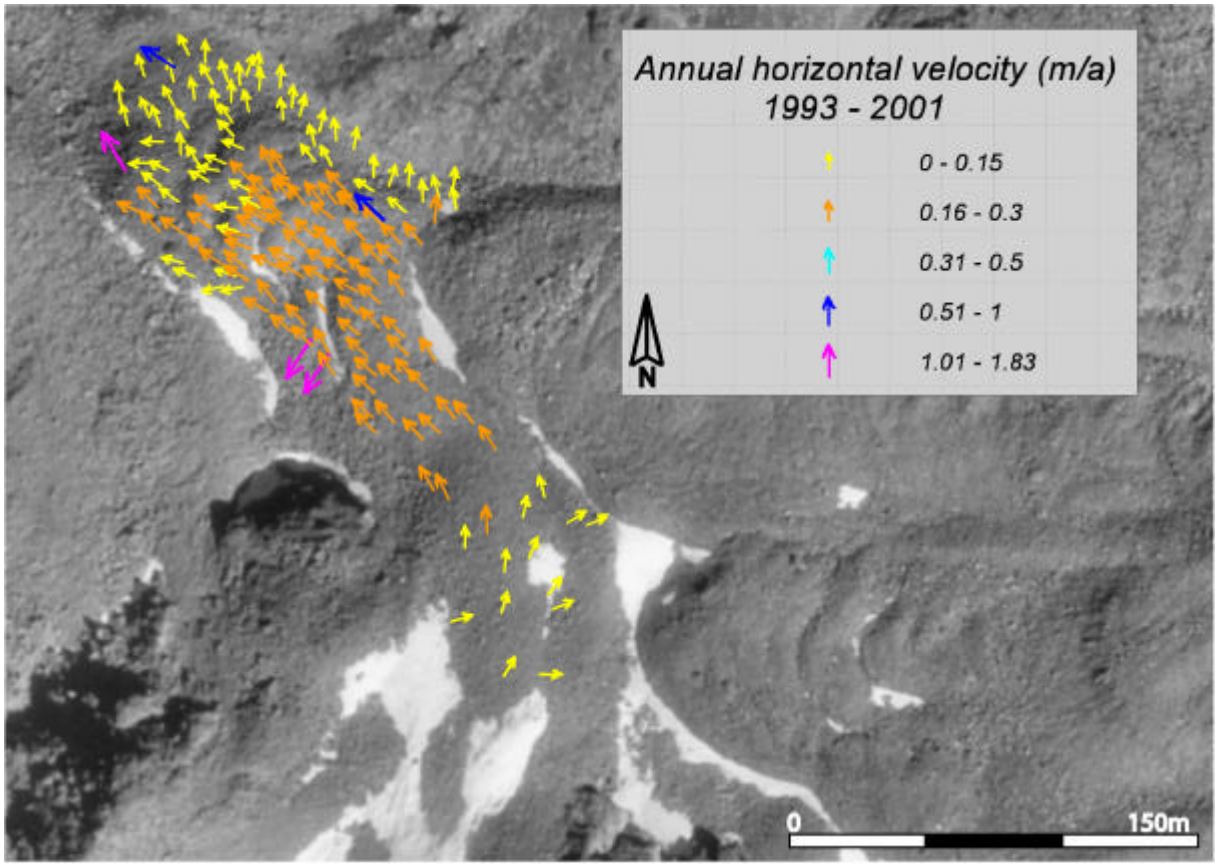

Figure 5.29: Mean annual surface velocities 1993 – 2001 on the rockglacier Brle. Underlying orthoimage of 20.08.1975 (flight line 22, aerial photographs taken by Swisstopo).

5.2.3 Hungerlitälli

5.2.3.1 Rockglacier Hufh

Horizontal velocities

On rockglacier Hufh (nr. 11 of the inventory) a high number of blocks was matched in the first period (figure 5.30). On the orographic right side as well as in the root zone of the permafrost body a measurement was impossible due to snowpatches. The vectorfield shows velocities in the range of uncertainty (up to 0.06 m/a) on the orographic left side of the lower lobe. Partially, these vectors are arranged in a whirl probably indicating vertical changes. Against that, velocities between 0.1 and 0.26 m/a are depicted on the other side of the lobe. Above, on the second lobe, constant values between 0.3 and 0.4 m/a are quantified. Both in the root zone and at the margins rates are again lower.

In the second period (1993 – 2001) the quantification of horizontal velocities was limited due to snow cover in one orthoimage (2001), which inhibited the measurement of corresponding grey-values. The depicted vectors indicate velocities between 0.1 and 0.2 m/a in the orographic left part of the lower lobe, while the right part and the upper lobe show rates up to 1.8 m/a (figure 5.31).

Vertical changes

The vertical surface changes on rockglacier Hufh are shown in figure 5.32 for the first investigated period (1975 – 1993). A cumulative increase in thickness of 2 – 5 m, which corresponds to a rate of 0.1 – 0.3 m/a, is indicated for a part of the lower lobe. Against that, a slight decrease is depicted above the front of the upper lobe. The orographic right side of the rockglacier has to be excluded in the interpretation, since the snowpatch causes errors in the measurement.

In the second period (1993 – 2001) a vertical increase (2 – 5 m; 0.25 – 0.6 m/a) is again revealed on the lower half of the rockglacier, while a decrease (partially up to -10 m; -1.25 m/a) is displayed in the root zone (figure 5.33).

Rockglacier Hufh is clearly active in the investigated period (1975 – 2001) and shows an increase in horizontal velocity in the second period. The topography of the feature with its two lobes situated one over the other is well reflected in the horizontal displacements. On the lower lobe movement is concentrated on the orographic right side, while the other side depicts small rates. The upper lobe reveals higher values and is overriding the lower lobe. Therefore, the vertical changes probably indicate mass balance effects with a thickening in the lower part and a thinning in the upper part of the rockglacier.

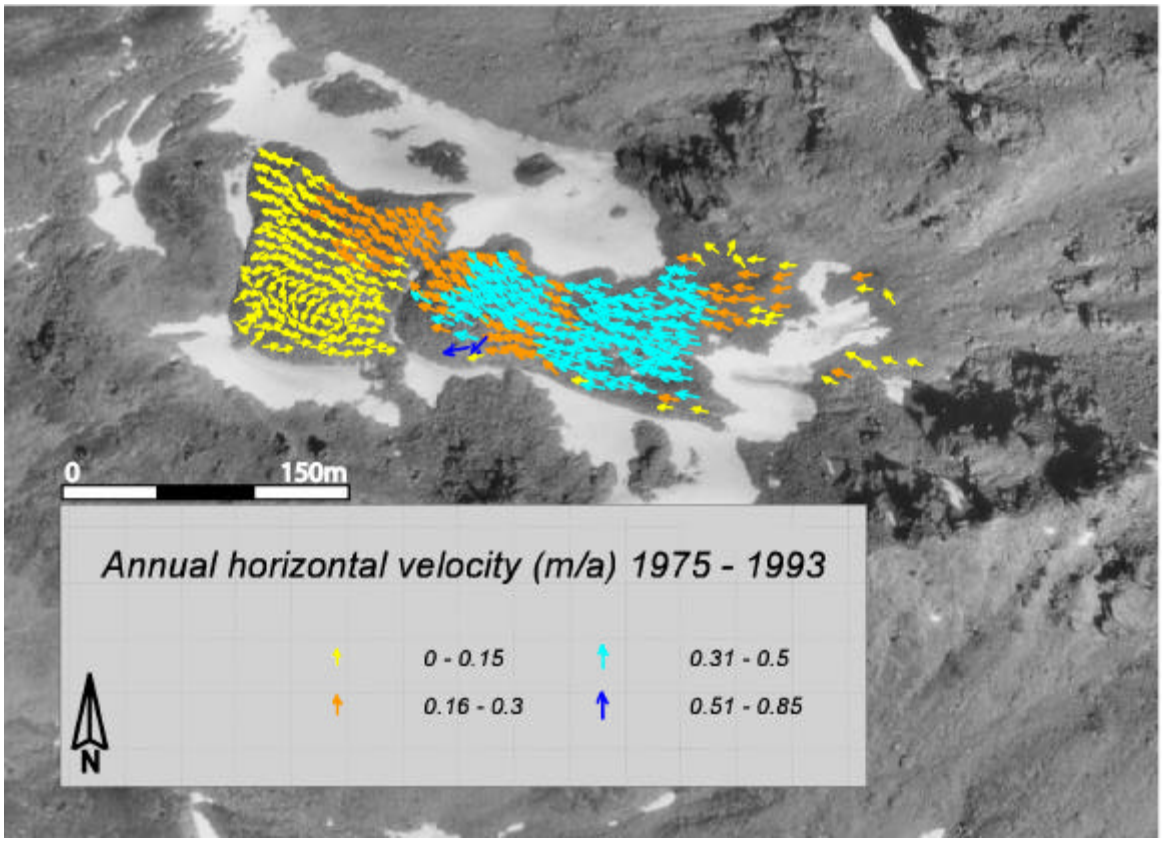

Figure 5.30: Mean annual surface velocities 1975 – 1993 on the rockglacier Hufh. Underlying orthoimage of 20.08.1975 (flight line 22, aerial photographs taken by Swisstopo).

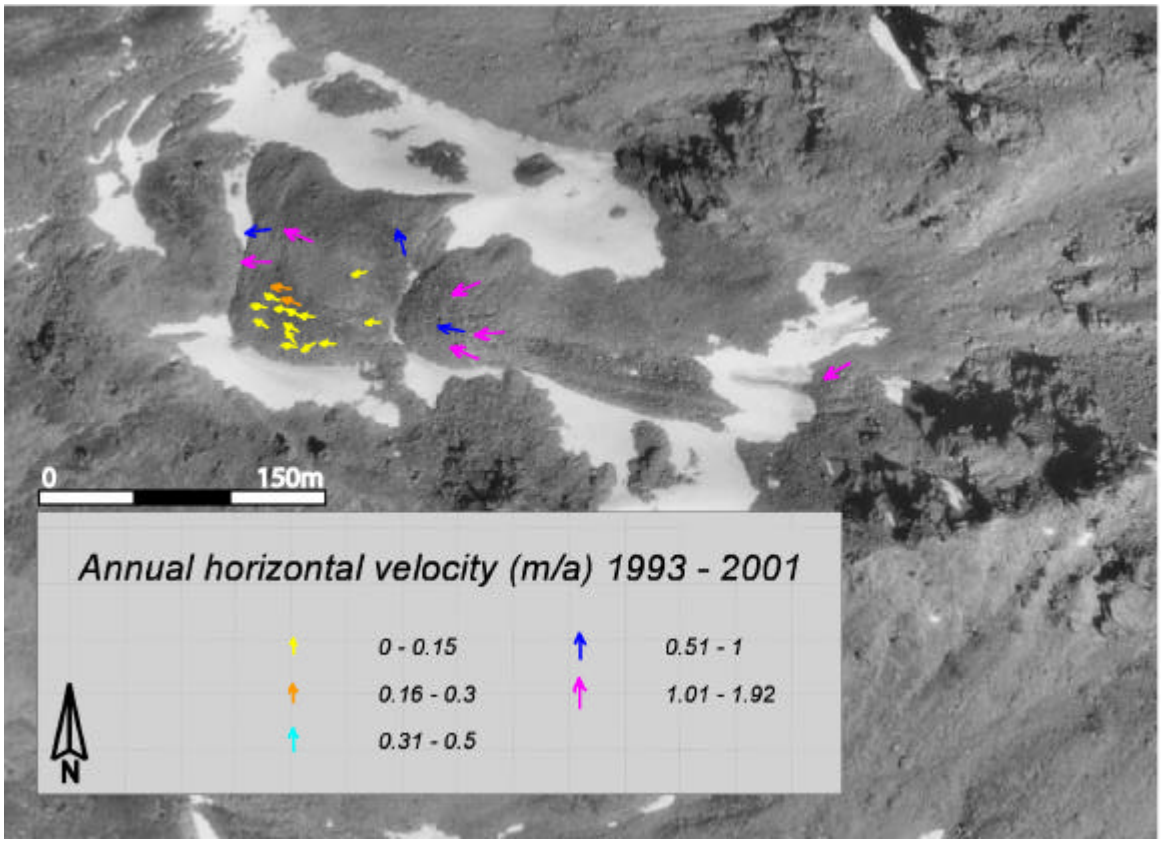

Figure 5.31: Mean annual surface velocities 1993 – 2001 on the rockglacier Hufh. Underlying orthoimage of 20.08.1975 (flight line 22, aerial photographs taken by Swisstopo).

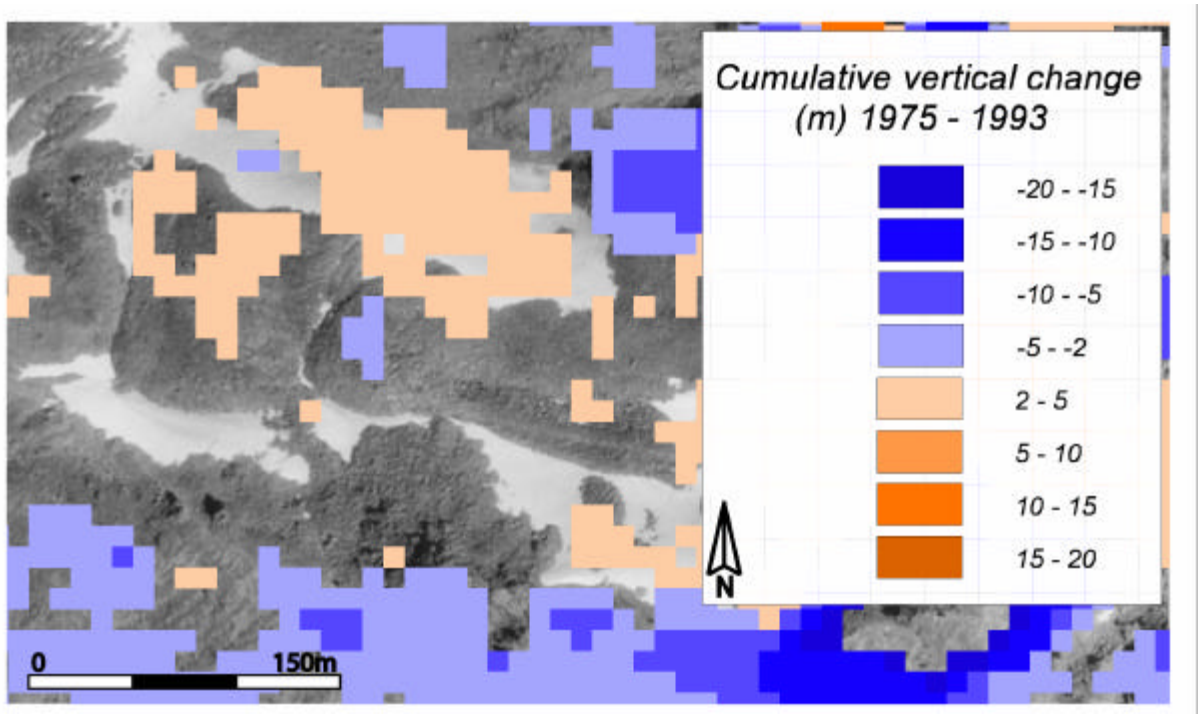

Figure 5.32: Cumulative vertical change on rockglacier Hufh between 1975 and 1993 (smoothed by a median-filter, window size 3x3). Underlying orthoimage of 20.08.1975 (flight line 22, aerial photographs taken by Swisstopo).

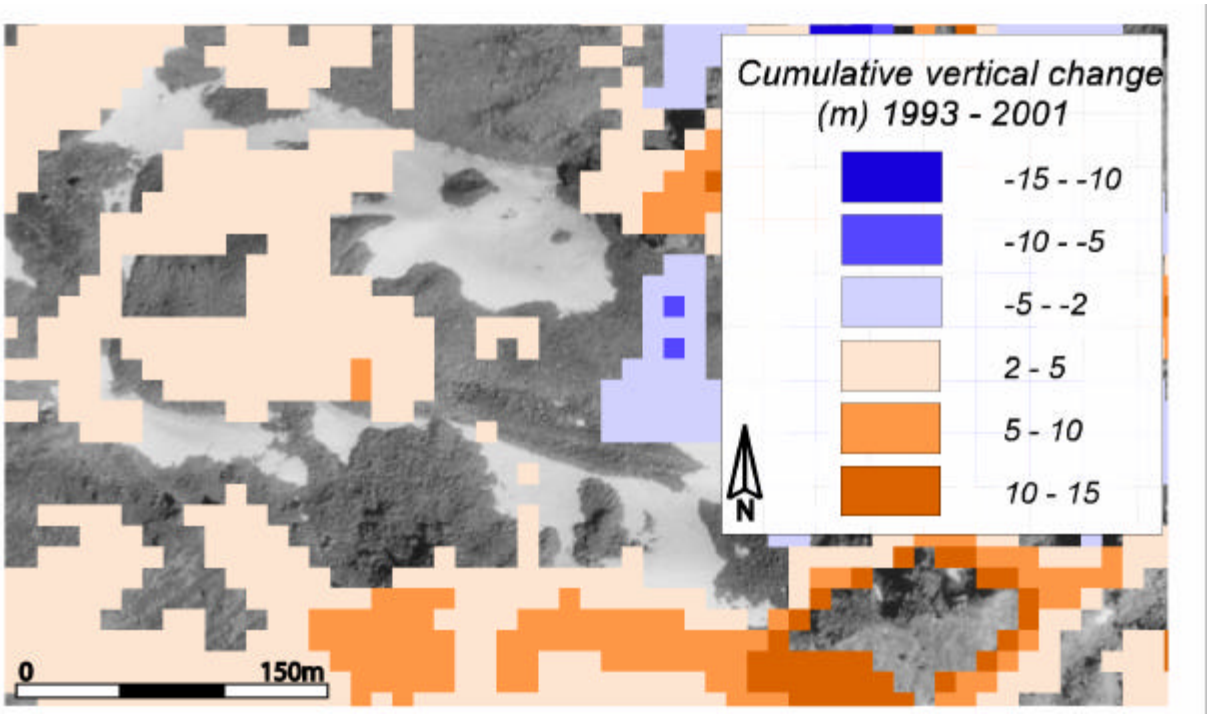

Figure 5.33: Cumulative vertical change on rockglacier Hufh between 1993 and 2001 (smoothed by a median-filter, window size 3x3). Underlying orthoimage of 20.08.1975 (flight line 22, aerial photographs taken by Swisstopo).

5.2.3.2 Rockglacier Hujp

Horizontal velocities

Also on rockglacier Hujp (nr. 12 of the inventory) a high number of blocks was matched, at least in the first period (1975 - 1993). The velocities display a very uniform vectorfield with only slight differences (figure 5.34). From the root zone to the centre of the rockglacier the values are low (0.06 – 0.08 m/a) but beyond the range of uncertainty. On the lower lobe rates are mainly between 0.1 and 0.12 m/a. More distinct differences are given at the front; while the orographic right part moves with about 0.2 m/a, the left part depicts values at about 0.02 m/a (within the range of uncertainty).

A similar pattern, although with clearly higher velocities, is shown for the period 1993 – 2001 (figure 5.35). The fast movement seems to spread from the front, since highest values (0.51 – 1.8 m/a) occur there, followed by a concentric field with rates between 0.31 and 0.5 m/a. The main part of the lobe depicts velocities between 0.16 and 0.3 m/a while lower rates are quantified at the margins and on the orographic left side of the front. In the upper part of the rockglacier a measurement was inhibited by snow cover in 2001.

Vertical changes

Between 1975 and 1993 changes in thickness on Hujp reveal negative values (-2 - -5 m; -0.1 - -0.3 m/a) in some parts of the lower lobe as well as in the middle of the rockglacier (figure 5.36). Against that, an increase in elevation (2 - 10 m; 0.1 – 0.6 m/a) occurs in the root zone.

In the second period an opposite pattern is indicated (figure 5.37). A thickening (2 – 5 m; 0.25 – 0.6 m/a) is indicated in major parts of the permafrost body, while a thinning (-5 - -10 m; -0.6 – -1.25 m/a) is depicted in the root zone.

Rockglacier Hujp is a monomorphic landform, which is overrunning the Egesen moraine and therefore has a very steep terminus. Between 1975 and 1993 it depicts only small movements slightly above the range of uncertainty as well as some higher rates at the front which probably result from the sliding or falling of individual blocks. Against that, a distinct increase in velocity is reflected in the second period (1993 – 2001), indicating the activity of the feature. Highest rates occur again at the front and seem to penetrate to the upper part. Vertical surface changes reveal diverse patterns in the two periods. The thickening in the lower part between 1993 and 2001 seems to be related to the high horizontal velocities.

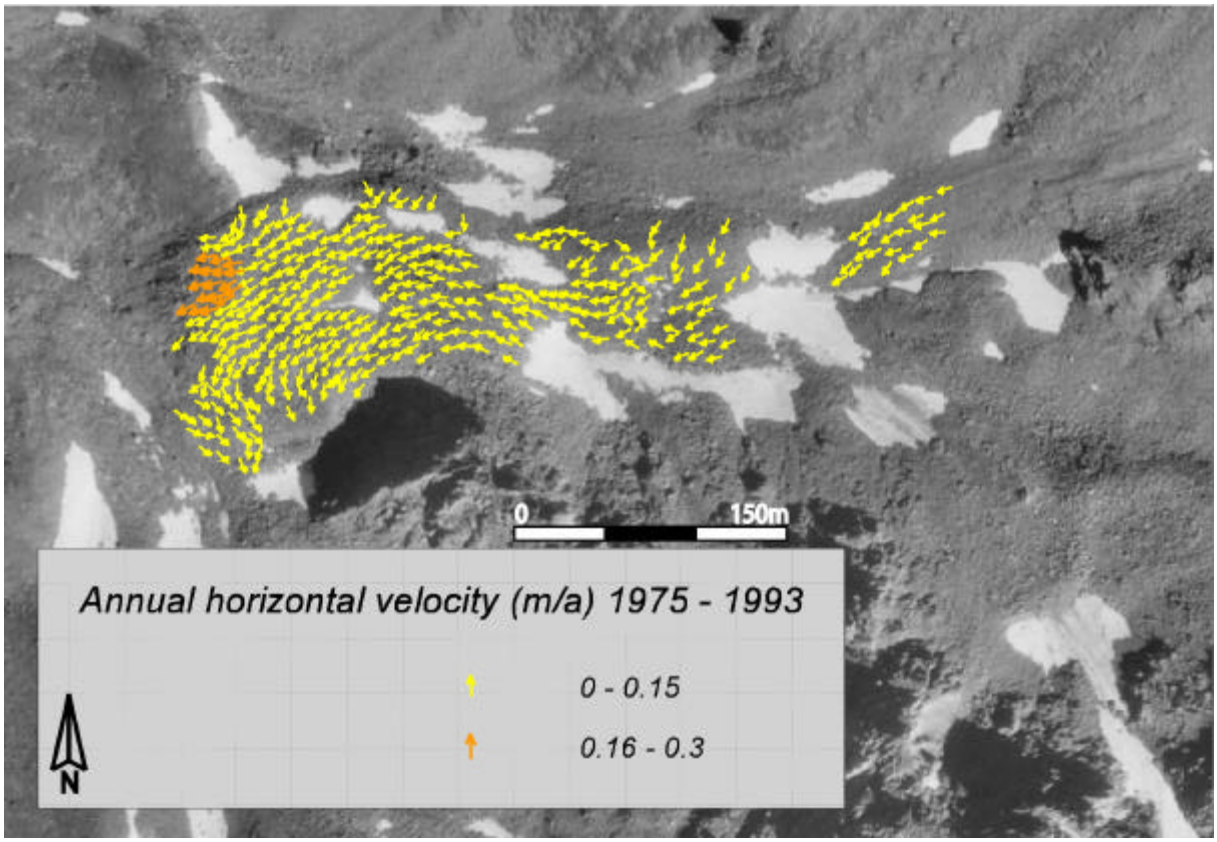

Figure 5.34: Mean annual surface velocities 1975 – 1993 on the rockglacier Hujp. Underlying orthoimage of 20.08.1975 (flight line 22, aerial photographs taken by Swisstopo).

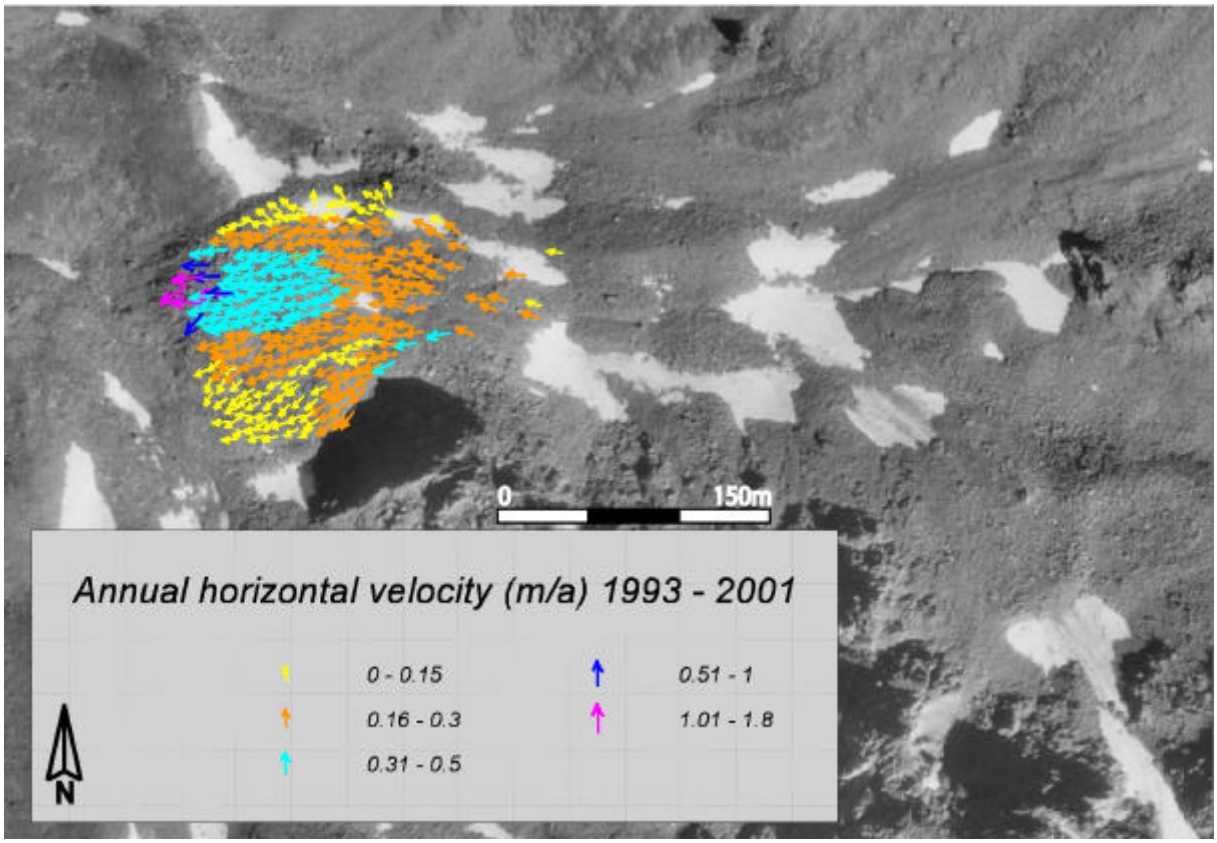

Figure 5.35: Mean annual surface velocities 1993 – 2001 on the rockglacier Hujp. Underlying orthoimage of 20.08.1975 (flight line 22, aerial photographs taken by Swisstopo).

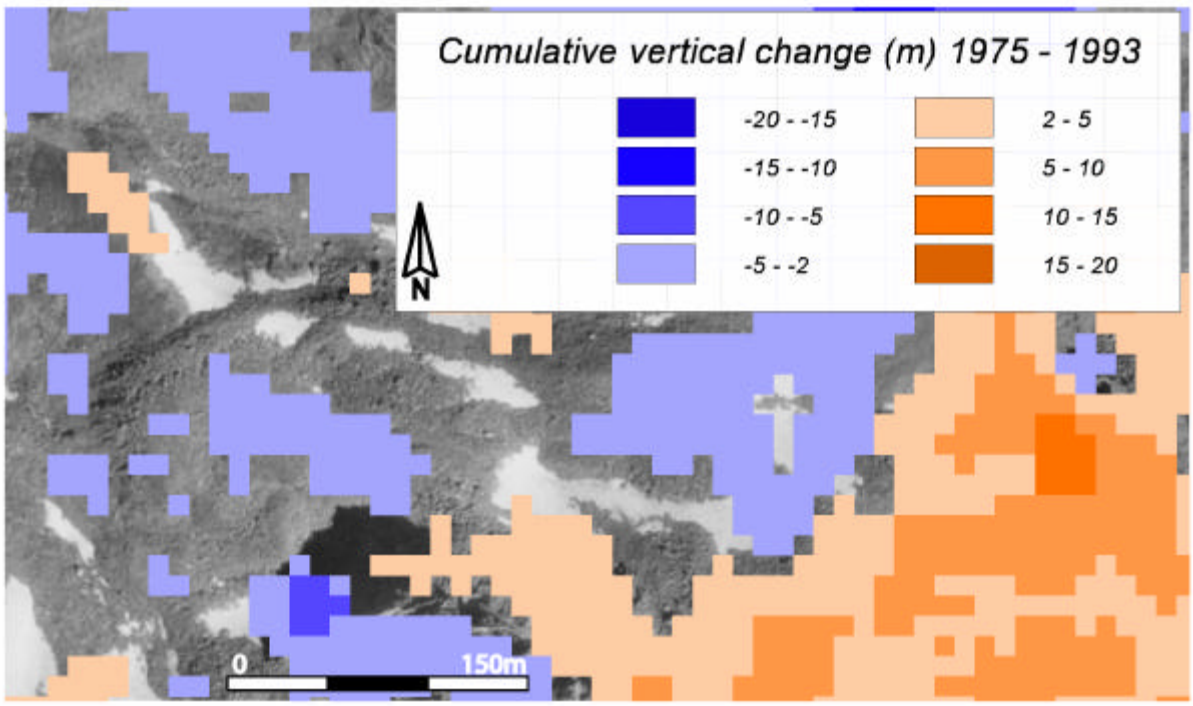

Figure 5.36: Cumulative vertical change on rockglacier Hujp between 1975 and 1993 (smoothed by a median-filter, window size 3x3). Underlying orthoimage of 20.08.1975 (flight line 22, aerial photographs taken by Swisstopo).

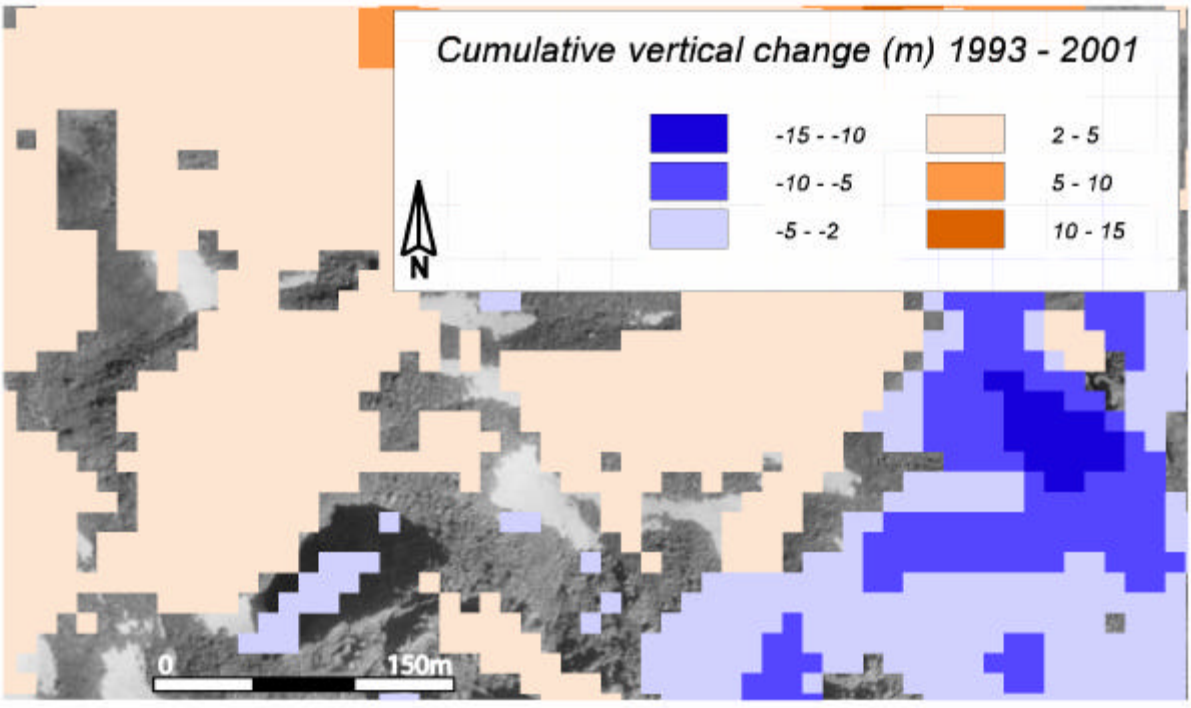

Figure 5.37: Cumulative vertical change on rockglacier Hujp between 1993 and 2001 (smoothed by a median-filter, window size 3x3). Underlying orthoimage of 20.08.1975 (flight line 22, aerial photographs taken by Swisstopo).

5.2.3.3 Rockglacier Hurh1

On rockglacier Hurh1 (nr. 13 of the inventory) which was mapped as active, several blocks were matched in both measurement periods in order to quantify horizontal velocities. All of them depict values in the range of uncertainty, apart from single rocks at the front. Additionally, the vectors reveal a great variety of directions. Thus, the inactivity of the feature is indicated by the photogrammetric data. Regarding the vertical changes, only a slight thickening occurred over the investigated period 1975 – 2001.

5.2.3.4 Rockglacier Hurh2

Horizontal velocities

Also on this rockglacier (nr. 14 of the inventory) which was mapped as inactive, the velocity vectors are clearly in the range of uncertainty in both investigated periods. Therefore, the inactivity of this rockglacier is confirmed. Changes in elevation were quantified over the entire period 1975 – 2001 (figure 5.4). A small area in the middle of the rockglacier depicts a decrease in elevation, while a slight thickening is indicated at the front as well as in the root zone.

5.2.3.5 Rockglacier Huhh1

Horizontal velocities

The velocity pattern of rockglacier Huhh1 (nr. 15 of the inventory) displays distinct fields of uniform movements between 1975 and 1993 (figure 5.38). At the rockglacier margins as well as on the orographic right part of the lower lobe rates between 0.04 and 0.1 m/a are quantified. Against it, the left part of the lower lobe depicts velocities up to 0.3 m/a. Further up, above a second steep front, an extensive area reveals velocities at about 0.45 m/a while only single blocks show higher values.

Between 1993 and 2001 the vectorfield is less uniform than in the first period, especially in the upper part of the rockglacier (figure 5.39). On the orographic right side of the lower lobe velocities between 0.1 and 0.15 m/a are depicted directly at the front while further up values are in the range of uncertainty and the vectors show a whirl-like orientation. To the left the rates increase and show a central flowline of up to 0.3 m/a and values at about 0.4 m/a at the orographic left margin. The upper lobe displays high velocities of mostly more than 1.0 m/a. Only in the root zone a small field of uniform velocities (0.51 - 1.0 m/a) is revealed.

In comparison to the first period the mass seems to creep no more as a whole, since the blocks move individually with diverse magnitudes and in slightly different directions.

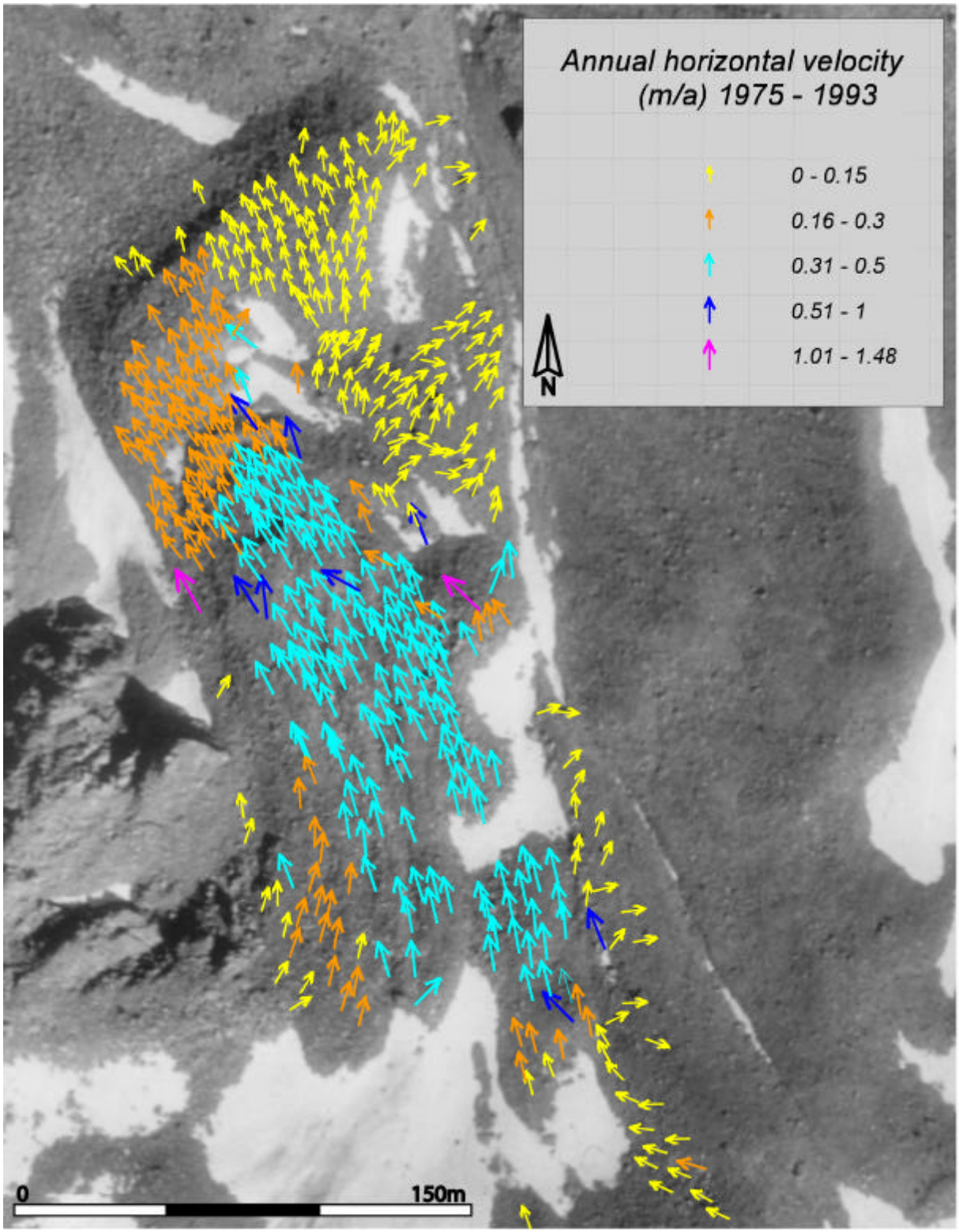

Figure 5.38: Mean annual surface velocities 1975 – 1993 on the rockglacier Huhh1. Underlying orthoimage of 20.08.1975 (flight line 22, aerial photographs taken by Swisstopo).

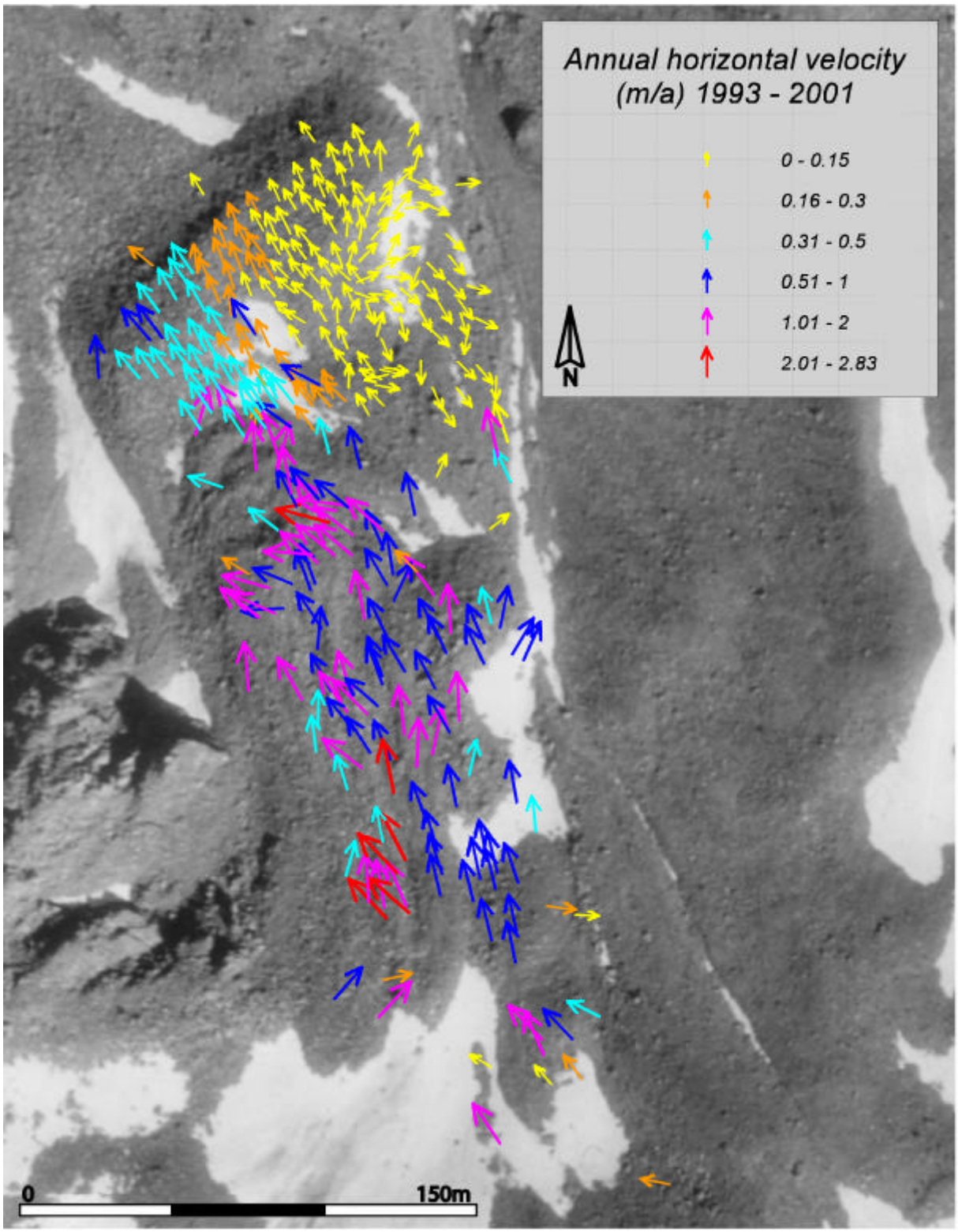

Figure 5.39: Mean annual surface velocities 1993 – 2001 on the rockglacier Huhh1. Underlying orthoimage of 20.08.1975 (flight line 22, aerial photographs taken by Swisstopo).

Vertical changes

Vertical surface changes on rockglacier Huhh1 depict for the first period an increase in elevation of 2 – 5 m (0.1 – 0.3 m/a) on the orograpic right side (figure 5.40). Directly below the cirque, a thickening is also revealed on the orographic left side. The rest of the feature shows no changes

in elevation. Between 1993 and 2001 (figure 5.41) again a large part of the rockglacier indicates no surface changes, but some areas on the lower lobe and below the cirque indicate an increase in thickness (up to 5 m; 0.6 m/a).

Rockglacier Huhh1 depicts a complex ridge-and-furrow topography and two lobes which are arranged over each other. The horizontal movements quantified between 1975 and 2001 confirm the activity of the feature. Additionally, a distinct acceleration is reflected in the data of the second period (1993 – 2001). Regarding the vertical changes, the thickening of the orographic right side in the first period is difficult to interpret. Between 1993 and 2001 at least the thickening below the second front can be explained by the high horizontal velocities and the advancing front.

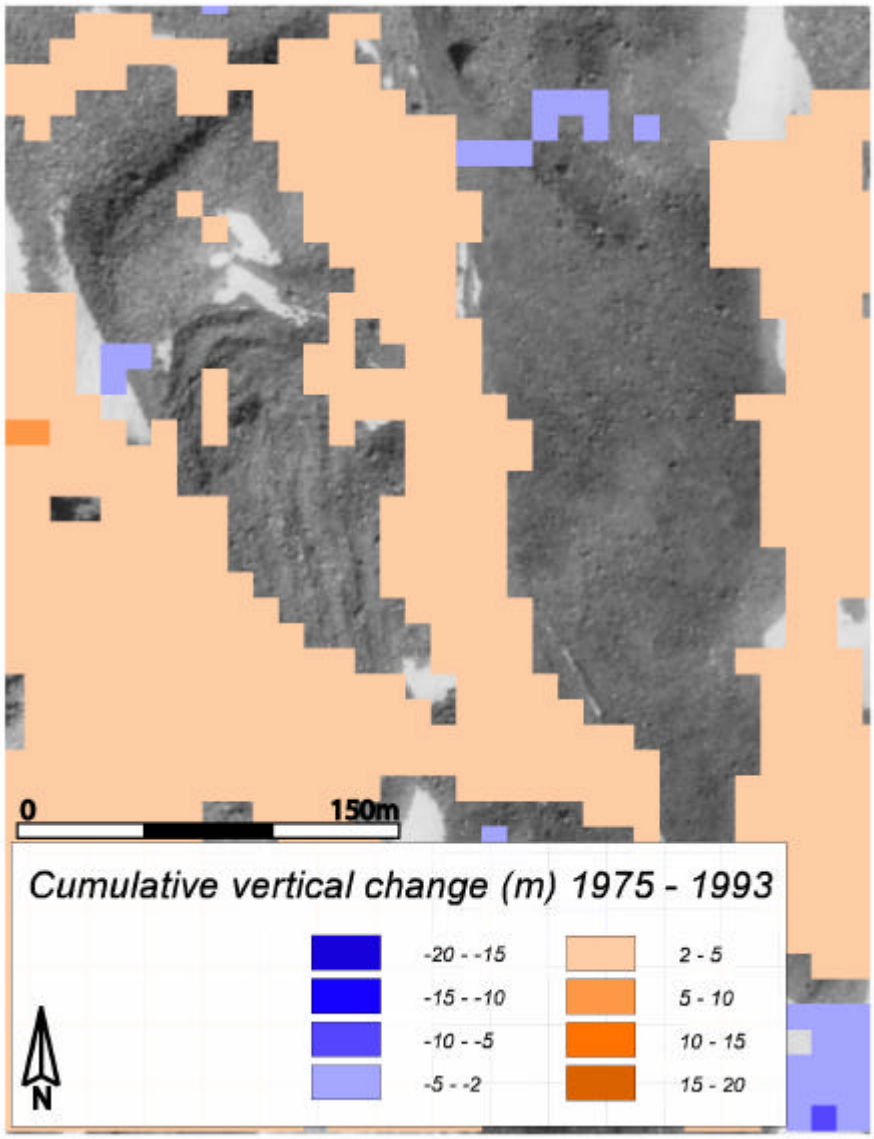

Figure 5.40: Cumulative vertical change on rockglacier Huhh1 between 1975 and 1993 (smoothed by a median-filter, window size 3x3). Underlying orthoimage of 20.08.1975 (flight line 22, aerial photographs taken by Swisstopo).

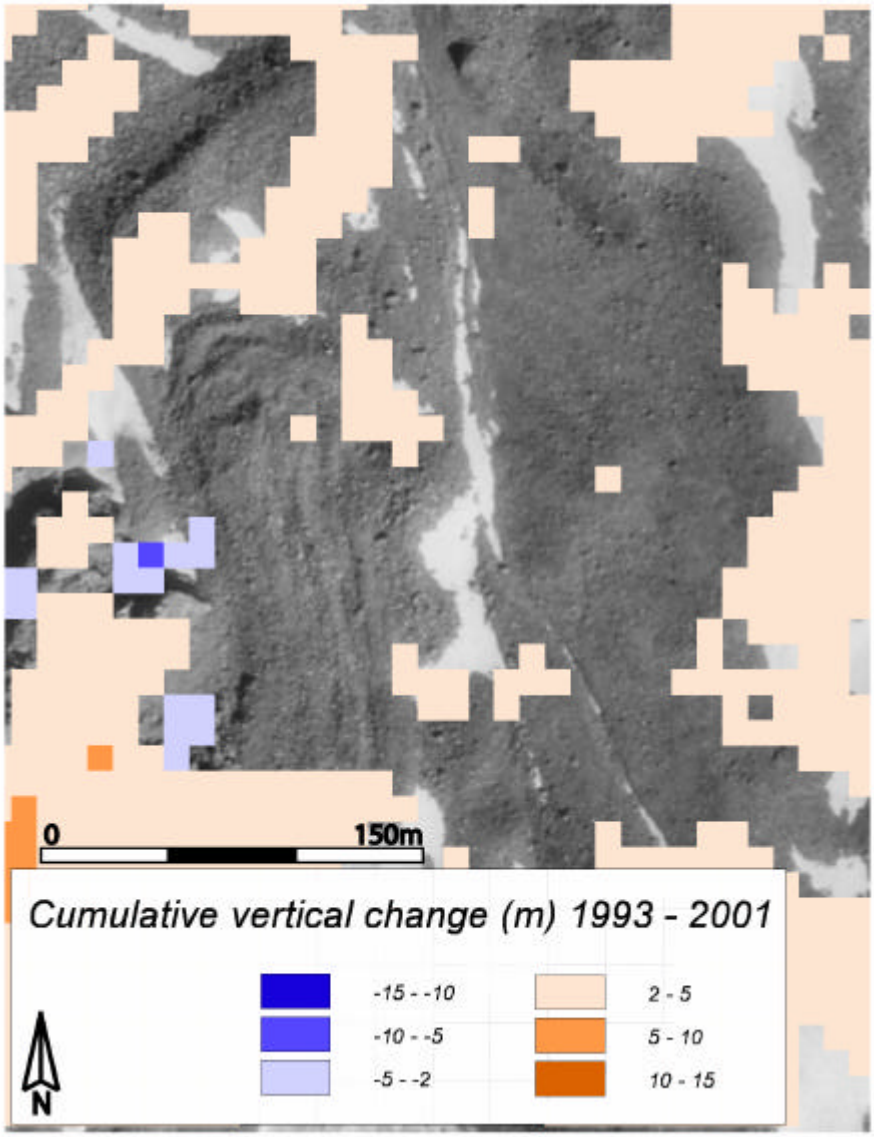

Figure 5.41: Cumulative vertical change on rockglacier Huhh1 between 1993 and 2001 (smoothed by a median-filter, window size 3x3). Underlying orthoimage of 20.08.1975 (flight line 22, aerial photographs taken by Swisstopo).

5.2.3.6 Rockglacier Huhh2

Horizontal velocities

The large complex of rockglacier Huhh2 (nr. 16 of the inventory) was mapped as inactive and thus, displacements were expected to be low respectively in the range of uncertainty. In both investigated periods this assumption appeared to be right (indicated both by the low magnitudes and the diverse directions of the vectors), apart from a slope in the root zone of Huhh2, directly below the front of rockglacier Huhh1. In the first period this slope depicts velocities between 0.07 and 0.13 m/a in the upper part, while the lower part is in the range of uncertainty but shows a distinct direction of the movement (figure 5.42). This pattern is similar between 1993 and 2001, but the rates increased significantly (up to 0.3 m/a) in the upper part (figure 5.43).

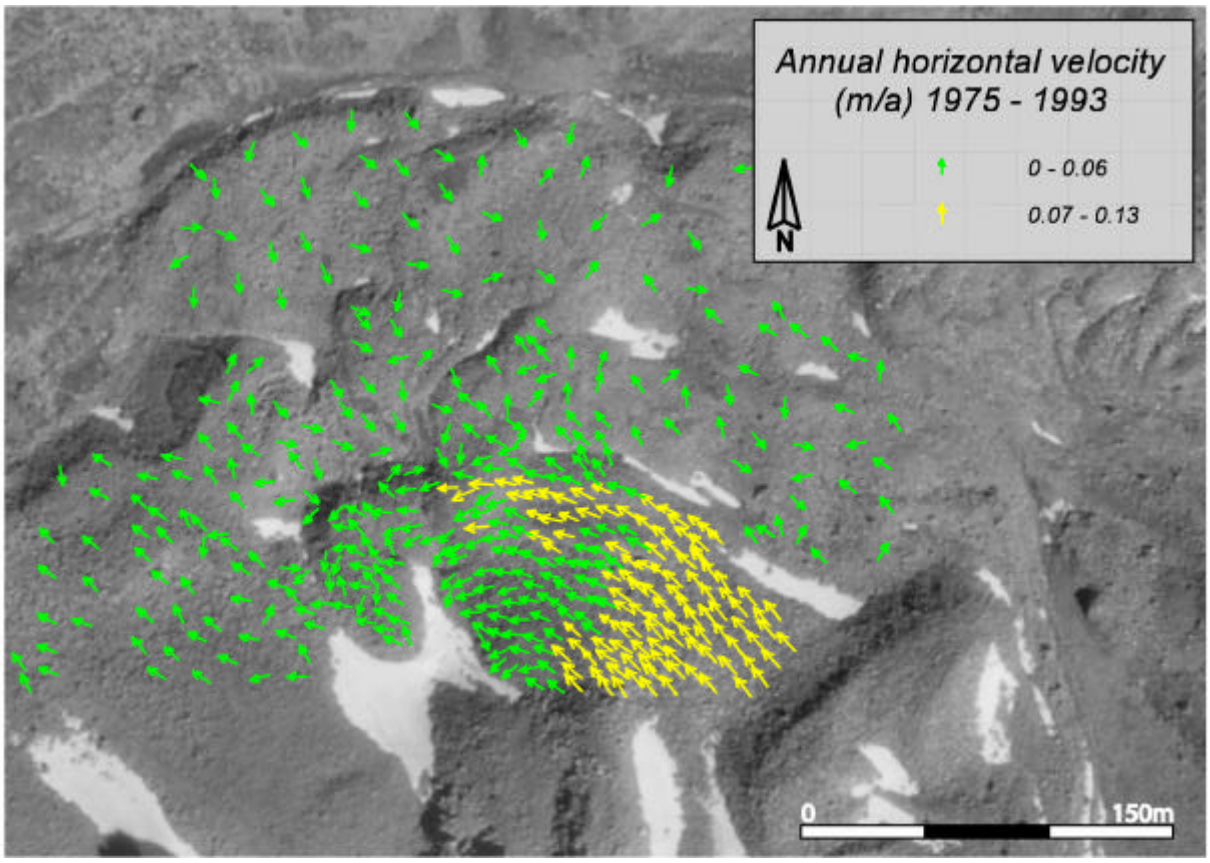

Figure 5.42: Mean annual surface velocities 1975 – 1993 on the rockglacier Huhh2. Underlying orthoimage of 20.08.1975 (flight line 22, aerial photographs taken by Swisstopo).

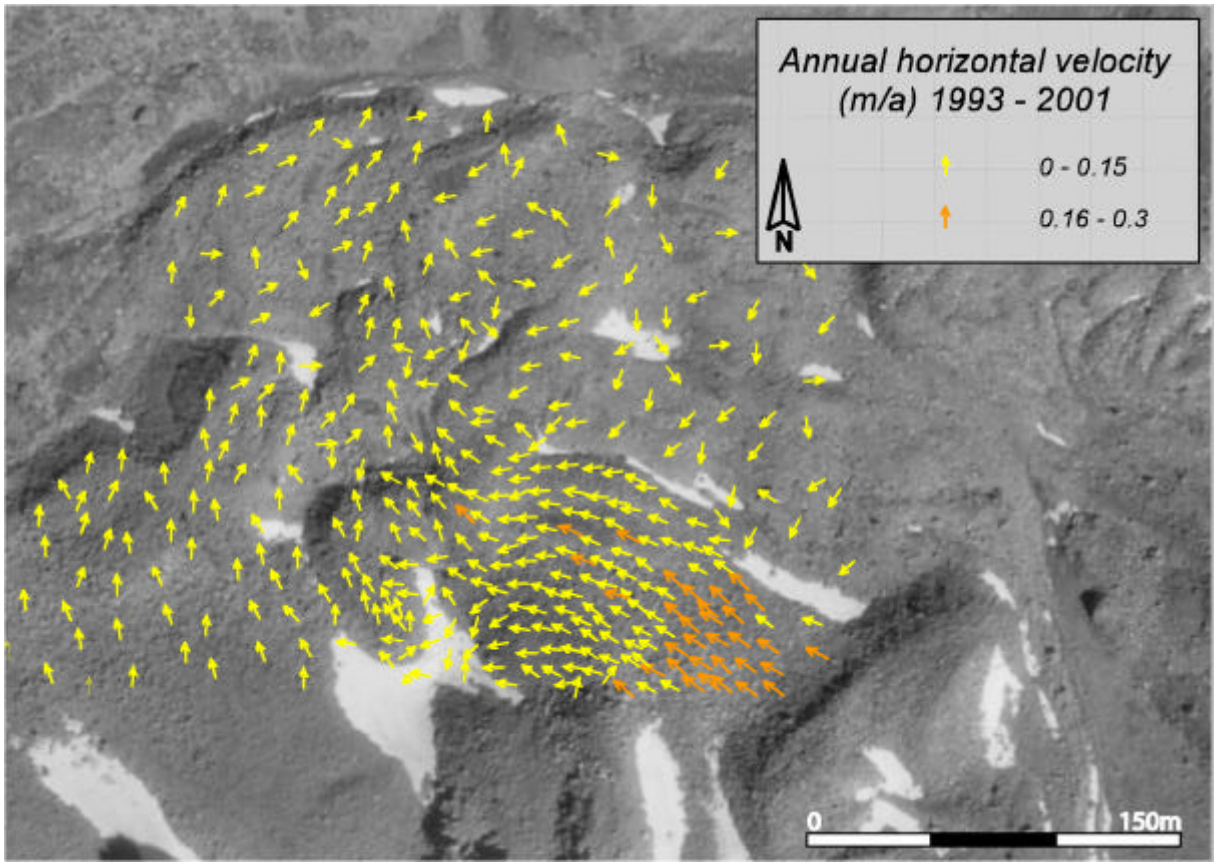

Figure 5.43: Mean annual surface velocities 1993 – 2001 on the rockglacier Huhh2. Underlying orthoimage of 20.08.1975 (flight line 22, aerial photographs taken by Swisstopo).

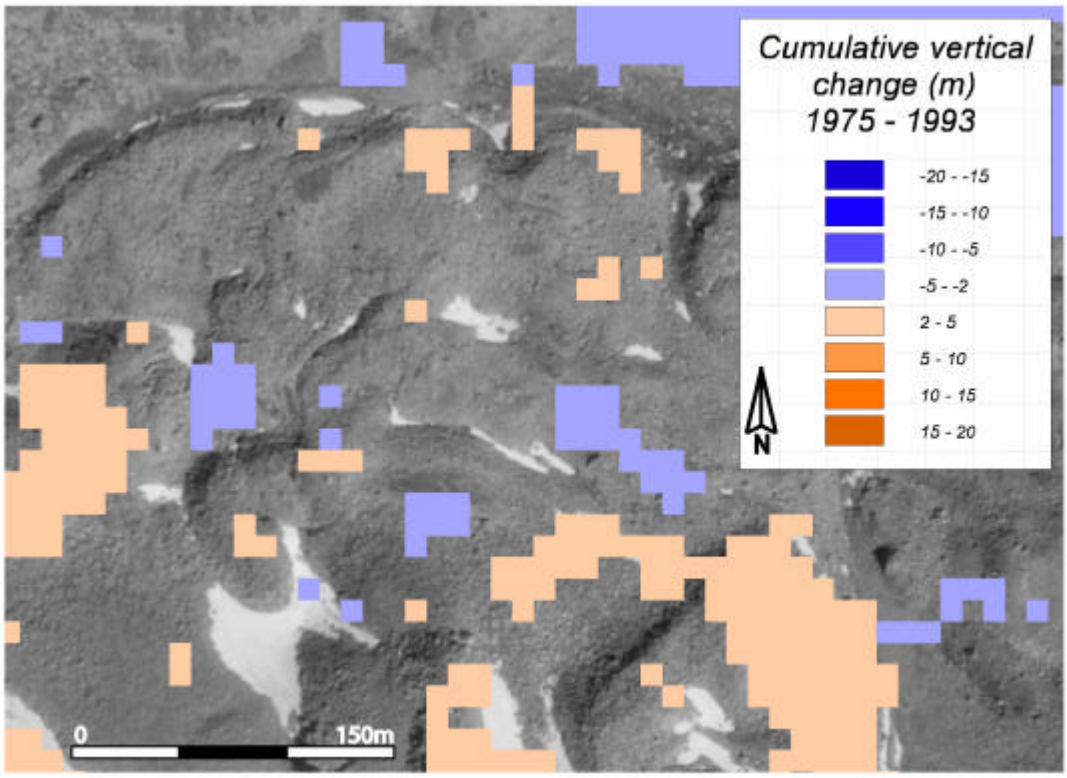

Figure 5.44: Cumulative vertical change on rockglacier Huhh2 between 1975 and 1993 (smoothed by a median-filter, window size 3x3). Underlying orthoimage of 20.08.1975 (flight line 22, aerial photographs taken by Swisstopo).

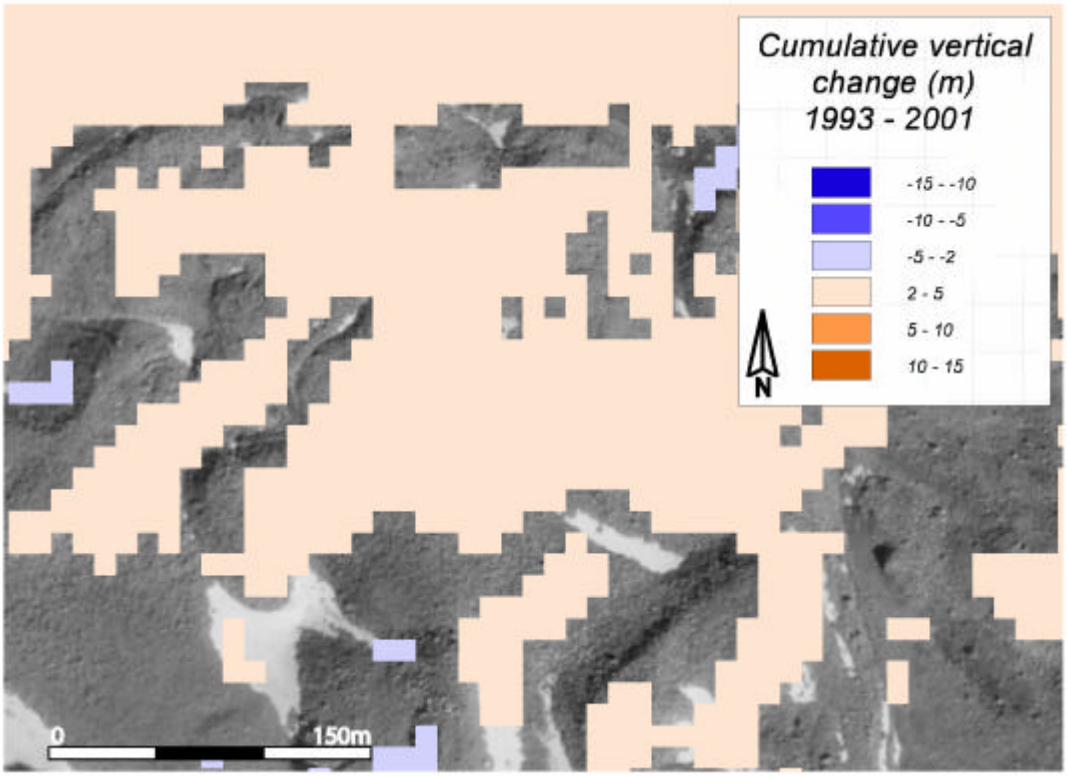

Figure 5.45: Cumulative vertical change on rockglacier Huhh2 between 1993 and 2001 (smoothed by a median-filter, window size 3x3). Underlying orthoimage of 20.08.1975 (flight line 22, aerial photographs taken by Swisstopo).

Vertical changes

Regarding the vertical change on rockglacier Huhh2, no clear signal is revealed between 1975 and 1993 (figure 5.44). Apart from an increase in elevation (2 – 5 m; 0.1 – 0.3 m/a) below the front of rockglacier Huhh1 and in the contact zone to the protalus rampart (orographic left), some small areas show a vertical decrease (-2 - -5 m; -0.1 - -0.3 m/a). Against that, a thickening (2 – 5 m; 0.25 – 0.6 m/a) occurs all over the rockglacier apart from the fronts between 1993 and 2001 (figure 5.45).

Rockglacier Huhh2 is a complex landform in the bottom of the hanging valley, which was mapped as inactive. The photogrammetric data confirm the inactivity of the feature, apart from a slope in the root zone adjacent to rockglacier Huhh1. Probably the slope is influenced by the advance of Huhh1, but since a relatively large area depicts the movements actively creeping permafrost has to be assumed. Concerning the vertical changes, the pattern of the first period seems to emphasise the inactivity of the feature. Against that, the changes between 1993 and 2001 are hard to explain.

5.2.3.7 Rockglacier Huhh3

Horizontal velocities

On rockglacier Huhh3 (nr. 17 of the inventory) a high number of blocks was matched in both investigated periods (figures 5.46, 5.47). Between 1975 and 1993 velocities up to 0.15 m/a are depicted in the root zone, at the rockglacier margins as well as in the lower lobes. The main lobe (above the third front) reveals uniform rates between 0.16 and 0.3 m/a with two small fields in the central flow line showing velocities up to 0.5 m/a.

In the second period (1993 – 2001) a slight increase in velocities is depicted at the rockglacier margins and on the lower lobes whereas the main lobe shows a distinct speed-up. Maximum rates (1.0 – 2.5 m/a) occur in the upper part, directly below the cirque. Further down a uniform field of values between 0.5 and 1.0 m/a spreads to the front. This field is surrounded by velocities up to 0.5 m/a.

Vertical changes

Between 1975 and 1993, vertical changes occur only in small areas on rockglacier Huhh3 (figure 5.48). A cumulative thickening (2 – 5 m; 0.1 – 0.3 m/a) is indicated in the upper part (directly below the cirque) and above the uppermost front. Punctually, thinning (-2 - -5 m) is depicted at the front on the orographic left side. In the second period (figure 5.49) the elevation changes are slightly different. A thickening (2 – 5 m; 0.25 – 0.6 m/a) occurs in the cirque and in the lower part of the rockglacier, while a thinning in the same order of magnitude is indicated in the upper part, directly below the cirque.

Rockglacier Huhh3 is again a complex rockglacier with several lobes indicating different generations. This pattern is well reflected in the velocityfields of the clearly active feature. High velocities represent the upper lobe which is overriding the lower one. This part of the rockglacier depicts a distinct acceleration in the second period, whereas the lowermost lobes show small movements in both periods. Concerning the vertical component, especially the changes between 1993 and 2001 fit well with the horizontal velocities. A distinct thinning occurs in the area of highest horizontal movements and results in a thickening in the lower part of the lobe. Thus, a change in flow balance in indicated. Due to the high velocities in the upper part, the creeping mass seems to lose connection to the source area. This becomes apparent in the clear boundary between thickening in the cirque (probably due to accumulation) and thinning in the root zone of the rockglacier.

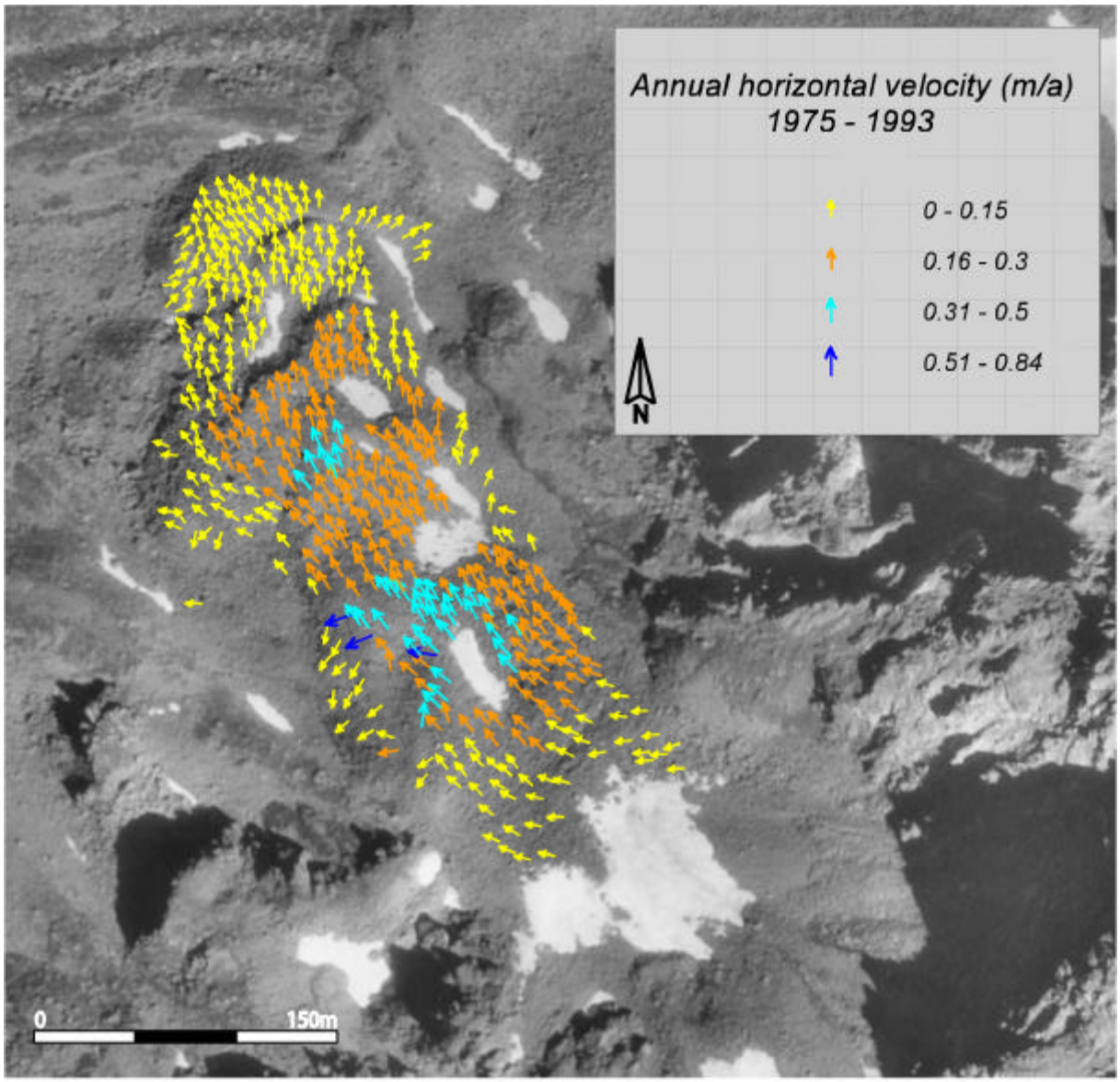

Figure 5.46: Mean annual surface velocities 1975 – 1993 on the rockglacier Huhh3. Underlying orthoimage of 20.08.1975 (flight line 22, aerial photographs taken by Swisstopo).

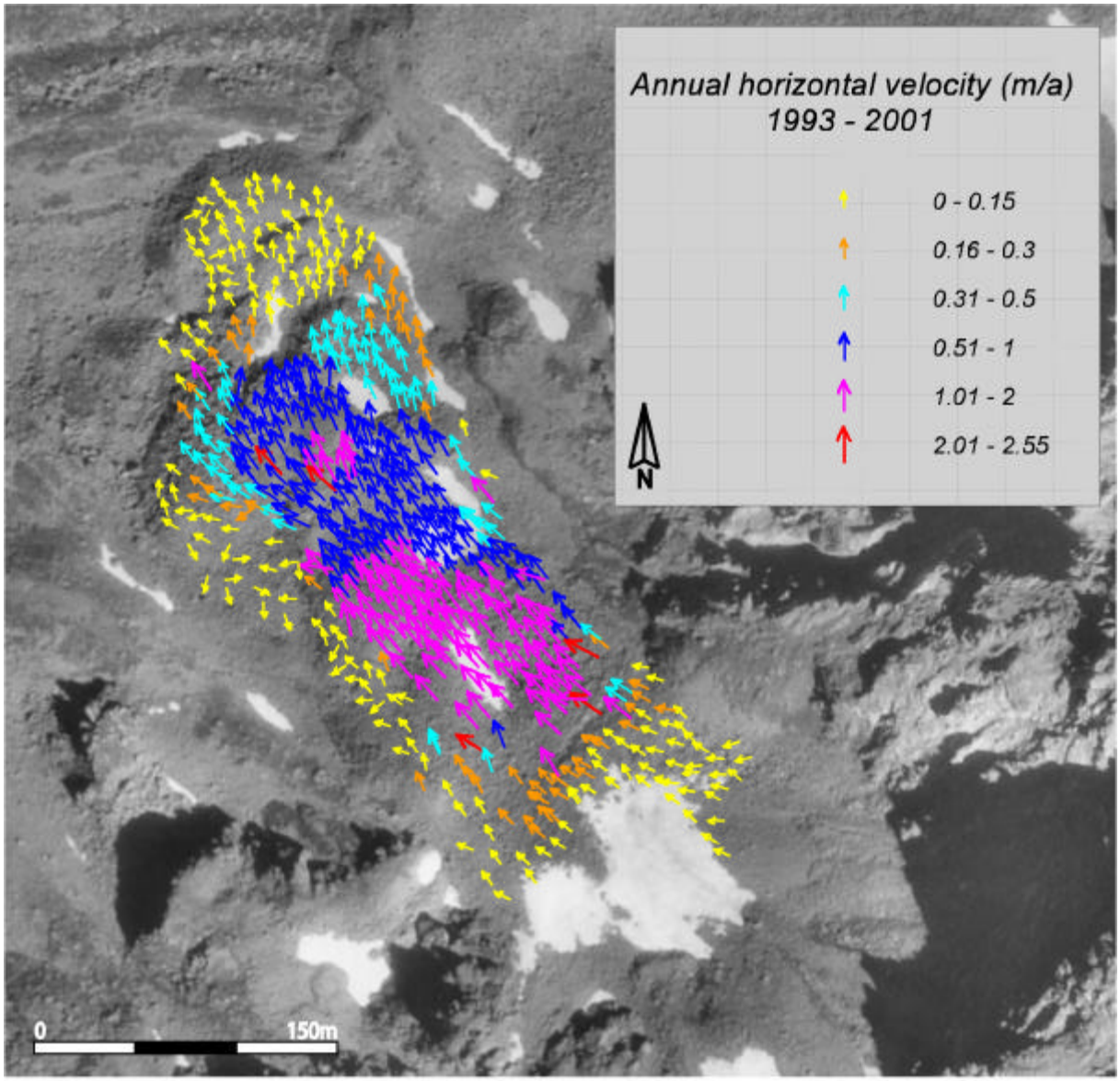

Figure 5.47: Mean annual surface velocities 1993 – 2001 on the rockglacier Huhh3. Underlying orthoimage of 20.08.1975 (flight line 22, aerial photographs taken by Swisstopo).

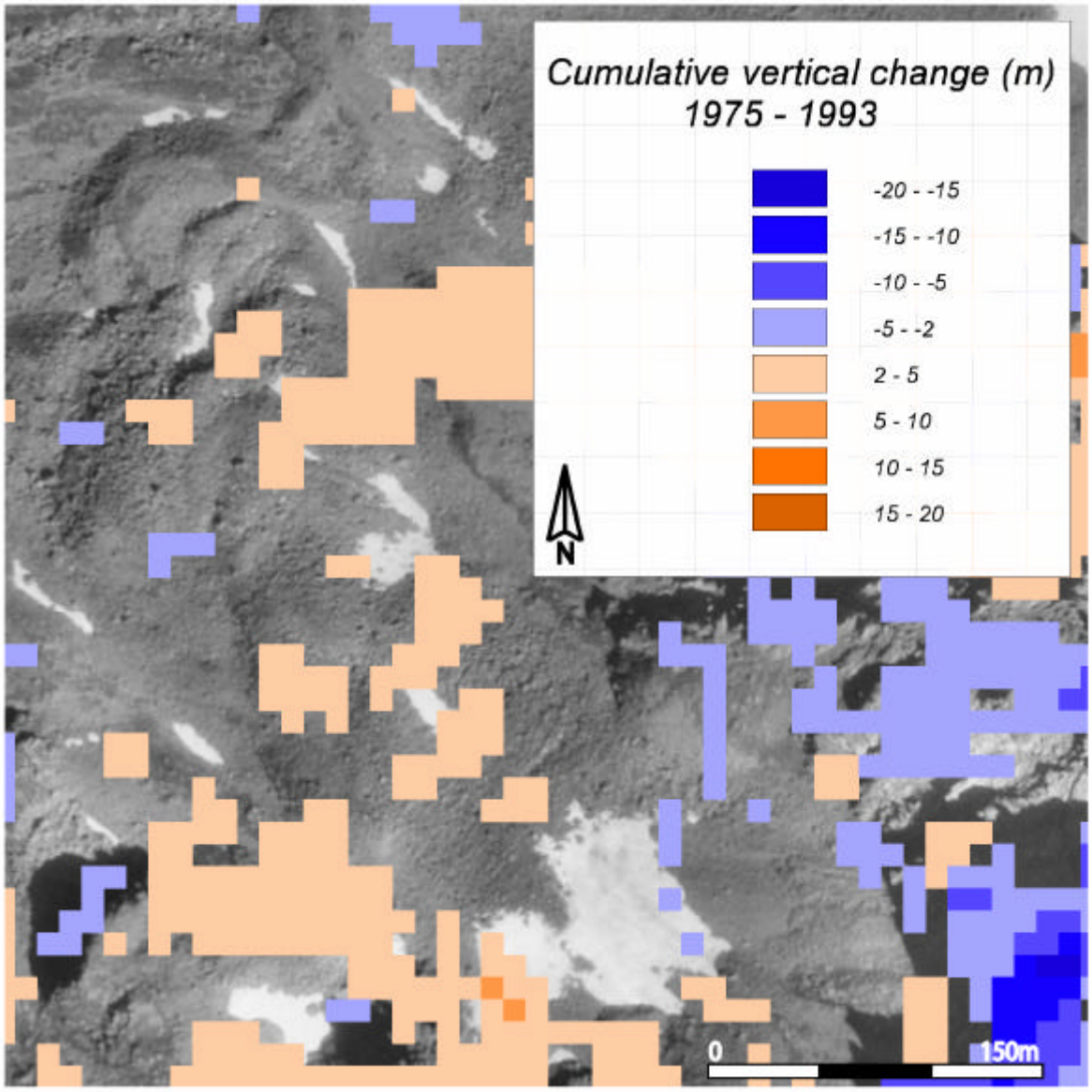

Figure 5.48: Cumulative vertical change on rockglacier Huhh3 between 1975 and 1993 (smoothed by a median-filter, window size 3x3). Underlying orthoimage of 20.08.1975 (flight line 22, aerial photographs taken by Swisstopo).

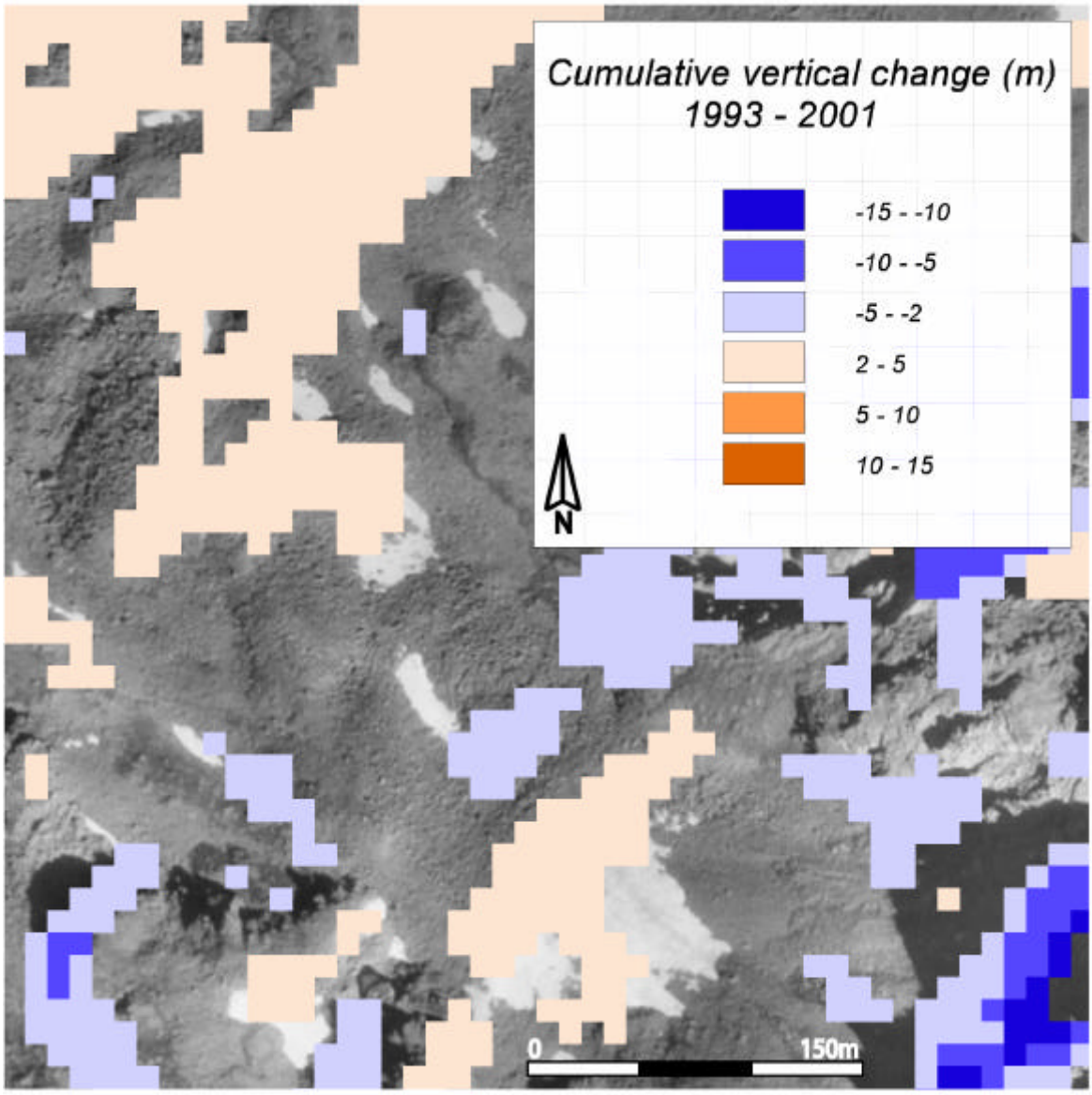

Figure 5.49: Cumulative vertical change on rockglacier Huhh3 between 1993 and 2001 (smoothed by a median-filter, window size 3x3). Underlying orthoimage of 20.08.1975 (flight line 22, aerial photographs taken by Swisstopo).

5.2.4 Grüobtälli

5.2.4.1 Rockglacier Grueo1

Horizontal velocities

This rockglacier (nr. 21 of the inventory) is one of the most striking landforms in the Turtmann valley. By visual interpretation of the orthoimages of the years 1975, 1993 and 2001 it shows major changes in its geometry (figure 5.50). Beside the outstanding advance of its front (~ 60 m in 26 years), the ripped surface is conspicuous. The crevasse-like features in the middle of the rockglacier are up to 12 metres deep. Due to these characteristics, its kinematics is quantified over four shorter periods (1975 – 1981; 1981 – 1987; 1987 – 1993; 1993 – 2001). A lot of blocks were matched in each period, apart from the root zone where a perennial snowfield inhibited the measurement.

In the first period (1975 – 1981), where the rockglacier topography was relatively smooth, the horizontal velocityfield was very uniform, but revealed already quite high speeds (figure 5.51). On the upper part of the rockglacier as well as at the margins velocities between 0.51 and 1.0 m/a are depicted while the lower part moves with rates up to 2 m/a. Single blocks, especially at the front, show even higher values up to 5 m/a. The gap in the vectorfield results from a wide snowpatch on the orthoimage of 1981.

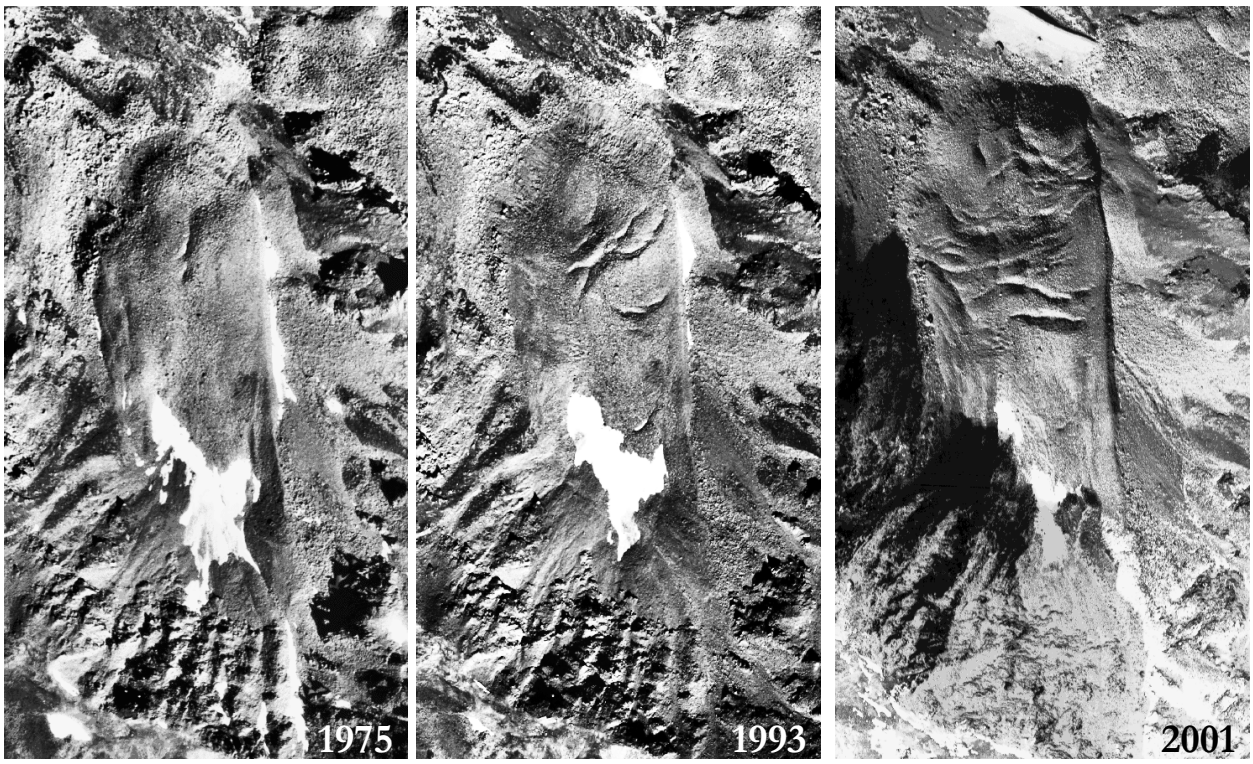

Figure 5.50: Change in surface geometry of rockglacier Grueo1. Underlying orthoimages of 20.08.1975, 20.08.1993 (aerial photographs taken by Swisstopo) and 28.09.2001 (HRSC-A survey).

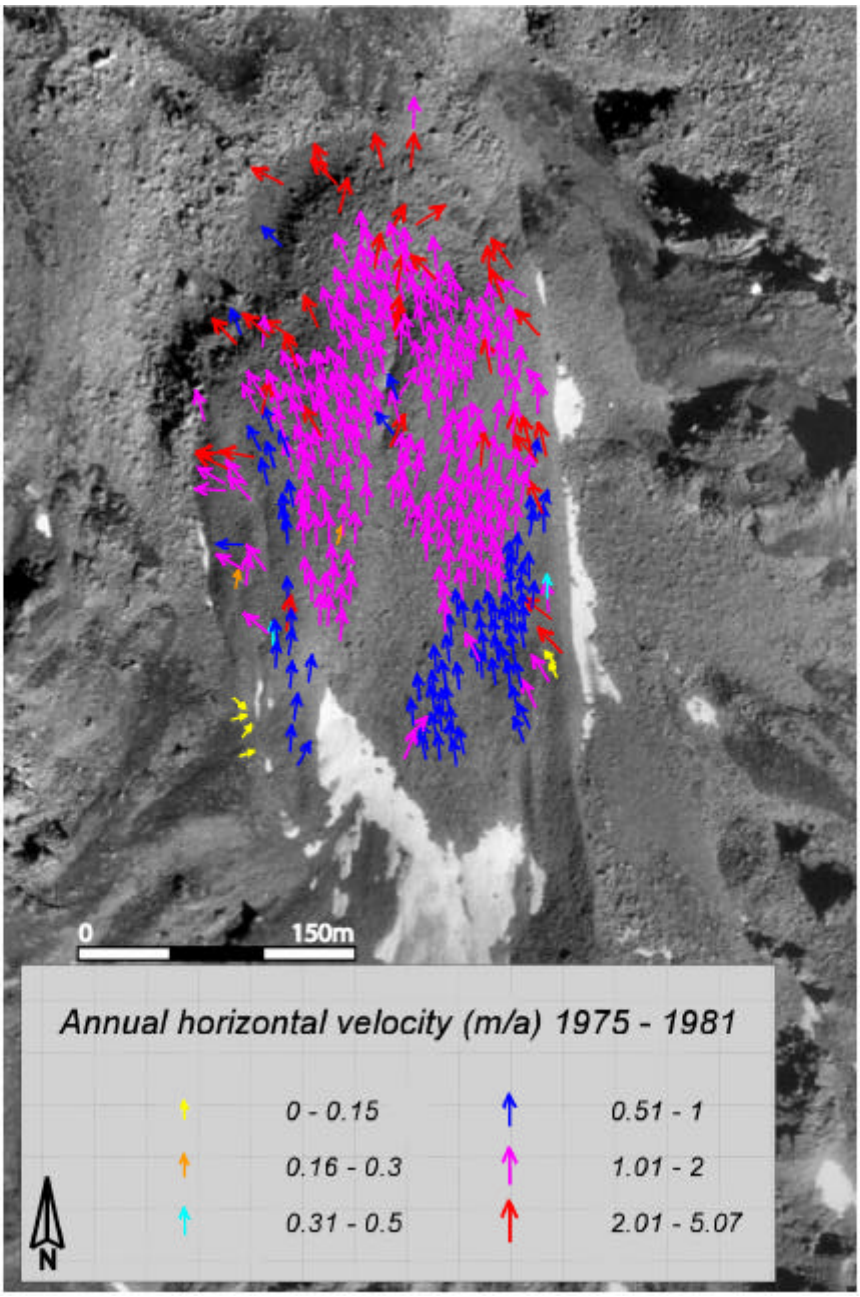

Figure 5.51: Mean annual surface velocities 1975 – 1981 on the rockglacier Grueo1. Underlying orthoimage of 20.08.1975 (flight line 22, aerial photographs taken by Swisstopo).

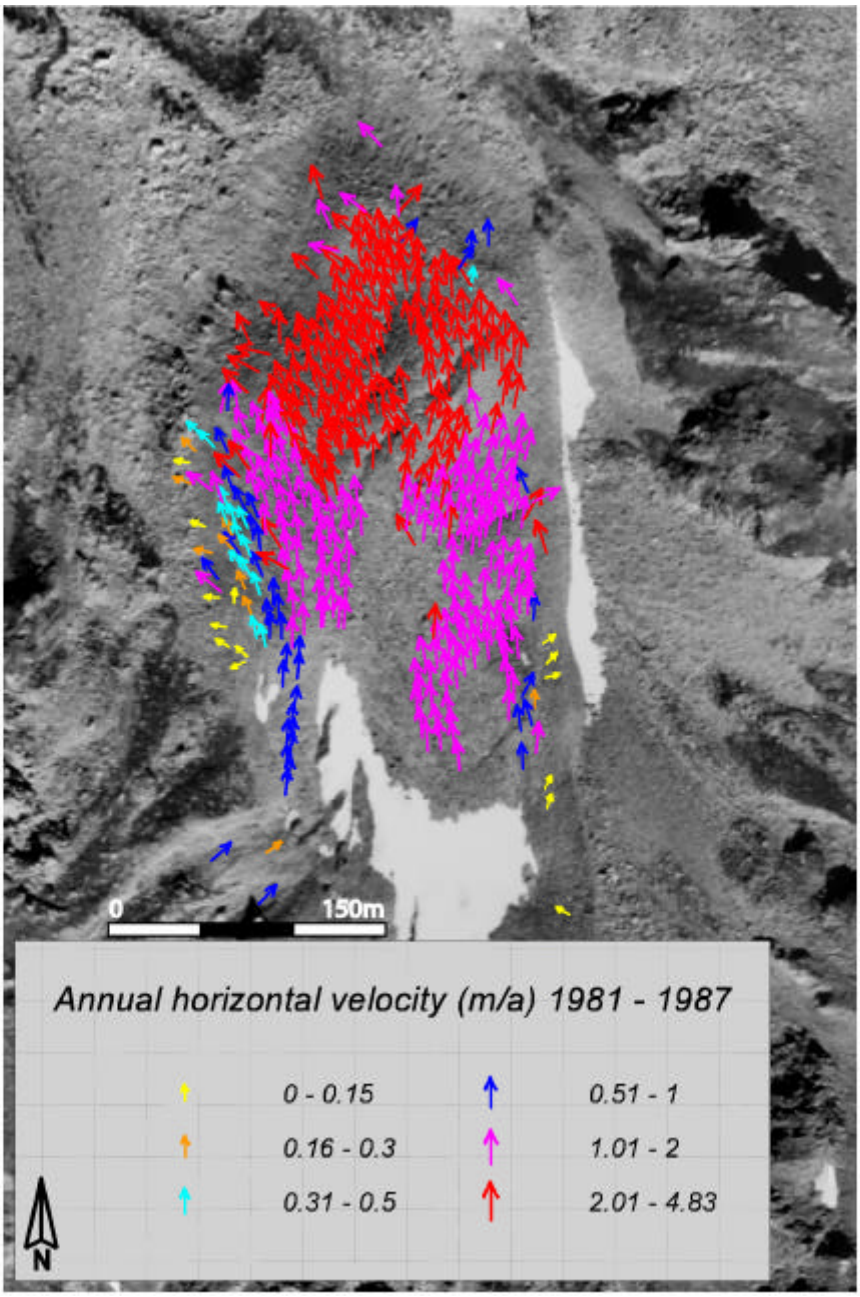

Figure 5.52: Mean annual surface velocities 1981 – 1987 on the rockglacier Grueo1. Underlying orthoimage of 16.08.1987 (flight line 34, aerial photographs taken by Swisstopo).

Also between 1981 and 1987 the vectorfield is clearly divided in two parts (figure 5.52). The surface of the root zone and the middle part moves with 1-2 m/a downwards, while the frontal part accelerates to up to 5 m/a. Additionally, a clearer differentiation of velocities is given at the margins of the rockglacier and reveals a nice gradient, especially on the orographic left side.

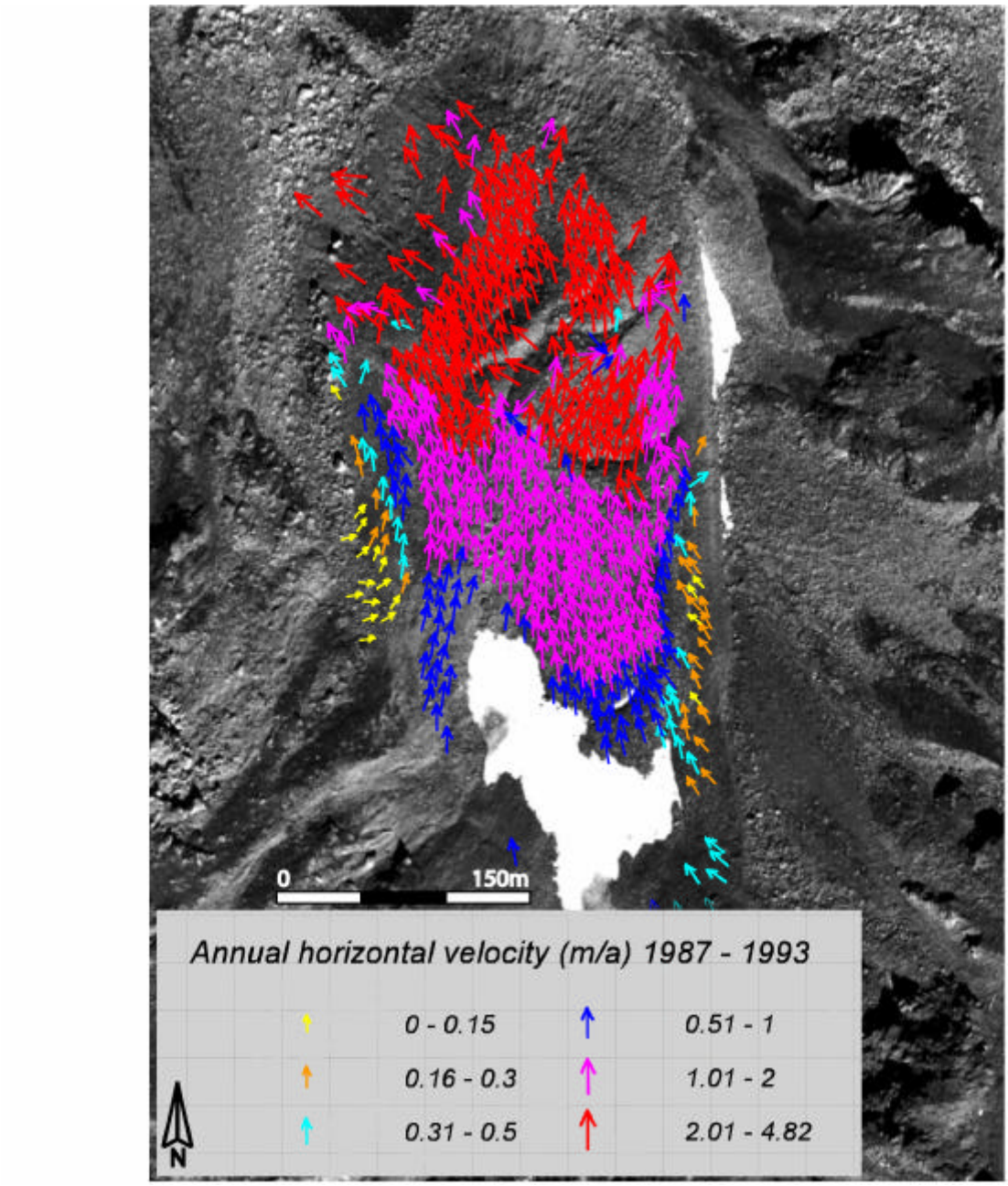

Figure 5.53: Mean annual surface velocities 1987 – 1993 on the rockglacier Grueo1. Underlying orthoimage of 20.08.1993 (flight line 16, aerial photographs taken by Swisstopo).

For the third investigated period (1987 – 1993) a nice sequence of velocityfields is depicted in figure 5.53. Relatively small values (up to 0.5 m/a) are indicated in the root zone and at the margins of the rockglacier. In the upper section, directly below the snowpatch, uniform velocities between 0.51 and 1.0 m/a are measured, while movements up to 2.0 m/a occur in the centre. The lower part of the rockglacier tongue shows the highest velocities between 2.0 and nearly 5.0 m/a. Even around the crevasse-like features the movement reveals no significant gradients.

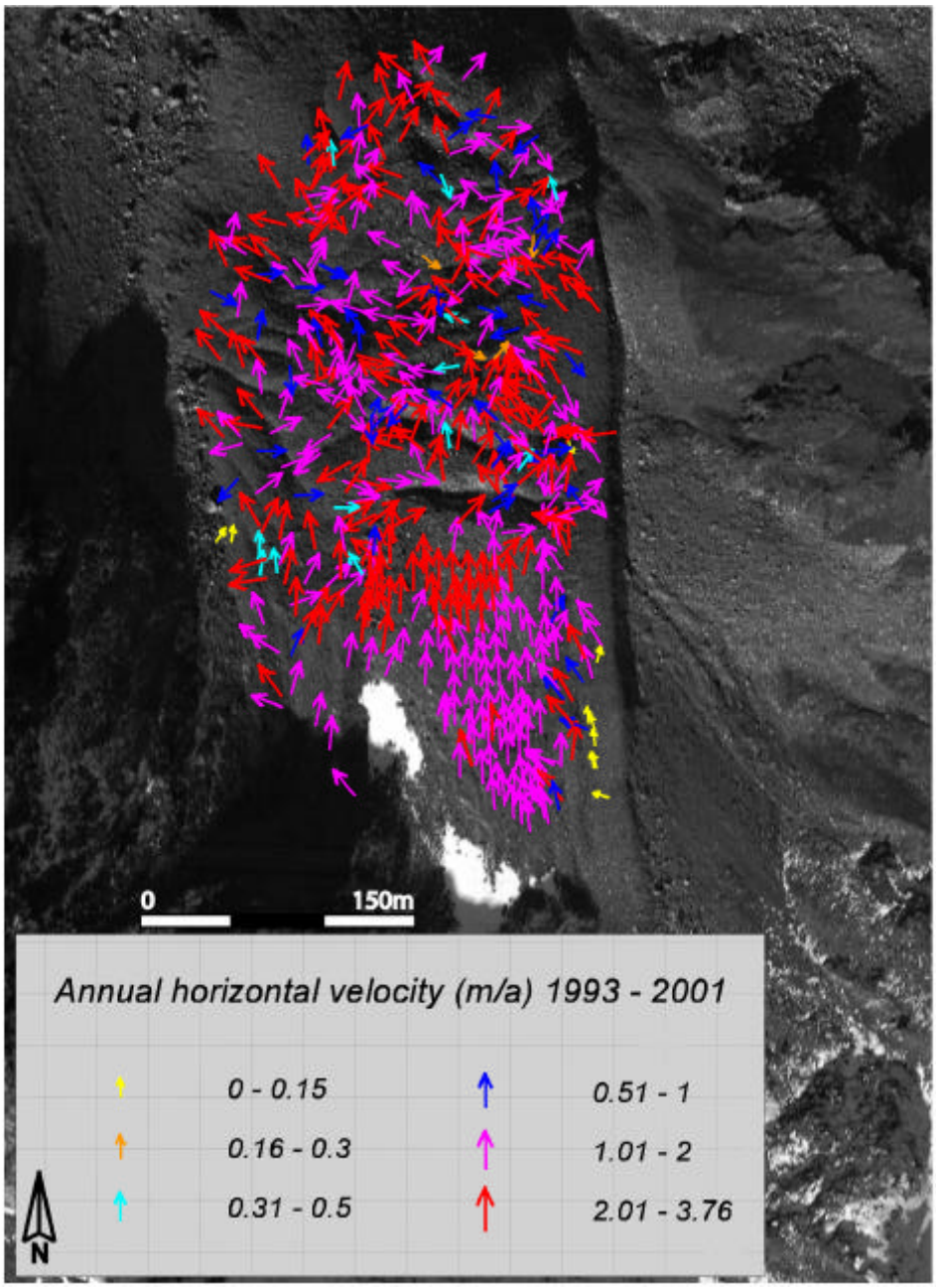

Figure 5.54: Mean annual surface velocities 1993 – 2001 on the rockglacier Grueo1. Underlying orthoimage of 28.09.2001 (HRSC-A data).

The last period (1993 – 2001) displays a drastically different behaviour (figure 5.54). While the upper half of the rockglacier shows horizontal velocities of 1.0 to more than 2 m/a, the vectorfield in the lower half is chaotic due to the ripped topography. Blocks were displaced individually into the crevasses and superimposed by other blocks. That process results in a loss of coherence in optical contrast, which inhibits the measurement of corresponding grey-value features.

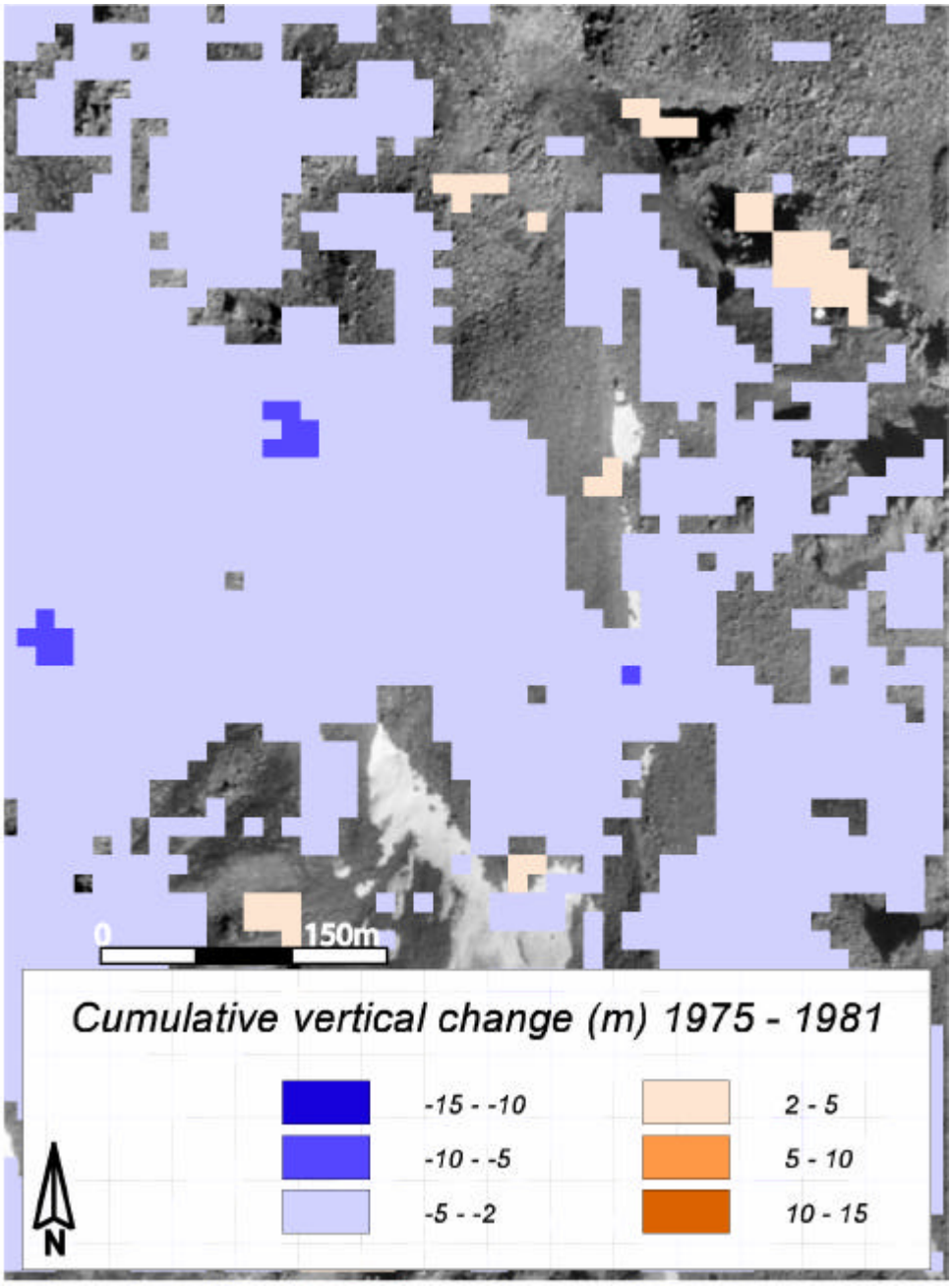

Figure 5.55: Cumulative vertical change on rockglacier Grueo1 between 1975 and 1981 (smoothed by a median-filter, window size 3x3). Underlying orthoimage of 20.08.1975 (flight line 22, aerial photographs taken by Swisstopo).

Vertical changes

The elevation changes on rockglacier Grueo1 depict different developments over the investigated period 1975 - 2001. Between 1975 and 1981, the surface appears to be stable in the root zone as well as in most parts of the front. Against that, a widespread decrease in thickness of -2 - -5 m, which corresponds to a rate of -0.3 - -0.8 m/a, is revealed in the middle part of the rockglacier (figure 5.55).

Over the period 1981-1987, the centre of the permafrost body depicts no vertical changes (figure 5.56). The front shows a cumulative thickening (2 – 5 m; 0.3 – 0.8 m/a), while a thinning occurs in the root zone, especially on the orographic left side of the rockglacier.
Between 1987 and 1993 the vertical changes reveal again a different pattern (figure 5.57). While the centre depicts still an unchanged surface, a uniform increase in thickness (2 – 5 m) occurs in the upper as well as in the lower part of the rockglacier. At the orographic right side of the front, a distinct thickening of 5 – 10 m or 0.8 – 1.7 m/a, respectively, is indicated.
During the last period (1993 – 2001) the rockglacier shows the strongest vertical changes (figure 5.58). These are concentrated in the lower part and depict an increase in thickness of up to 15 m (2.5 m/a) at the front, which is due to the advance of the permafrost body. Directly above the front, a distinct thinning in the same order of magnitude is revealed. This occurs in the area of the deepest crevasse. In the root zone, a slight thinning is depicted, which results probably from the reduction of the snowpatch (compare figures 5.53, 5.54).
In 1997/1998 two avalanche dams were constructed directly below the rockglacier, without directly affecting it. Regarding the change in elevation, the dams give a good opportunity to validate the measurements of vertical movements (cf., Roer et al. 2005).

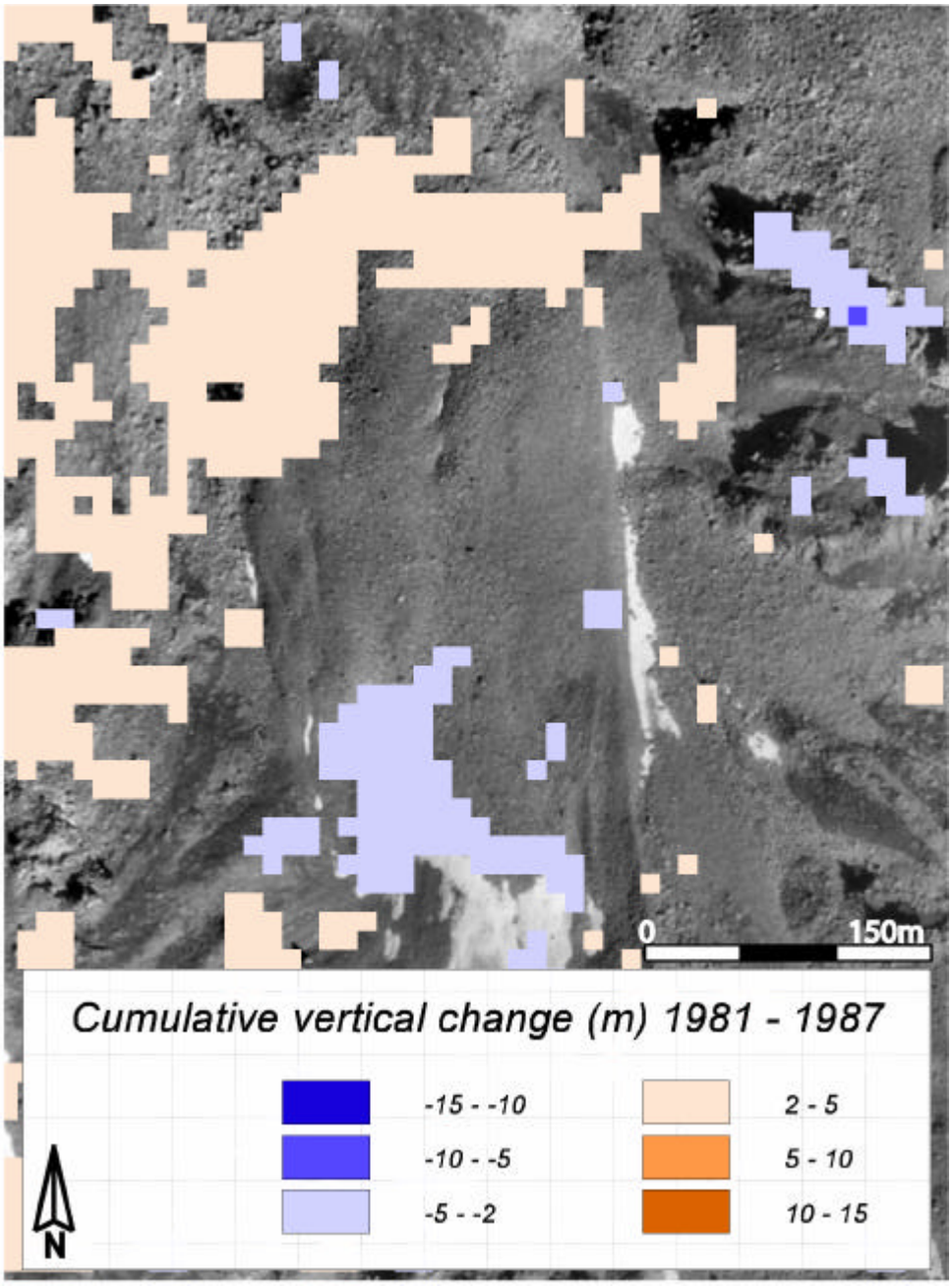

Figure 5.56: Cumulative vertical change on rockglacier Grueo1 between 1981 and 1987 (smoothed by a median-filter, window size 3x3). Underlying orthoimage of 20.08.1975 (flight line 22, aerial photographs taken by Swisstopo).

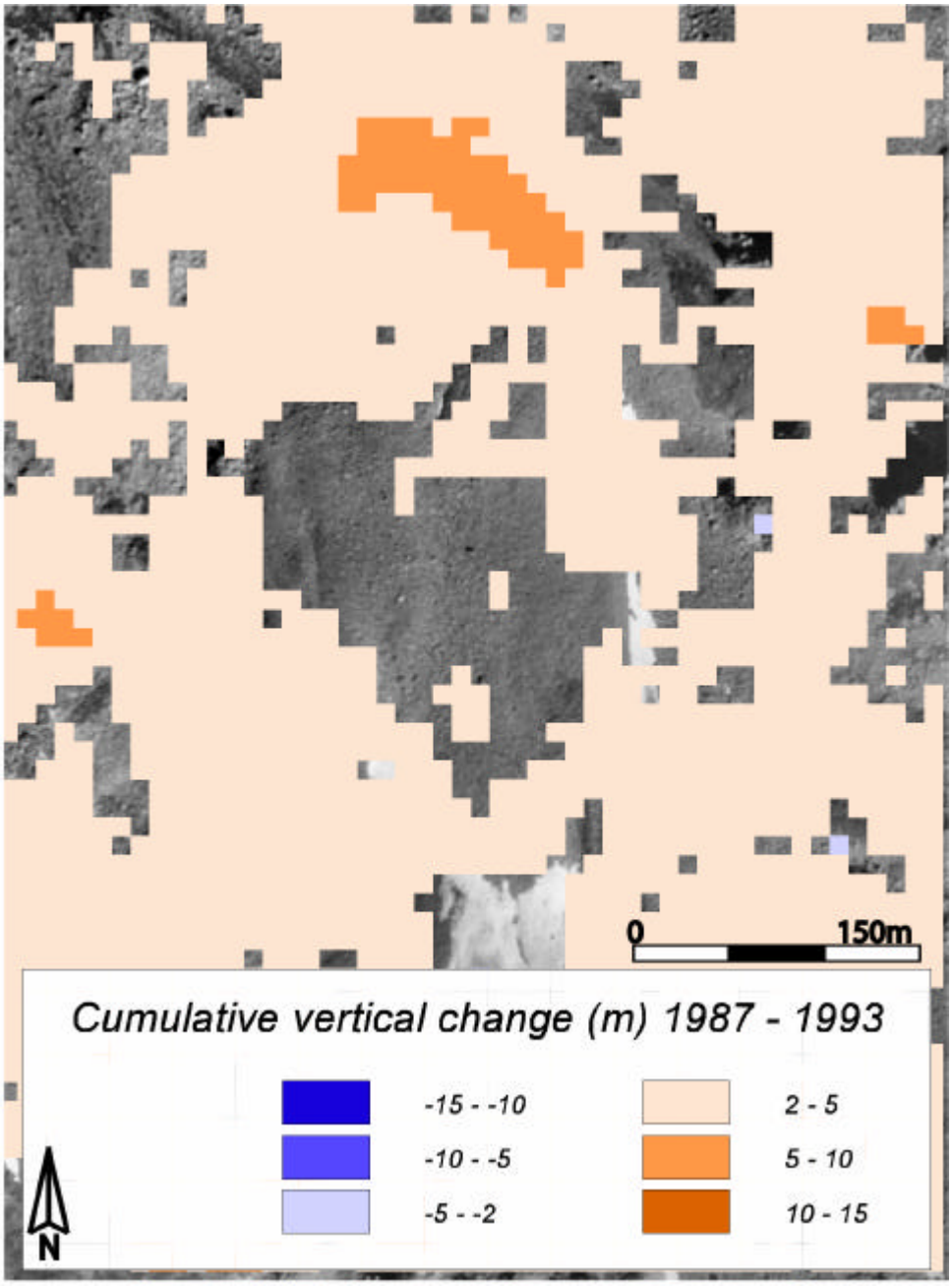

Figure 5.57: Cumulative vertical change on rockglacier Grueo1 between 1987 and 1993 (smoothed by a median-filter, window size 3x3). Underlying orthoimage of 20.08.1975 (flight line 22, aerial photographs taken by Swisstopo).

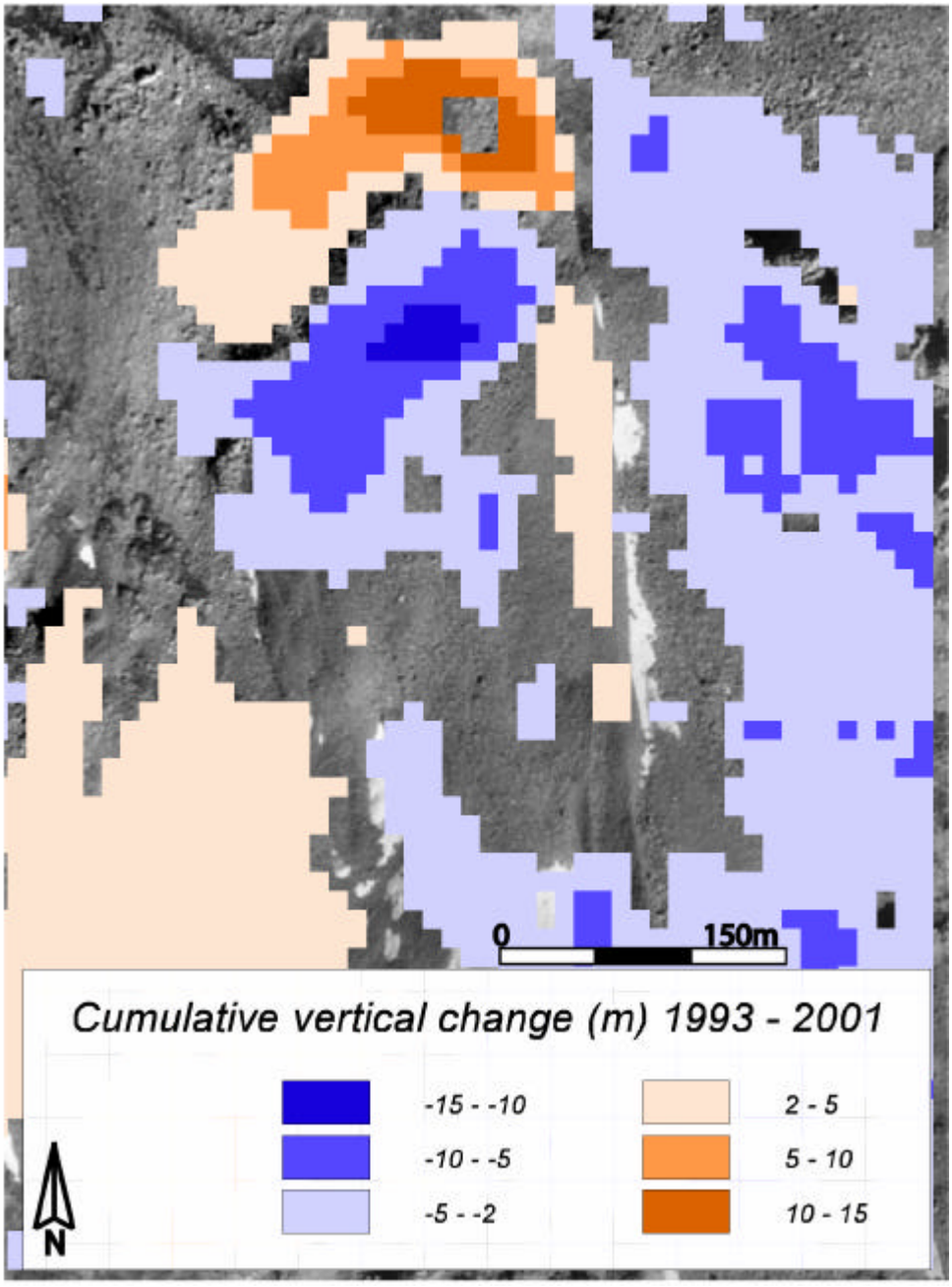

Figure 5.58: Cumulative vertical change on rockglacier Grueo1 between 1993 and 2001 (smoothed by a median-filter, window size 3x3). Underlying orthoimage of 20.08.1975 (flight line 22, aerial photographs taken by Swisstopo).

The exceptional horizontal velocities and vertical changes on Grueo1 underline the conspicuous development of the rockglacier. By the combined analysis of horizontal and vertical changes over four investigated periods, further details on the ongoing processes are hoped for.

The distinct increase in elevation at the front results from the advance of the permafrost body. Only in the last period (1993 – 2001) a corresponding thinning above the front depicts the shift of mass. In this part of the rockglacier, marked signs of instability, such as e.g. development of crevasses and surface destruction, indicate a probable change in process regime. Against that, the middle part of the rockglacier shows no significant losses or gains after 1981 and therefore a

uniform permafrost creep can be assumed here. Regarding the upper part of the rockglacier, it astonishes that in spite of the high horizontal rates and the corresponding flow of rockglacier mass, only a slight thinning occurs in the root zone. Thus, a regular input of mass has to be suspected. This can at least partly be confirmed, since debris-flow deposits were mapped - on orthoimages (1975, 1987) and in the field (2002, 2003) – in the root zone. Additional influence from avalanches can be assumed.

5.2.4.2 Rockglacier Grueo2

Horizontal velocities

On rockglacier Grueo2 (nr. 22 of the inventory) the displacement of a high number of rocks was measured in the first period (1975 – 1993). The vectors depict a uniform field of velocities below 0.15 m/a clearly indicating the creep direction (figure 5.59). In comparison, an adjacent debris-covered slope shows small movements without a clear orientation. In the middle part of the rockglacier higher velocities of up to 0.3 m/a occur.

Between 1993 and 2001 the movement of fewer blocks was quantified, but nevertheless they clearly reveal the acceleration of the rockglacier (figure 5.60). Velocities below 0.15 m/a are indicated by single vectors in the upper part of Grueo2. Against that, the middle part of the rockglacier shows rates mostly between 0.31 and 1.0 m/a. To the front, the velocities are again smaller (0.16 – 0.3 m/a).

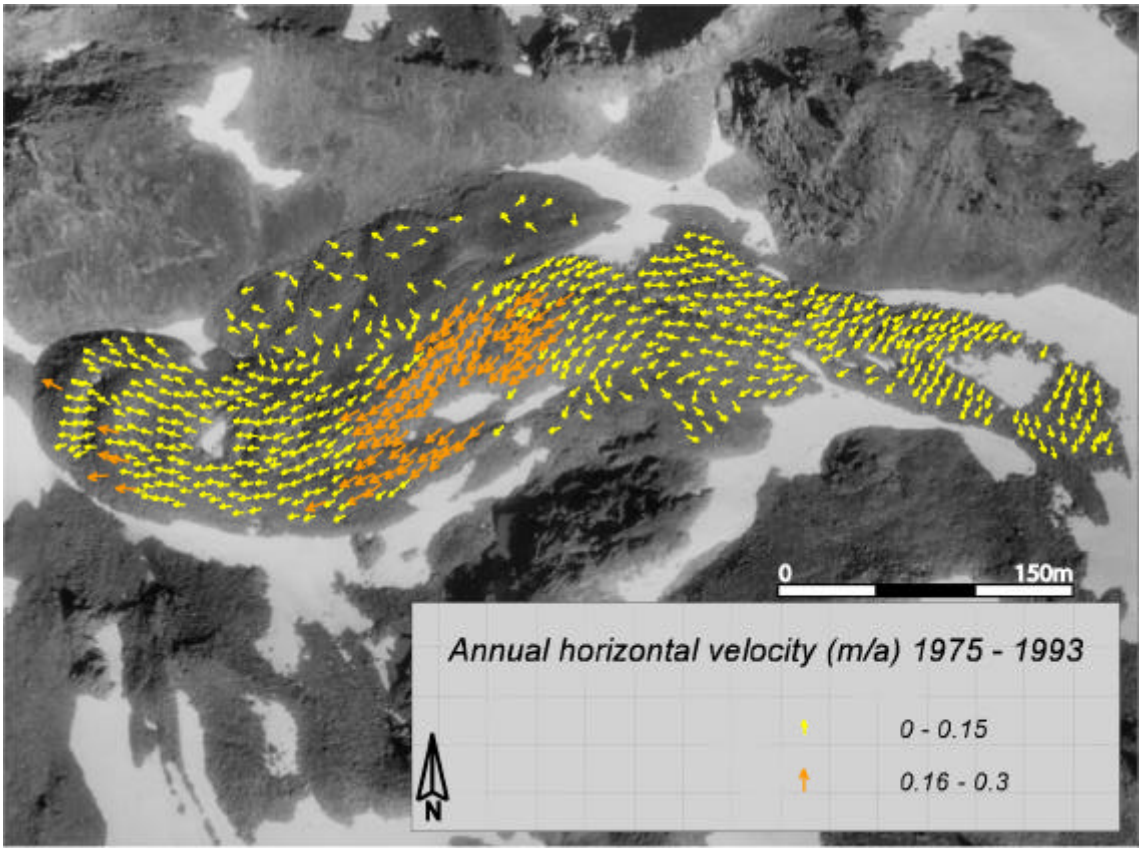

Figure 5.59: Mean annual surface velocities 1975 – 1993 on the rockglacier Grueo2. Underlying orthoimage of 20.08.1975 (flight line 22, aerial photographs taken by Swisstopo).

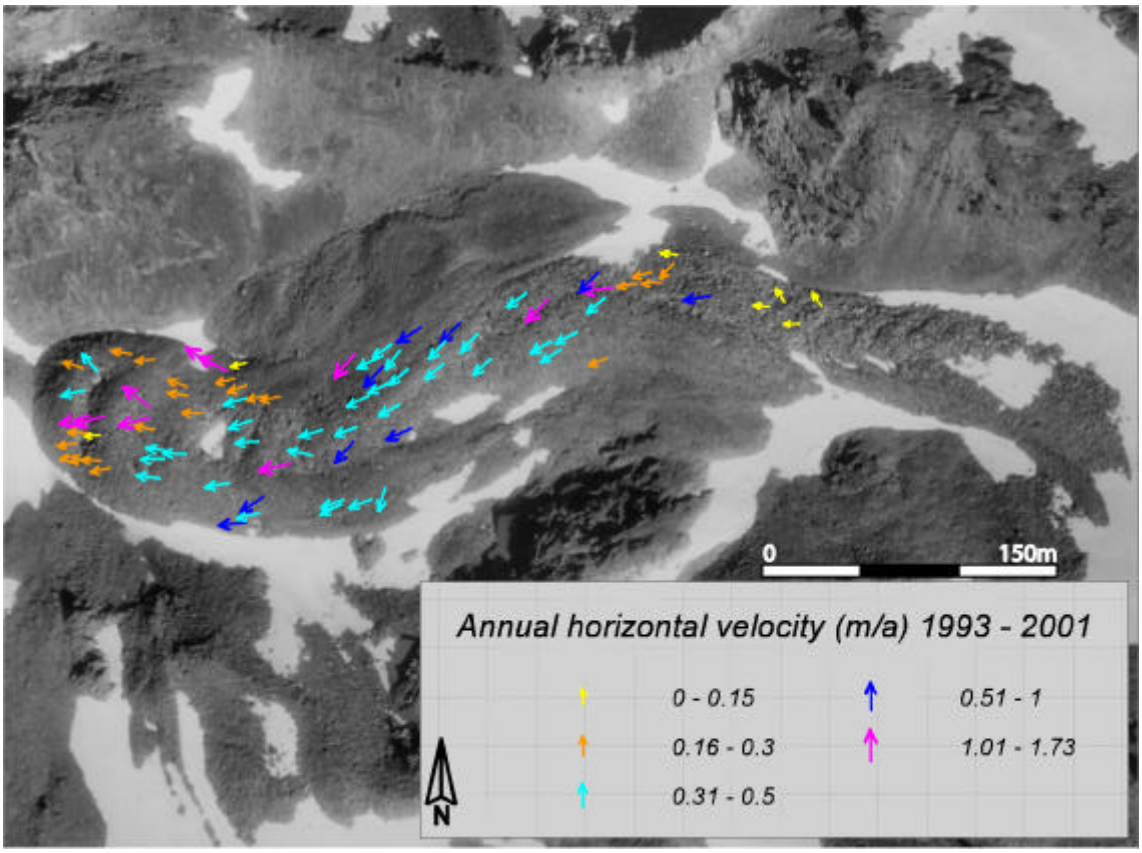

Figure 5.60: Mean annual surface velocities 1993 – 2001 on the rockglacier Grueo2. Underlying orthoimage of 20.08.1975 (flight line 22, aerial photographs taken by Swisstopo).

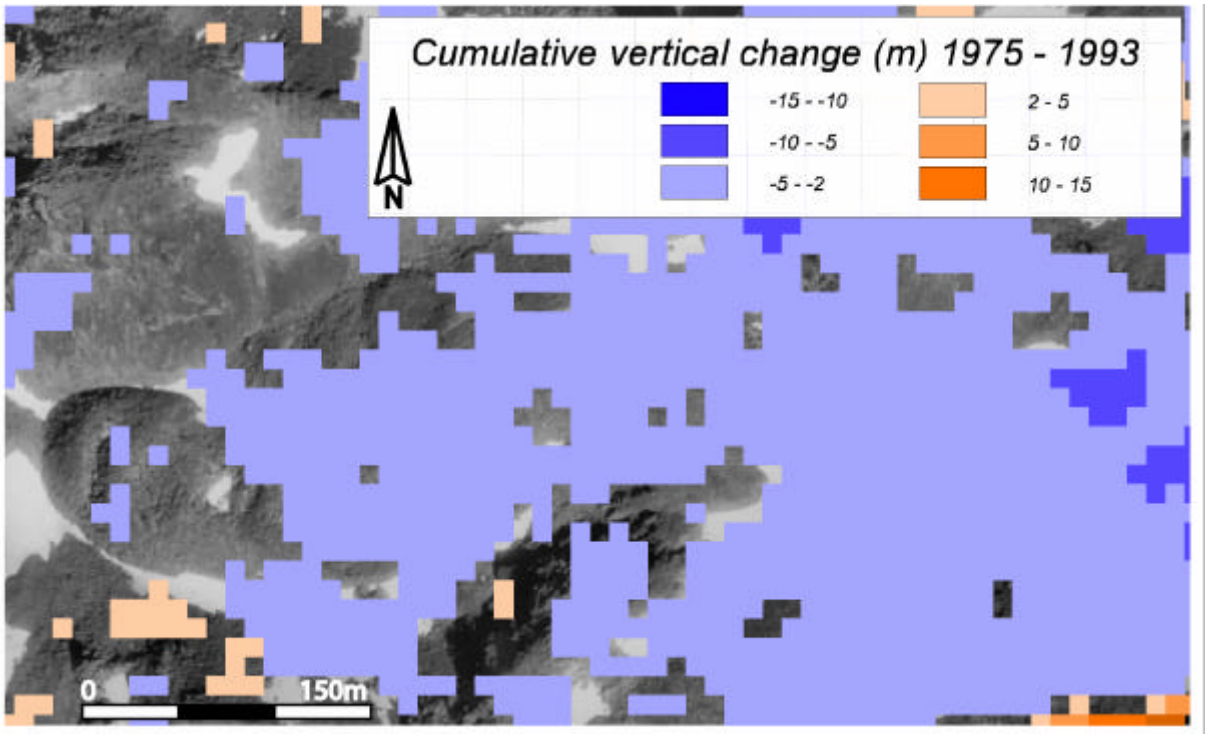

Figure 5.61: Cumulative vertical change on rockglacier Grueo2 between 1975 and 1993 (smoothed by a median-filter, window size 3x3). Underlying orthoimage of 20.08.1975 (flight line 22, aerial photographs taken by Swisstopo).

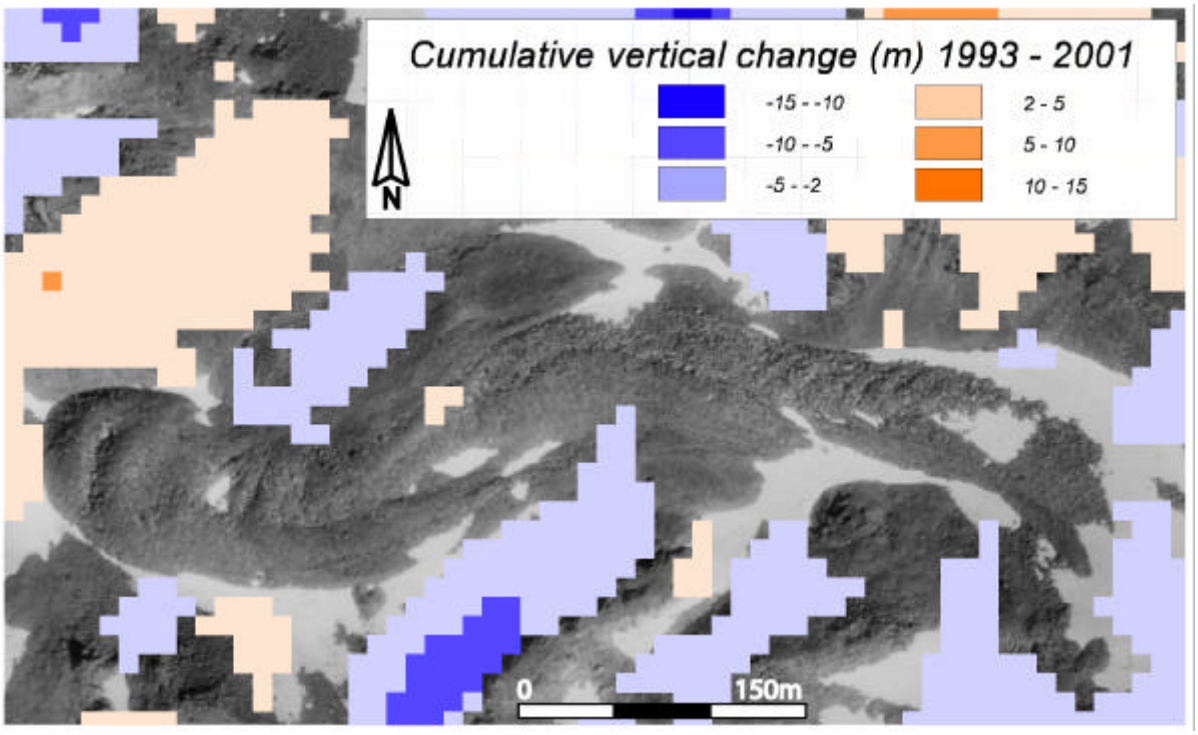

Figure 5.62: Cumulative vertical change on rockglacier Grueo2 between 1993 and 2001 (smoothed by a median-filter, window size 3x3). Underlying orthoimage of 20.08.1975 (flight line 22, aerial photographs taken by Swisstopo).

Vertical changes

The elevation change between 1975 and 1993 depicts a general lowering of the surface (-2 - -5 m; -0.1 – -0.3 m/a), except for the lowermost part of the rockglacier (figure 5.61). Against that, nearly no changes occur in the second investigated period (figure 5.62).

Because of its shape and the distinctive surface topography, this rockglacier represents an interesting landform. Its activity is depicted by a uniform flowfield with higher velocities only in the steeper part of the rockglacier and by a clear speed-up in the second period. Corresponding possible changes in flow balance are not indicated in the vertical changes.

5.2.4.3 Rockglacier Grueo3

Horizontal velocities

In the first period (1975 – 1993), velocities in the range of uncertainty (0.06 m/a) are measured all over rockglacier Grueo 3 (nr. 23 of the inventory). Only individual blocks at the front show higher movements (figure 5.63).

Between 1993 and 2001, the velocities are again in the range of uncertainty (0.13 m/a) apart from single blocks (figure 5.64). Thus, the inactivity of the feature has to be assumed, even if the orientation of the vectors indicates a uniform direction in both periods.

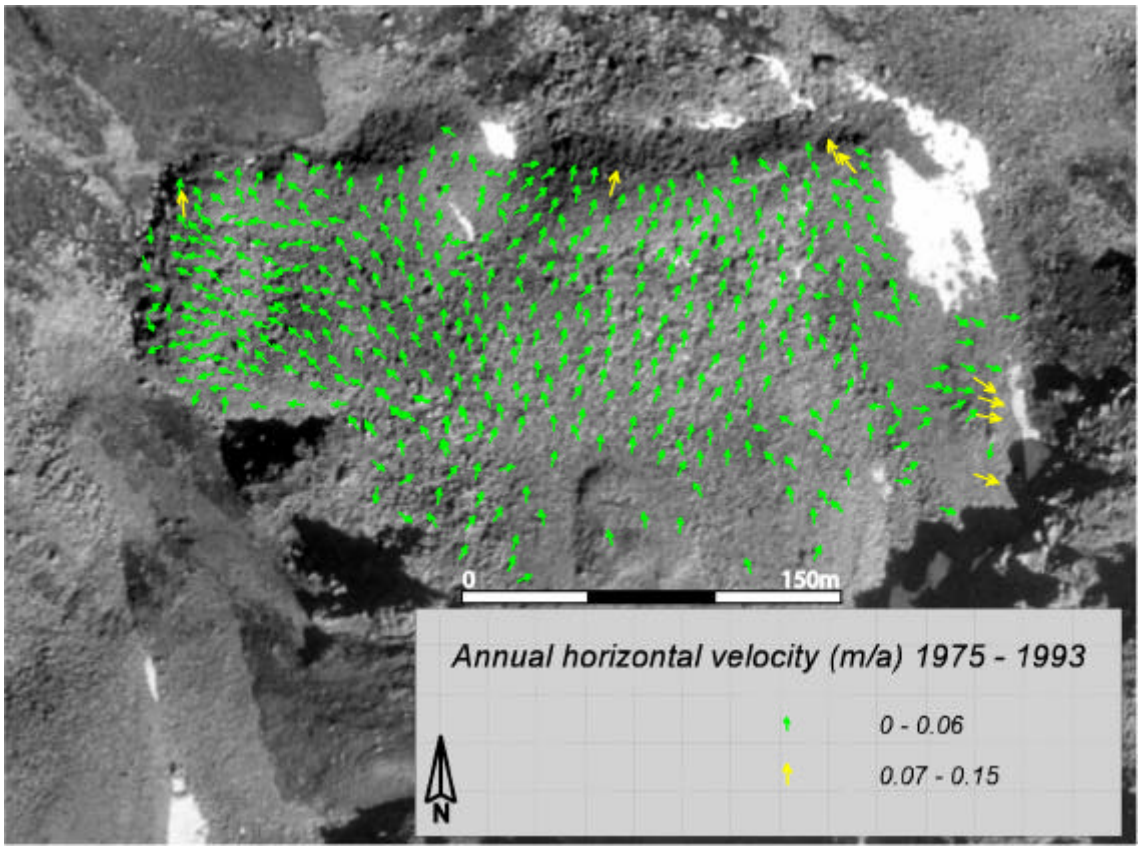

Figure 5.63: Mean annual surface velocities 1975 – 1993 on the rockglacier Grueo3. Underlying orthoimage of 20.08.1975 (flight line 22, aerial photographs taken by Swisstopo).

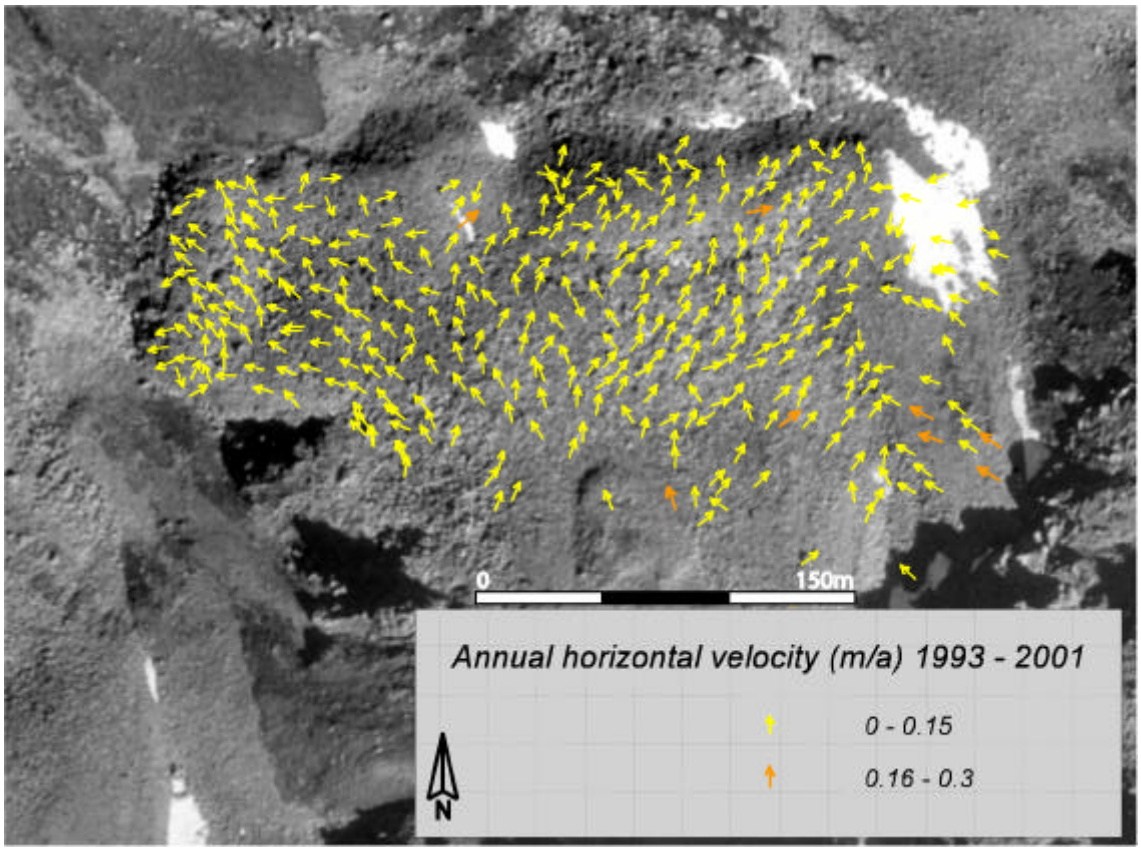

Figure 5.64: Mean annual surface velocities 1993 – 2001 on the rockglacier Grueo3. Underlying orthoimage of 20.08.1975 (flight line 22, aerial photographs taken by Swisstopo).

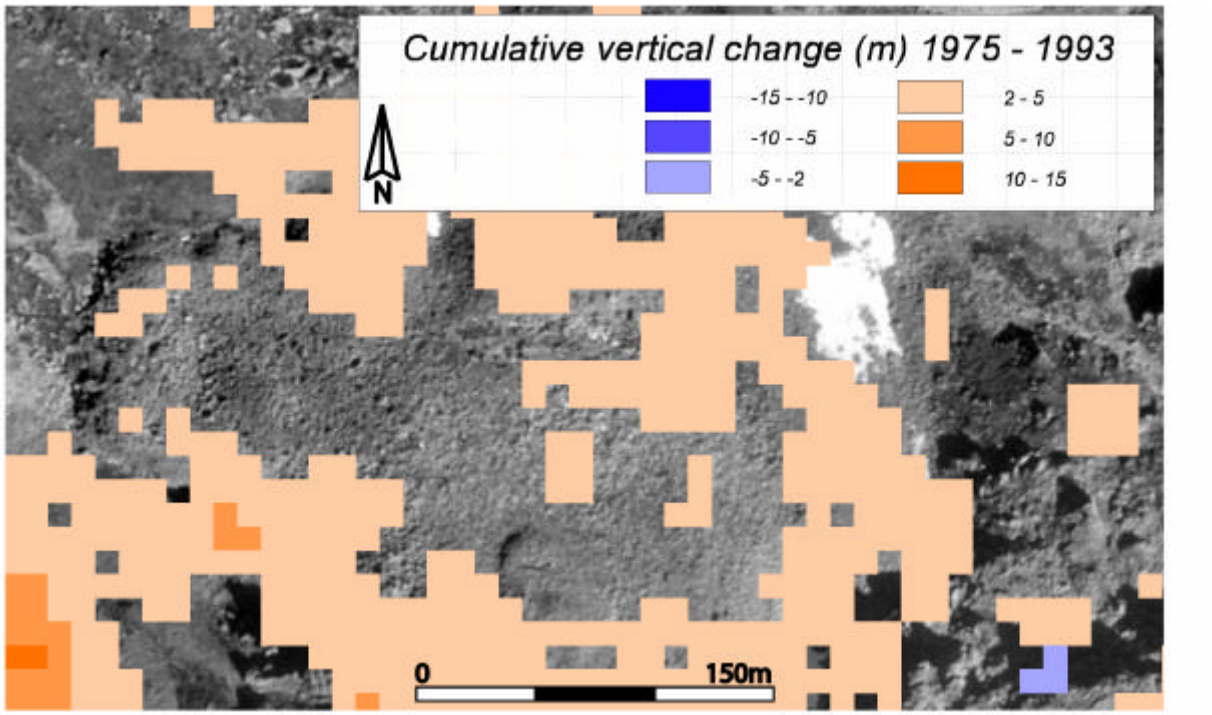

Figure 5.65: Cumulative vertical change on rockglacier Grueo3 between 1975 and 1993 (smoothed by a median-filter, window size 3x3). Underlying orthoimage of 20.08.1975 (flight line 22, aerial photographs taken by Swisstopo).

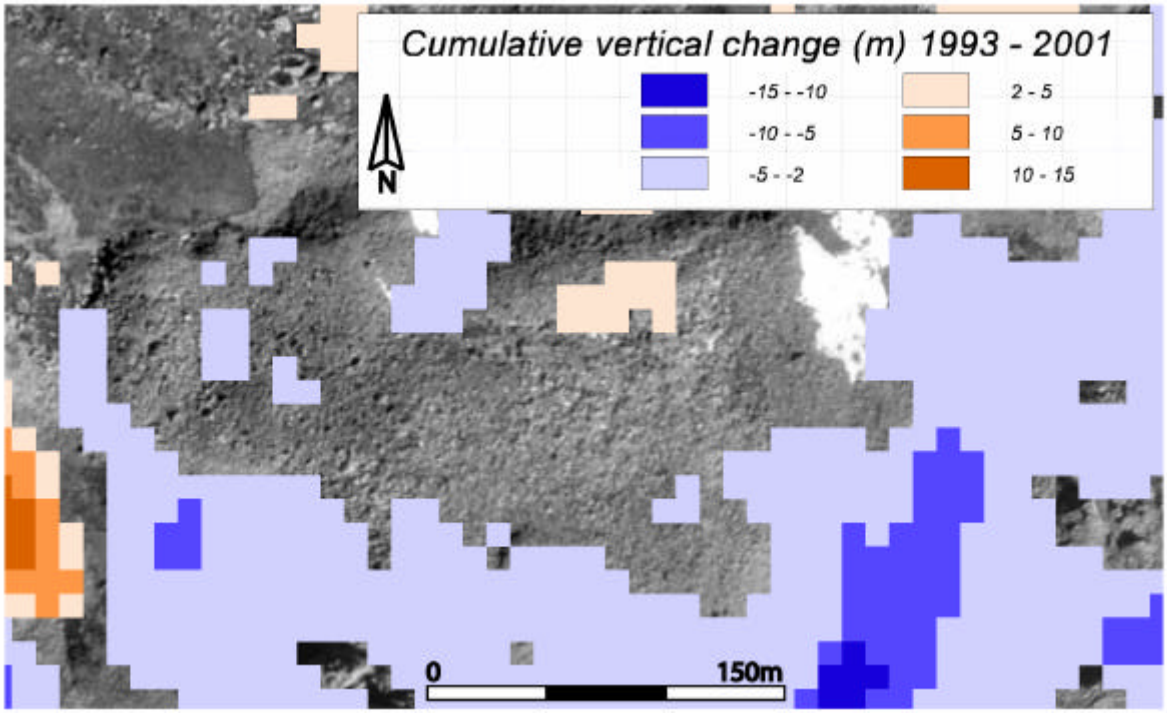

Figure 5.66: Cumulative vertical change on rockglacier Grueo3 between 1993 and 2001 (smoothed by a median-filter, window size 3x3). Underlying orthoimage of 20.08.1975 (flight line 22, aerial photographs taken by Swisstopo).

Vertical changes

Between 1975 and 1993 rockglacier Grueo3 shows an increase in thickness (2 – 5 m; 0.1 – 0.3 m/a) which is widespread in the orographic right part (figure 5.65). In contrast to that, a decrease in thickness (-2 - -5; -0.25 - -0.6 m/a) is revealed in some parts at the rockglacier margin over the second period (figure 5.66).

5.2.4.4 Rockglacier Grueo4

Horizontal velocities

This rockglacier (nr. 24 of the inventory) is situated in a similar position like Grueo3 and shows a similar vectorfield. In the first period (1975 – 1993) the rockglacier reveals velocities in the range of uncertainty apart from one lobe which is superimposed on the main body of the rockglacier. This lobe depicts speeds mostly between 0.07 and 0.15 m/a (figure 5.67).

In the second period (1993 – 2001) a similar pattern is given in the data (figure 5.68). The main part of the rockglacier shows again rates in the range of uncertainty (0.13 m/a), but the aforementioned lobe depicts clearly higher values. Especially in the upper part of this lobe, some blocks move up to 1.0 m/a.

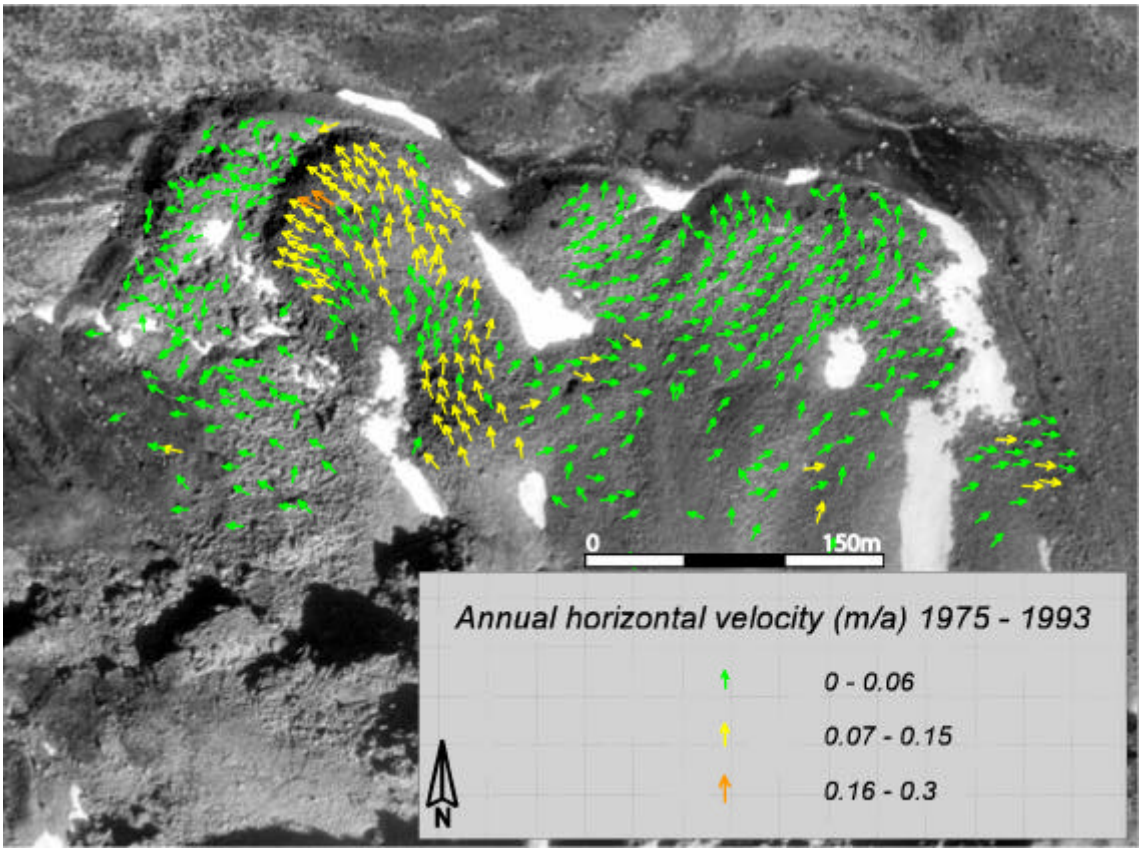

Figure 5.67: Mean annual surface velocities 1975 – 1993 on the rockglacier Grueo4. Underlying orthoimage of 20.08.1975 (flight line 22, aerial photographs taken by Swisstopo).

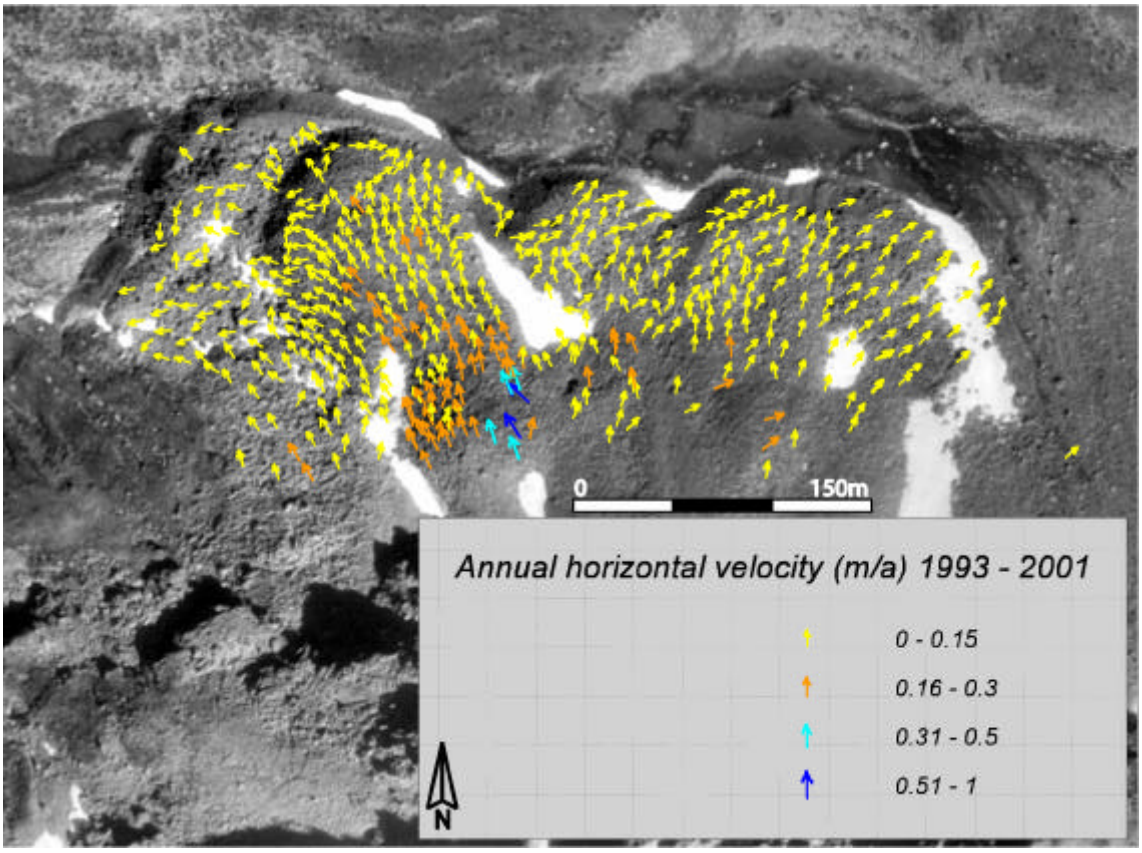

Figure 5.68: Mean annual surface velocities 1993 – 2001 on the rockglacier Grueo4. Underlying orthoimage of 20.08.1975 (flight line 22, aerial photographs taken by Swisstopo).

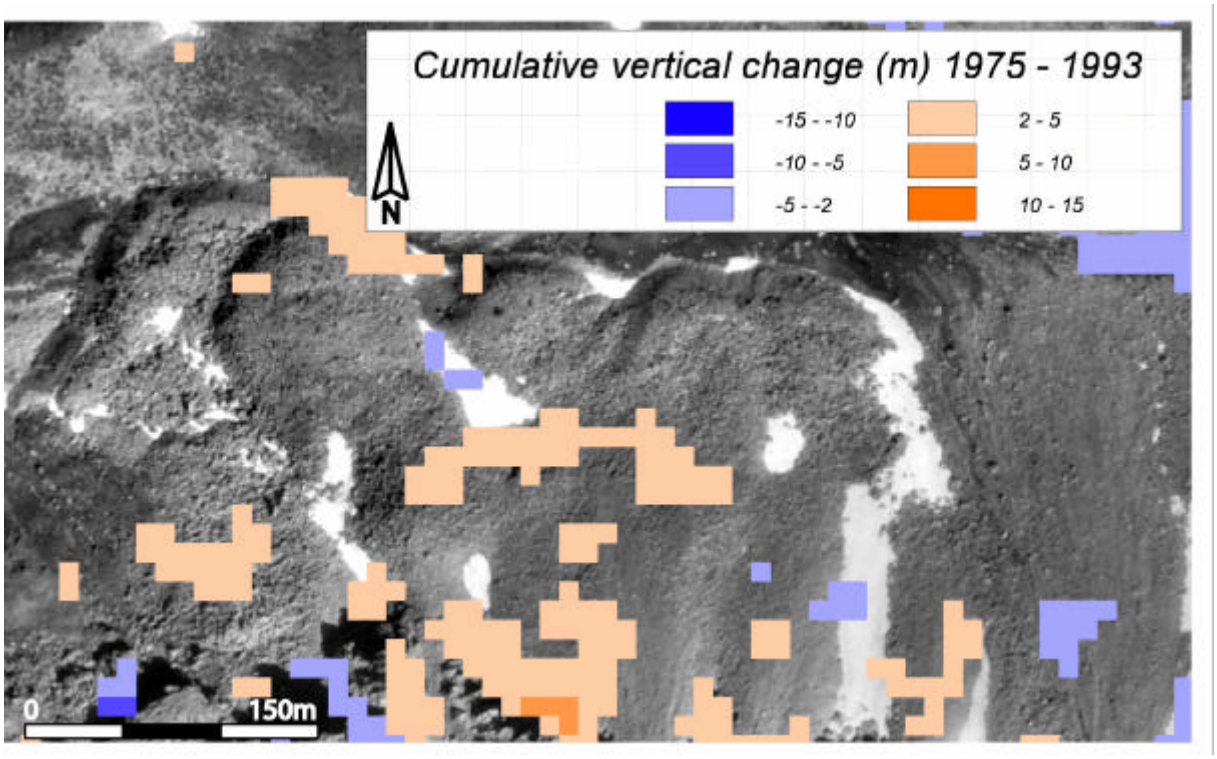

Figure 5.69: Cumulative vertical change on rockglacier Grueo4 between 1975 and 1993 (smoothed by a median-filter, window size 3x3). Underlying orthoimage of 20.08.1975 (flight line 22, aerial photographs taken by Swisstopo).

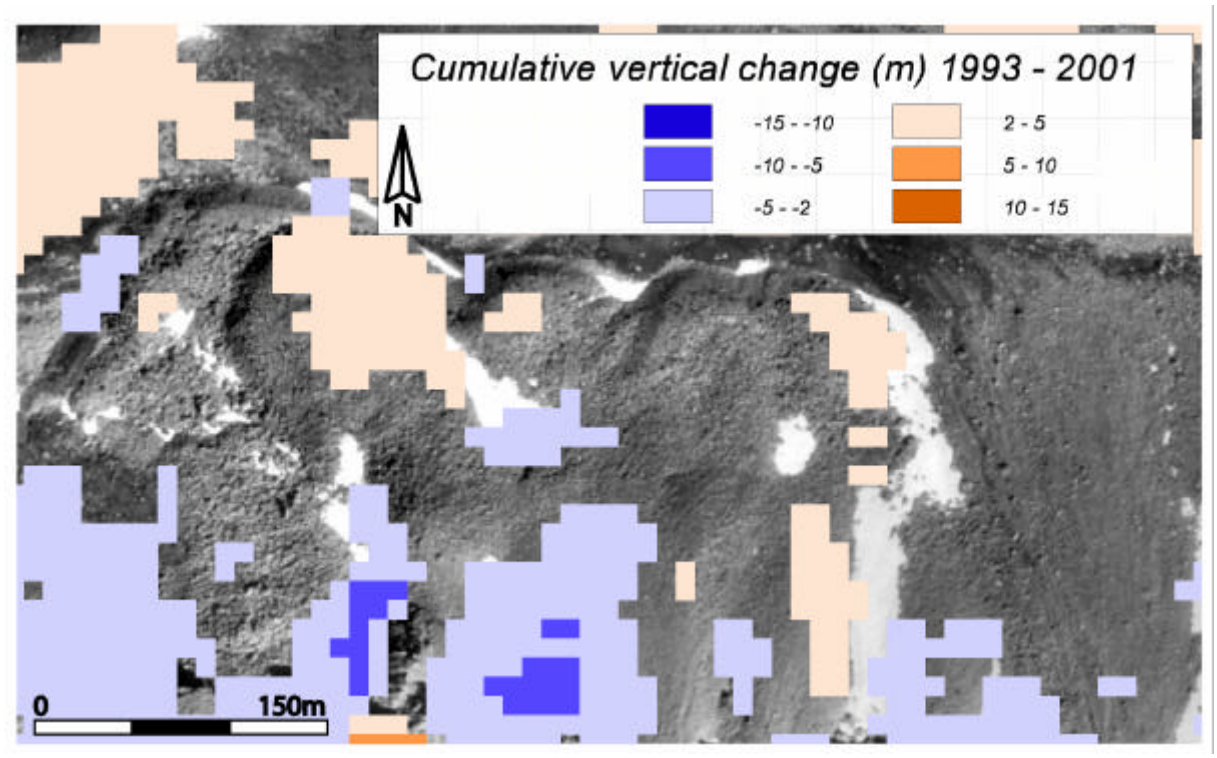

Figure 5.70: Cumulative vertical change on rockglacier Grueo4 between 1993 and 2001 (smoothed by a median-filter, window size 3x3). Underlying orthoimage of 20.08.1975 (flight line 22, aerial photographs taken by Swisstopo).

Vertical changes

In a small area in the central part of the rockglacier Grueo4 and at the front of the superimposed lobe an increase in thickness is depicted in the first period (figure 5.69). Between 1993 and 2001 wider areas on the mentioned lobe as well as on the orographic right side reveal a cumulative thickening (2 – 5 m; 0.25 – 0.6 m/a). Thinning occurs in the area of the snowpatch. Additionally, the high values in the root zone of the rockglacier result from measurement errors due to shadows (figure 5.70).

Grueo3 and Grueo4 depict typical lobe-shaped rockglaciers situated in the bottom of a hanging valley. They reveal inactivity or small movements, apart from single lobes moving on top of the older lobes.

5.2.4.5 Rockglacier Grueo5

Horizontal velocities

On this rockglacier (nr. 25 of the inventory) the velocities were predominantly in the range of uncertainty in the first period (1975 – 1993). Additionally, measurements were impossible in the second period (1993 – 2001) due to snow on the 2001 orthoimage. Thus, the state of activity of this rockglacier is hard to determine, but inactivity has to be assumed due to the low rates in the first period.

Vertical changes

Regarding the elevation changes over the entire period 1975 – 2001 (figure 5.6), decrease in thickness is depicted in the root zone while an increase occurs in the lower part of the rockglacier. Due to the before mentioned snow on the orthoimage of 2001 and the possible measurement errors, the vertical changes are not included in the activity assessment of Grueo5.

5.2.4.6 Rockglacier Grueo6

Horizontal velocities

Rockglacier Grueo6 (nr. 26 of the inventory) is a large feature with the main part of the permafrost body situated in a cirque, while the frontal part is creeping over a steep slope into the hanging valley. Between 1975 and 1993 the movement of a lot of blocks was quantified (figure 5.71). On the main body the velocities are completely below 0.15 m/a, but above the front rates between 0.16 and 0.5 m/a are depicted. At the foot of the front movements are in the range of uncertainty.

In the second period (1993 – 2001) only a few blocks were matched, again due to a loss in optical contrast resulting from snow on the orthoimage of 2001 (figure 5.72). The vectors indicate again

velocities below 0.15 m/a on the main body and values up to 0.5 m/a above the front. Directly at the front and at its foot, higher rates up to 2.0 m/a are depicted.

Vertical changes

Over the first period the elevation changes on Grueo6 reveal an increase in thickness (2 – 5 m; 0.1 – 0.3 m/a) on the orographic right side as well as in the steep part at the rockglacier front (figure 5.73). The distinct decrease in elevation indicated in the orographic right part of the front probably result from errors in the measurements due to shadows in the orthoimages. The rest of the permafrost body depicts an unchanged surface.

Between 1993 and 2001, some patchy thickening (2 – 5 m; 0.25 – 0.6 m/a) occurs in the upper part of the rockglacier, while to the front the surface appears to be stable (figure 5.74). Again, the distinct lowering depicted at both sides of the front results from measurement errors.

Rockglacier Grueo6 is a very interesting landform because of its shape and the extraordinary position. The front depicts no signs of instability, although it is situated on a very steep slope. In the upper part of the rockglacier (around the large snowpatch) a new lobe seems to develop. This is indicated in the orientation of the vectors and by a thickening in both investigated periods. Unfortunately, only very few blocks were matched in the second period and thus it is not clear how this part of the rockglacier developed.

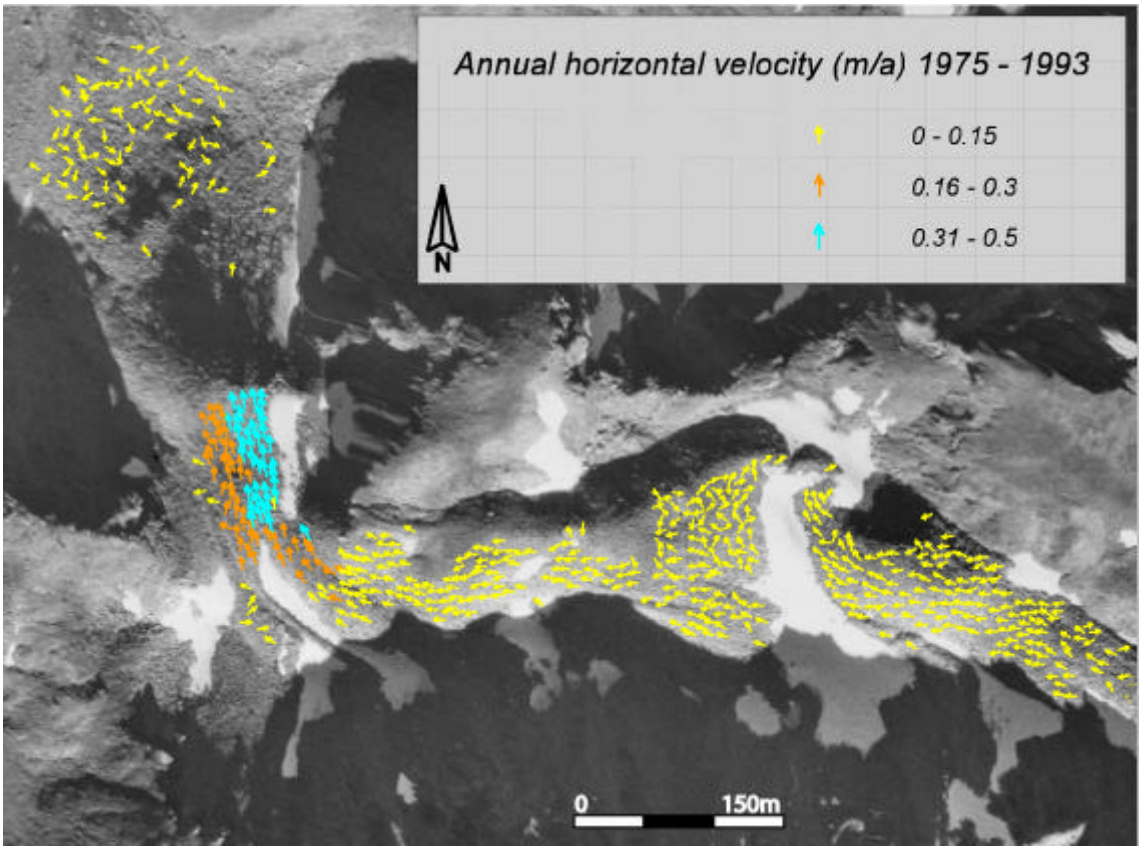

Figure 5.71: Mean annual surface velocities 1975 – 1993 on the rockglacier Grueo6. Underlying orthoimage of 06.10.1975 (flight line 21, aerial photographs taken by Swisstopo).

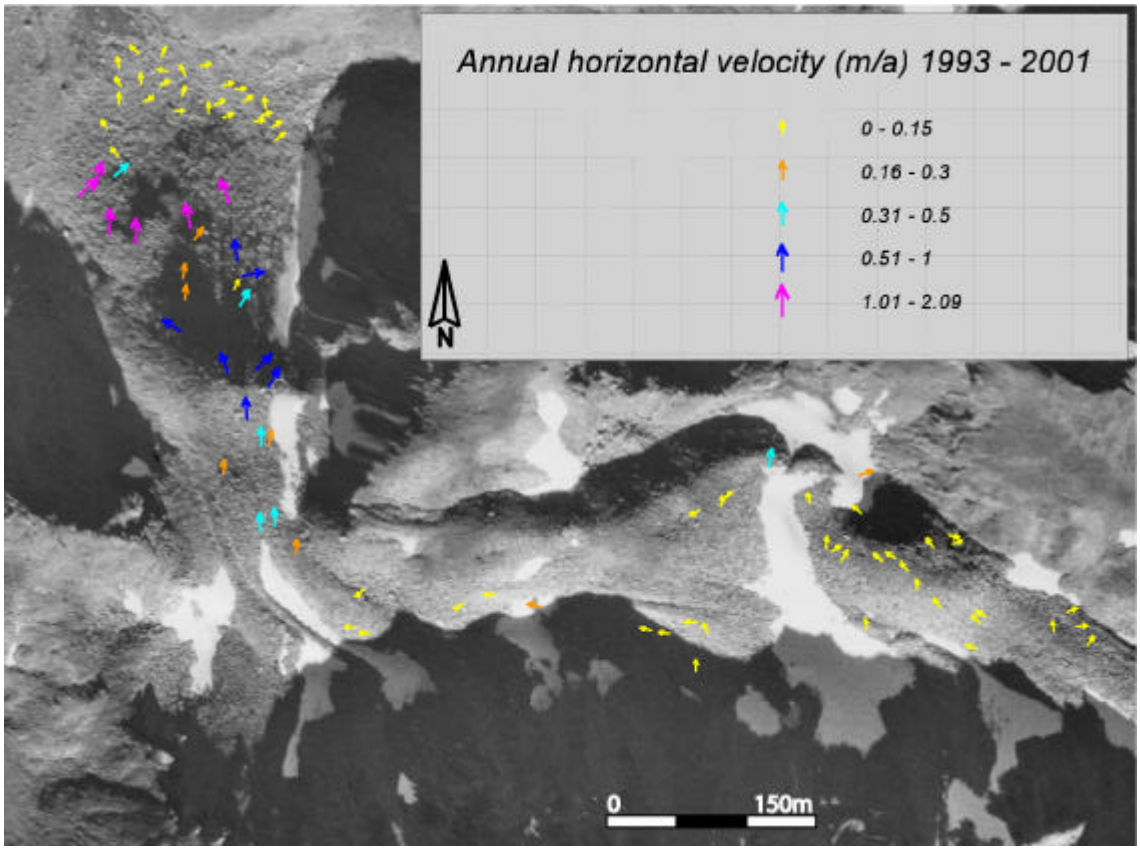

Figure 5.72: Mean annual surface velocities 1993 – 2001 on the rockglacier Grueo6. Underlying orthoimage of 06.10.1975 (flight line 21, aerial photographs taken by Swisstopo).

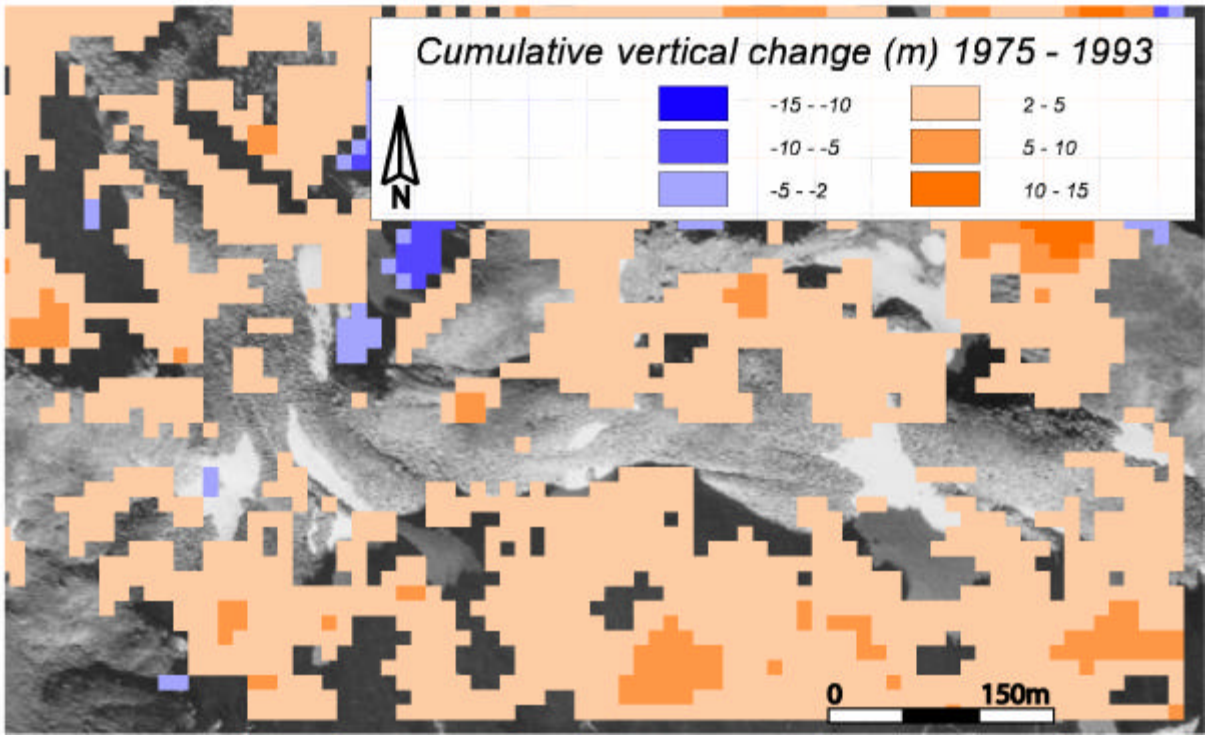

Figure 5.73: Cumulative vertical change on rockglacier Grueo6 between 1975 and 1993 (smoothed by a median-filter, window size 3x3). Underlying orthoimage of 06.10.1975 (flight line 21, aerial photographs taken by Swisstopo).

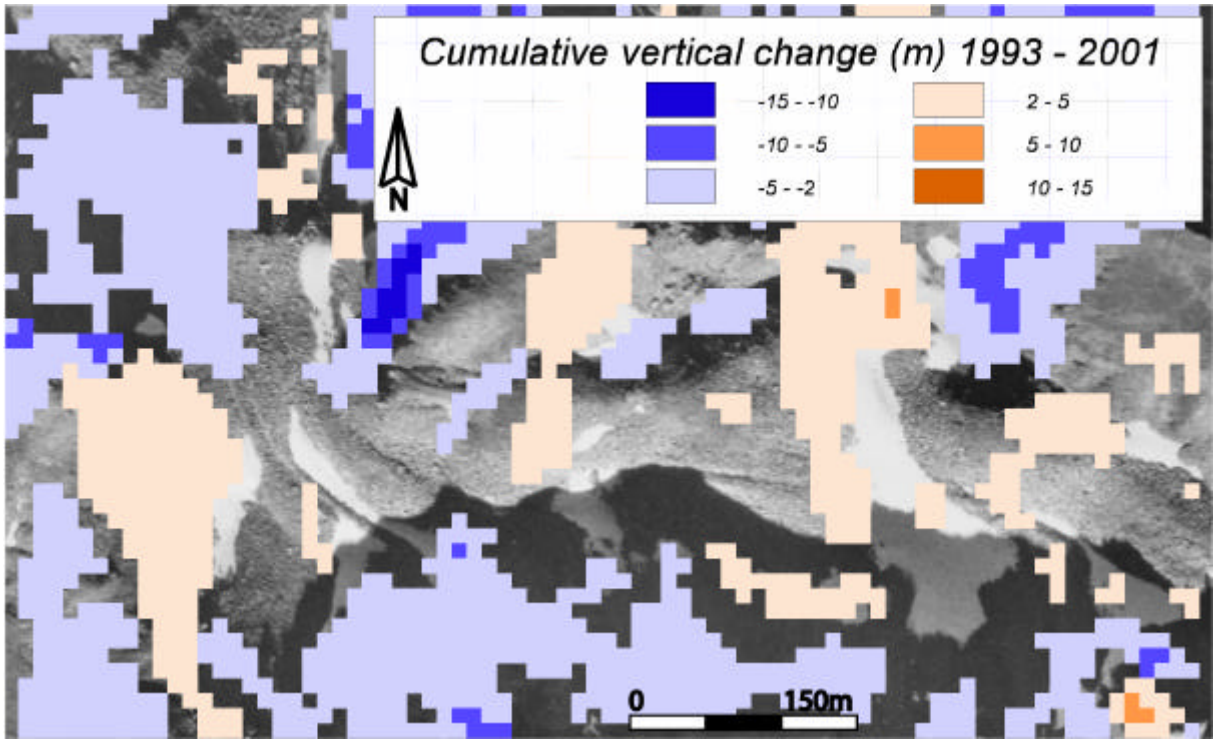

Figure 5.74: Cumulative vertical change on rockglacier Grueo6 between 1993 and 2001 (smoothed by a median-filter, window size 3x3). Underlying orthoimage of 06.10.1975 (flight line 21, aerial photographs taken by Swisstopo).

5.2.4.7 Rockglacier Grueo7

Horizontal velocities

Grueo7 (nr. 27 of the inventory) is a complex rockglacier situated in the bottom of the hanging valley. In the first investigated period (1975 – 1993) it shows a uniform velocityfield with rates up to 0.15 m/a (figure 5.75). Only single blocks reveal higher values.

Between 1993 and 2001 the rockglacier shows a distinct increase in speed (figure 5.76). While rates are below 0.15 m/a on the lowermost lobe, they depict a uniform field between 0.16 and 0.3 m/a in the middle part of the rockglacier with a small field of high velocities (up to 1.9 m/a) in the central flowline (above the fourth front). In the root zone, measurements were not possible.

Vertical changes

Between 1975 and 1993 the vertical changes on Grueo7 reveal an increase in thickness (2 – 5 m; 0.1 – 0.3 m/a), which occurs mostly at the margin of the rockglacier (figure 5.77). Against that, the rockglacier surface depicts only a patchy thickening (2 – 5 m; 0.25 – 0.6 m/a) in the second period (figure 5.78). A decrease in thickness of up to -10 m (-1.25 m/a) is indicated at the rockglacier front. The noisy pattern at the border of the image results from errors due to shadows and snowcover. Therefore, mass gains or losses can not be determined for the root zone of the rockglacier.

Grueo7 is a complex tongue-shaped rockglacier situated in the bottom of the hanging valley. But, compared to other rockglaciers in a similar position, it depicts a clear activity and a very distinct speed-up in the second period.

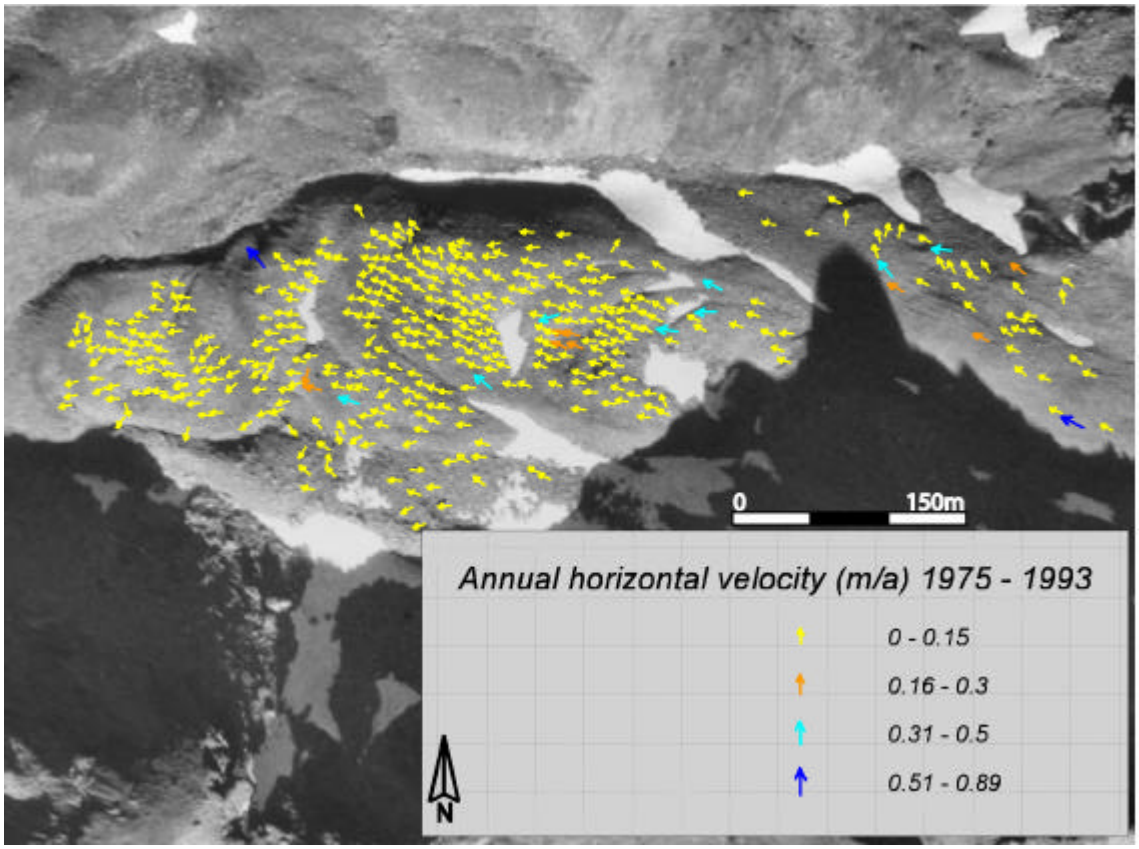

Figure 5.75: Mean annual surface velocities 1975 – 1993 on the rockglacier Grueo7. Underlying orthoimage of 06.10.1975 (flight line 21, aerial photographs taken by Swisstopo).

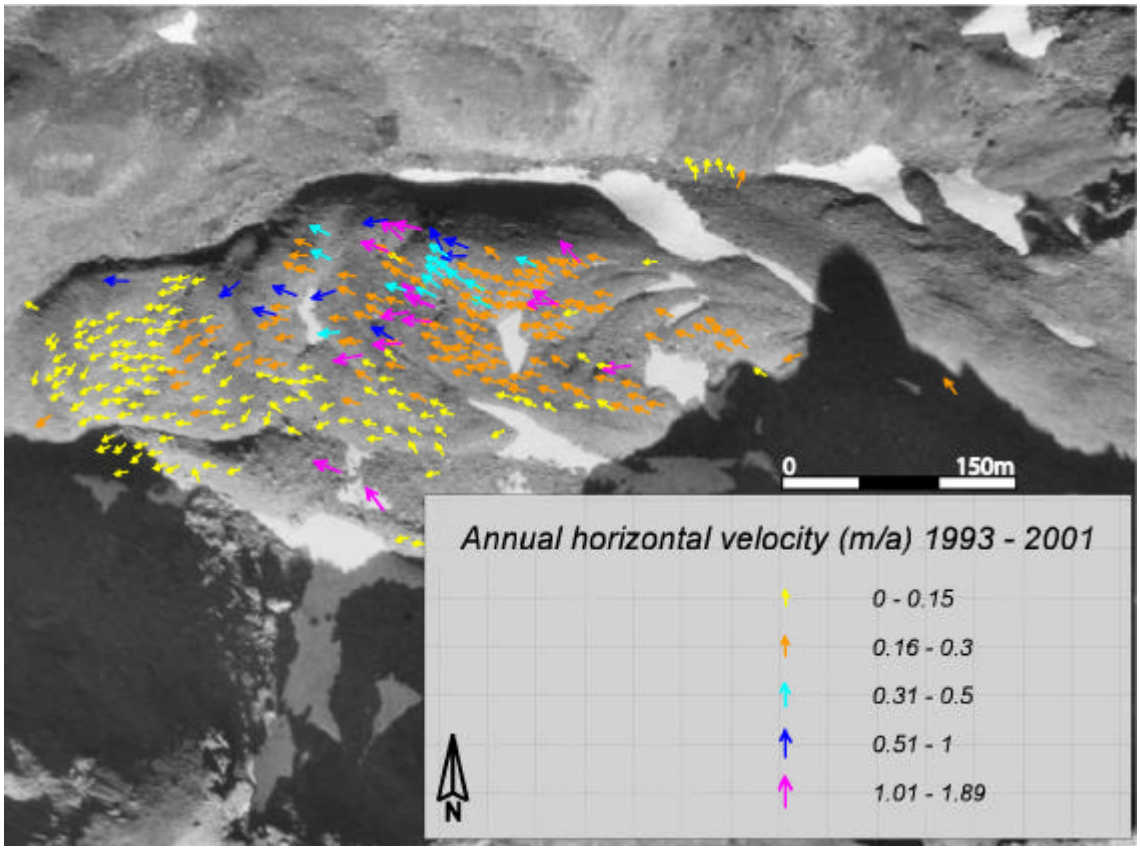

Figure 5.76: Mean annual surface velocities 1993 – 2001 on the rockglacier Grueo7. Underlying orthoimage of 06.10.1975 (flight line 21, aerial photographs taken by Swisstopo).

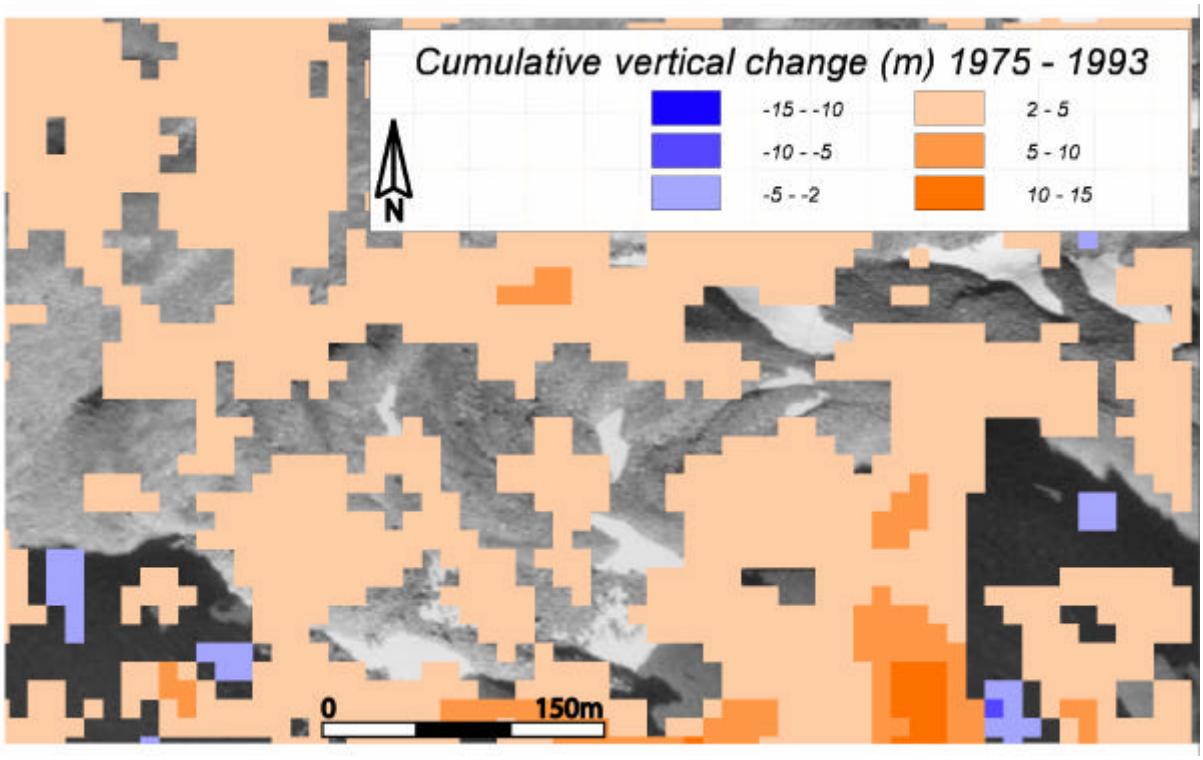

Figure 5.77: Cumulative vertical change on rockglacier Grueo7 between 1975 and 1993 (smoothed by a median-filter, window size 3x3). Underlying orthoimage of 06.10.1975 (flight line 21, aerial photographs taken by Swisstopo).

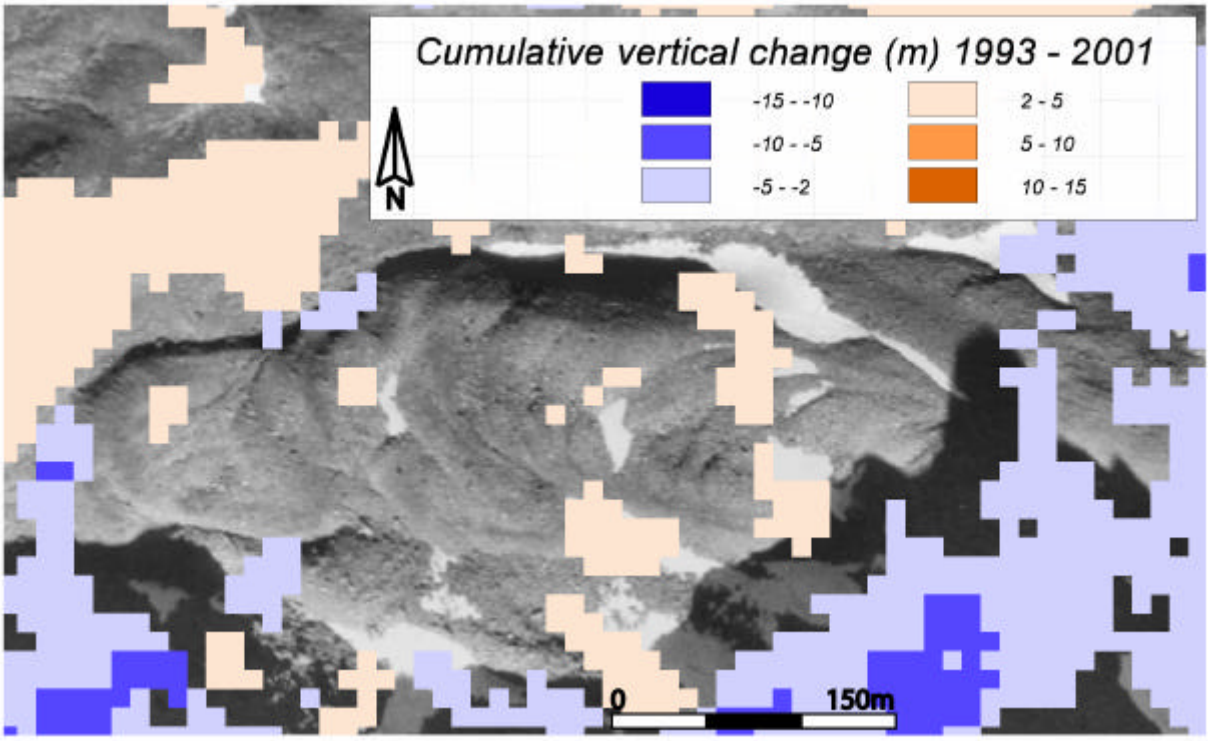

Figure 5.78: Cumulative vertical change on rockglacier Grueo7 between 1993 and 2001 (smoothed by a median-filter, window size 3x3). Underlying orthoimage of 06.10.1975 (flight line 21, aerial photographs taken by Swisstopo).

5.2.4.8 Rockglacier Grueo8

On this feature (nr. 28 of the inventory) velocities in the range of uncertainty were measured in both periods. Therefore, inactivity is assumed for this rockglacier. Additionally, vertical changes seemed to be strongly influence by the occurrence of snow and thus are not included in the interpretation.

5.2.5 Niggelingtälli

5.2.5.1 Rockglacier Niggel1

Horizontal velocities

Rockglacier Niggel1 (nr. 31 of the inventory) is a very small rockglacier situated below a small cirque. Between 1975 and 1993 the measured displacements are mostly in the range of uncertainty and the vectors show differences in their orientation (figure 5.79). Some blocks in the upper part and in the central flowline depict slightly higher velocities (up to 0.15 m/a).
Over the second period (1993 – 2001) a uniform vectorfield is displayed in figure 5.80. Rates are mostly in the range of uncertainty but some blocks in the central flowline and at the lower front depict velocities up to 0.3 m/a. Thus, it is suspected that the rockglacier is active or was rather reactivated.

Vertical changes

The elevation changes over the period 1975 – 1993 reveal only a small decrease in the root zone, while the most part of the rockglacier depicts an unchanged surface (figure 5.81). Between 1993 and 2001 an increase in thickness (2 – 5 m; 0.25 – 0.6 m/a) is observed in large parts of the permafrost body (figure 5.82).

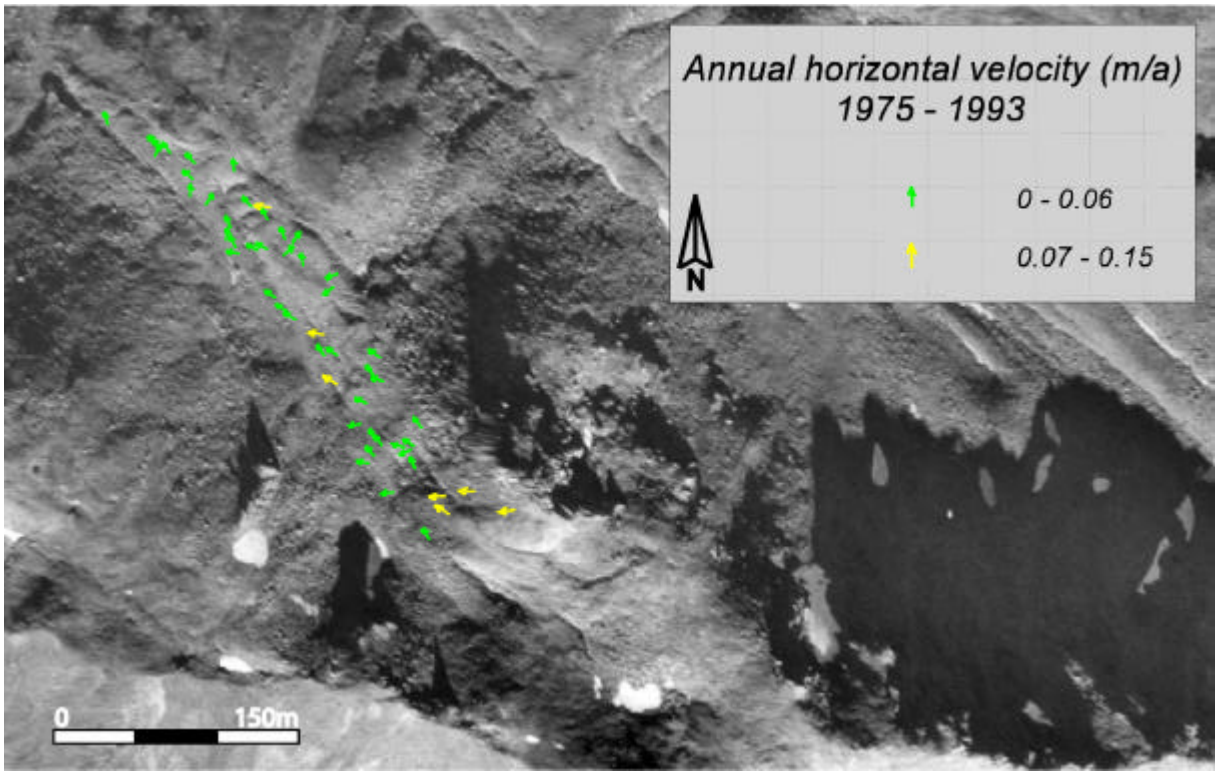

Figure 5.79: Mean annual surface velocities 1975 – 1993 on the rockglacier Niggel1. Underlying orthoimage of 20.08.1975 (flight line 22, aerial photographs taken by Swisstopo).

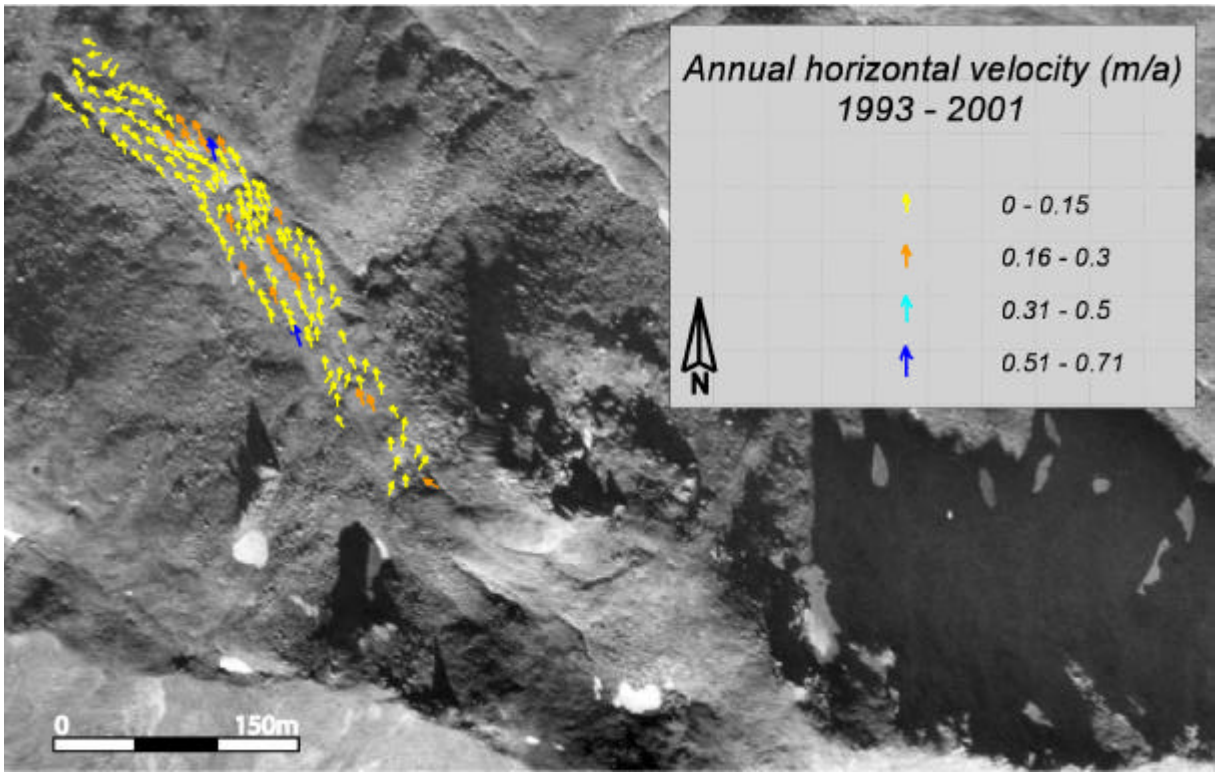

Figure 5.80: Mean annual surface velocities 1993 – 2001 on the rockglacier Niggel1. Underlying orthoimage of 20.08.1975 (flight line 22, aerial photographs taken by Swisstopo).

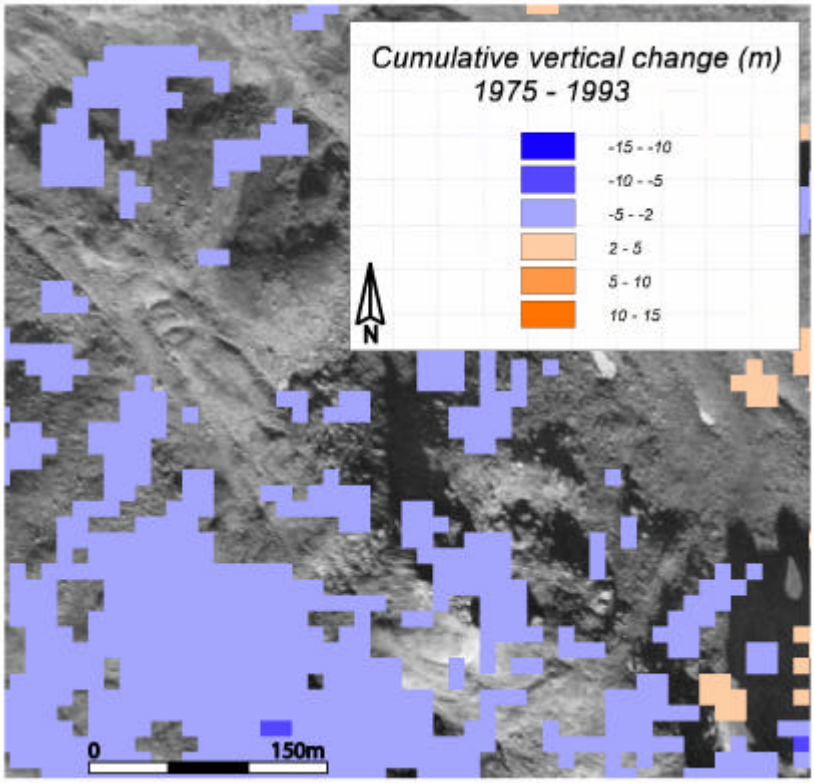

Figure 5.81: Cumulative vertical change on rockglacier Niggel1 between 1975 and 1993 (smoothed by a median-filter, window size 3x3). Underlying orthoimage of 20.08.1975 (flight line 22, aerial photographs taken by Swisstopo).

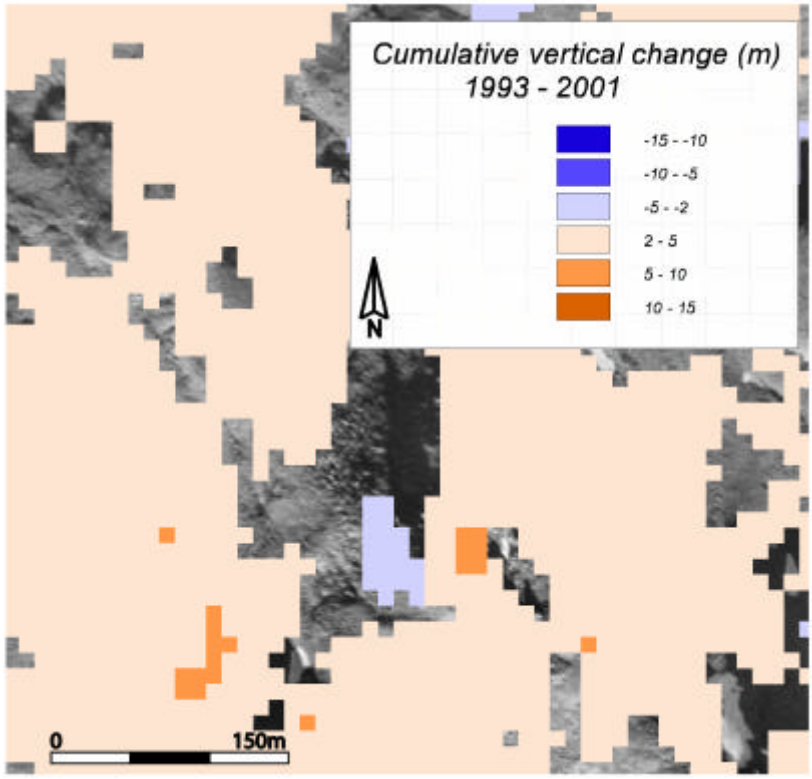

Figure 5.82: Cumulative vertical change on rockglacier Niggel1 between 1993 and 2001 (smoothed by a median-filter, window size 3x3). Underlying orthoimage of 20.08.1975 (flight line 22, aerial photographs taken by Swisstopo).

5.2.5.2 Rockglacier Niggel2

Horizontal velocities

Niggel2 (nr. 32 of the inventory) depicts the most complex rockglacier since at least 5 lobes are situated one over the other indicating different generations. A lot of blocks were matched in the first period (1975 – 1993) but in the middle part of the rockglacier shadows and snowpatches inhibited more measurements (figure 5.83). For the most part of the rockglacier, the horizontal creep rates at the surface amount to 0.15 m/a. Only in the central flowline of the upper lobe some individual blocks depict higher values. The lowermost lobe as well as the adjacent lobe in the root zone reveal velocities in the range of uncertainty and show diverse directions.

Over the period 1993 – 2001 a uniform vectorfield is given in figure 5.84. Again, the velocities depict mainly rates up to 0.15 m/a. But in the middle of the rockglacier several blocks show higher values (0.16 - 0.3 m/a). The lowermost and the adjacent lobe indicate again inactivity by small displacements and diverse directions of the vectors.

Vertical changes

The elevation changes on Niggel2 reveal for the most part a stable surface. Between 1975 and 1993 an increase in thickness (2 – 5 m; 0.1 – 0.3 m/a) is indicated on the adjacent lobe as well as in the root zone of the rockglacier (figure 5.85). Further down, similar changes occur in some places at the lateral fronts. On the lowermost lobe, a decrease in thickness (-2 - -5 m; -0.1 - -0.3 m/a) is depicted directly below the second front. Over the second investigated period (1993 – 2001) a lowering of the surface is indicated in the root zone and on the adjacent lobe (figure 5.86). Against that, an increase in thickness is again shown at the different fronts, which is most apparent on the second lobe.

The complex rockglacier Niggel2 reveals a distinct activity and an increase in horizontal velocity, which appears less distinctive in comparison to the other rockglaciers.

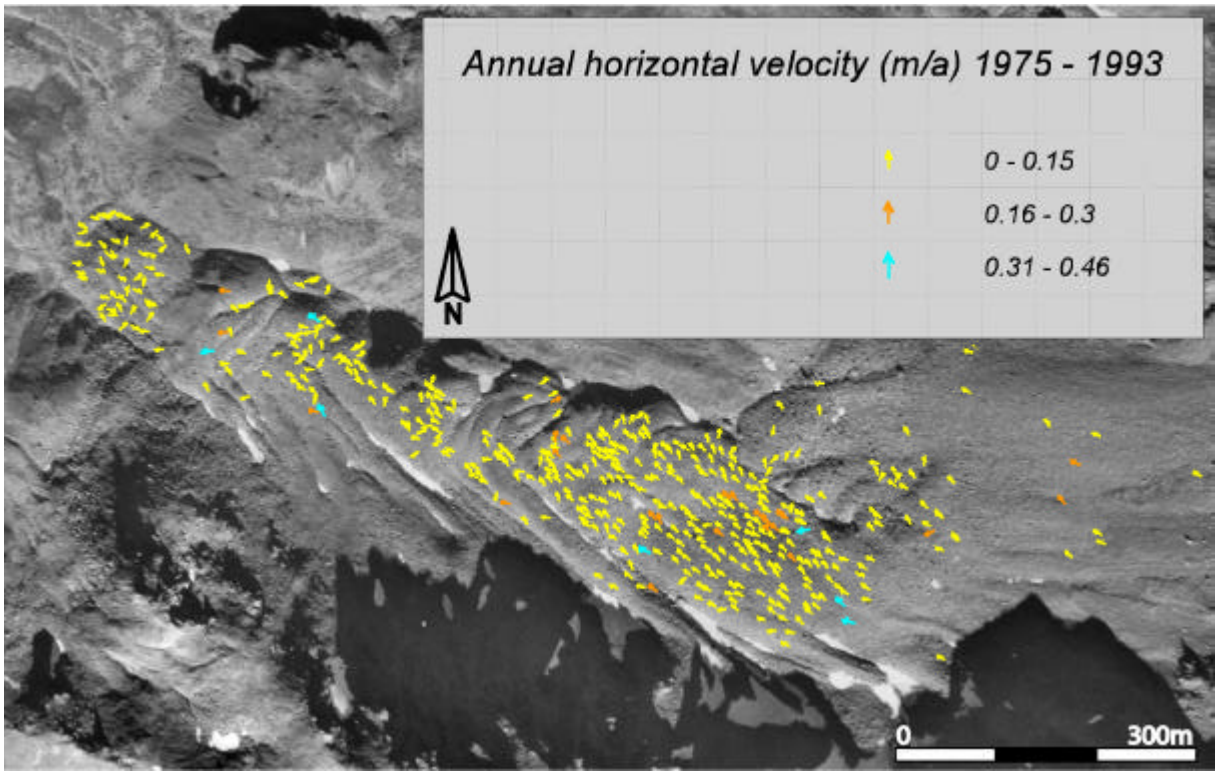

Figure 5.83: Mean annual surface velocities 1975 – 1993 on the rockglacier Niggel2. Underlying orthoimage of 20.08.1975 (flight line 22, aerial photographs taken by Swisstopo).

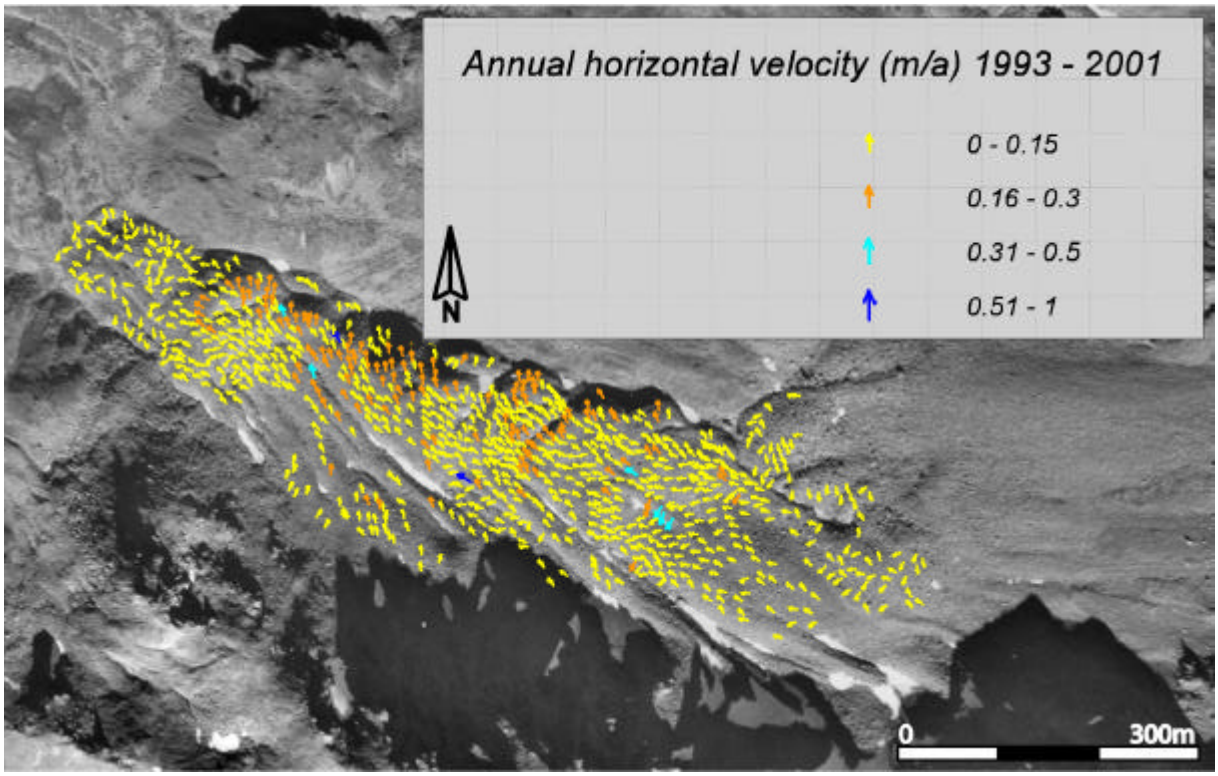

Figure 5.84: Mean annual surface velocities 1993 – 2001 on the rockglacier Niggel2. Underlying orthoimage of 20.08.1975 (flight line 22, aerial photographs taken by Swisstopo).

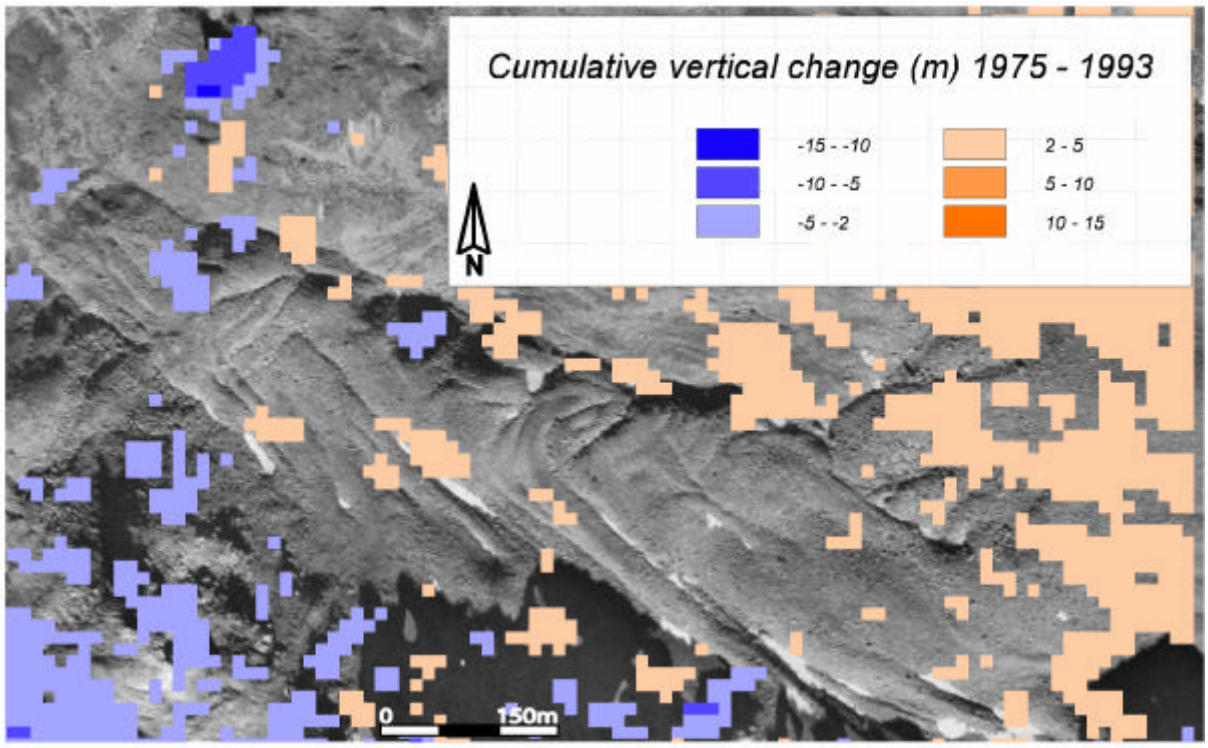

Figure 5.85: Cumulative vertical change on rockglacier Niggel2 between 1975 and 1993 (smoothed by a median-filter, window size 3x3). Underlying orthoimage of 20.08.1975 (flight line 22, aerial photographs taken by Swisstopo).

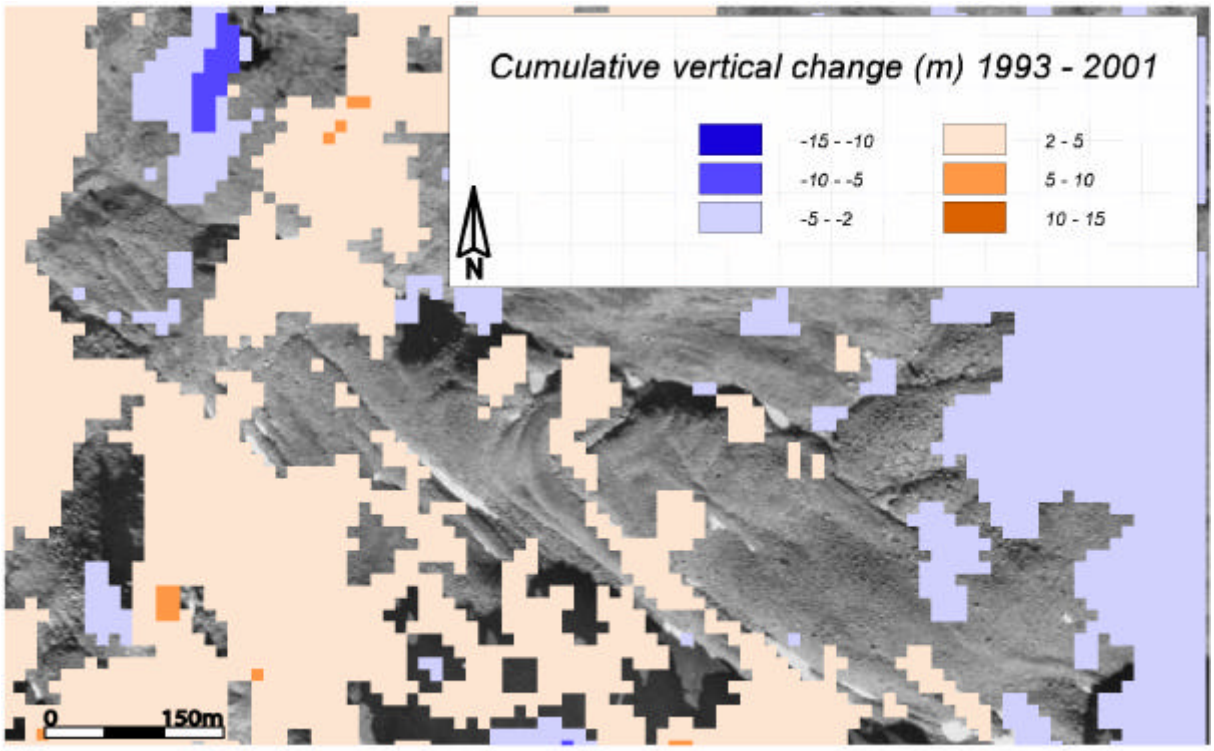

Figure 5.86: Cumulative vertical change on rockglacier Niggel2 between 1993 and 2001 (smoothed by a median-filter, window size 3x3). Underlying orthoimage of 20.08.1975 (flight line 22, aerial photographs taken by Swisstopo).

5.2.5.3 Rockglaciers Niggel3-7

All of these rockglaciers (nr. 33 - 37 of the inventory) indicated no significant movement. Velocities were quantified for Niggel3 (nr. 33), Niggel4 (nr. 34) and Niggel5 (nr. 35) and depicted rates in the range of uncertainty in both investigated periods. On Niggel 6 (nr. 36) and Niggel7 (nr. 37) a simple comparison of orthoimages (by flickering) revealed no displacements. Thus, the inactivity of all these rockglaciers is determined.

5.2.6 Chummetjitälli

5.2.6.1 Rockglacier Chummet1

Horizontal velocities

On rockglacier Chummet1 (nr. 40 of the inventory) relatively few blocks were matched by the CIAS program since snowpatches cover large parts of the feature. Over the first period (1975 – 1993), a uniform field of movements up to 0.15 m/a is indicated in the uppermost part of the rockglacier (figure 5.87). Further down, a gradient of higher values (0.25 – 0.57 – 0.8 m/a) is depicted by several blocks in the central flowline. The lower lobe shows an irregular velocityfield with rates between 0.16 and 1.0 m/a.

Between 1993 and 2001 non-uniform velocities of up to 1.0 m/a are indicated on the upper lobe, while the lower part of the rockglacier depicts a uniform vectorfield with rates mostly in the range of 0.23 – 0.27 m/a (figure 5.88). Higher rates occur individually at the front.

Vertical changes

Regarding the vertical surface changes on rockglacier Chummet1 (figure 5.89) a cumulative increase in thickness (2 – 5 m; 0.1 – 0.3 m/a) is depicted on the lower lobe between 1975 and 1993. Against that, the upper part of the rockglacier shows only patchy changes which are mainly negative (-2 - -5 m; -0.1 - -0.3 m/a). In the second period (1993 – 2001) thickening is revealed on the whole feature (figure 5.90). Apart from two areas with higher values (5 – 10 m; 0.6 – 1.25 m/a) the vertical changes are generally in the range of 2 to 5 m (0.25 – 0.6 m/a).

Chummet1 is a polymorphic rockglacier with two distinct lobes. Although the data on horizontal velocities are limited, the activity of the feature is indicated. Whether this rockglacier shows also higher creep rates in the second period is difficult to determine. Regarding the vertical changes, possible mass balance effects are difficult to assess, especially in the second period.

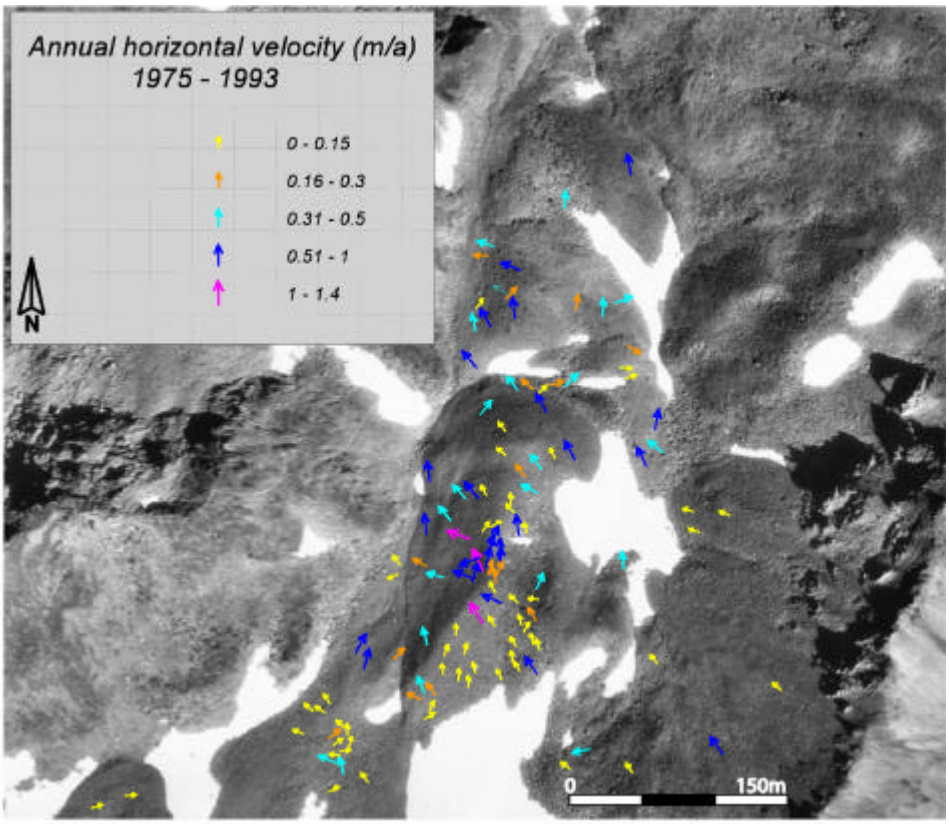

Figure 5.87: Mean annual surface velocities 1975 – 1993 on the rockglacier Chummet1. Underlying orthoimage of 20.08.1975 (flight line 22, aerial photographs taken by Swisstopo).

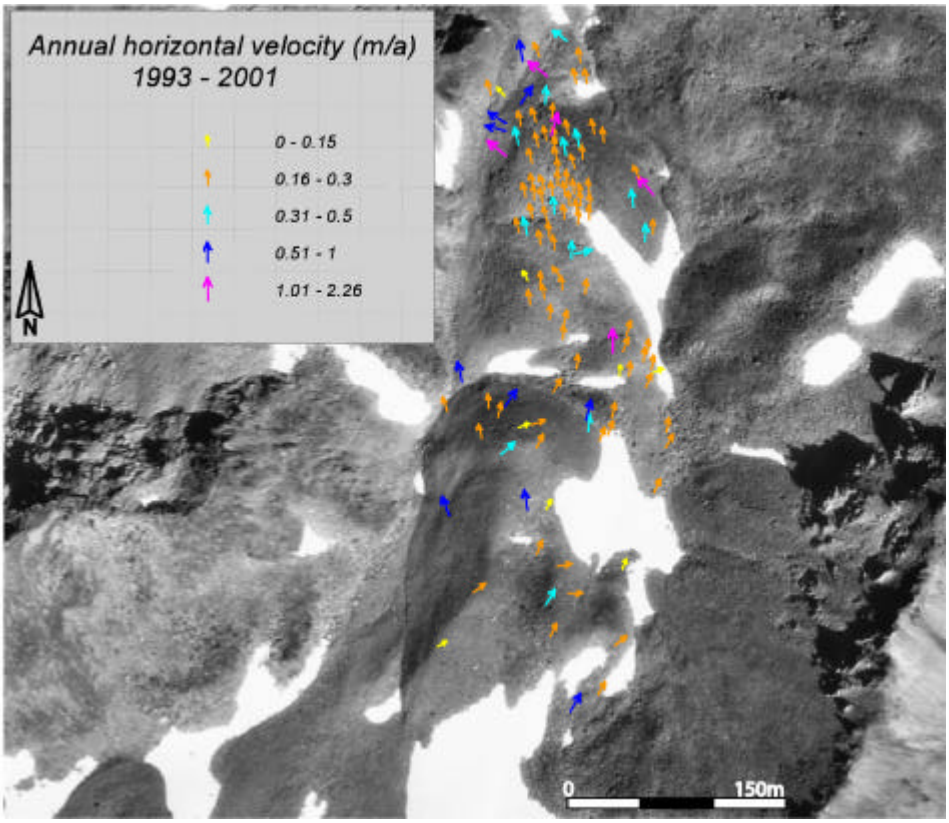

Figure 5.88: Mean annual surface velocities 1993 – 2001 on the rockglacier Chummet1. Underlying orthoimage of 20.08.1975 (flight line 22, aerial photographs taken by Swisstopo).

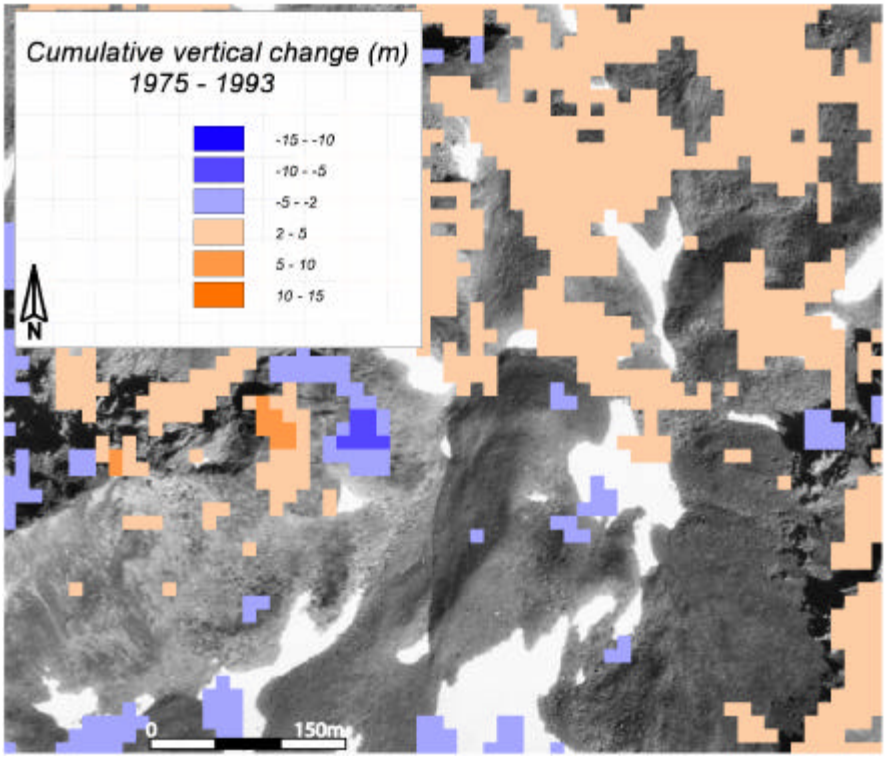

Figure 5.89: Cumulative vertical change on rockglacier Chummet1 between 1975 and 1993 (smoothed by a median-filter, window size 3x3). Underlying orthoimage of 20.08.1975 (flight line 22, aerial photographs taken by Swisstopo).

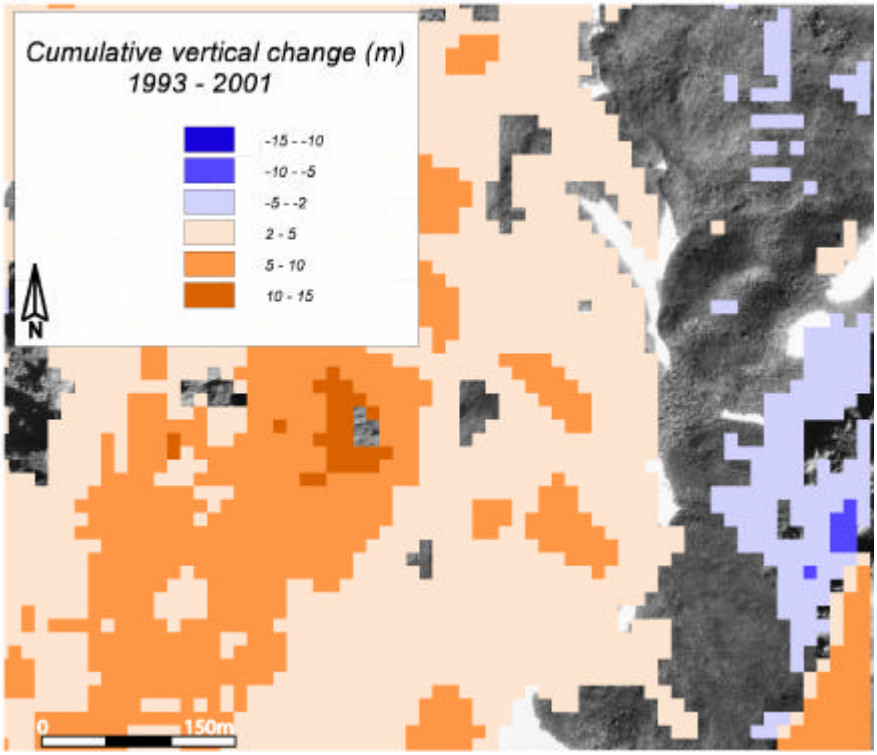

Figure 5.90: Cumulative vertical change on rockglacier Chummet1 between 1993 and 2001 (smoothed by a median-filter, window size 3x3). Underlying orthoimage of 20.08.1975 (flight line 22, aerial photographs taken by Swisstopo).

5.2.6.2 Rockglaciers Chummet2-4

The other rockglaciers in the Chummetjitälli (nr. 41, 42 and 43 of the inventory), which are partially very small, showed velocities in the range of uncertainty over both investigated periods. Therefore, the mapped inactivity of these features is confirmed by the measurements. Considering the vertical changes nearly no differences are quantified in the first period, whereas a general increase (2 – 5 m; 0.25 – 0.6 m/a) is revealed between 1993 and 2001 (figure 5.10). Perhaps this general thickening may result from errors in one of the DTMs.

5.2.7 Summary

On the east flank of the Turtmann valley the surface kinematics of 33 rockglaciers was investigated on the basis of photogrammetric products (DTMs and orthoimages). Horizontal velocities were quantified by digital image matching in the CIAS program, while vertical changes were derived from comparison of multitemporal DTMs. The accuracy of the horizontal and vertical displacements is estimated to lie within a range of 2 pixels (RMS) or 5.5 cm/a (for 1975 - 1993) and 12.5 cm/a (for 1993 – 2001) for the small-scale aerial photographs applied here.

For most of the rockglaciers, the state of activity was determined with good confidence, since displacement for a large number of surface blocks was measured reliably. The horizontal surface velocityfields often display single lobes situated one over the other and terminating with steep fronts. Inactive lobes, indicating former activity, are found in the lower part of most rockglaciers. To the borders of the rockglaciers, the displacement often decreases abruptly due to lateral friction. In parts where horizontal creep compression takes place, the velocities are in general lower than in parts with extensional flow. Hence, spatial variations in horizontal velocities agree with certain patterns in surface topography

For 18 of the 33 studied rockglaciers, a current activity was ascertained. Apart from rockglacier Brho2, which was investigated over the entire period (1975-2001), as well as rockglacier Grueo1, which was studied over four phases due to its extraordinary behaviour, the individual rockglaciers were monitored over two time periods (1975-1993 and 1993-2001) (table 5.7). Therefore, it was possible to deduce temporal changes in surface displacements. An overview of the temporal changes in the entire hanging valleys is illustrated in appendix 3. From the measurements it was ascertained, that the horizontal velocities on all active rockglaciers depict a distinct increase between 1993 and 2001, compared to the period 1975-1993. This signal is given in the mean values, while the median-values are slightly different and reveal, for instance, on rockglacier hufh a decrease in velocity (table 5.7). This difference results from the small number of measured blocks in the second period. In general, between 1993 and 2001 fewer blocks were matched on most rockglaciers because of snowcover in the orthoimage of 2001. Mean-, median- and maximum values of horizontal displacements as well as the acceleration are given in figure 5.91 – 5.93, and emphasise the enormous differences between the two investigated periods.

Rockglacier Grueo1 depicted extraordinarily large displacements over all investigated periods (table 5.8). Regarding the temporal changes, an increase in velocity is revealed in the second period (1981-1987), while a decrease occurs in the third period (1987-1993), followed by a slight increase between 1993 and 2001.

Vertical changes showed less uniform signals on most rockglaciers. This is due to the diverse components influencing the mass- and the flow balance (cf., chapter 2.3.5.4). Because of its striking development, rockglacier Grueo1 affords a good opportunity to show vertical changes in geometry. The conspicuous increase in thickness at the rockglacier front (up to 20 m over the period 1993-2001) results from the advance of the feature. In parallel, a thinning in the same order of magnitude is revealed in the centre of the permafrost body. Thus, an enormous transfer

of mass is depicted by the vertical changes. On other rockglaciers vertical thinning or thickening occurred more individually on single lobes.

Table 5.7: Comparison of horizontal velocities (mean, median, maximum) between 1975-1993 and 1993-2001 of all investigated active rockglaciers.

		1975 - 1993				**1993 - 2001**				
Nr.	Name of rockgl.	Number of measured blocks	**Mean** velocity (m/a)	**Median** velocity (m/a)	**Max** velocity (m/a)	Number of measured blocks	**Mean** velocity (m/a)	**Median** velocity (m/a)	**Max** velocity (m/a)	Acceleration **mean/median**
1	Pibw	348	0.09	0.08	1.21	97	0.14	0.11	0.65	55% / 37 %
2	Pipp1	986	0.18	0.09	1.19	939	0.3	0.18	2.19	66% / 100 %
6	Brho1	1185	0.15	0.05	1.21	737	0.19	0.07	2.0	26 % / 40 %
8	Brle	97	0.15	0.1	1.14	172	0.2	0.17	1.83	33 % / 70 %
11	Hufh	432	0.21	0.22	0.85	27	0.49	0.19	1.92	133 % / -14 %
12	Hujp	403	0.07	0.06	0.9	323	0.27	0.22	1.8	286 % / 266 %
15	Huhh1	515	0.24	0.23	1.48	339	0.5	0.32	2.83	108 % / 39 %
16	Huhh2	458	0.04	0.03	0.13	375	0.08	0.06	1.78	100 % / 100 %
17	Huhh3	529	0.16	0.14	0.84	573	0.55	0.43	2.55	244 % / 207 %
22	Grueo2	701	0.1	0.09	0.7	100	0.49	0.35	1.88	390 % / 289 %
24	Grueo4	525	0.05	0.04	0.6	545	0.11	0.09	2.34	120 % / 125 %
26	Grueo6	689	0.08	0.04	0.87	140	0.27	0.09	2.09	238 % / 125 %
27	Grueo7	500	0.09	0.07	1.12	329	0.25	0.18	1.89	178 % / 157 %
31	Niggel1	107	0.05	0.04	0.34	177	0.1	0.09	0.71	100 % / 125 %
32	Niggel2	696	0.08	0.06	0.76	1144	0.11	0.1	2.15	38 % / 67 %
40	Chu1	316	0.26	0.14	1.4	197	0.41	0.25	2.26	58 % / 79 %

Table 5.8: Comparison of horizontal velocities (mean, median, maximum) of rockglacier Grueo1 over four investigated periods.

		1975 - 1981				**1981 - 1987**				
Nr.	Name of rockgl.	Number of measured blocks	**Mean** velocity (m/a)	**Median** velocity (m/a)	**Max** velocity (m/a)	Number of measured blocks	**Mean** velocity (m/a)	**Median** velocity (m/a)	**Max** velocity (m/a)	Acceleration **mean/median**
21	Grueo1	420	1.34	1.24	5.07	503	1.67	1.83	4.83	25 % / 48 %
		1987 - 1993				**1993 - 2001**				
21	Grueo1	688	1.6	1.61	4.82	509	1.76	1.76	3.76	10 % / 10 %

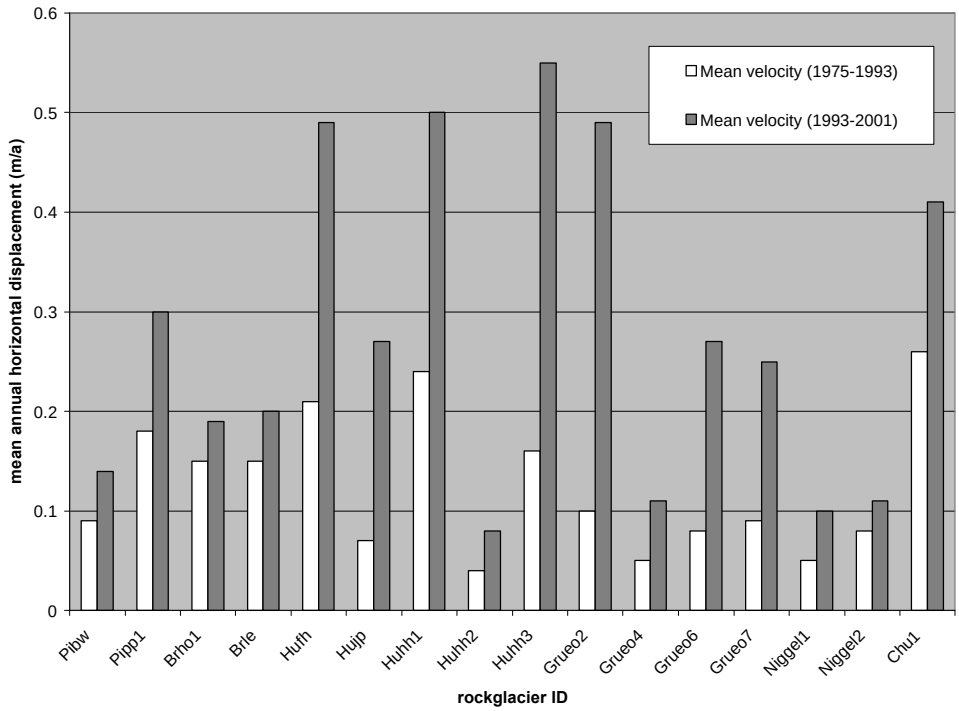

Figure 5.91: Comparison of mean annual horizontal velocities (m/a) between 1975-1993 and 1993-2001.

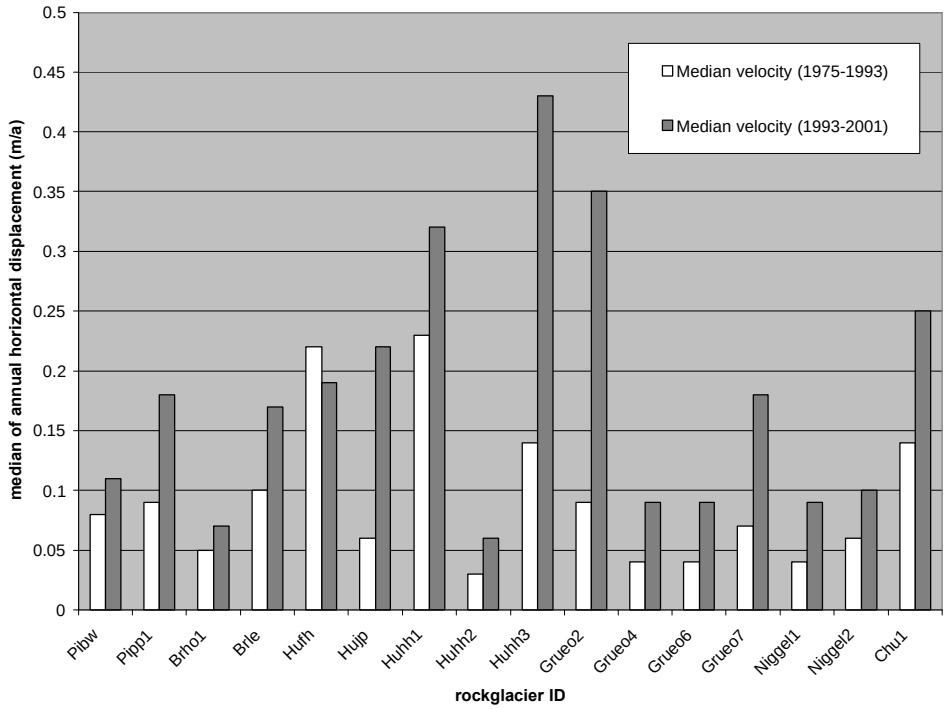

Figure 5.92: Comparison of median values of annual horizontal velocities (m/a) between 1975-1993 and 1993-2001.

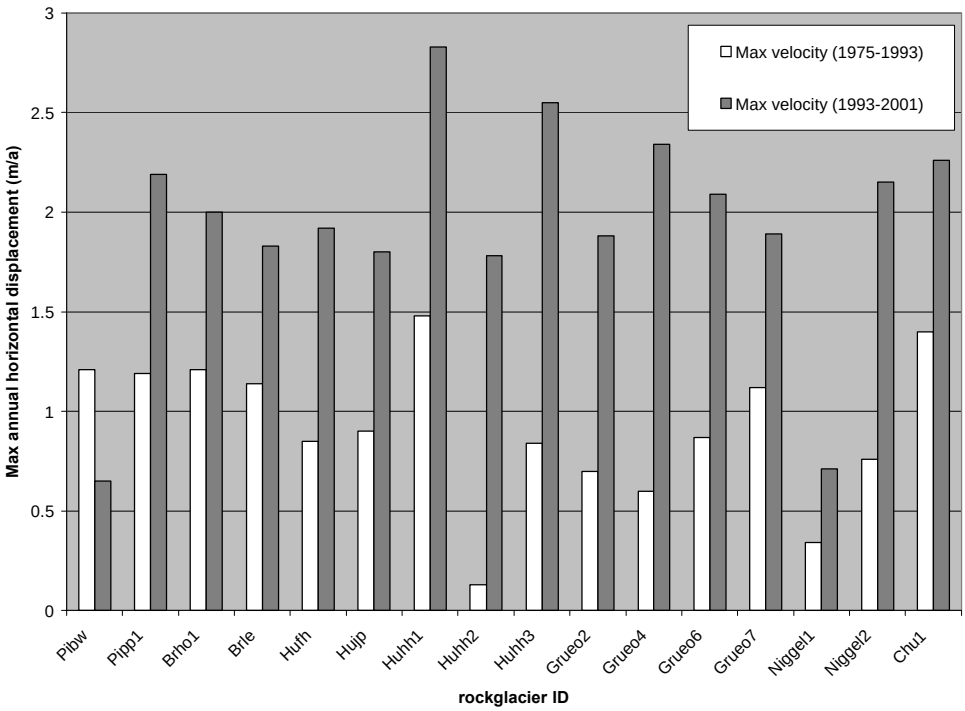

Figure 5.93: Comparison of maximum annual horizontal velocities (m/a) between 1975-1993 and 1993-2001.

5.3 Terrestrial geodetic survey

Two rockglaciers in the Hungerlitälli were monitored by terrestrial geodetic survey during the years 2001 to 2004. The measurement campaign depended on suitable weather conditions and thus was not conducted at a certain time. But, the survey at approximately annual intervals was strived for. Additionally, seasonal differences in rockglacier kinematics were documented in some years by a further survey in early summer (June or July, depending on the duration of the snow cover). A measurement during winter was not feasible due to snow cover and avalanches.
The 'annual' data are not really comparable since they cover not a whole year (the period is mostly reduced to about 3 weeks) and since they cover slightly different periods of each year. Thus, the interpretation of similarities and differences in the velocities needs to be conducted carefully. At least the data gives an impression of the magnitude of the displacements as well as their spatial pattern.
All velocities measured on the rockglaciers are clearly beyond the range of uncertainty (2-3 cm) of the method (see chapter 3.3). Thus they show significant displacements and ascertain the activity of the features.

5.3.1 Rockglacier Huhh1

For rockglacier Huhh1, data on horizontal and vertical changes as well as the direction of the displacement are summarised in table 5.9 for the periods 2001/2002 and 2002/2003 while the following table 5.10 contains the data of the year 2003/2004 and includes 'seasonal' values of the early summer 2003 (5.7.-10.8.2003). Velocities of the entire period (2001 – 2004) are compiled in table 5.11 by the calculated changes in coordinates (left columns) and for comparison by simple addition of the values in tables 5.9 and 5.10 (right columns).

The survey was started in September 2001 with 15 prominent blocks on the lower half of the rockglacier and was expanded in the following summer (August 2002). At that time, two blocks (106 and 114) were still covered by snow. Therefore, values are missing in table 5.9.
As depicted in figure 5.94, where the magnitude of movement is illustrated both by the length and the colour of the vector, the first data (10.9.2001 – 30.8.2002) show small displacements (0.05 – 0.12 m) on the orographic right side of the lower lobe while the velocities on the left part are significantly higher (0.38 – 0.48 m). Above the second steep front highest movements (0.62 – 0.84 m) occur. The pattern described is additionally emphasised by the vertical changes (figure 5.95), which show positive values between 0.7 and 1.0 m on the upper lobe and between 1.0 and 1.2 m on the lower lobe. Thus, the surface topography with its different lobes is clearly reflected by the respective horizontal and vertical velocities.

Table 5.9: Velocities of blocks at the surface of rockglacier HuHH1 in the period 2001/2002 and 2002/2003.

	10.09.2001 - 30.08.2002			**30.08.2002 - 10.08.2003**		
Block	direction	horizontal change (m)	vertical change (m)	direction	horizontal change (m)	vertical change (m)
101	45.978	0.099	1.169	217.557	0.451	0.125
102	35.653	0.119	1.178	293.946	0.079	0.123
103	-13.665	0.056	1.211	195.995	0.047	0.152
104	62.606	0.387	1.105	276.368	0.392	0.049
105	54.734	0.484	1.113	266.793	0.508	0.019
106						
107	53.741	0.619	0.819	134.181	1.735	-0.097
108	52.827	0.623	0.817	103.716	2.583	-0.417
109	54.131	0.762	0.855	262.330	0.868	-0.311
110	54.571	0.756	0.826	260.600	0.838	-0.298
111	65.769	0.839	0.788	269.926	0.985	-0.331
112	63.355	0.776	0.800	209.603	3.515	-1.426
113	63.692	0.771	0.781	179.136	2.905	0.851
114						
115	66.840	0.458	0.988	282.152	0.475	-0.099
116				277.714	0.328	-0.070
117				291.948	1.037	-0.433
118				285.879	0.917	-0.306
119				283.312	0.854	-0.352
120				286.668	0.889	-0.490
121				289.972	0.566	-0.306
122				250.411	1.406	-0.212
123				110.634	0.607	-0.324
124				132.693	0.228	-0.009
125				243.033	2.026	-0.306

Table 5.10: Velocities of blocks at the surface of rockglacier HuHH1 in the period 2003/2004 and between July and August of 2003.

	10.08.2003 - 31.07.2004			5.7.2003 - 10.8.2003		
Block	direction	horizontal change (m)	vertical change (m)	direction	horizontal change (m)	vertical change (m)
101	191.332	0.477	0.042	269.593	0.896	-0.200
102	272.829	0.130	0.035	294.427	0.812	-0.198
103	279.115	0.015	0.115	268.395	0.682	-0.209
104	268.653	0.487	-0.052	288.086	1.070	-0.208
105	259.992	0.585	-0.072	285.528	1.251	-0.224
106	262.390	0.662	-1.969	281.512	1.233	0.499
107	262.409	2.247	-2.147	265.886	1.265	-0.247
108	256.186	0.796	-0.407	266.442	1.210	-0.237
109	257.537	0.960	-0.400	256.720	1.349	-0.337
110	253.571	3.611	-0.436	250.724	1.303	-0.292
111	255.641	2.405	-0.523	246.688	1.289	-0.270
112	267.536	1.030	-0.455	194.728	2.946	-7.653
113	268.780	0.990	-0.438	174.957	2.473	0.891
114	201.209	0.816	-0.478	242.994	2.548	-0.258
115	279.167	0.483	-0.191	239.263	0.920	-2.286
116	279.947	0.337	-0.187	228.593	1.056	-2.660
117	294.727	1.250	-0.645	226.708	1.307	-0.311
118	286.807	1.218	-0.558	225.745	1.362	-0.250
119	282.696	1.011	-0.580	228.438	1.397	-0.282
120	285.204	1.078	-0.672	234.498	1.480	-0.363
121	291.171	0.626	-0.447	103.451	3.766	-0.324
122	209.541	1.209	-0.300	236.648	2.785	-0.352
123	105.966	0.606	-0.424	243.990	1.706	-5.980
124	145.813	0.177	-0.062	234.591	1.650	-0.292
125	201.846	1.969	-0.397	228.179	3.395	-0.475

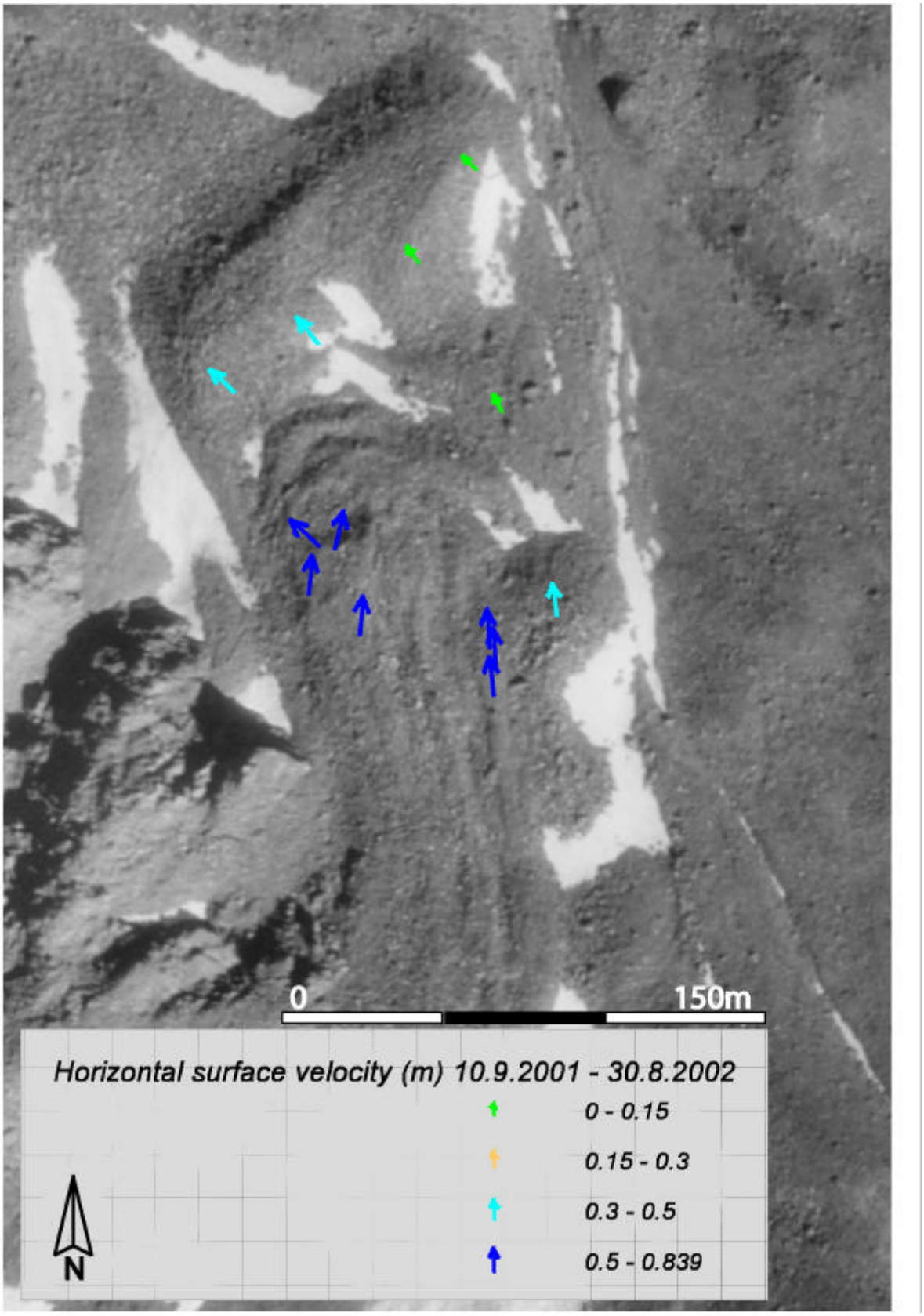

Figure 5.94: Horizontal surface velocity (m) of blocks on rockglacier Huhh1 between 10.9.2001 and 30.8.2002. Underlying orthophoto of 20.08.1975 (flight-line 22, aerial photographs taken by swisstopo).

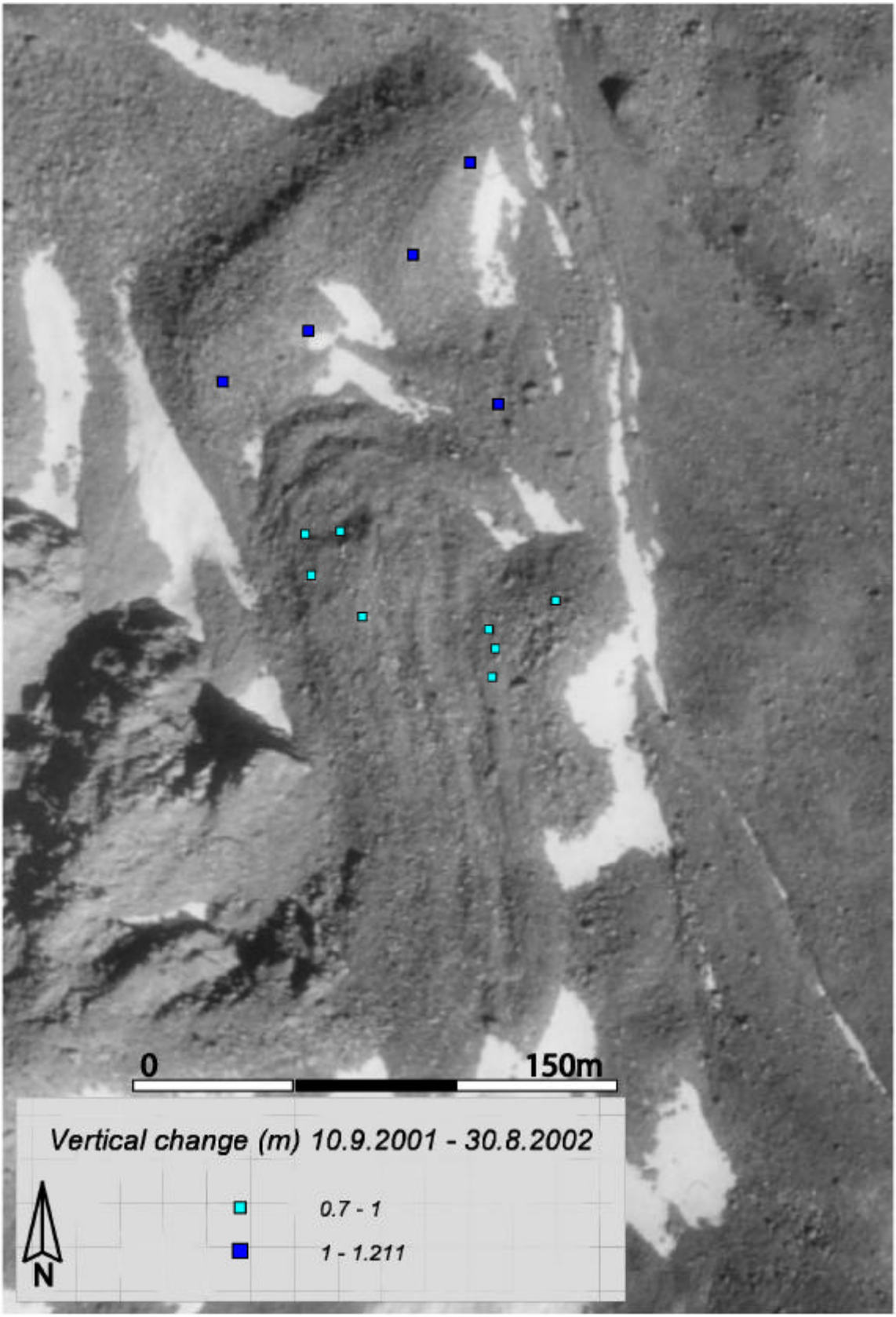

Figure 5.95: Vertical change (m) of blocks on rockglacier Huhh1 between 10.9.2001 and 30.8.2002. Underlying orthophoto of 20.08.1975 (flight-line 22, aerial photographs taken by swisstopo).

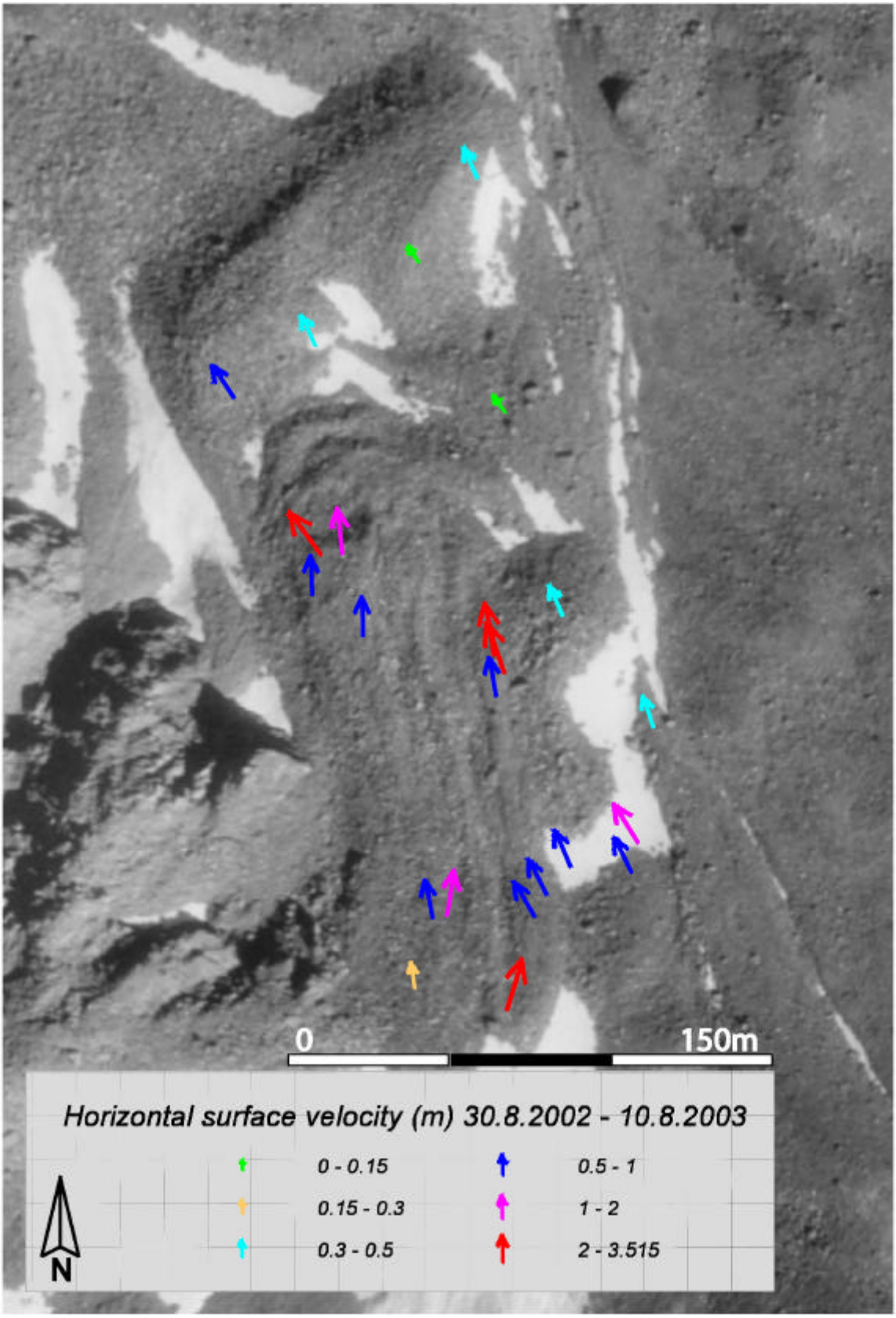

Figure 5.96: Horizontal surface velocity (m) of blocks on rockglacier Huhh1 between 30.8.2002 and 10.8.2003. Underlying orthophoto of 20.08.1975 (flight-line 22, aerial photographs taken by swisstopo).

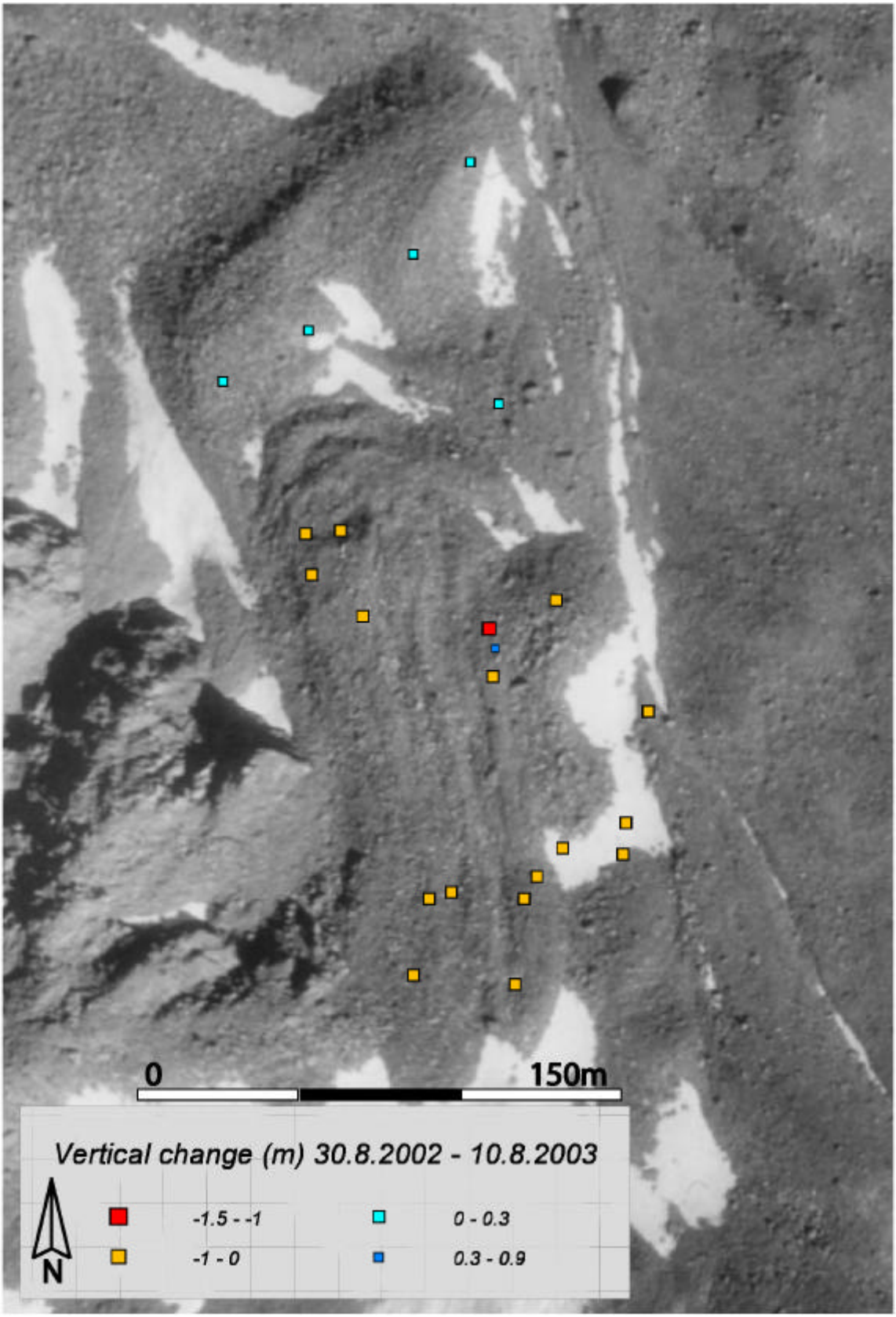

Figure 5.97: Vertical change (m) of blocks on rockglacier Huhh1 between 30.8.2002 and 10.8.2003. Underlying orthophoto of 20.08.1975 (flight-line 22, aerial photographs taken by swisstopo).

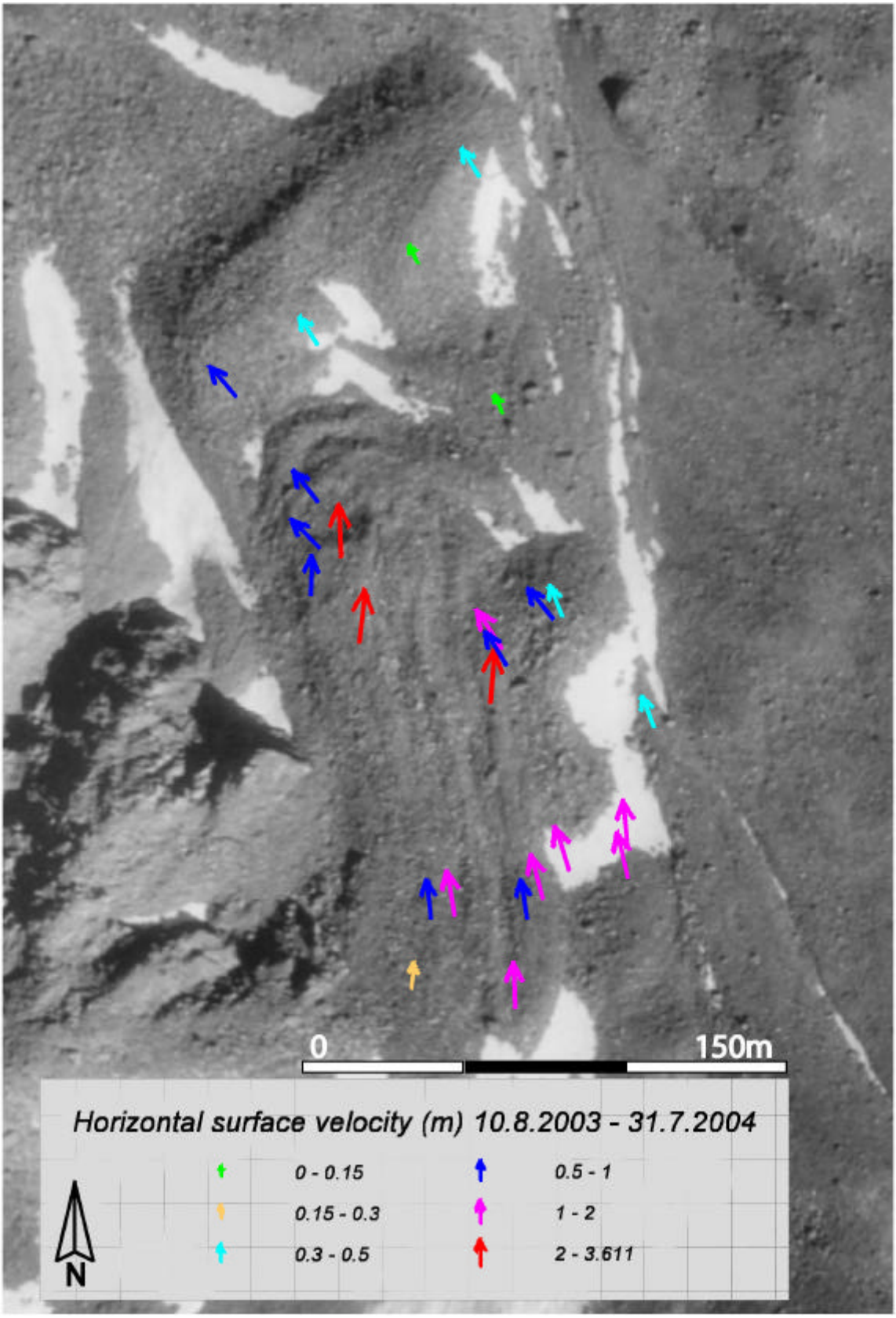

Figure 5.98: Horizontal surface velocity (m) of blocks on rockglacier Huhh1 between 10.8.2003 and 31.7.2004. Underlying orthophoto of 20.08.1975 (flight-line 22, aerial photographs taken by swisstopo).

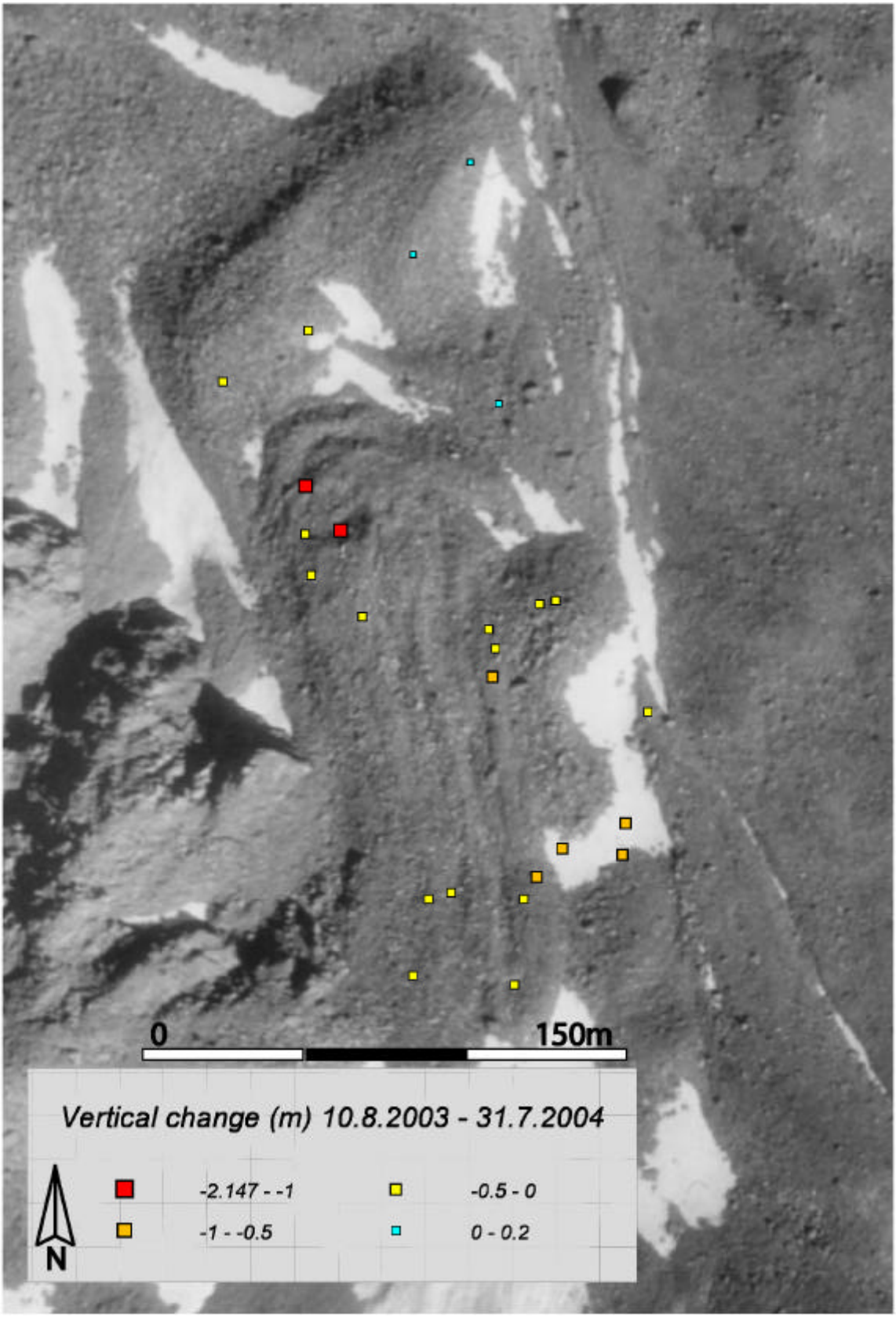

Figure 5.99: Vertical change (m) of blocks on rockglacier Huhh1 between 10.8.2003 and 31.7.2004. Underlying orthophoto of 20.08.1975 (flight-line 22, aerial photographs taken by swisstopo).

Regarding the data of the second year (30.8.2002 – 10.8.2003) (figure 5.96), the horizontal displacements on the lower lobe indicate similar values as before, apart from block 101 which accelerated from 0.1 to 0.45 m. On the upper lobe, the velocities are very high (1.0 – 3.5 m) at the front and between 0.8 and 1.0 m at the centre. At the orographic right margin of the second front, the velocities are clearly smaller (0.3 – 0.5 m). The vertical changes (figure 5.97) depict a slight increase in altitude (0 – 0.3 m) on the lower lobe and a uniform decrease (mostly between -0.2 and -0.5 m) on the upper lobe.

The results of the third year (10.8.2003 – 31.7.2004) reveal a very similar pattern to the previous year, with slightly higher velocities in the rooting zone (figure 5.98). Against that, differences appear in the vertical displacements (figure 5.99). The orographic right side of the lower lobe shows positive values up to 0.2 m. The rest of the rockglacier depicts uniform negative values (between -0.05 and -0.5 m) with more significant losses (-0.5 - -1.0 m) in the orographic right side of the rooting zone. At the front of the upper lobe two blocks show a reduction in altitude at about -2.0 m.

In addition to the 'annual' velocities the total changes between 2001 and 2004 were measured and were compared to the added values of the single years (table 5.11). By the combined analysis of horizontal and vertical changes, the previously described pattern is confirmed. On the lower lobe the horizontal velocities are small, especially on the orographic right side, and they are accompanied by a vertical thickening between 1.0 and 1.5 m. On the upper lobe the horizontal displacements are significantly higher, apart from blocks at the rockglacier margin, and reveal vertical thinning, which is at least partly due to the horizontal movement parallel to the surface. Comparing the measured with the added values, most blocks reach a good agreement. Deviations in horizontal velocities result from changes in the direction of the movement over the years. Thus, the added values overestimate the total displacement in some cases.

Table 5.11: Measured velocities of blocks at the surface of rockglacier HuHH1 for the entire period 2001/2004 (only for the blocks measured in 2001) and addition of the single periods (as check).

	10.09.2001 - 31.7.2004			**check (t1+t2+t3)**	
Block	direction	horizontal change (m)	vertical change (m)	horizontal change (m)	vertical change (m)
101	291.224	0.255	1.336	1.027	1.336
102	264.581	0.306	1.336	0.327	1.336
103	223.618	0.014	1.478	0.118	1.478
104	269.185	1.262	1.102	1.267	1.102
105	260.578	1.573	1.060	1.577	1.060
106	264.367	1.710	-1.117	0.662	-1.969
107	220.235	2.685	-1.425	4.602	-1.425
108	286.679	3.734	-0.007	4.002	-0.007
109	258.139	2.586	0.144	2.590	0.144
110	254.842	5.201	0.092	5.205	0.092
111	260.982	4.209	-0.066	4.229	-0.066
112	228.075	4.866	-1.081	5.321	-1.081
113	141.367	3.087	1.194	4.665	1.194
114	270.848	2.520	0.103	0.816	-0.478
115	276.191	1.407	0.698	1.415	0.698
116				0.666	-0.257
117				2.287	-1.078
118				2.135	-0.864
119				1.865	-0.932
120				1.967	-1.162
121				1.192	-0.753
122				2.615	-0.512
123				1.213	-0.748
124				0.405	-0.071
125				3.995	-0.703

On rockglacier Huhh1 an additional survey allowed the calculation of displacements during one month (5.7.-10.8.) in the summer of 2003 (table 5.10). The results show overall high horizontal velocities (0.7 – 3.7 m) exceeding the 'annual' displacements (30.8.2002 – 10.8.2003). The vertical changes reveal a general lowering of the surface. Such high velocities are quite possible; especially in the summer of 2003 which was extraordinarily warm. But, since the high values are not reflected in the 'annual' velocities, this phenomenon is hard to explain. Either displacements into an opposite direction occur in the rest of the year (which is unlikely, since this would be an upslope movement) or, an error occurred during the survey in July 2003 (this was checked and can be excluded).

5.3.2 Rockglacier Huhh3

The 'annual' data on direction, horizontal and vertical change of blocks on rockglacier Huhh3 are compiled in table 5.12 and visualised in figures 5.100 – 5.103. In order to check the data, corresponding values of the entire period (2.09.2002 – 1.08.2004) as well as the added values of t1 (2.09.2002 – 13.08.2003) and t2 (13.08.2003 – 1.08.2004) are given in table 5.13.

Table 5.12: Velocities of blocks at the surface of rockglacier Huhh3 between 2002-2003 and 2003-2004.

	2.09.2002 - 13.08.2003			**13.08.2003 - 1.08.2004**		
Block	direction	horizontal change (m)	vertical change (m)	direction	horizontal change (m)	vertical change (m)
201	274.523	0.275	1.242	261.768	0.223	0.300
202	259.026	0.130	1.224	195.298	0.094	0.275
203	256.160	0.271	1.176	246.652	0.311	0.178
204	286.438	0.364	1.284	241.933	0.482	0.155
205	269.553	0.524	1.072	262.645	0.627	0.059
206	168.282	1.700	0.878	264.313	1.234	-0.207
207	264.277	1.208	0.562	267.075	1.563	-0.631
208	268.822	0.963	0.721			
209	198.663	1.375	1.064	159.115	1.664	0.017
210	238.880	1.111	1.000	241.453	1.450	-0.098
211	267.971	1.630	0.827	270.823	2.163	-0.375
212	265.003	0.551	0.991	277.841	0.756	-0.104
213	253.173	1.124	0.792	261.910	1.654	-0.346
214	252.769	1.634	0.455	256.970	2.236	-0.794
215	252.211	1.700	0.412	256.995	2.359	-0.844
216	249.936	1.722	0.439	258.957	2.333	-0.870
217	236.872	0.601	1.015	263.089	0.301	0.175
218	248.767	1.649	0.251	256.467	2.281	-1.029
219	250.786	1.863	0.275	257.464	2.560	-1.090
220	245.978	1.830	0.284	251.643	2.587	-1.045
221	239.051	1.469	0.276	253.486	2.116	-1.244
222	230.326	0.667	0.782	261.809	1.530	-1.087
223	248.800	1.243	0.265	246.049	3.948	-3.749
224	213.604	0.306	1.120	110.163	0.359	0.085
225	218.262	0.275	1.169	294.652	0.286	0.140
226	200.509	0.259	1.208	295.701	0.207	0.177
227	191.207	0.247	1.208	103.669	0.156	0.257
228	183.271	0.285	1.229	116.473	0.176	0.261
229	200.828	0.239	1.207	278.941	0.176	0.202
230	207.352	0.208	1.137	281.621	0.172	0.250
231	213.117	0.205	1.178	100.370	0.172	0.194

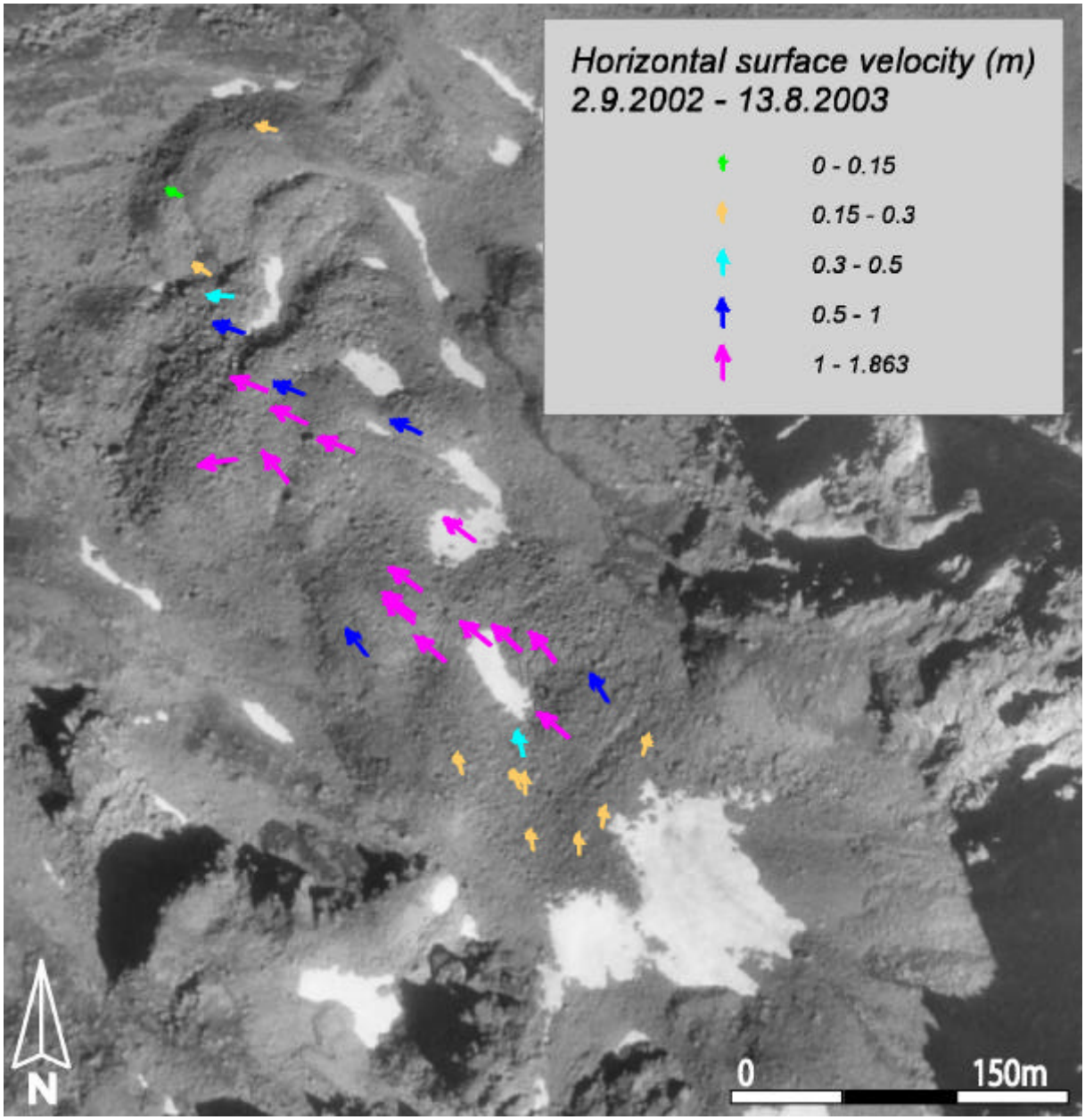

Figure 5.100: Horizontal surface velocity (m) on rockglacier Huhh3 between 2.9.2002 and 13.8.2003. Underlying orthophoto of 20.08.1975 (flight-line 22, aerial photographs taken by swisstopo).

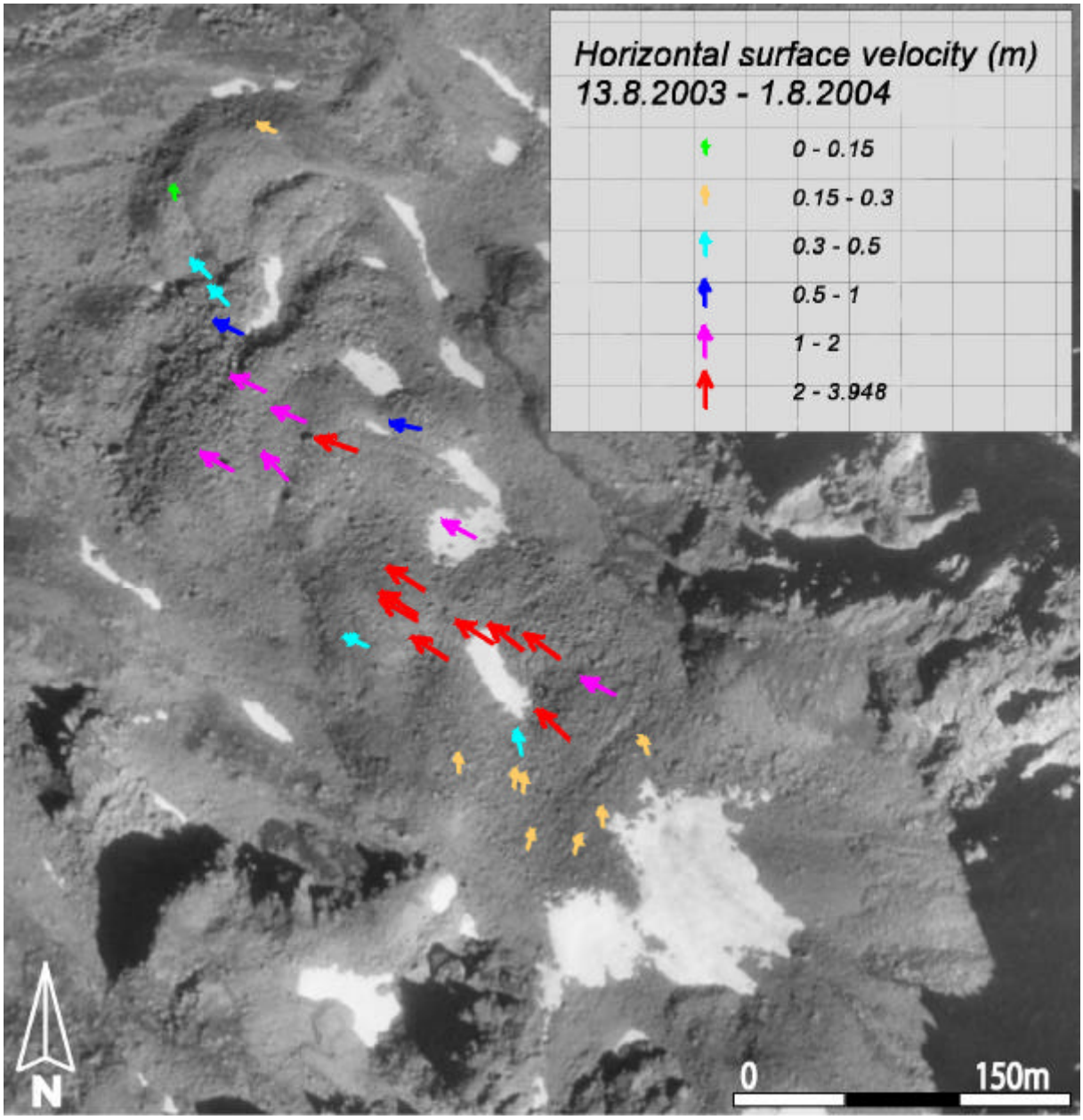

Figure 5.101: Horizontal surface velocity (m) on rockglacier Huhh3 between 13.8.2003 and 1.8.2004. Underlying orthophoto of 20.08.1975 (flight-line 22, aerial photographs taken by swisstopo).

The horizontal and vertical changes measured on rockglacier Huhh3 show great spatio-temporal variations within the considered period. The observation points near the front (blocks 201 – 205) and those in the rooting zone (224 - 231) depict horizontal changes between 0.1 and 0.6 m in both years. Against that, the blocks in the centre of the rockglacier mostly show horizontal displacements between 1.0 and 1.8 m in the year 2002/2003 and about 2.0 m and up to 3.9 m in the year 2003/2004 (figures 5.100, 5.101). In general, the displacements follow the direction of the slope with some deviations in the rooting zone at the border of the cirque, where velocities are low.

Regarding the vertical changes, a similar pattern is given. In the period 2002/2003 (figure 5.102) the blocks in the lower part of the rockglacier (201 – 210) indicate a thickening of about 1.0 m, while the increase is much lower (0.2 – 0.4 m) in the centre of the rockglacier. In the rooting zone (224 – 231) again a distinct thickening (1.0 – 1.3 m) is quantified. In the year 2003/2004 this division into three fields remains, but with totally different values (figure 5.103). A slight thickening of about 0.05 – 0.3 m occurs in the lower part and in the rooting zone, while the blocks in the centre show a vertical thinning which is very distinct (-1.0 - -3.7 m) in the area below the cirque, resulting from the high horizontal velocities. In total (2002 - 2004) the upper and the lower part of the rockglacier show horizontal compression, while the middle part depicts extensional creep (table 5.13). This pattern is additionally supported by the horizontal velocities of the whole period (2002 – 2004). Like in the single years, values are low at the front and on the lower lobe as well as in the rooting zone. Against that, values of 1.2 m to more than 5 m are reached in the centre of the rockglacier. Comparisons of measured displacements and added data of the single years show good agreements (table 5.13).

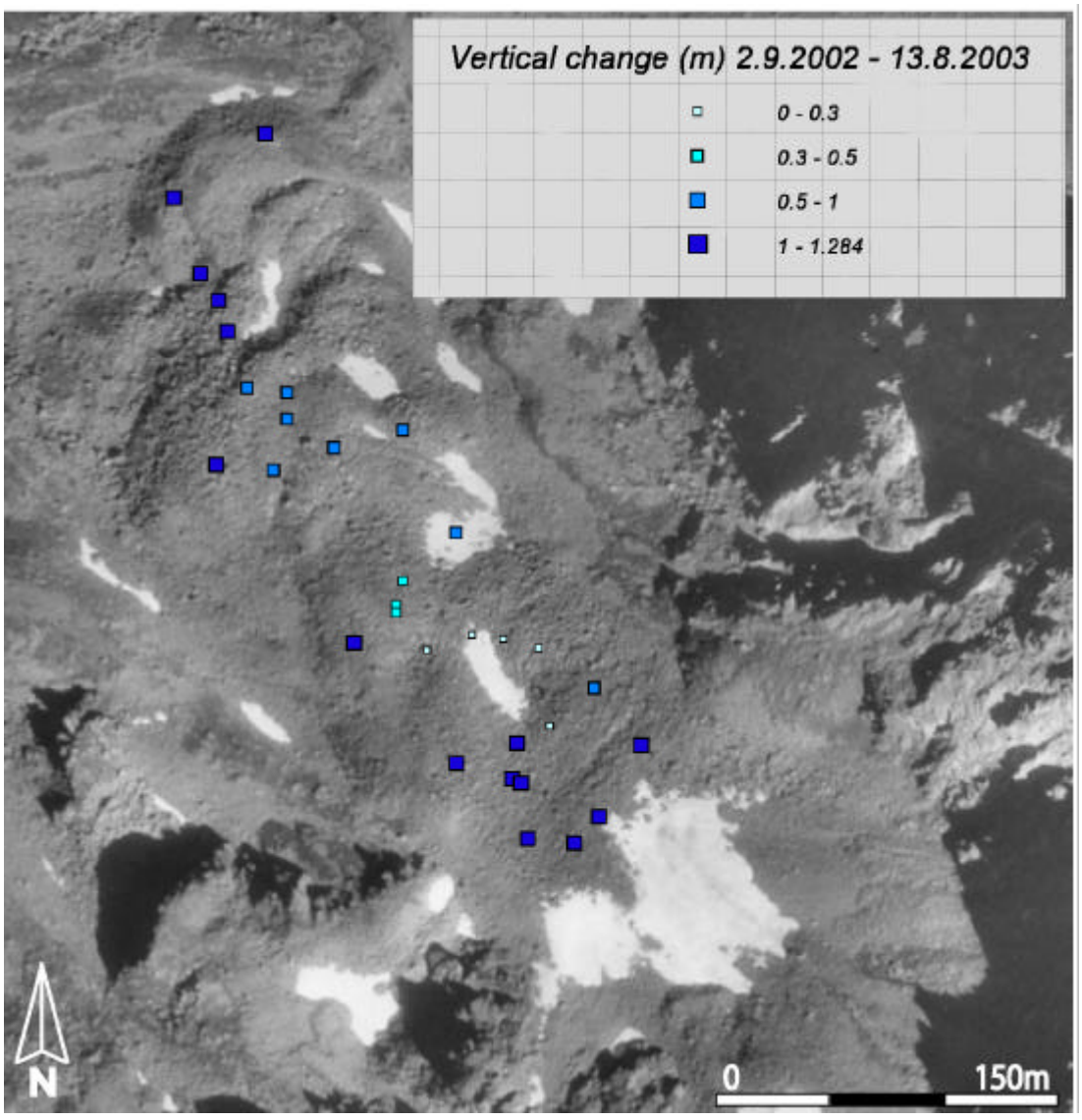

Figure 5.102: Vertical change (m) on rockglacier Huhh3 between 2.9.2002 and 13.8.2003. Underlying orthophoto of 20.08.1975 (flight-line 22, aerial photographs taken by swisstopo).

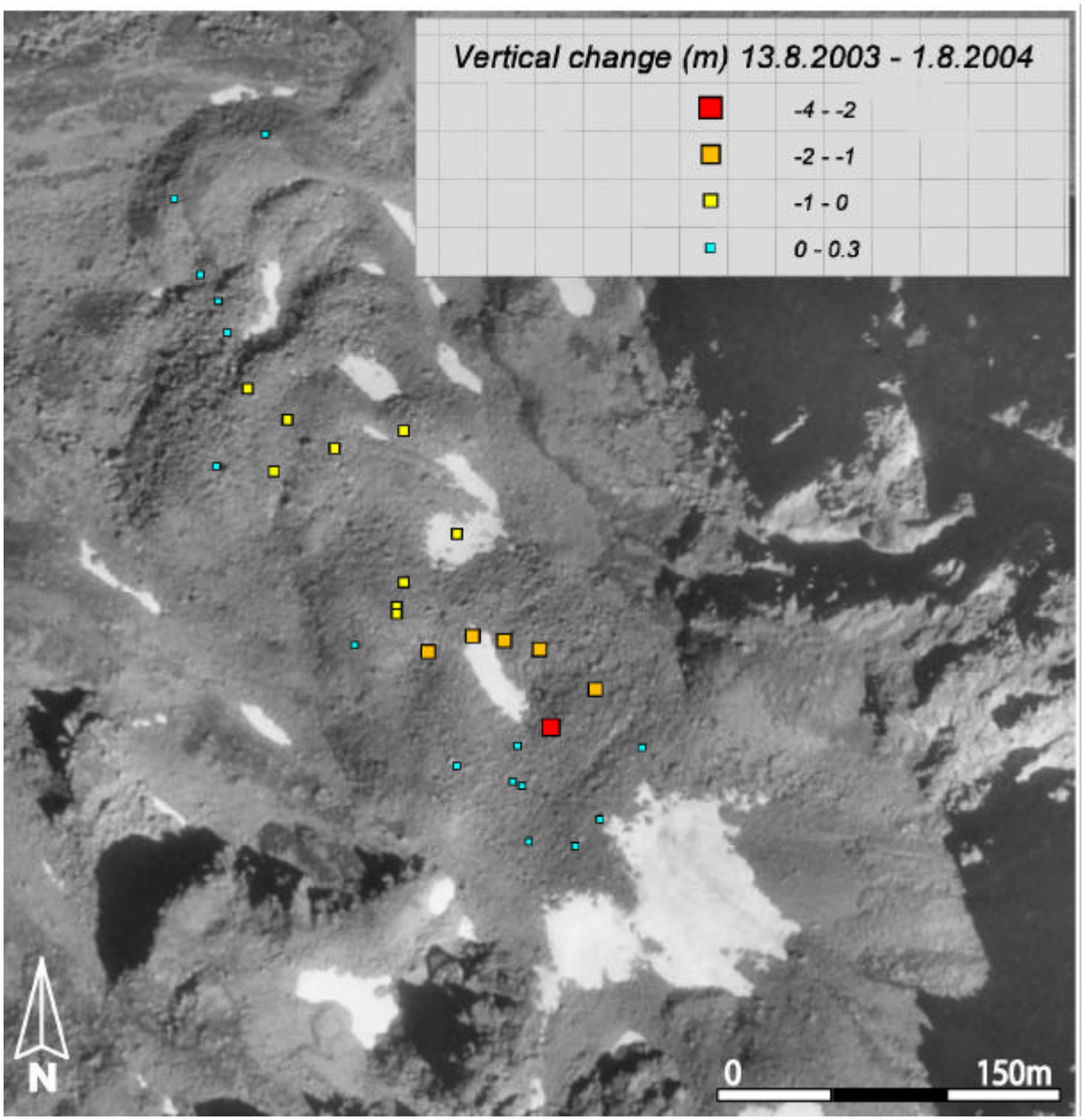

Figure 5.103: Vertical change (m) on rockglacier Huhh3 between 13.8.2003 and 1.8.2004. Underlying orthophoto of 20.08.1975 (flight-line 22, aerial photographs taken by swisstopo).

Table 5.13: Velocities of blocks on Huhh3 over the whole period 2002-2004 and for comparison check of horizontal and vertical changes by addition of the values 2002-2003 (t1) and 2003-2004 (t2).

	2.09.2002 - 1.08.2004			**check: t1 + t2**	
Block	direction	horizontal change (m)	vertical change (m)	horizontal change (m)	vertical change (m)
201	268.822	0.495	1.542	0.498	1.542
202	232.692	0.197	1.499	0.224	1.499
203	251.095	0.580	1.354	0.582	1.354
204	260.961	0.796	1.439	0.846	1.439
205	265.803	1.149	1.131	1.151	1.131
206	126.954	2.037	0.671	2.933	0.671
207	265.852	2.771	-0.069	2.772	-0.069
208					
209	176.937	2.895	1.081	3.039	1.081
210	240.351	2.560	0.902	2.561	0.902
211	269.593	3.792	0.452	3.793	0.452
212	272.431	1.301	0.887	1.308	0.887
213	258.375	2.772	0.446	2.778	0.446
214	255.191	3.868	-0.339	3.870	-0.339
215	254.977	4.056	-0.432	4.059	-0.432
216	255.138	4.045	-0.431	4.055	-0.431
217	245.581	0.885	1.190	0.902	1.190
218	253.230	3.922	-0.778	3.929	-0.778
219	254.653	4.417	-0.815	4.423	-0.815
220	249.292	4.413	-0.761	4.417	-0.761
221	247.589	3.563	-0.968	3.585	-0.968
222	252.359	2.141	-0.305	2.198	-0.305
223	246.688	5.190	-3.484	5.191	-3.484
224	266.650	0.484	1.205	0.665	1.205
225	257.292	0.463	1.309	0.561	1.309
226	241.613	0.344	1.385	0.466	1.385
227	230.377	0.266	1.465	0.404	1.465
228	225.151	0.249	1.490	0.461	1.490
229	233.029	0.341	1.409	0.415	1.409
230	240.475	0.318	1.387	0.381	1.387
231	252.152	0.293	1.372	0.377	1.372

As on the other rockglacier, an additional survey in July 2003 enabled the deduction of 'summer' - movement rates for a five-week period (8.7. – 13.8.2003). Horizontal velocities up to 0.15 m occur on the lowermost lobe and at the border of the cirque while the rest of the rockglacier depicts velocities between 0.15 and 0.9 m (table 5.14, figure 5.104). The comparison with the 'annual' horizontal velocities (2.9.2002 – 13.8.2003) reveals contributions mostly between 13 and 21 % (table 5.14). Some blocks at the orographic left front (209, 210) and in the upper part (223 – 230) show contributions of 46 - 80 % to the annual displacement. The 190 % value is assumed

to be incorrect. If the rockglacier would creep with a steady movement, the contributions of a five-week period would lie at about 10 %. Thus, at least at the centre of the rockglacier the presented results indicate intraannual variations with maximum velocities during summer.
The vertical displacements show a general lowering of the surface with values between -0.1 and -0.3 m in the marginal areas and up to -0.8 m in the central part of the rockglacier (figure 5.105). Since the 'annual' values depict a general rise of the surface, the main vertical movements seem to occur during another period of the year.

Table 5.14: Direction, horizontal and vertical change of blocks on Huhh3 between 8.07. and 13.08.2003 as well as contribution to the 'annual' displacement (2.9.2002 – 13.8.2003) in percent.

	8.07.2003 - 13.08.2003			% of period 2.9.02-13.8.03
Block	direction	horizontal change (m)	vertical change (m)	horizontal change
201	128.506	0.056	-0.257	20.36
202	134.449	0.019	-0.238	14.62
203	102.456	0.027	-0.258	9.96
204	157.435	0.130	-0.183	35.71
205	270.509	0.072	-0.274	13.74
206	274.687	0.428	-0.314	25.18
207	260.254	0.165	-0.343	13.66
208	255.377	0.131	-0.798	13.60
209	178.851	0.654	-0.27	47.56
210	271.386	0.893	-0.297	80.38
211	254.842	0.240	-0.312	14.72
212	216.372	0.118	-0.297	21.42
213	231.669	0.199	-0.305	17.70
214	238.965	0.266	-0.344	16.28
215	242.722	0.273	-0.368	16.06
216	230.527	0.314	-0.352	18.23
217				
218	236.334	0.279	-0.779	16.92
219	237.580	0.306	-0.402	16.43
220	230.477	0.322	-0.391	17.60
221	223.894	0.295	-0.41	20.10
222	211.646	0.208	-0.349	31.18
223	235.009	0.576	-0.676	46.34
224	185.065	0.241	-0.298	78.76
225	194.160	0.153	-0.267	55.64
226	180.805	0.154	-0.246	59.46
227	174.795	0.164	-0.258	66.40
228	240.185	0.542	-0.247	190.18
229	183.093	0.114	-0.27	47.70
230	181.387	0.097	-0.3	46.63
231				

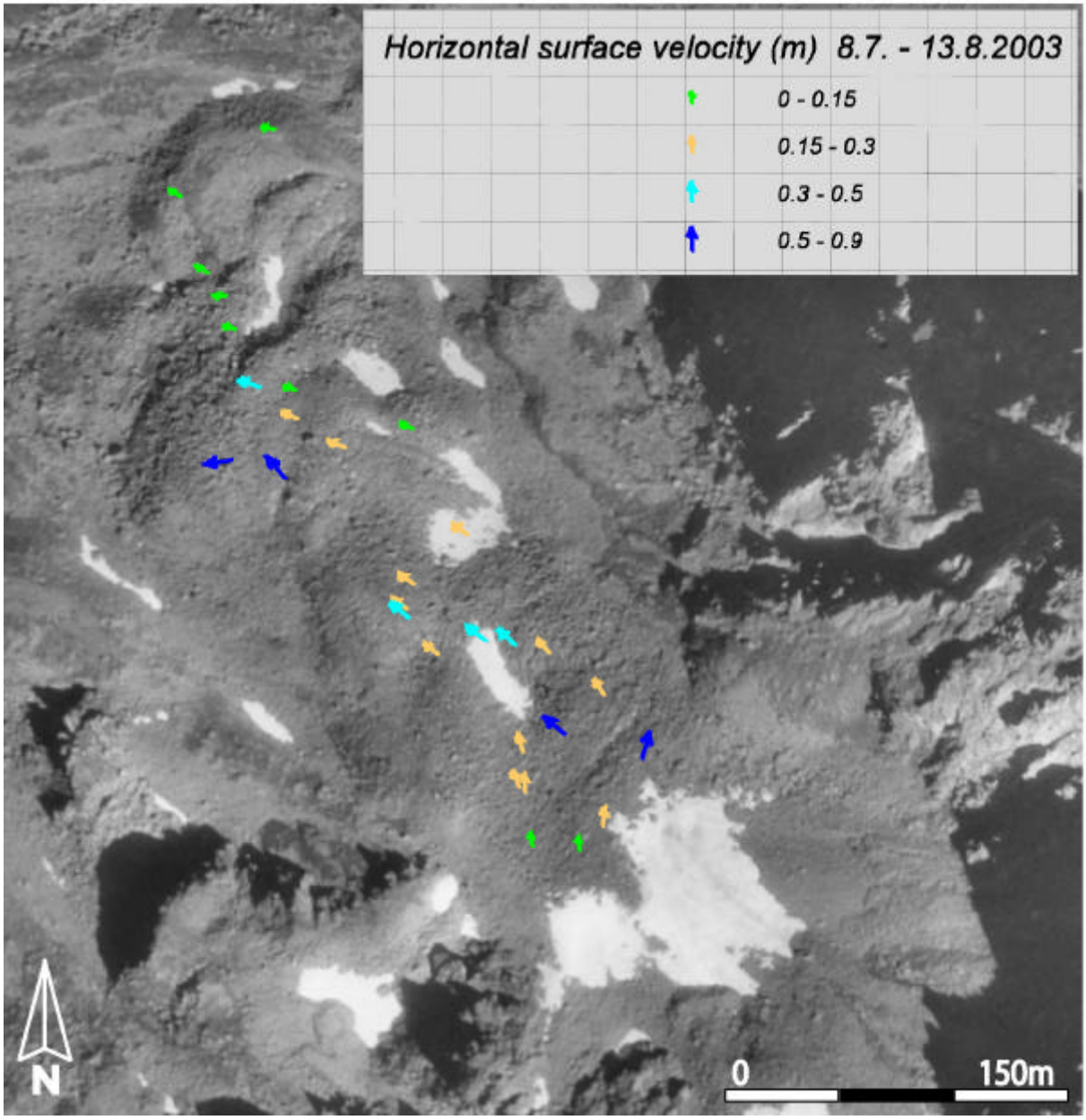

Figure 5.104: Horizontal surface velocity (m) on rockglacier Huhh3 between 8.7. and 13.8.2003. Underlying orthophoto of 20.08.1975 (flight-line 22, aerial photographs taken by swisstopo).

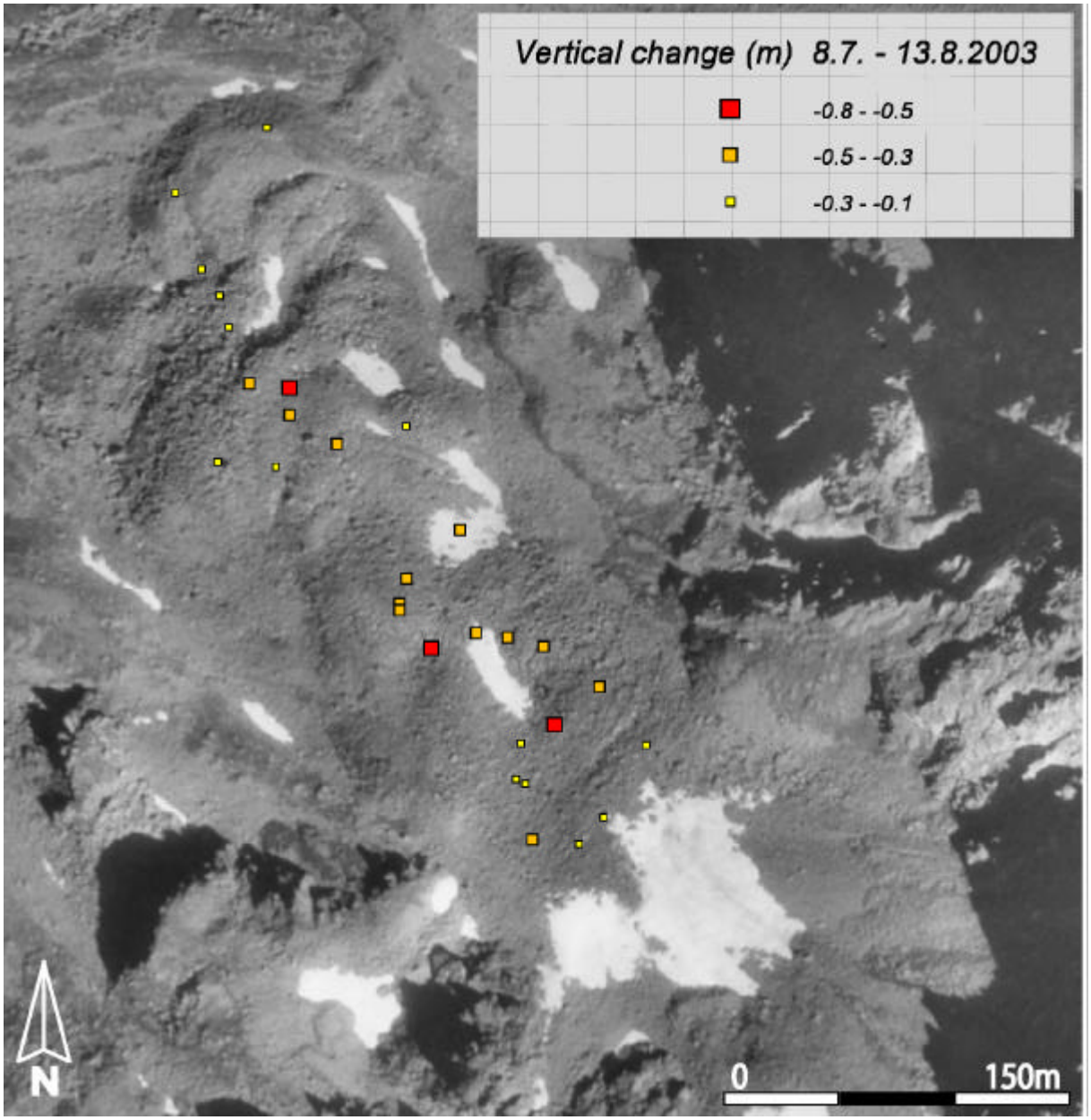

Figure 5.105: Vertical change (m) on rockglacier Huhh3 between 8.7. and 13.8.2003. Underlying orthophoto of 20.08.1975 (flight-line 22, aerial photographs taken by swisstopo).

5.3.3 Summary

The compiled high-resolution data on rockglacier kinematics derived from terrestrial geodetic survey contain valuable information on spatio-temporal variations. Distinct activity was deduced on the rockglaciers Huhh1 and Huhh3, even on the lowermost lobes which appeared inactive.

Interannual variations were investigated on both rockglaciers and indicated a general acceleration of horizontal velocities in the last years. This speed-up combined with a vertical thinning is most conspicuous in the central part of the rockglaciers.

Regarding intraannual variations in both horizontal and vertical velocities, the results from Huhh3 showed different components. While a large part of the annual horizontal displacement

occurred during summer, the majority of the vertical movement seems to happen in another period of the year.

On both rockglaciers the surface topography is clearly reflected in the pattern of horizontal and vertical velocities. Additionally, a strong link between horizontal and vertical displacements was observed. This is due to the general downslope movement of the blocks. Thus, a vertical component (normally negative) is automatically associated with the horizontal displacement. Additionally, great influence is given by the gradient. On gentle slopes (e.g., on the lower lobes of the rockglaciers or in the rooting zone at the cirque) the horizontal velocities are generally lower and the vertical component is mostly positive due to compression. Against that, horizontal velocities are higher on steep slopes and cause vertical thinning (extension). This pattern is clearly visible on the investigated rockglaciers. But, on both features an overall thickening was quantified in the corresponding first year of the measurement (2001/2002 on Huhh1, 2002/2003 on Huhh3). This phenomenon is not easy to explain but may be influenced by the timing of the first survey in September. If thinning is at least partially influenced by loss of mass, e.g. melting of ice, this occurs within a very short period in summer (probably in August or September). Therefore, if melting occurred before the first survey (September) and after the second survey (August of following year) it was left out and was not quantified. In the following years the survey was carried out earlier and thickening was quantified on the lower lobes while the main part of the permafrost bodies depicted thinning. Another reason for the thickening in the first periods may be the overall lower horizontal velocity in comparison to the following years. But, since movement takes place it must have been associated by at least a minimal decrease in height resulting from the before mentioned downslope movement. Thus, the argumentation is weak.

Especially on rockglacier Huhh3 the thinning in the upper part is very distinct in the year 2003/2004. The inspection in the field revealed very loose blocks in this area and the development of a spoon-like depression. Thus, the material is transported with high movement rates while the creeping mass loses connection to the debris supply from the cirque. Melting of ice may play an additional role by the thinning.

This dynamic interpretation of the rockglacier kinematics quantified in the years 2001 – 2004 gives an interesting insight but is unsatisfactory so far. Due to the shortness of the monitoring, inter- and intraannual variations are difficult to analyse and extraordinary values are hard to differentiate from ‘normal’ rates. Therefore, the survey is to be continued.

5.4 Dendrogeomorphology

5.4.1 Reaction wood in *Pinus cembra* stem

At the front of rockglacier Huhh3, a *Pinus cembra* tree was cropped in 2000 (cf., Roer 2001). The tree, which had an age of 34 years, showed distinct reaction wood indicating the tilting of the stem (figure 5.106). After a stable growing between 1966 and 1969, compression wood, which is directed upslope, occurred in 1970 for the first time. From 1990 it appeared more distinct and in the outermost rings (1997 – 2000) it depicted major influences. In addition, the occurrence of resin ducts in the late wood of the rings 1987, 1988, 1990 as well as 1997-1999 indicated strong mechanical stresses on the stem in the end of the growing season (Schweingruber 1996).

The observations include different signals: on the one hand, the front of the rockglacier had to be rather stable, due to the growing of the tree, while on the other hand, the data revealed mechanical stresses resulting from ground movement. In comparison with the photogrammetric results (figures 5.46, 5.47), the change in horizontal velocity is even indicated in the compression wood. Thus, the speed-up on rockglacier Huhh3 probably started in 1990 and appeared to be very distinct between 1997 and 2000.

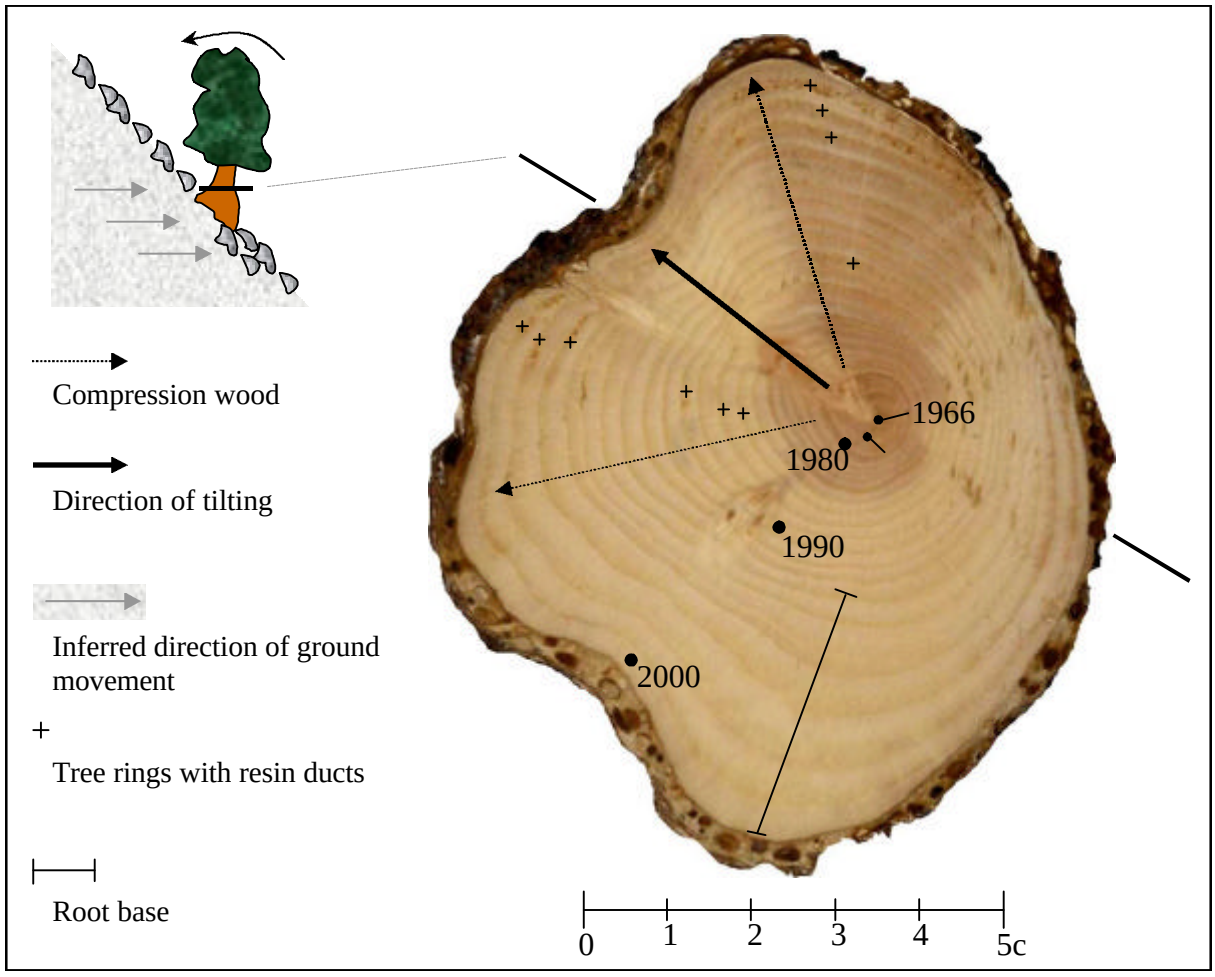

Figure 5.106: Compression wood in *Pinus cembra* stem and inferred movement of the ground.

5.4.2 Anatomical variations in *Salix helvetica* roots

In a first phase, the micro photos taken from the different root micro-sections of the eight *Salix helvetica* shrubs were analysed for variations observable visually. No obvious differences in ring width variations between the samples from the unstressed, inactive rockglacier lobe (Ref) and the stressed, active lobe (BG) were found. This also applies to differences in tracheid structure of the ground tissue, which is mainly formed to stabilize the plant. But comparing the vessels within the rings of the stressed and unstressed samples revealed general differences in size (figure 5.107). The vessels in roots taken from the inactive rockglacier tend to be larger than the ones from the stressed site.

To analyse this visual impression further, vessel sizes of all micro-sections (stressed and unstressed) were quantified using the image analysis program WinCELL. First results showed that it was possible to apply an automated, comparable measurement of vessel sizes within the rings of the *Salix helvetica* roots. In addition, a filter which excluded all cells with an area smaller than 0.0002 mm^2 was applied. These cells are defined to be tracheids, cells of the ground tissue of the rings. All cells larger than 0.0002 mm^2 were identified as vessels. As a result, an average of 1000 vessels was measured per micro-section. As a consequence from the filtering technique, the data do not have a normal but skewed distribution (compare figure 5.108).

In order to analyse the data from table 5.15 visually, box-plots are presented (figure 5.108), that is, for each measurement the median, maximum and minimum values as well as their statistical spread are determined (table 5.15). Within the box plot diagrams, the scale was manually adjusted to a maximum value of 0.004 mm^2 for better visualisation.

A detailed quality control of the cell measurements showed, that maximum values up to 0.0098 mm^2 for single vessels were caused by errors in defining cell wall boundaries of vessels within the micro photos. Nevertheless, maximum sizes of about 0.006 mm^2 for single vessels were proven as correct.

The vessel-size measurements confirm the visual impression. Although no obvious differences in ring-width variation are revealed, the size of vessels in stressed roots from the active rockglacier compared to those from roots of the inactive lobe is reduced. The calculated median for vessel sizes in roots of all plants taken from the active part are in average 60% lower than the values in roots of the inactive rockglacier. Even the statistical spread of about 75% to the related median values is lower in each of these plants (yellow boxes in figure 5.108).

The box-plots of the averaged data (diagram (C) in figure 5.108) are overlapping in the upper parts of the stressed roots and the lower parts of the unstressed roots, hence, the differences are not statistically significant. Nevertheless, the visual differences are still obvious. Vessels, formed to support the plant by transporting nutrients, are known to be variable in size (at least in stems) due to environmental stress (Kozlowski 1979). Although the difference is not statistically significant in this dataset, the findings fit to physiological patterns described for vessels in stems of trees (Lindorf 1994), but this has not been described for roots of shrubs yet.

As the most obvious reason for the differences in vessel size growth stresses in the ground are assumed, since the same topographic and climatic conditions exist at both sites. Thus, either

temperature conditions in the permafrost body or mechanical stresses due to rockglacier creep caused the changes in the wood-anatomy. Obviously, this argumentation is weak and further analyses need to be conducted. But the first-time application of this technique in rockglacier studies appears to be feasible and the preliminary results are promising.

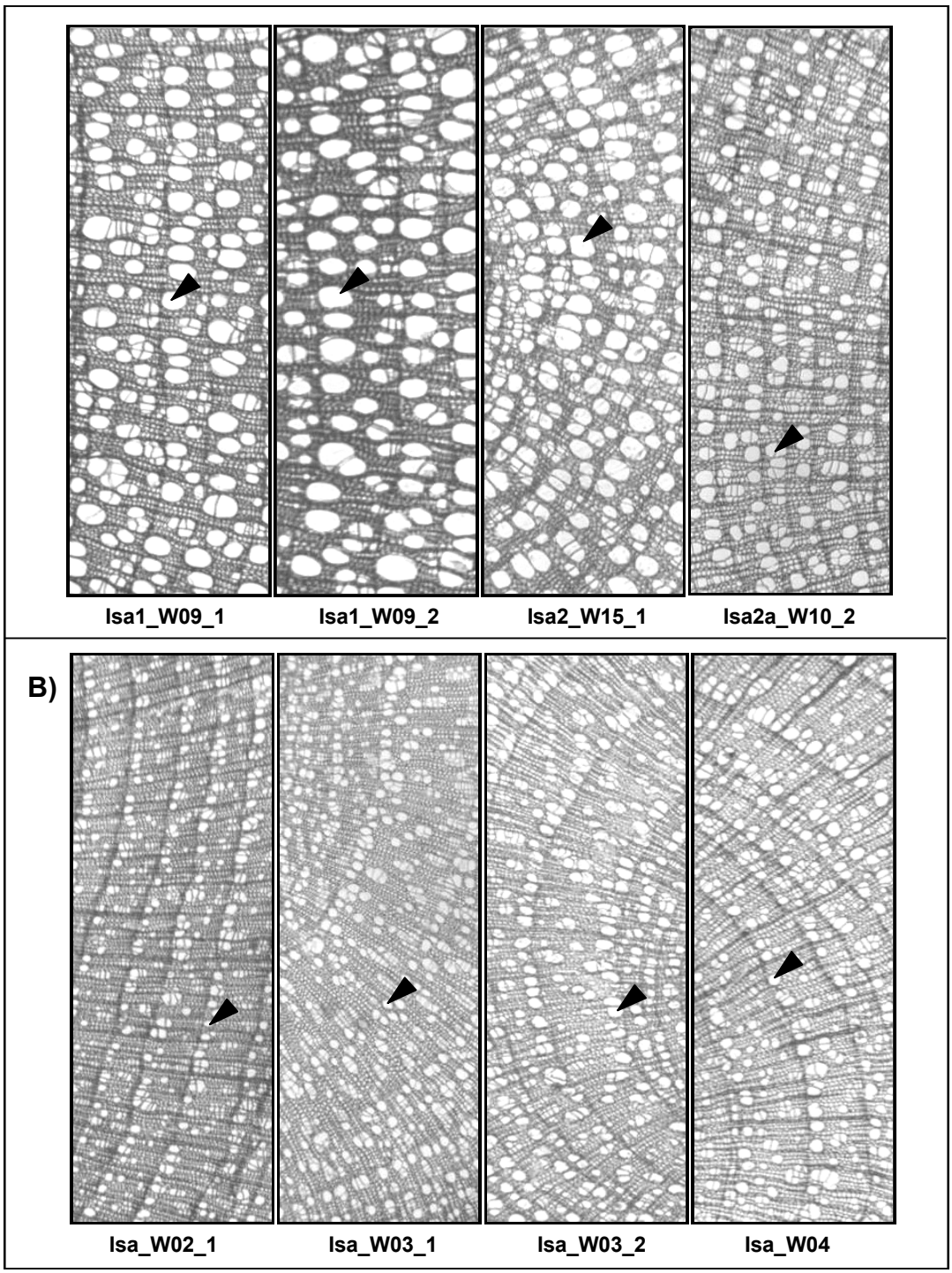

Figure 5.107: Micro sections of *Salix helvetica* roots from an inactive rockglacier (Ref) (**A**) and an active rockglacier (BG) (**B**); Black arrows indicate vessels (magnification: 40x). The differences in size of the vessels of unstressed (**A**) and stressed (**B**) roots are remarkable.

Table 5.15: Median, maximum, minimum values of vessel sizes and their statistical spread (*Salix helvetica* roots); inactive (Ref) and active (BG) rockglacier.

	Shrub ID (Ref)				
	Isa1_W09_1	**Isa1_W09_2**	**Isa2a_W10_2**	**Isa2_W15_1**	**Average_Ref**
Median	0.0014	0.0015	0.0009	0.0012	0.00125
Upper Quant.	0.0023	0.0029	0.0016	0.0022	0.00225
Max	0.0059	0.0098	0.0063	0.0064	0.0071
Min	0.0002	0.0002	0.0002	0.0002	0.0002
Lower Quant.	0.0006	0.0005	0.0004	0.0005	0.0005
	Shrub ID (BG)				
	Isa_W02_1	**Isa_W03_1**	**Isa_W03_2**	**Isa_W04**	**Average_BG**
Median	0.0005	0.0006	0.00055	0.0006	0.0005625
Upper Quant.	0.0007	0.001	0.0009	0.0009	0.000875
Max	0.0072	0.0043	0.0053	0.0056	0.0056
Min	0.0002	0.0002	0.0002	0.0002	0.0002
Lower Quant.	0.0003	0.0004	0.0003	0.0003	0.000325

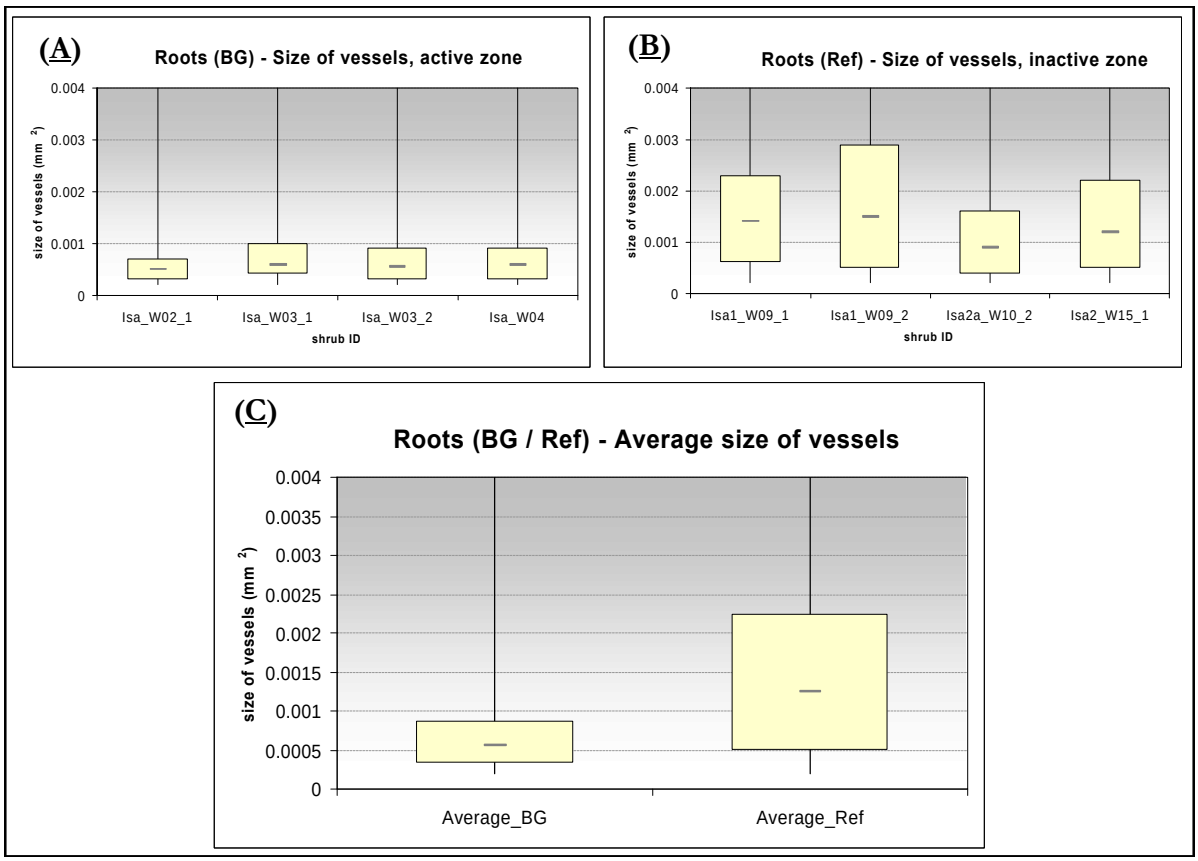

Figure 5.108: Boxplot visualisation of vessel size data (compare table 5.15): (A) active; (B) inactive rockglacier; (C) average values of vessel sizes (A) and (B). The skewed distribution is due to the exclusion of all cells < 0.0002 mm^2 (tracheids), the scale was adjusted to a max. value of 0.004 mm^2 for better visualisation.

5.5 Temperature monitoring:

A temperature monitoring was started in 2001 using Universal Temperature Loggers (UTL) (cf., Krummenacher et al. 1998). About 45 thermistors were placed in one hanging valley (Hungerlitälli) in various situations (on rockglaciers and surrounding terrain) between 2500 and 2780 m a.s.l. The data serve to determine the distribution of permafrost by the calculation of Mean Annual Ground Surface Temperatures (MAGST) as well as the interpretation of the Bottom Temperature of the winter Snow cover (BTS) (cf., Nyenhuis 2005) and to compare temperatures on different rockglaciers.

5.5.1 Active rockglacier Huhh1

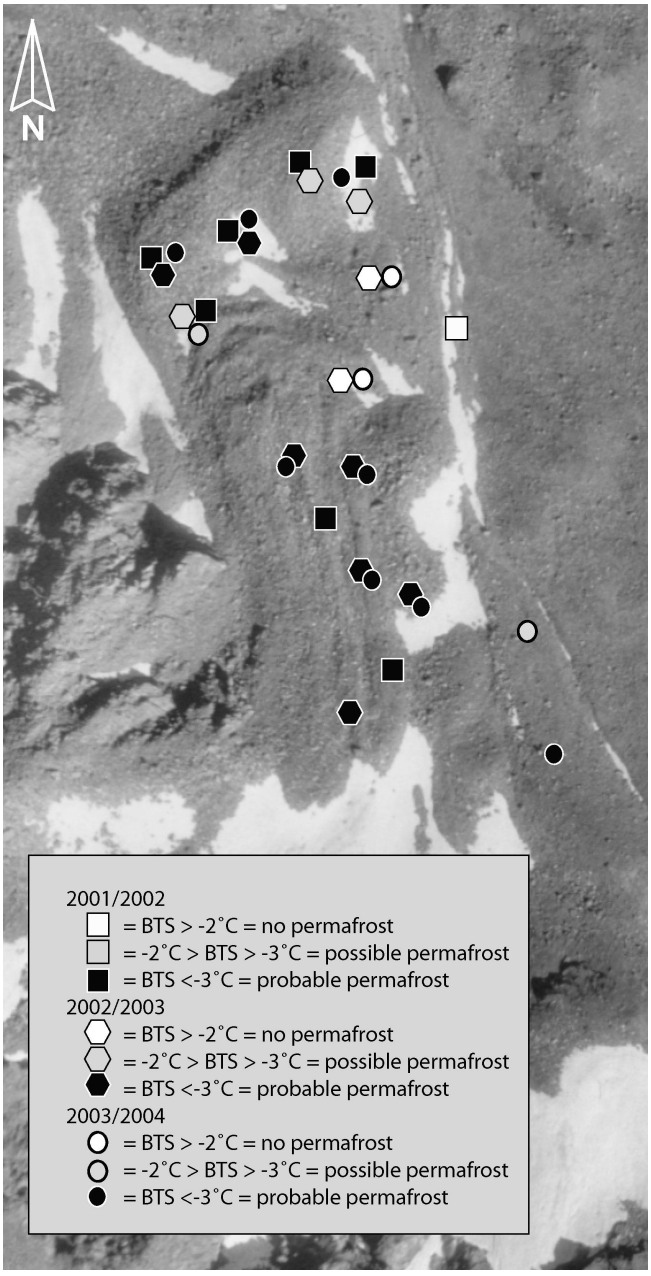

Figure 5.109: Bottom Temperatures of the winter Snow cover (BTS) on rockglacier Huhh1 in three successive years. Underlying orthophoto of 20.08.1975 (flight-line 22, aerial photographs taken by swisstopo).

As depicted in figure 5.109, the monitored BTS values on rockglacier Huhh1 were quite steady over the years. All thermistors on the upper lobe and at the terminal front (orographic left side) indicate clear permafrost temperatures (< -3°C), while clearly no-permafrost (temperatures > -2°C) is monitored in the orographic right part of the lower lobe and in the furrow beside the rockglacier. At the front, two loggers measured possible permafrost in the winter 2002/2003, while it was probable in the other winters. Of interest is the front of the upper lobe; at its orographic left side, permafrost was probable in the first winter (2001/2002), whereas it was only possible in the following winters.

5.5.2 Active rockglacier Huhh3

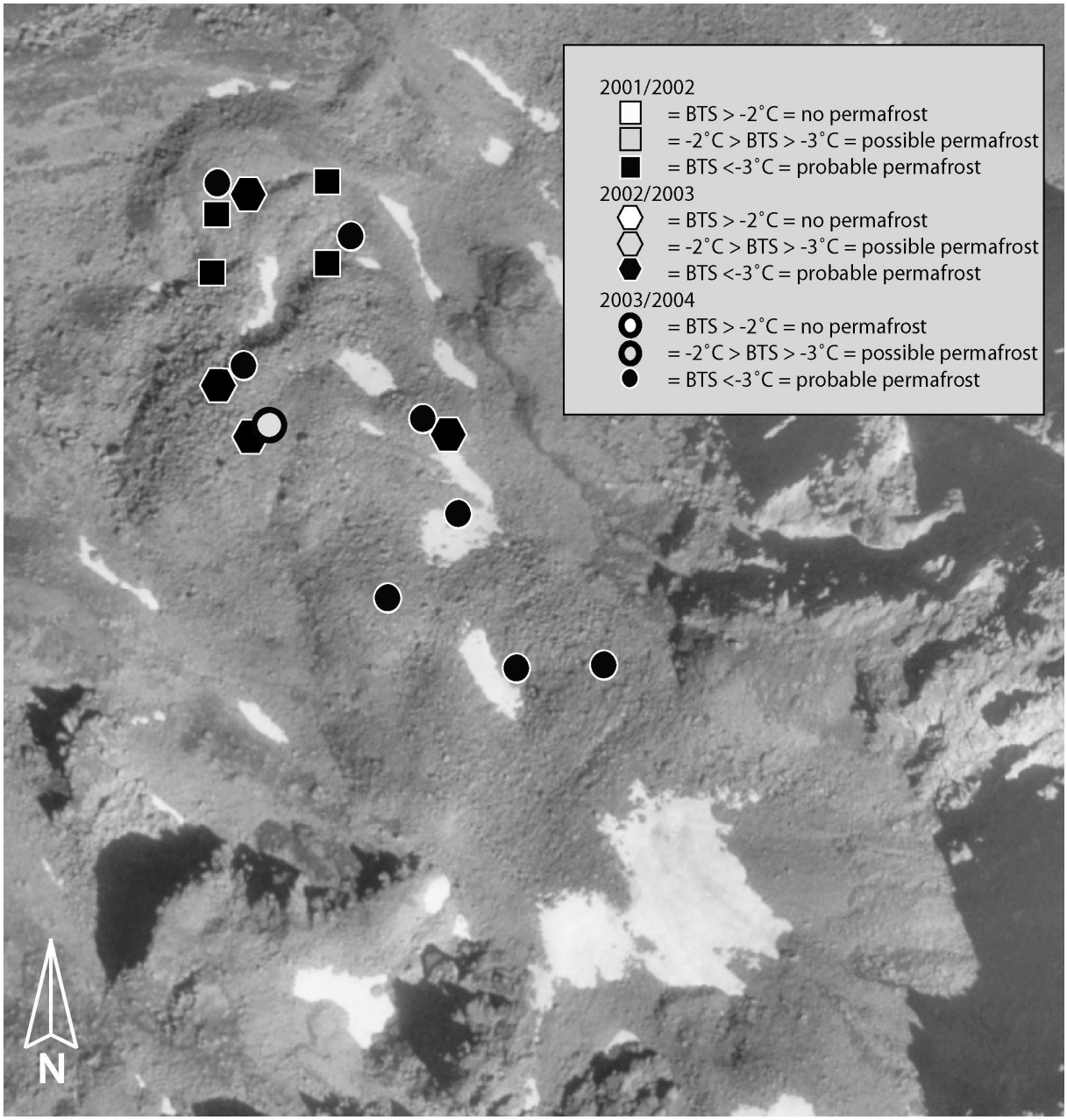

Figure 5.110: Bottom Temperatures of the winter Snow cover (BTS) on rockglacier Huhh3 in three successive years. Underlying orthophoto of 20.08.1975 (flight-line 22, aerial photographs taken by swisstopo).

On rockglacier Huhh3, all thermistors revealed clear permafrost temperatures over the monitoring period, even on the lower lobes which are mapped as inactive (figure 5.110). In the last winter (2003/2004) one exception is observed near the active front, where the BTS value was only -2.3°C (possible).

5.5.3 Inactive rockglacier Hurh2

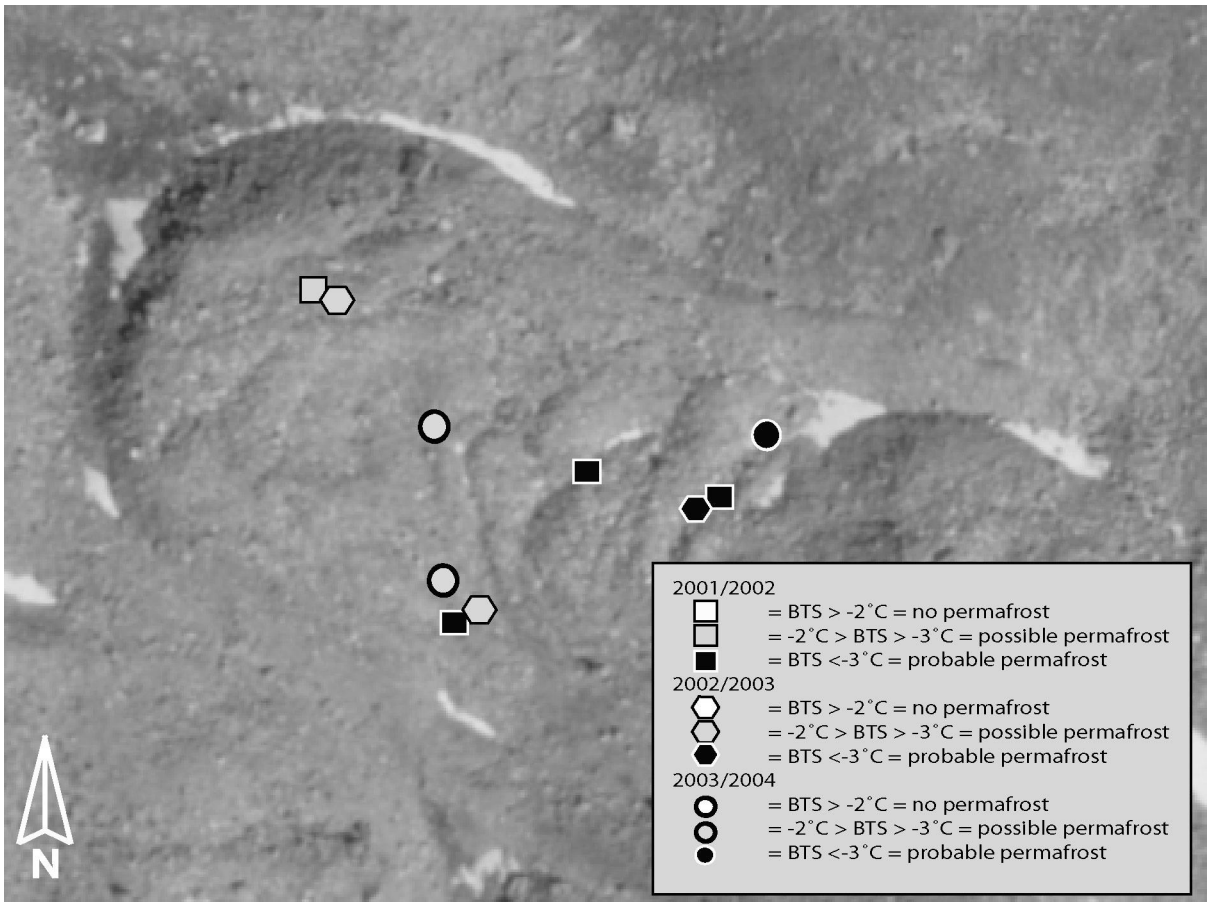

Figure 5.111: Bottom Temperatures of the winter Snow cover (BTS) on the inactiverockglacier Hurh2 in three successive years. Underlying orthophoto of 20.08.1975 (flight-line 22, aerial photographs taken by swisstopo).

On rockglacier Hurh2, bottom temperatures of the snow cover between -3° and -2°C (possible permafrost) were measured in the lower part of the tongue (figure 5.111). Thus, the values confirm the inactivity of the feature. Against that, in the rooting zone and thus in the vicinity to the terminus of Hurh1, the BTS values are clearly deeper and display probable permafrost conditions.

5.5.4 Inactive rockglacier Huhh2

Figure 5.112 shows, that on the inactive rockglacier Huhh2 only a few data loggers were placed in the winters 2002/2003 and 2003/2004. In most cases they showed a probable permafrost occurrence, apart from one thermistor which depicted a BTS value of – 2.8°C in the winter 2003/2004 and thus indicate only possible permafrost.

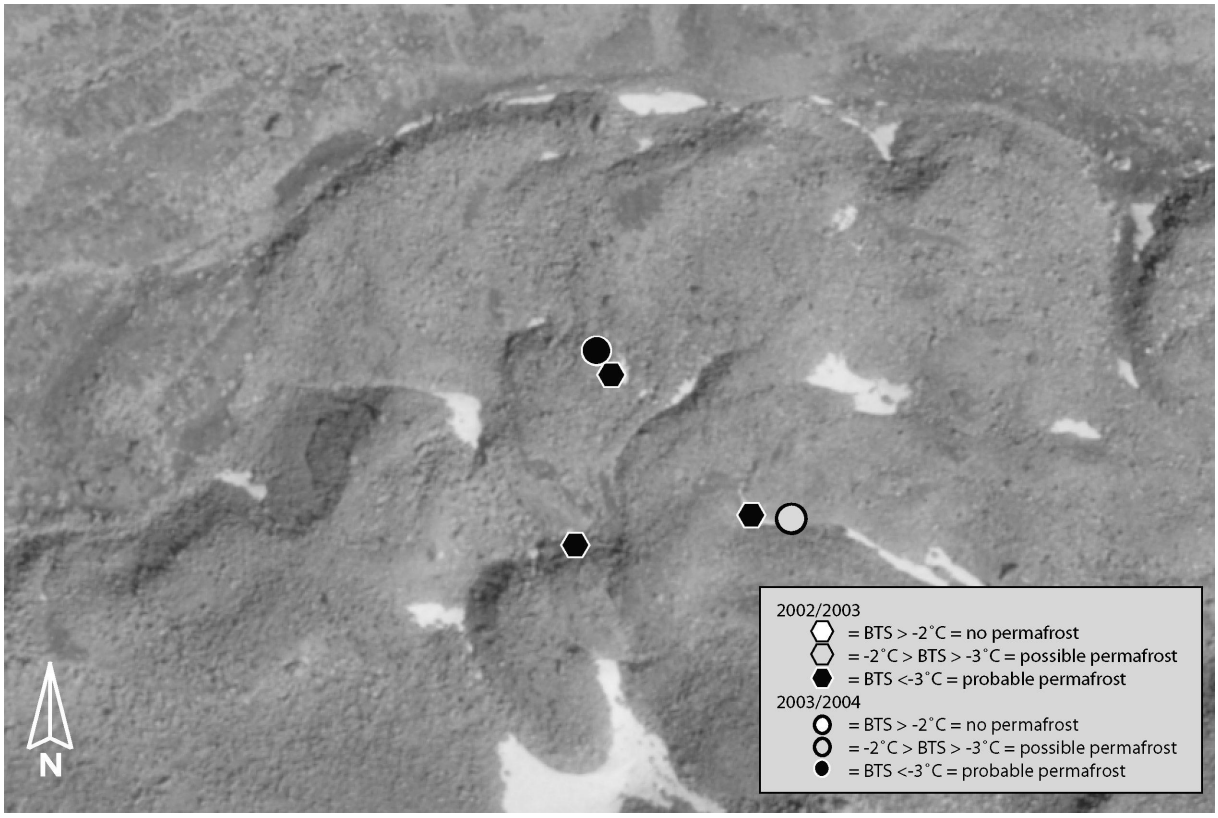

Figure 5.112: Bottom Temperatures of the winter Snow cover (BTS) on the inactive rockglacier Huhh2 in three successive years. Underlying orthophoto of 20.08.1975 (flight-line 22, aerial photographs taken by swisstopo).

5.5.5 Summary

The thermistor data depicted permafrost conditions on all investigated rockglaciers over a period of three winters (2001 – 2004), independent of their state of activity. Probably this results from the distribution of coarse debris, which favours the penetration of deep temperatures into the ground. Nyenhuis (2005) ascertained this assumption by a comparison of BTS values on and beyond rockglaciers. Thus, areas with small-grained material (e.g., moraines, glacier forefield) reveal mostly temperatures > -2°C, even directly next to a rockglacier with clear permafrost temperatures, and therefore are permafrost unfavourable. This phenomenon is visible on rockglacier Huhh1, where a thermistor was situated beside the rockglacier during the winter 2001/2002.

Probable permafrost was ascertained everywhere on rockglacier Huhh3 and at the front as well as on the upper lobe of Huhh1. On the inactive rockglacier Hurh2, the permafrost occurrence appeared a little bit patchy. Statements about the permafrost distribution on Huhh2 are limited due to the small number of thermistors.

In a few positions, a slight – but not significant – warming trend is reflected in initially monitored probable-permafrost conditions and later depicted possible-permafrost conditions (cf., Huhh2, Huhh3).

Since BTS values may vary in time, measurements over at least 3 years and better over 5 years are required for reliable interpretations (Matsuoka 2004, personal communication). Thus, with the existing data conclusions on permafrost occurrence are possible. For the analysis of temporal variations the temperature monitoring is to be continued.

6 DISCUSSION

Applied methods

By a combination of different methods, rockglacier movements in the Turtmann valley were analysed qualitatively and quantitatively on various spatial and temporal scales. Geomorphic mapping allowed the estimation of the degree of activity and served as base for the application of the other methods. By the use of digital photogrammetry and terrestrial geodetic survey the quantification of horizontal velocities and vertical changes was enabled. The photogrammetric results (chapter 5.2) demonstrate that the small-scale aerial photographs are highly useful to measure changes in rockglacier geometry. Also the combination with high resolution imagery (from HRSC-A), which was applied for the first time in rockglacier studies, has been successful (Roer et al. 2005). Thus, displacements were investigated in a large area (meso-scale) and over a time span of 26 years (1975 – 2001). Regarding the life-time of rockglaciers of some thousand years (cf., Frauenfelder & Kääb 2000) this period covers not a long time, but compared to other studies this is quite a long data series. The accuracy of the horizontal and vertical displacements is estimated to lie in the range of 6 – 13 cm/a, depending on the considered interval. Against that, the terrestrial geodetic survey enabled the quantification of block displacements on two rockglaciers over a period of 3 years. Due to the high accuracy of this technique and the temporal resolution of the measurements, inter- and intraannual changes of the displacements were recorded. Hence, even if the survey is restricted to the snow free period, movements during summer were distinguished from movements during the rest of the year. The determination of permafrost creep using dendrogeomorphic techniques, which strongly depend on the occurrence of trees or shrubs, was applied on two rockglaciers. With the investigated plants, a period of 30 to 40 years is covered. On one permafrost body, the increase in horizontal velocity in the beginning of the 1990s is clearly reflected in the reaction wood. On the other rockglacier, anatomical variations were investigated in the roots of shrubs. Due to the first-time application in rockglacier research and therefore low experiences in interpretation, it was not possible to conclude whether the observed growth variations result from low temperature conditions or from movements of the ground.

The combination of the described methods allows the thorough description of rockglacier kinematics and a careful interpretation of the findings in the Turtmann valley.

Rockglacier activity

Rockglacier activity was investigated and quantified by different methods (appendix 2). While the geomorphic mapping covered all rockglaciers (45) on the eastside of the Turtmann valley, digital photogrammetry was applied on all intact rockglaciers (34). For 85 % of the investigated features, the mapped activity or inactivity was confirmed by the photogrammetric data (appendix 2). Thus, the more qualitative mapping represents a valuable base for the determination of rockglacier

activity. Regarding the intact rockglaciers, an active state was ascertained for 53 % of them. Inactivity was sometimes hard to define due to the range of uncertainty of the displacements in digital photogrammetry. In addition, one rockglacier (Huhh2) revealed large areas with velocities below the level of significance, apart from a small area in the root zone, which showed a clear activity. In such a case the state of activity is hard to define. By the use of terrestrial geodetic survey, two rockglaciers (Huhh1, Huhh3) were monitored with high temporal resolution, and the activity of the permafrost bodies was again confirmed. Due to the high accuracy of this method (~ 3 cm), small displacements were quantified on the lower lobe of Huhh3, which was found to be inactive by photogrammetric measurements. Therefore, it is assumed that some of the inactive rockglaciers are possibly active, but reveal only very small displacements. The application of dendrogeomorphic techniques allowed the determination of activity on rockglacier Huhh3, while the data from rockglacier Grueo1 gave no clear evidence.

Horizontal velocities

Most of the rockglaciers in the Turtmann valley indicate above-average horizontal velocities compared to other rockglaciers in the Alps, which show normal rates in the range of centimetres to one meter per year (Haeberli 1985). Highest velocities are described for the Inneres Reichenkar (Austria) with max. 6.94 m/a (Chesi et al. 1999) and for the Äusseres Hochebenkar rockglacier (Austria) with up to 5 m/a (Vietoris 1972) (appendix 1). In Switzerland (Grisons) maximum horizontal velocities of 2 m/a are documented for the Val da l' Aqua rockglacier (Jäckli 1978, from Barsch 1992) and for the Suvretta rockglacier (Kääb 2000). Values in the same order of magnitude are also determined on the Gruben rockglacier in the Valais (Strozzi et al. 2004.). In the study presented here, maximum horizontal displacements in the range of 3 – 5 m/a were observed on several rockglaciers, e.g. Huhh1, Huh3, Grueo1.

Vertical changes

Regarding the vertical changes, no uniform signal is depicted on the rockglaciers. This is due to the diverse factors, such as 3-dimensional straining, climate forcing, debris supply, formation of ice from snow or water, etc. influencing this component (cf., chapter 2.3.5). Thus, differing processes may have occurred during the investigated periods. On some rockglaciers vertical changes are clearly correlated with the horizontal velocities (e.g., Grueo1, Huhh3). In these cases, high horizontal movements cause a thinning (vertical compression) in the upper part and a thickening (vertical extension) in the lower part of the rockglacier and thus indicate the shifting mass. It is presumed that if this creep behaviour continues for a while, the rockglacier body will loose connection to the sediment source in the root zone, since the sediment supply can not compensate the high velocities (cf., Lambiel & Delaloye 2004). On rockglacier Huhh3 this became, for instance, visible in a spoon-shaped depression directly below the cirque. Hence, the probably climatically driven speed-up might be followed by dynamic inactivation.

Over the period 1975-1993, in three hanging valleys (Pipjitälli, Brändjitälli, and Hungerlitälli) rockglacier kinematics was already investigated by the application of digital photogrammetry (Elverfeldt 2002). This affords the opportunity for a comparison of the measured velocities. Although a relatively small number of blocks was measured in this previous study, they correspond well in the horizontal as well as in the vertical displacements. Thus, the state of activity of the individual rockglaciers can be assessed with a small number of measured blocks and thus with less expenditure. But, for the investigation of single flowfields on a rockglacier and the interpretation of spatio-temporal variations in permafrost creep, a dense data pool is required.

Spatial variations

On the individual rockglaciers (micro-scale), spatial variations in horizontal velocities and vertical changes mostly emphasize the rockglacier topography or rather vice versa. As it was described also for other rockglaciers, horizontal velocities are highest in the central flowline of the individual lobes and depict a distinct decrease toward the margins, which is caused by increased friction (Haeberli 1985). In areas with transverse ridges and furrows indicating horizontal compression, speeds are in general smaller than in areas with extending flow (cf., chapter 2.3.5.2). As it was described by Kääb et al. (2003), the root zones often depict a continuous transition zone (with small displacements) to the bordering slopes. Therefore it is hard to define the upper border or the initiation line of the feature. On some rockglaciers below cirques (Huhh1, Huhh3) a distinct increase in velocity over a distance of a few meters was observed directly at the border of the cirque. A similar pattern is revealed for permafrost bodies which creep over steep slopes (e.g., border of a cirque, moraine) and therefore depict highest velocities at the front (Hujp, Grueo6). These observations emphasise the significance of the slope for small-scale variations in permafrost creep. In addition, in some places active lobes are superimposed on inactive ones and thus indicate a younger generation and the reactivation of the permafrost bodies (e.g., Brho1, Grueo4).

Considering all investigated rockglaciers (meso-scale), spatial variations reveal only slight regularities. In general, the active rockglaciers are concentrated in altitudes between 2600 and 2800 m a.s.l. (front altitude) and on north and north-west exposed slopes. The two rockglaciers showing the highest maximum velocities (Grueo1, Huhh3) indicate the lowermost positions of the investigated active rockglaciers. Thus, they are situated close to the lower boundary of the discontinuous permafrost occurrence. Regarding mean horizontal velocities, high or low rates, respectively, are depicted in diverse altitudes and aspects as well as on different slopes. By the classification of different types or settings of rockglaciers, it became apparent that the highest velocities are revealed on those below cirques (Hufh, Huhh1, Huhh3, Grueo2, Grueo6, Chu1). Apart from Grueo7, generally lower values are measured on rockglaciers which are situated in the bottom of a hanging valley (Huhh2, Grueo4, Niggel2). Against that, the permafrost bodies below glaciers (Pipp1, Brho1) showed no comparable behaviour.

Temporal variations

An increase in horizontal velocity within 26 years of photogrammetric monitoring was ascertained for all investigated active rockglaciers (figure 5.91). Since the results were averaged over the measurement periods of 18 and 8 years, respectively, it is not possible to date the beginning of the acceleration exactly. It is assumed, that the speed-up started in the beginning of the 1990s. At least, this is indicated by dendrogeomorphic data from Huhh3, which revealed a distinct reaction to mechanical stress from 1993, caused by an increase in rockglacier movement. Using geodetic survey between 2001 and 2004 on two rockglaciers (Huhh1, Huhh3), continued high velocities are confirmed. In addition, even within this short period an increase in horizontal velocity was quantified on both rockglaciers. Since the general speed-up appears to be the most distinct signal given in the data, probable controls are later discussed in more detail. In most cases, the changes in thickness also showed distinct temporal variations. But due to the diverse processes influencing the vertical component, a uniform signal is not indicated in the data.
Inraannual variations in horizontal velocities and vertical changes are recorded by terrestrial geodetic survey. For instance, the findings of rockglacier Huhh3 give rise to the assumption that most of the horizontal displacements occur in late summer and autumn, while most of the vertical changes seem to occur during another period of the year.

Rheological considerations

According to the current knowledge of rockglacier rheology, several parameters may cause a change in flow. Regarding the flow law, differences in ice content and thickness, ice temperature as well as changes in slope or a combination thereof, are possible explanations (Kääb et al. 1997). These parameters are influenced by the input of water (precipitation, meltwater), debris supply, snowcover characteristics (duration, thickness, etc.), and temperature variations. One parameter recently often stressed is the increase in ground temperature, which results in a warming of the ice, a subsequent decrease in ground ice viscosity and thus leads to higher deformation rates (Kääb et al. 2003). For instance, this is concluded by Arenson et al. (2002), who documented degrading permafrost with a decrease in ice content, an increase in creep velocity and rise of shear zones towards the surface. This observation is contrary to the assumption by Barsch (1996), who described the reaction of rockglaciers to an increase in temperatures by a distinct decrease in velocity and a subsequent inactivation. It should be noted, however, that the above hypotheses, that apparently contradict each other, could both apply if different time scales are considered. In addition to a rise in temperature, also other factors like an increase in ice content, for instance by refreezing meltwater, or an increased debris supply may cause higher deformation rates. The effectiveness of all these individual parameters on different spatial and temporal scales is to a large extent unknown.

Probable controls on the investigated rockglacier speed-up

In order to interpret the observed speed-up of rockglaciers in the Turtmann valley, some geomorphic and climatic parameters are investigated for their individual influence on rockglacier

movement. Obviously, these simple correlations will not allow a deduction of ongoing processes or dynamics within this complex system, but probably they help to get a better idea of major controls.

- Geomorphic controls

Different terrain parameters are correlated with mean annual horizontal displacements to ascertain geomorphic controls on rockglacier creep.

First of all, the relation between average slope (°) and mean annual horizontal velocity is investigated for both periods (1975 – 1993 and 1993 – 2001). As depicted in figure 6.1, very different trends are revealed for the two periods. Hence, the slope seems to be of greater importance in the second period, where velocities are in general higher. With r-values of 0.15 (1975-1993) and 0.31 (1993-2001) and a corresponding level of significance (r*95 = 0.497), the relation between slope angle and horizontal velocity is statistically not significant. A similar correlation was determined by Frauenfelder et al. (2003) for rockglaciers from the European Alps and the Rocky Mountains. Thus, it is indicated that in general the influence of stress on the magnitude of flow is less important than other factors (Frauenfelder et al. 2003).

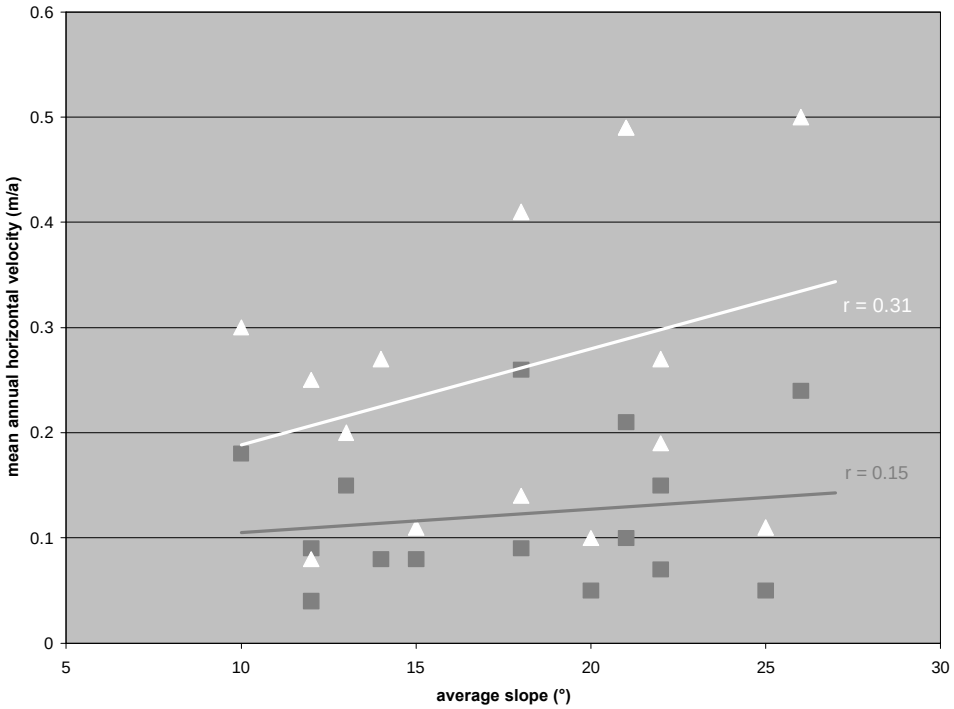

Figure 6.1: Relation between average slope (°) and mean annual horizontal velocity (m/a) of all active rockglaciers (apart from Grueo1) for both investigated periods. = mean velocity 1975 – 1993; Ä = mean velocity 1993 – 2001. Total sample size n = 16.Thus, r* 95 = 0.497, r* 99 = 0.623, r*99.9 = 0.742.

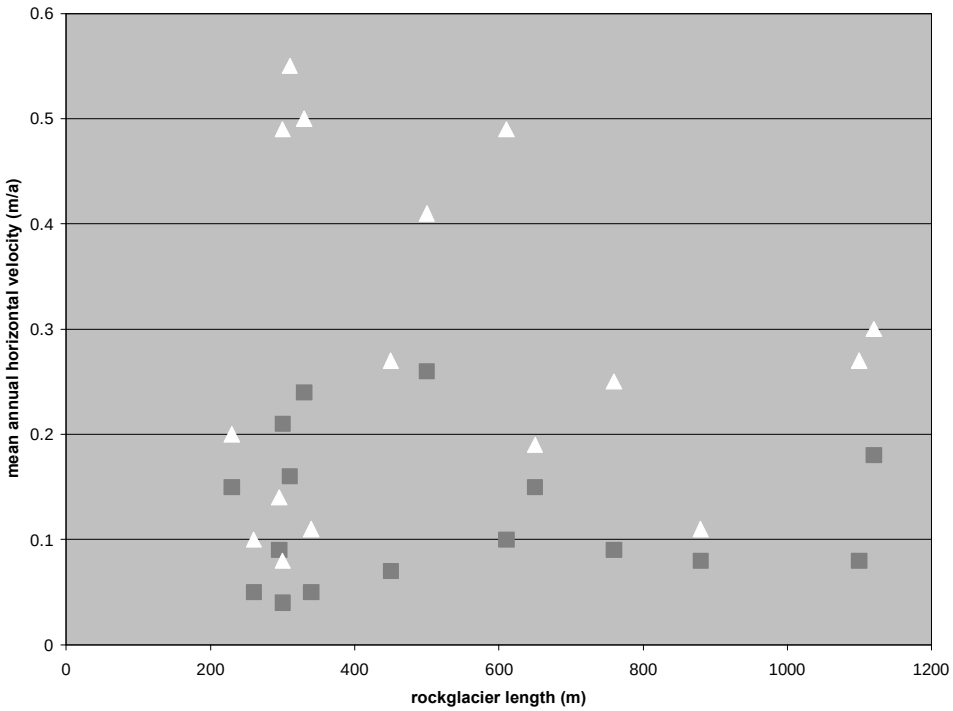

Figure 6.2: Relation between rockglacier length (m) and mean annual horizontal velocity (m/a) of all active rockglaciers (apart from Grueo1) for both investigated periods. □ = mean velocity 1975 – 1993; Ä = mean velocity 1993 – 2001. Total sample size n = 16.

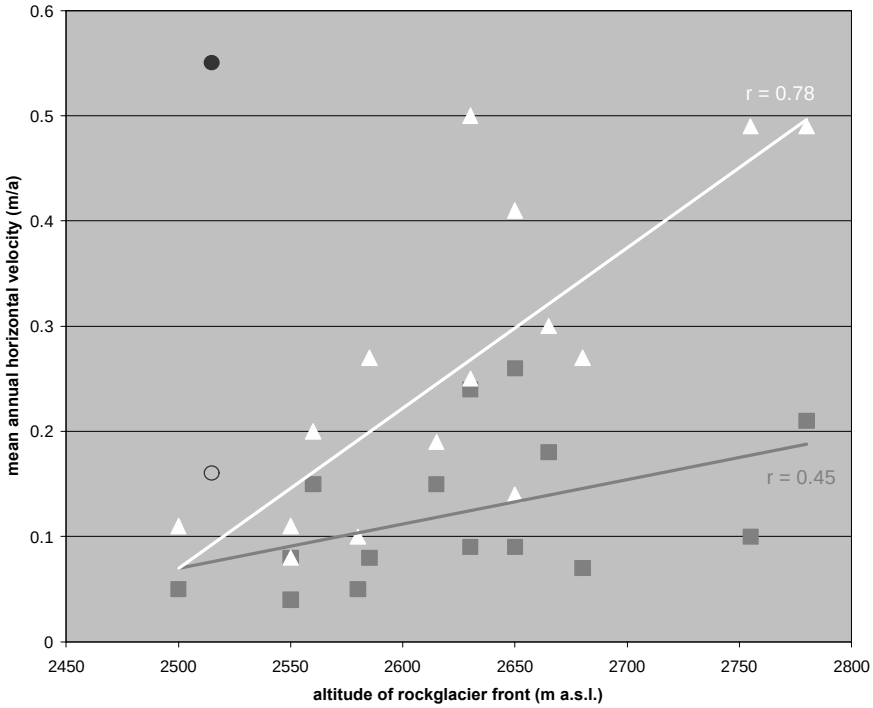

Figure 6.3: Relation between altitude of rockglacier front (m a.s.l.) and mean annual horizontal velocity (m/a) of all active rockglaciers (apart from Grueo1) for both investigated periods. □ = mean velocity 1975 – 1993; Ä = mean velocity 1993 – 2001; □ = Huhh3 mean velocity 1975 – 1993 (not included in the trendline – analysis); □ = Huhh3 mean velocity 1993 – 2001 (not included in the trendline-analysis).

Second, the correlation of rockglacier length and mean annual horizontal velocity is analysed (figure 6.2). Again, great differences are revealed for the two periods and for both of them the relation is statistically not significant. This is in contrast to the findings by Frauenfelder et al. (2003), who revealed a clear correlation (r = 0.63) between the two parameters.

Third, the velocity is correlated with the altitude at the rockglacier front and thus with the minimum altitude of the rockglaciers (figure 6.3). Also here, the trendlines depict major differences for the two time spans. Surprisingly, the values indicate that velocities increase with increasing altitude. Regarding all investigated rockglaciers, a weak correlation is given by r-values of 0.37 (1975 - 1993) and 0.49 (1993 – 2001) with r*95 = 0.497. By excluding the outlier Huhh3 (marked by□ and□) still a weak correlation (r-value = 0.45, r*95 = 0.514) is depicted for the first period (1975-1993). But, a distinct correlation with an r-value of 0.78 is revealed for the second period (1993 – 2001). Thus, the relation between the altitude and the increased velocities of the second period is even included in r*99.9 = 0.76 and therefore depicts a high statistical significance. By this correlation, the influence of air temperature (as a function of altitude) is indicated. Therefore, further analyses concentrate on temperature conditions and changes on different spatial scales (meso- and micro-scale).

- Climatic controls

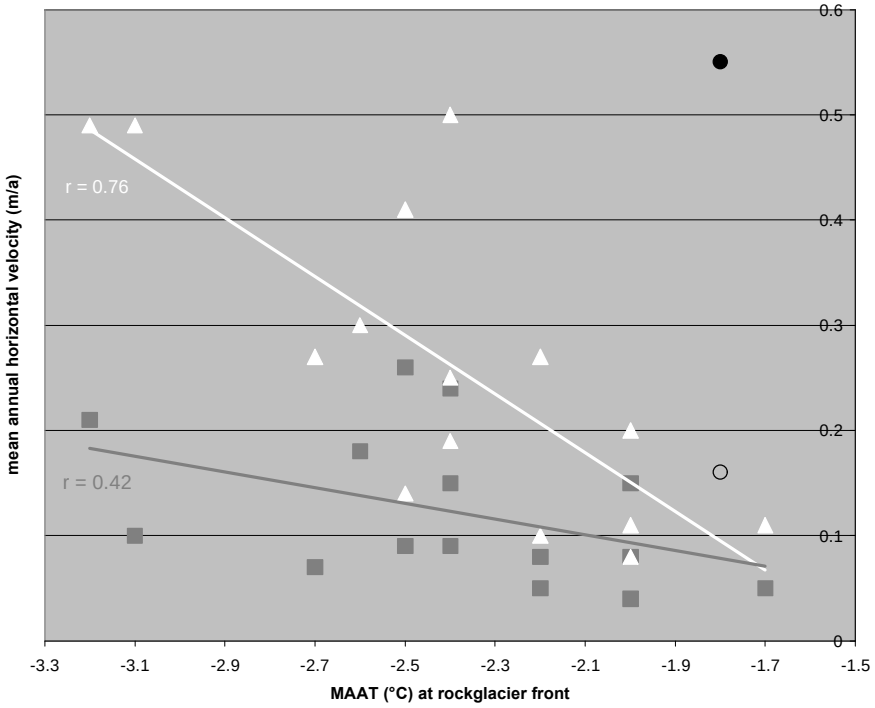

Figure 6.4: Relation between MAAT (°C) at rockglacier front and mean annual horizontal velocity (m/a) of all active rockglaciers (apart from Grueo1) for both investigated periods. □ = mean velocity 1975 – 1993; Ä = mean velocity 1993 – 2001; □ = Huhh3 mean velocity 1975 – 1993 (not included in the trendline – analysis); □ = Huhh3 mean velocity 1993 – 2001 (not included in the trendline-analysis).

In order to correlate surface velocities with temperature data and due to the lack of meteorological data for the study site, the mean annual air temperatures (MAAT) at the rockglacier fronts were calculated by the application of a regional temperature gradient (cf., chapter 4). Since the estimated temperature data are conditional upon altitude, great similarities are depicted in the figures 6.3 and 6.4. The correlation of velocity and MAAT shows that – again by exclusion of the outlier Huhh3 (marked by □ and □) - especially the velocities between 1993 and 2001 are clearly correlated to the MAAT with an r-value of 0.76 (r*99.9 = 0.76). The velocities of the first period (1975-1993) reveal only a weak correlation with the MAAT (r = 0.42; r*95 = 0.514), which is statistically not significant.
Interesting is the depicted trend, which indicates an increasing horizontal velocity with decreasing temperatures. This finding is contrary to the observation made by Frauenfelder et al. (2003), who described a decrease in mean surface velocity with decreasing temperatures (r = 56) for rockglaciers all over Europe and from the Rocky Mountains. In this context it has to be considered, that the mentioned study included also rockglaciers from high latitudes and thus from cold environments. Regarding the great number of features with a MAAT between 0 and -2°C, great differences in mean velocities are also revealed (Frauenfelder et al. 2003: 256). On the other hand it has to be considered, that in the here presented study one rockglacier (Huhh3), which is situated in a low altitude and depicts high velocities, was excluded in the analysis.

Increasing horizontal velocities were not only ascertained for all investigated active rockglaciers in the Turtmann valley, but were currently also observed on other rockglaciers in the Alps (e.g., Schneider & Schneider 2001; Ikeda et al. 2003; Lambiel & Delaloye 2004). Due to the dimension of this signal, it is suspected to be caused by changes on a corresponding scale (e.g., climatic changes such as a rise in air temperature). Therefore, the regional (meso-scale) signal of rockglacier acceleration is compared to the general temperature development in the Alps (meso- to macro-scale), which is detailed by Böhm et al. (2001) and Böhm (2003). In homogenised data from around 100 climatic stations in the Alps he observed a distinct warming trend, starting in 1890 (with two peaks in the 1950s and in the 1990s). This alpine warming since the middle of the 19th century is twice as high as the global value. Reactions of the high mountain system are described by Böhm (2003) for example in the rise of the 0°C isotherm of about 250m since 1890 in the western Alps (Monte-Rosa/Mont-Blanc area); 150m of the total 250m occurred in the last 20 years!
For the study area, temperature data from the nearby 'Sion' station (distance to the Turtmann valley is about 26 km) is given in figure 6.5. Beside the mean annual temperatures, summer (June-August) and winter (December-February) temperatures are displayed separately. The series indicates a general warming trend since the end of the 19th century. Especially the strong increase in winter temperatures, from -1.2° C to 0.9° C over the investigated period, is depicted in the trendline. Similar trends are also revealed in data from high altitude stations such as Jungfraujoch (3576 m a.s.l., ~ 40 km distance to the Turtmann valley) and Grosser St. Bernhard (2472 m a.s.l., ~ 65 km distance to the Turtmann valley). The rockglacier speed-up fits well with the general rise

in temperature (long time scale) and also with the warming starting in the early 1990s (short time scale). Since rockglacier sensitivity is not known in detail and depends on several parameters, both scales need to be considered.

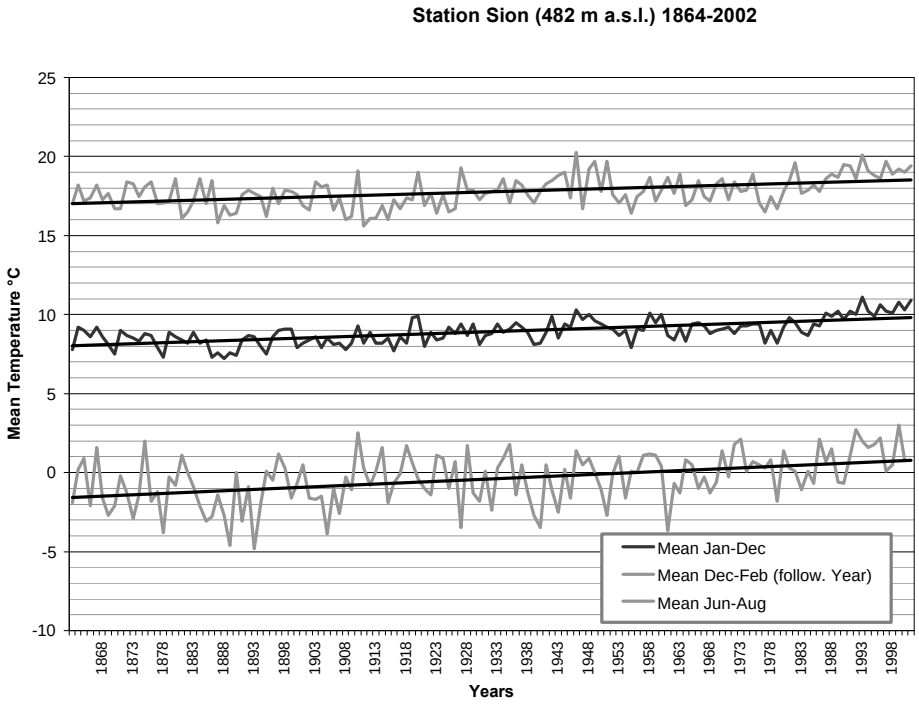

Figure 6.5: Mean annual air temperatures (black line), mean summer air temperatures (upper grey line) and mean winter air temperatures (lower grey line) at the Sion station (482 m a.s.l.) between 1864 and 2002 (according to Böhm et al. 2001). The distance to the Turtmann valley is about 26 km. The depicted trendline demonstrates the positive trend of the temperature.

Since the MAAT values represent only estimated values and since the alpine data set gives only regional information, a validation on the local scale is required. Thus, in order to link rockglacier movement to ground thermal conditions on the micro-scale, a comparison of horizontal velocities and BTS-values is given in the figures 6.6 and 6.7. The velocity pattern depicted in figure 6.6 A (1993-2001) displays lowest rates at the margins and at the front. Especially in the lower orographic right side of the rockglacier the velocities are close to the measurement error and thus may indicate inactivity. High velocities between 0.5 and more than 2.0 m/a represent the upper lobe which is overriding the lower one. Comparing the distribution of BTS-values (figure 6.6 B) to the horizontal velocities, the described pattern is well reflected. Low BTS values strongly suggesting the presence of permafrost are measured at the lowermost front of the rockglacier and on the upper lobe. The inactive area in the lower right part of the rockglacier yields BTS temperatures > -2°C. The front of the upper lobe is of interest, since permafrost was present in the first winter (2001/2002) and was only 'possible' in the following winters.

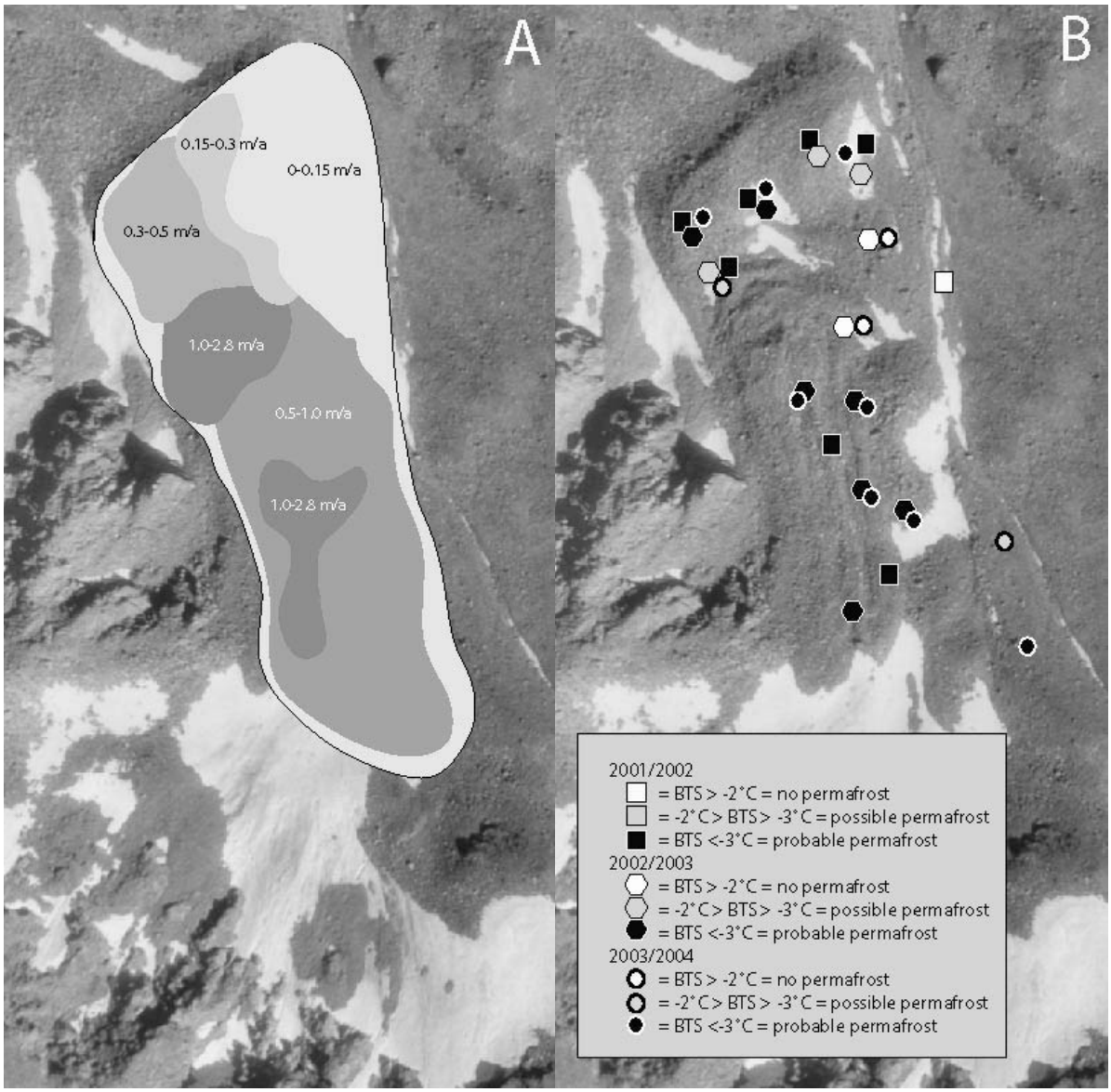

Figure 6.6: Comparison of flow fields (A) and BTS-temperatures (B) on rockglacier Huhh1 (front orientation to the north). A: Mean annual horizontal velocity (m/a) of the period 1993-2001 measured by digital photogrammetry, summarised in several flow fields. B: BTS-values of the winters 2001/2002, 2002/2003 and 2003/2004 on rockglacier Huhh1 (from: Roer et al. in press).

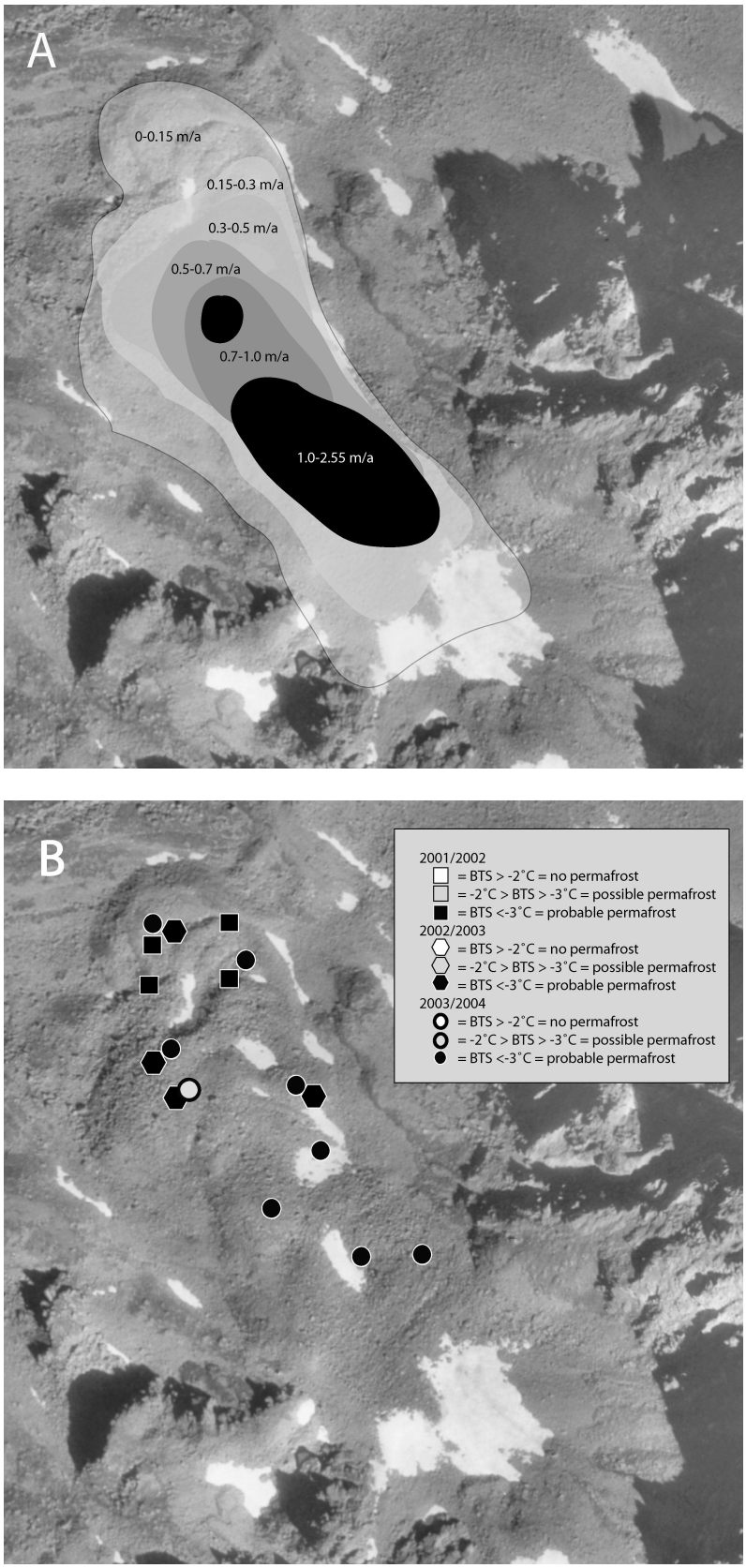

Figure 6.7: Comparison of flow fields (A) and BTS-temperatures (B) on rockglacier Huhh3 (front orientation to the northwest). A: Mean annual horizontal velocity (m/a) of the period 1993 – 2001 measured by digital photogrammetry, summarised in several flow fields. B: BTS-values of the winters 2001/2002, 2002/2003 and 2003/2004 on rockglacier Huhh3.

On rockglacier Huhh3, the differences in horizontal velocities (1993 – 2001) are not reflected in the BTS-temperatures, since low BTS values indicating the presence of permafrost are measured by all thermistors (figure 6.7). Only at one site on the active front, possible permafrost is suggested during the winter 2003/2004. In contrast to rockglacier Huhh1, low BTS values are even revealed on the lowermost lobe which depicts very small displacements. Also in the centre of the rockglacier, where velocities up to 2.55 m/a and a distinct thinning indicate possible 'warm' permafrost, low BTS –temperatures were determined.

Summary

The increase in horizontal velocities is difficult to explain as a large number of parameters influence rockglacier rheology and corresponding data are limited. Since the increase was ascertained on all investigated active rockglaciers in diverse positions, parameters operating on the micro-scale (e.g., change in slope, debris supply) are probably not decisive for the general speed-up. In order to get a better idea of major controls, some parameters are correlated with annual horizontal velocities. Obviously, it has to be considered that different scales are regarded in the interpretation and therefore, conclusions are probably limited.

Concerning geomorphic controls, both surface slope and length of the rockglaciers showed no significant correlations, while the altitude (of the front) revealed a clear correlation with the mean annual horizontal velocity (1993-2001). The latter parameter indicated the influence of air temperature, since it is a function of altitude.

The comparison of calculated MAAT and surface velocities showed a distinct trend of increasing velocities with an increase in altitude. But, it has to be considered that the rockglaciers Grueo1 and Huhh3, which are situated in the lowermost positions of the active rockglaciers and depict the highest velocities, were not included in the correlation. Therefore, greatest changes seem to occur on the lowermost as well as on the uppermost rockglaciers. Thus, a complex set of forcing factors which is not reflected in simple correlations is indicated.

The link between the meso-scale signal of rockglacier speed-up and the increase in alpine temperatures is general in nature, but at least it suggests one probable explanation for the velocity increase in the 1990s and supports the hypothesis by Schneider & Schneider (2001), who observed rockglaciers reacting directly to temperature changes. Another possibility is a delayed reaction to long-term climatic trends. But in this context, the sudden increase in surface movement within a few years (beginning of the 1990s), which was ascertained on all investigated active rockglaciers, is not explicable.

The comparison of horizontal velocities and BTS-values on the micro-scale reveals a different result than the study by Ikeda et al. (2003). In the here presented study, areas with high velocities show clear permafrost-temperatures over a period of 3 winters, while Ikeda et al. (2003) described BTS-values of > -3°C indicating a marginal condition of permafrost presence. Thus, the results do not fit with the observation that rockglaciers with high surface velocities show ground surface temperatures close to the thawing point (e.g., Arenson et al. 2002; Ikeda et al.

2003; Kääb et al. 2003). Since the finding was confirmed for two rockglaciers in the Turtmann valley, probably the interpretation needs to be reconsidered.

In addition, the atypical flow behaviour of rockglacier Grueo1 raises other aspects. This permafrost body indicates the lowermost position of an active rockglacier in the Turtmann valley (2420 m a.s.l.) and revealed already in the first investigated period (1975-1981) mean velocities of 1.34 m/a. The apportioned flowfield of the rockglacier depicts uniform deformation rates in the upper part and chaotic deformation in the lower part, which becomes clearly visible in the surface topography (especially from 1987). It is assumed that in the root zone permafrost creep is still the decisive process, while the occurrence of sliding cause the movements at the lower part of the rockglacier and thus indicate a shift in process regime. A similar surface topography as well as deformation behaviour was only described for the rockglacier Hinteres Langtalkar, Austrian Alps (Kaufmann & Ladstädter 2003). In this case, an abrupt change in base topography, e.g. a bedrock dam, was determined as reason for the cracks as well as the acceleration. Such conditions do not apply for rockglacier Grueo1. From the position of the permafrost body it is assumed that it is actually situated at or below the lower limit of the discontinuous permafrost, which is also confirmed by the permafrost distribution modelling from Nyenhuis et al. (in press). Therefore, marginal or degrading permafrost conditions are indicated and stress the hypothesis of Kääb et al. (2002) that 'warm' rockglaciers (i.e. permafrost temperatures close to 0° C) creep, in general, faster than 'cold' rockglaciers. Thus, the described flow behaviour probably reflects the final stage of an active rockglacier. Similar conditions can also be assumed for rockglacier Huhh3, which is situated in a comparable position (altitude of front at 2515 m a.s.l.) and also reveals high horizontal velocities. But, as mentioned before, measured BTS values do not indicate marginal permafrost conditions. Thus, it has to be questioned to what extend the BTS values are indicators for permafrost occurrence at every scale.

Due to a lack of observations on internal structures, temperatures and velocities, further suggestions on the observed rockglacier acceleration can only be evaluated at a qualitative level.

Since borehole measurements show most of the deformation to be concentrated within narrow shear horizons at several meters depth (e.g., Arenson et al. 2002), it is possible that dynamic changes are concentrated to such horizons and result in increased surface velocities. Generally it is assumed that rockglaciers react gradually to changes in the system, mainly affected by long-term climatic trends (e.g., Barsch 1996; Kääb et al. 1997). Thus, it is supposed that it takes a long time (decades or centuries) till a change in temperature reaches the base of the rockglacier body and leads to an adjustment of the movement (rheological response). Although it is not clear how the temperature penetrates into the ground, such effects would indicate a gradual adaptation to changes in air temperature. Hence, the here observed speed-up possibly reflects the temperature increase after the little ice age. But nevertheless it seems surprising, that the acceleration occurs within a very short period and parallel on all active rockglaciers, independent of their thickness. Another aspect would be the occurrence of different processes in various depths of the rockglacier body. For instance, this was also described by Arenson et al. (2002), who measured seasonal changes in shallow shear zones, while greater depths are more affected by longterm

variations (cf., Kääb et al. 2002, 2003). Perhaps, a large part of the movement is limited to the upper layer or even the active layer. Another explanation would be the crossing of a certain internal threshold due to some changes, which leads to a uniform reaction in all rockglaciers.
The 'kinematic boundary condition on the surface' enables the distinction of internal mass balance effects and external influences, by the combined analysis of horizontal and vertical changes in rockglacier geometry (chapter 2.3.5.4). The observed thickening of some permafrost bodies may reflect an increased material supply (ice or debris) which can be a local driving force for the horizontal acceleration. Other rockglaciers in the Turtmann valley show a distinct thinning in the root zone and thickening in the lower part, indicating that the sediment supply can not compensate the high velocities (cf., Lambiel & Delaloye 2004). Thus, the significance of material supply – which is also climatically driven – seems to play an important role and needs to be monitored in detail.
In addition, also short-term climatic variations in the snow cover (thickness, duration, etc.), the summer temperatures controlling the thickness of the active layer or the amount of melt water may play an important role. Since all these types of information are not available for the study area, further research is required to clarify this.

Although the acceleration took place at rockglaciers in diverse altitudes and different topographic situations, it is assumed that the increase in air temperature and the corresponding changes in ground thermal conditions indicate the prevailing reason for the observed changes. Greatest displacements were revealed on rockglaciers in the lowermost positions and in high elevations. Thus, either the changes in boundary conditions are effective in the entire system, or diverse parameters or combinations thereof are decisive in the different altitudes. Since all of the rockglaciers showed a distinct increase in horizontal velocity, local parameters are probably not decisive. It is assumed that all features seem to indicate 'warm' permafrost conditions and are therefore very sensitive.

As it becomes apparent in the discussion, conflicting interpretations and conclusions arise from the given findings. Probably, this results from the high complexity of the considered system as well as the limited data and knowledge on the prevailing processes. The latter are conditional upon diverse parameters acting on different spatial and temporal scales. Therefore, the individual scale dependency makes the correlation of single parameters more difficult.

7 CONCLUSIONS

In view of the research questions for the here presented study (chapter 1) and from the given findings (chapter 5) and discussions (chapter 6), the following conclusions are compiled:

- The applied methods enabled the thorough investigation of kinematics on 45 rockglaciers in the Turtmann valley. Especially the use of small-scale aerial photography and the first-time combination with digital airborne pushbroom imagery (HRSC-A), appeared to be highly useful for the area-wide measurement of changes in rockglacier geometry. Thus, horizontal velocities and vertical changes were determined over a period of 26 years. The application of terrestrial geodetic survey, allowed the evaluation of the findings on the micro-scale, due to the higher accuracy of the technique and the measurement at annual intervals. The first-time application of dendrogeomorphology regarding rockglacier kinematics gave preliminary results but appeared to be feasible.
- The applied techniques and especially the combination of geomorphic mapping and digital photogrammetry allowed the reliable assessment of the rockglacier activity.
- Some rockglaciers revealed exceptionally high horizontal velocities (up to several meters per year) and also distinct vertical changes, compared to other rockglaciers in the Alps.
- One rockglacier (Grueo1) showed a conspicuous flow behaviour, which is probably not related to permafrost creep alone. Very high surface velocities (2-5 m/a) extend from the front upwards to the root zone and cause deep crevasses at the surface. The front revealed an advance of about 60 m in 26 years.
- Clear spatio-temporal variations in horizontal velocities and vertical changes were observed on most rockglaciers. On the micro-scale the spatial variations indicated to be mostly influenced by the surface slope, while on the meso-scale no clear signal was revealed. Regarding the temporal variations, a distinct increase in horizontal velocities – probably from the beginning of the 1990s - was ascertained on all active rockglaciers.
- The correlations of increased horizontal velocities with terrain parameters as well as with general temperature data and ground surface temperatures showed different signals, partially contradicting each other. High movement rates occur in low as well as in high altitudes. On rockglaciers close to the lower limit of the discontinuous permafrost distribution, where marginal or degrading permafrost conditions are assumed, low BTS values strongly suggesting the presence of permafrost were measured. Due to the limited knowledge on rockglacier dynamics it is far from known, how a change in forcing factors is translated into a

rheological response and therefore the drawing of conclusions is limited. But, since the speed-up was ascertained on all investigated active rockglaciers in the Turtmann valley and was also observed on other rockglaciers in the Alps, it is assumed that it is linked to climatic changes and an increase in ground temperatures, respectively. But, the relation between temperature and rockglacier dynamics seems to be much more complex and is not easily described by simple correlations.

- Considering geomorphodynamics, the described findings emphasise the significance of rockglaciers in the geomorphology of the Turtmann valley.
- In addition, even if the probable controls and corresponding reaction times are not known in detail, the sudden increase in permafrost creep within a few years supports the role of rockglaciers as sensitive indicators for changes of boundary conditions in the high mountain geosystem.

8 PERSPECTIVES

Spatio-temporal variations in rockglacier kinematics were described elaborately for the Turtmann valley by means of different methods. Beside the methodological novelties, the area-wide determination of rockglacier speed-up reveals the most interesting finding of the presented study. Thus, the perspectives target on the better understanding of rockglacier dynamics.

Although more data on rockglacier kinematics will not automatically improve the knowledge on rockglacier dynamics, statements on rheological driving forces may be derived from observed spatio-temporal variations, since changes are related either by changes in input of ice or debris or by warming/cooling effects. Parallel to this, suspected influencing parameters need to be quantified on their relevant scale and need to be included in the analysis of rockglacier kinematics, in order to understand the mechanism by which a change in forcing factors is translated into a rheological response. Therefore, an intensified monitoring including data on internal structures, temperatures and velocities as well as climatic changes is demanded to get a profound knowledge on the underlying processes. In this context a combination of different methods (field investigations, laboratory tests as well as modelling) is required. In addition, the investigation of system immanent or self-organised developments as possible reasons for rheological changes is suggested.

Since most investigations are concentrated on single rockglaciers, meso-scale information on rockglacier and permafrost development is limited. As a consequence, selected and representative rockglaciers from all over the Alps are to be investigated by a uniform monitoring program in future. Additionally, long-term observations are necessary to distinguish inter-annual variations from long-term trends.

Concerning the investigations in the Turtmann valley, the measurement of rockglacier movement should definitely be continued. Additional investigations on rockglaciers close to the lower limit of the discontinuous permafrost, e.g., by using drillings or geophysical soundings, would be appreciated to analyse in detail the debris-ice mixture at boundary conditions. In particular, rockglacier Grueo1 should be monitored carefully in order to prevent the nearby constructions from slope failure.

Regarding the distinct changes in permafrost creep within the last decade and considering the suspected changes in thermo-dynamics, one has to be aware of related hazards in regions with mountain permafrost. This became apparent in the large number of rockfalls during the hot summer of 2003. Depending on their position in the terrain, also rockglaciers may be a source area or initiation zone for rockfall – or debris flow events (Kääb 2004). Therefore, rockglaciers in certain positions as well as those with indications for instabilities (e.g., Grueo1) should be monitored in at least annual intervals.

From the given observations, a high sensitivity of rockglaciers was concluded. In this context, it should be investigated in future, to what extent the depicted changes are also visible in other processes (e.g., gelifluction), in order to evaluate the sensitivity of the high mountain geosystem in terms of environmental changes.

9 ACKNOWLEDGEMENTS

First of all I thank Richard Dikau for initiating this project as well as for his interest and support in the ongoing research. Further, I am particularly grateful to Andreas Kääb for the possibility to conduct the photogrammetric investigations at the Department of Geography in Zürich and for several helpful discussions.

The study was funded by the Deutsche Forschungsgemeinschaft (DFG) as a PhD-project within the Research Training Group 'Landform – a structured and variable boundary layer' (Graduiertenkolleg 437). The availability of aerial photographs by the Swiss Federal Office of Topography (Swisstopo) is acknowledged. Additionally, I want to thank Walter Werlen for providing reference points for the Turtmann valley. Thanks are also dedicated to Reinhard Böhm for the homogenised temperature data of the Alps.

I gratefully acknowledge the support of Christoph Kany (surveying technician) for his assistance in setting up the geodetic network and the check of the measurements. In this context I want to thank all the helping hands in various field campaigns (Susanne Wolfart, Ingo Wolff, Jan Busch, Raphael Holland, Susanne Lenz, and Mamke Oehmisch) and the logistic support from Wilhelm Berckum, Marcel Bregy, Rosmarie & Volkher Teuffel as well as from the municipality of Oberems.

Thanks are due to Kirsten von Elverfeldt, who provided first data on rockglacier kinematics in the Turtmann valley from small-scale aerial photography. Further thanks are given to Philippe Meuret, Bruno Weber and Stephan Imfeld for their valuable support in smoothly running the digital photogrammtric workstation at the Department of Geography, University of Zurich.

Holger Gärtner enabled the use of the Dendrolab at the WSL to prepare and analyse the microsections. I thank him and Ingo Heinrich for valuable discussions on the findings.

Several intense and constructive discussions with colleagues of the working group and of the Research Training Group (in particular with Michael Nyenhuis, Jan-Christoph Otto, Thomas Hoffmann, Susanne Schmidt, Lothar Schrott, and Thomas Glade) are gratefully acknowledged. Additionally I thank Andreas Kääb, Reynald Delaloye, Christophe Lambiel and Michael Avian for the cooperation in analysing the facts about rockglacier speed-up in the Alps.

Thanks are dedicated to Susan Busse for thoroughly editing and improving the language.

In particular, I thank my family for their understanding, love and care as well as financial contributions.

And finally: a big hug to my friends (above all to Holger, Tina, Jean-Claude, Marion, Vera, Michael, Jana, Axel, Vanessa, Inge, Philipp, Robby, Felix, Lilly & others) for a lot of motivational and relaxing moments.

10 BIBLIOGRAPHY

Alestalo, J. (1971): Dendrochronological interpretation of geomorphic processes. Fennia 105: 140.

Anderson, M. G. & T. P. Burt (1981): Methods of geomorphological investigation. In: Goudie, A. (ed.): Geomorphological Techniques. George Allen and Unwin, London: 3-11.

Anisimov, O. A. & F. E. Nelson (1996): Permafrost distribution in the northern hemisphere under scenarios of climate change. Global and Planetary Change, 14: 59-72.

Arenson, L. U., Hoelzle, M. & S. Springman (2002): Borehole deformation measurements and internal structure of some rock glaciers in Switzerland. Permafrost and Periglacial Processes 13: 117-135.

Arenson, L. U., Springman, S. M. & P. G. Hawkins (2003a): Pressuremeter tests within an active rock glacier in the Swiss Alps. In: Proceedings of the 8th International Conference on Permafrost, Zürich, Balkema, 1: 33-38.

Arenson, L. U., Almasi, N. & S. M. Springman (2003b): Shearing response of ice-rich rock glacier material. In: Proceedings of the 8th International Conference on Permafrost, Zürich, Balkema, 1: 39-44.

Bachrach, T., Jakobsen, K., Kinney, J., Nishimura, P., Reyes, A., Laroque, C. P. & D. J. Smith (2004): Dendrogeomorphological assessment of movement at Hilda rock glacier, Banff National Park, Canadian Rocky Mountains. Geografiska Annaler 86A, 1: 1-9.

Baltsavias, E. P. (1996): Digital ortho-images – a powerful tool for the extraction of spatial- and geo-information. ISPRS Journal of Photogrammetry and Remote Sensing 51, 2: 63-77.

Baltsavias, E. P., Favey, E., Bauder, A., Bösch, H. & M. Pateraki (2001): Digital surface modelling by airborne laser scanning and digital photogrammetry for glacier monitoring. Photogramm. Rec. 17, 98: 243-273.

Barsch, D. (1969): Studien und Messungen an Blockgletschern in Macun, Unterengadin. Zeitschrift für Geomorphologie, Suppl. 8: 11-30.

Barsch, D. (1977): Nature and importance of mass-wasting by rock glaciers in alpine permafrost environments. Earth Surface Processes 2: 231-245.

Barsch, D. (1987a): Rock glaciers: an approach to their systematics. In: Giardino, J. R., Shroder, J. F. Jr. & J. D. Vitek (eds.) Rock glaciers. Allen and Unwin, Boston: 41-44.

Barsch, D. (1987b): The problem of the ice-cored rock glacier. In: Giardino, J. R., Shroder, J. F. Jr. & J. D. Vitek (eds.) Rock glaciers. Allen and Unwin, Boston: 45-53.

Barsch, D. (1988): Rock glaciers. In: Clark, M.J. (ed.) Advances in periglacial geomorphology. Wiley, Chichester: 69-90.

Barsch, D. (1992): Permafrost Creep and Rockglaciers. Permafrost and Periglacial Processes 3: 175-188.

Barsch, D. (1996): Rockglaciers: Indicators for the present and former geoecology in high mountain environments. Springer, Berlin: 331.

Barsch, D. & N. Caine (1984): The nature of mountain geomorphology. Mountain research and development, 4, 4: 287-298.

Barsch, D. & G. Hell (1975): Photogrammetrische Bewegungsmessungen am Blockgletscher Murtèl I, Oberengadin, Schweizer Alpen. Zeitschrift für Gletscherkunde und Glazialgeologie 11, 2: 111-142.

Barsch, D. & M. Jakob (1998): Mass transport by active rockglaciers in the Khumbu Himalaya. Geomorphology 26: 215 – 222.

Barsch, D. & L. King (1975): An attempt to date fossil rock glaciers in Grison, Swiss Alps (a preliminary note). Quaestiones Geographicae 2: 5-14.

Barsch, D. & L. King (1989): Origin and geoelectrical resistivity of rockglaciers in semi-arid subtropical mountains (Andes of Mendoza, Argentinia). Zeitschrift für Geomorphologie N. F. 33, 2: 151-163.

Barsch, D. & W. Zick (1991): Die Bewegungen des Blockgletschers Macun I von 1965-1988 (Unterengadin, Graubünden, Schweiz). Zeitschrift für Geomorphologie, N. F. 35, 1: 1-14.

Bearth, P. (1980): Erläuterungen zu Atlasblatt 71 (1308 St. Niklaus) des „Geologischen Atlas der Schweiz 1:25.000". Schweizerische Geologische Kommission. Zürich.

Berthling, I., Eiken, T., Madsen, H. & J. L. Sollid (2001): Downslope displacement rates of ploughing boulders in a mid-alpine environment: Finse, Southern Norway. Geografiska Annaler 83 A, 3: 103-116.

Berthling, I., Etzelmüller, B., Eiken, T. & J. L. Sollid (1998): Rock glaciers on Prins Karls Forland, Svalbard. I: Internal structure, flow velocity and morphology. Permafrost and Periglacial Processes 9: 135-145.

Berthling, I., Etzelmüller, B., Eiken, T. & J. L. Sollid (2003): Short communication - the rock glaciers on Prins Karls Forland: corrections of surface displacement rates. Permafrost and Periglacial Processes 14: 291-293.

Bishop, M. P. & J. F. Shroder, Jr. (2004): Geographic Information Science and Mountain Geomorphology. Springer, Berlin: 486.

Böhm, R. (2003): Systematische Rekonstruktion von zweieinhalb Jahrhunderten instrumentellem Klima in der groesseren Alpenregion – ein Statusbericht. In: Gamerith, W., Messerli, P., Meusburger, P. & H. Wanner (eds.): Alpenwelt – Gebirgswelten, Inseln, Bruecken, Grenzen. Tagungsbericht und wissenschaftliche Abhandlungen. 54. Deutscher Geographentag, Bern: 123-131.

Böhm, R., Auer, I., Brunetti, M., Maugeri, M., Nanni, T. & W. Schöner (2001): Regional temperature variability in the European Alps: 1760-1998 from homogenized instrumental time series. International Journal of Climatology 21: 1779-1801.

Bräuning, A. (1995): Zur Anwendung der Dendrochronologie in den Geowissenschaften. Die Erde 126: 189-204.

Brazier, V., Kirkbride, M. P. & I. F. Owens (1998): The relationship between climate and rock glacier distribution in the Ben Ohau Range, New Zealand. Geografiska Annaler 80A, 3-4: 193 – 207.

Broccard, A. (1998): Géomorphologie du Turtmanntal (Valais). Diploma thesis, Department of Geography, University of Lausanne.

Büdel, J. (1948): Die klimamorphologischen Zonen der Polarländer. Erdkunde 2: 22-53.

Büdel, J. (1977): Klima-Geomorphologie. Borntraeger, Berlin.

Bundesamt für Landestopographie (2001): Hydrologischer Atlas der Schweiz. Wabern, Bern.

Burger, K. C., Degenhardt Jr., J. J. & J. R. Giardino (1999): Engineering geomorphology of rock glaciers. Geomorphology 31: 93-132.

Chaix, A. (1923): Les coulées de blocs du Parc National Suisse d´Engadine (Note préliminaire). Le Globe 62: 1-35.

Chaix, A. (1943): Les coulées de blocs du Parc National Suisse: Nouvelles measures et comparaison avec les "rock stream" de la Sierra Nevada de Californie. Le Globe 82: 121-128.

Chandler, J. (1999): Effective application of automated digital photogrammetry for geomorphological research. Earth Surface Processes and Landforms 24, 1: 51-63.

Chesi, G., Krainer, K. & W. Mostler (1999): Bewegungsmessungen am aktiven Blockgletscher Inneres Reichenkar mit der GPS-Methode. X. Int. Geodätische Woche, Obergurgl: 223-227.

Chorley, R. J. (1962): Geomorphology and general systems theory. US Geological Survey Professional Paper 500-B: 1-10.

Chorley, R. J. & B. A. Kennedy (1971): Physical geography: a systems approach. Prentice Hall, London.

Clark, D. G., Steig, E. J., Potter, N. & A. R. Gillespie (1998): Genetic variability of rock glaciers. Geografiska Annaler 80A: 175-182.

Corte, A. E. (1987): Rock glacier taxonomy. In: Giardino, J. R., Shroder, J. F. & J. D. Vitek (eds.): Rock glaciers. Allen & Unwin, London: 27-39.

Davies, M. C. R., Hamza, O. & C. Harris (2001): The effect of rise in mean annual temperature on the stability of rock slopes containing ice-filled discontinuities. Permafrost and Periglacial Processes 12: 137-144.

De Boer, D. H. (1992): Hierarchies and spatial scale in process geomorphology: a review. Geomorphology 4: 303-318.

Dikau, R. (1978): Refraktionsseismische Untersuchungen an Blockgletschern im Turtmanntal (Wallis, Schweiz). Master thesis (unpublished). Department of Geography, University of Heidelberg.

Dikau, R. (1989): The application of a digital relief model to landform analysis in geomorphology. In: Raper, J. (ed.): Three dimensional applications in Geographical Information Systems, London, Taylor & Francis: 51-77.

Dikau, R. & J. Schmidt (1999): Georeliefklassifikation. In: Schneider-Sliwa, R., Schaub, D. & G. Gerold (eds.): Angewandte Landschaftsökologie. Springer: 217-244.

Douglass, A. E. (1941): Crossdating in Dendrochronology. Journal of Forestry 39: 825 - 831.

Elconin, R. F. & E. R. LaChapelle (1997): Flow and internal structure of a rock glacier. Journal of Glaciology 43, 144: 238-244.

Elverfeldt, K. von (2002): Analyse der Blockgletscherkinematik im Turtmanntal, Wallis, mittels digitaler Photogrammetrie. Diploma thesis (unpublished), Department of Geography, University of Bonn.

Etzelmüller, B. & M. Hoelzle (2001): IPA-Taskforce for mapping and modelling the occurrence and distribution of mountain permafrost, status report (draft). http://www.geo.uio.no/taskforcedraft.

Eugster, H. (1973): Bericht über die Untersuchungen des Blockstroms in der Val Sassa im Schweiz. Nationalpark (GR) von 1917-1971. Ergebnisse der wissenschaftlichen Untersuchungen im Schweizerischen Nationalpark 11: 368-384.

Evans, D. J. A. (1993): High-latitude rock glaciers: a case study of form and processes in the Canadian Arctic. Permafrost and Periglacial Processes 4: 17-35.

Evin, M. & A. Assier (1983): Glacier et glaciers rocheux dans le Haut-Vallon du Loup, (Haute-Ubaye, Alpes du sud, France). Zeitschrift für Gletscherkunde und Glazialgeologie. 19, 1: 27 – 41.

Evin, M., Assier, A. & D. Fabre (1990): Les glaciers rocheux du Marinet (Haut-Ubaye, France). Rev Géomorphol Dyn. 39: 139 – 155.

Fantucci, R. & A. McCord (1995): Reconstruction of landslide dynamic with dendrochronological methods. Dendrochronologia 13: 1-22.

Francou, B. & L. Reynaud (1992): 10 year surficial velocities on a rock glacier (Laurichard, French Alps). Short communication. Permafrost and Periglacial Processes 3: 209-213.

Frauenfelder, R. (1998): Permafrostuntersuchungen mit GIS. Eine Studie im Fletschhorngebiet. In: Beiträge aus der Gebirgsgeomorphologie. Jahresversammlung 1997 der Schweizerischen Geomorphologischen Gesellschaft der SANW. Mitteilungen der VAW/ETH Zürich 158: 55-68.

Frauenfelder, R. & A. Kääb (2000): Towards a palaeoclimatic model of rock-glacier formation in the Swiss Alps. Annals of Glaciology 31: 281-286.

Frauenfelder, R., Haeberli, W. & M. Hoelzle (2003): Rockglacier occurrence and related terrain parameters in a study area of the Eastern Swiss Alps. In: Proceedings of the 8th International Conference on Permafrost, Zürich, Balkema, 1: 253-258.

Frauenfelder, R., Haeberli, W., Hoelzle, M. & M. Maisch (2001): Using relict rockglaciers in GIS-based modelling to reconstruct Younger Dryas permafrost distribution patterns in the Err-Julier area, Swiss Alps. Norwegian Journal of Geography 55: 195-202.

Frauenfelder, R., Laustela, M. & A. Kääb (2004): Velocities and relative surface ages of selected Alpine rockglaciers. Turbulenzen in der Geomorphologie. Jahrestagung der SGMG 2003, Erstfeld. VAW 184: 103-118.

French, H. M. (1996): The periglacial environment. Longman, Essex: 341.

Funk, M. & M. Hoelzle (1992): Application of a potential direct solar radiation model for investigating occurrences of mountain permafrost. Permafrost and Periglacial Processes 3, 2: 139-142.

Gärtner, H. (2003a): The applicability of roots in dendrogeomorphology. In: Schleser, G., Winiger, M., Bräuning, A., Gärtner, H., Helle, G., Jansma, E., Neuwirth, B. & K. Treydte (eds.) (2003): TRACE – Tree Rings in Archaeology, Climatology and Ecology 1: 120-124.

Gärtner, H. (2003b): Holzanatomische Analyse diagnostischer Merkmale einer Freilegungsreaktion in Jahrringen von Koniferenwurzeln zur Rekonstruktion geomorphologischer Prozesse. Dissertationes Botanicae 378: 118.

Gärtner, H., Schweingruber, F. H. & R. Dikau (2001): Determination of erosion rates by analyzing structural changes in the growth pattern of exposed roots. Dendrochronologia 19: 1-11.

Gärtner, H., Esper, J. & K. Treydte (2004): Geomorphologie und Jahrringe – Feldmethoden in der Dendrogeomorphologie. Schweizerische Zeitschrift für Forstwesen 155, 6: 198-207.

Garcia Gonzales, I. & D. Eckstein (2003): Climatic signal of earlywood vessels of oak on a maritime site. Tree Physiology 23: 497–504.

Gerrard, A. J. (1990): Mountain environments: an examination of the physical geography of mountains. Belhaven Press, London: 317.

Gers, E., Florin, N., Gärtner, H., Glade, T., Dikau, R. & F. H. Schweingruber (2001): Application of shrubs for dendrogeomorphological analysis to reconstruct spatial and temporal landslide movement patterns. -A preliminary study- In: Dikau, R. & K.-H. Schmidt (eds.): Mass Movements in South, West and Central Germany. Zeitschrift für Geomorphologie, Suppl. 125: 163-175.

Giardino, J. R., Shroder, J. F. & M. P. Lawson (1984): Tree-ring analysis of movement of a rock-glacier complex on Mount Mestas, Colorado, U.S.A. Arctic and Alpine Research 16, 3: 299-309.

Gilliéron, F. (1946): Geologische-petrographische Untersuchungen an den Ni-Co-Lagerstätten Kaltenberg (Turtmanntal, Wallis). Beiträge zur Geologie der Schweiz - Geotechnische Serie, 25: 19-34.

Gorbunov, A. P. (1983): Rock glaciers of the mountains of middle Asia. 4th International Conference on Permafrost. Fairbanks, Alaska. National Academic Press, Washington: 359-362.

Gorbunov, A. P., Titkov, S. N. & V. G. Polyakov (1992): Dynamics of rock glaciers of the Northern Tien Shan and the Djungar Ala Tau, Kazahkstan. Permafrost and Periglacial Processes 3: 29-39.

Gregory, K. J. (2000): The changing nature of physical geography. Arnold, London: 368.

Gruber, S. & M. Hoelzle (2001): Statistical modelling of mountain permafrost distribution: Local calibration and incorporation of remotely sensed data. Permafrost and Periglacial Processes 12, 1: 69-77.

Gruber, S., Hoelzle, M. & W. Haeberli (2004): Rock-wall temperatures in the Alps: Modelling their topographic distribution and regional differences. Permafrost and Periglacial Processes 15: 299-307.

Gruber, S., Peter, M., Hoelzle, M., Woodhatch, I. & W. Haeberli (2003): Surface temperatures in steep alpine rock faces – A strategy of regional-scale measurement and modelling. In: Proceedings of the 8th International Conference on Permafrost, Zürich, Balkema, 1: 325-330.

Guglielmin, M., Adighieri, B. & B. Testa (2003): PERMACLIM: a model for the distribution of mountain permafrost, based on climatic observations. Geomorphology 51, 4: 245-257.

Gwinner, K., Hauber, E., Hoffmann, H., Scholten, F., Jaumann, R., Neukum, G., Coltelli, M. & G. Puglisi (1999): The HRSC-A experiment on high resolution imaging and DEM generation at the Aeolian Islands. In: Proc. 13th Int. Conf. Appl. Geol. Remote Sens., Proc. 1: 560-569. Vancouver, Canada.

Hack, J. T. (1960): Interpretation of erosional topography in humid temperate regions. American Journal of Science 256: 80 – 97.

Haeberli, W. (1973): Die Basis-Temperatur der winterlichen Schneedecke als möglicher Indikator für die Verbreitung von Permafrost in den Alpen. Zeitschrift für Gletscherkunde und Glazialgeologie 9, 1-2: 221-227.

Haeberli, W. (1975): Untersuchungen zur Verbreitung von Permafrost zwischen Flüelapass und Piz Grialetsch (Graubünden). Mitteilungen der VAW/ETH Zürich 17: 221.

Haeberli, W. (1985): Creep of mountain permafrost: Internal structure and flow of alpine rock glaciers. Mitteilungen der VAW/ETH Zürich 77: 119.

Haeberli, W. (1990): Permafrost. In: Internationale Fachtagung über Schnee, Eis und Wasser in den Alpen in einer wärmeren Atmosphäre. Mitteilungen der VAW/ETH Zürich 108: 71-88.

Haeberli, W. (1992a): Possible effects of climate change on the evolution of alpine permafrost. Catena Supplement 22: 23-35.

Haeberli, W. (1992b): Construction, environmental problems and natural hazards in periglacial mountain belts. Permafrost and Periglacial Processes 3, 2: 111-124.

Haeberli, W. (1995): Permafrost und Blockgletscher in den Alpen. Vierteljahrsschrift der Naturforschenden Gesellschaft in Zürich 140, 3: 113-121.

Haeberli, W. (2000): Modern research perspectives relating to permafrost creep and rock glaciers: a discussion. Permafrost and Periglacial Processes 11: 290-293.

Haeberli, W. & F. Epifani (1986): Mapping the distribution of buried glacier ice – an example from Lago Delle Locce, Monte Rosa, Italian Alps. Annals of Glaciology 8: 78-81.

Haeberli, W. & G. Patzelt (1982): Permafrostkartierung im Gebiet der Hochebenkar-Blockgletscher, Obergurgl, Ötztaler Alpen. Zeitschrift für Gletscherkunde und Glazialgeologie 18: 127-150.

Haeberli, W., Wegmann, M. & D. Vonder Mühll (1997): Slope stability problems related to glacier shrinkage and permafrost degradation in the Alps. Eclogae geol. Helv 90: 407-414.

Haeberli, W., Harris, S. A., Goudong, C. & A. P. Gorbunov (1993): Mountain permafrost and climatic change. Permafrost and Periglacial Processes 4: 165-174.

Haeberli, W., Hoelzle, M., Kääb, A., Keller, F., Vonder Mühll, D. & S. Wagner (1998): Ten years after drilling through the permafrost of the active rock glacier Murtèl, eastern Swiss Alps: Answered questions and new perspectives. Proceedings of the 7th International Conference on Permafrost, Yellowknife. Nordicana 57, Université Laud: 403-410.

Haeberli, W., Brandova, D., Burga, C., Egli, M., Frauenfelder, R., Kääb, A., Maisch, M., Mauz, B., & R. Dikau (2003): Methods of absolute and relative age dating of rock-glacier surfaces in alpine permafrost. In: Proceedings of the 8th International Conference on Permafrost, Zürich, Balkema, 1: 343-348.

Hagedorn, J. (1980): The montane periglacial zone and its morphological lower limit. Zeitschrift für Geomorphologie N.F. Suppl.-Bd. 36: 96-103.

Hamilton, S. J. & W. B. Whalley (1995): Rock glacier nomenclature: A re-assessment. Geomorphology 14: 73-80.

Hanson, S. & M. Hoelzle (2004): The thermal regime of the active layer at the Murtèl rock glacier based on data from 2002. Permafrost and Periglacial Processes 15: 273-282.

Harris, S. A. (2001): Twenty years of data on climate-permafrost-active layer variations at the lower limit of alpine permafrost, Marmot Basin, Jasper National Park, Canada. Geografiska Annaler 83 A, 1-2: 1-14.

Harris, C. & W. Haeberli (2003): Warming permafrost in the mountains of Europe. Bulletin of the World Meteorological Organization 52, 3: 1-6.

Hauber, E., Slupetzky, H., Jaumann, R., Wewel, F., Gwinner, K. & G. Neukum (2000): Digital and automated high resolution stereo mapping of the Sonnblick Glacier (Austria) with HRSC-A. EARSeL eProceedings 1: 246-254.

Hauck, C. (2001): Geophysical methods for detecting permafrost in high mountains. Mitteilungen der VAW/ETH Zürich 171: 204.

Hauck, C., Guglielmin, M., Isaksen, K., & D. Vonder Mühll (2001): Applicability of frequency-domain and time-domain electromagnetic methods for mountain permafrost studies. Permafrost and Periglacial Processes 12: 39-52.

Herz, T., King, L. & H. Gubler (2003): Microclimate within coarse debris of talus slopes in the alpine periglacial belt and its effect on permafrost. In: Proceedings of the 8th International Conference on Permafrost, Zürich, Balkema, 1: 383-387.

Höllermann, P. (1973): Some reflections on the nature of high mountains, with special reference to the western United States. Arctic and Alpine Research, 5, 3: A149-A160.

Höllermann, P. (1983): Blockgletscher als Mesoformen der Periglazialstufe. Studien aus europäischen und nordamerikanischen Hochgebirgen. Bonner Geographische Abhandlungen 67: 73.

Höllermann, P. (1985): The periglacial belt of mid-latitude mountains from a geoecological point of view. Erdkunde 39: 259-270.

Hoelzle, M. (1989): Untersuchungen zur Permafrostverbreitung im Oberengadin. Diploma thesis (unpublished), Department of Geography, ETH Zürich: 79.

Hoelzle, M. (1992): Permafrost occurrence from BTS measurements and climatic parameters in the Eastern Swiss Alps. Permafrost and Periglacial Processes 3, 2: 143-147.

Hoelzle, M. (1994): Permafrost und Gletscher im Oberengadin. Grundlagen und Anwendungsbeispiele für automatisierte Schätzverfahren. Mitteilungen der VAW/ETH Zürich 132: 121.

Hoelzle, M., Haeberli, W. & F. Keller (1993): Applications of BTS-measurements for modelling permafrost distribution in the Swiss Alps. 6th International Conference on Permafrost. Proceedings, Beijing: 272-277.

Hoelzle, M., Wegmann, M. & B. Krummenacher (1999): Miniature temperature dataloggers for mapping and monitoring of permafrost in high mountain areas: First experience from the Swiss Alps. Permafrost and Periglacial Processes 10, 2: 113-124.

Hoelzle, M., Wagner, S., Kääb, A. & D. Vonder Mühll (1998): Surface movement and internal deformation of ice-rock mixtures within rock glaciers at Pontresina-Schafberg, Upper Engadin, Switzerland. In: 7th International Conference on Permafrost, Yellowknife, Canada. Collection Nordicana 57: 465-471.

Hoelzle, M., Mittaz, C., Etzelmüller, B. & W. Haeberli (2001): Surface energy fluxes and distribution models of permafrost in European mountain areas: An overview of current developments. Permafrost and Periglacial Processes 12, 1: 53-68.

Hoffmann, A. (2000): Neue Ansätze zur Auswertung und Klassifikation von sehr hochauflösenden Daten: Methoden der Segmentierung, der hierarchischen Klassifizierung und der per-Pacel-Methode mit Daten der Digitalen Kamera HRSC-A und ihre Anwendbarkeit für die Aktualisierung topographischer Karten. PhD thesis, Humboldt-University Berlin.

Hoffmann, A., Van Der Vegt, J. W. & F. Lehmann (2000): Towards automated map updating: is it feasible with new digital data-acquisition and processing techniques? IAPRS 33: 295-302.

Hsü, K. J. & U. Briegel (1991): Geologie der Schweiz: Ein Lehrbuch für den Einstieg und eine Auseinandersetzung für Experten. Bern.

Humboldt, A. von (1807): Ideen zu einer Geographie der Pflanzen nebst einem Naturgemälde der Tropenländer. Tübingen.

Humlum, O. (1982): Rock glacier types on Disko, central West Greenland. Geografisk Tidsskrift 82: 59-66.

Humlum, O. (1988): Rock glacier appearance level and rock glacier initiation line altitude: a methodological approach to the study of rock glaciers. Arctic and Alpine Research 20, 2: 160-178.

Humlum, O. (1996): Origin of rock glaciers: Observations from Mellemfjord, Disko Island, central West Greenland. Permafrost and Periglacial Processes 7: 361-380.

Humlum, O. (1998a): Active layer thermal regime at three rock glaciers in Greenland. Permafrost and Periglacial Processes 8, 4: 383-408.

Humlum, O. (1998b): The climatic significance of rock glaciers. Permafrost and Periglacial Processes 9: 375-395.

Humlum, O. (1998c): Active layer thermal regime 1991 – 1996 at Qeqertarsuaq, Disko Island, central Greenland. Arctic and Alpine Research 30, 3: 295-305.

Humlum, O. (2000): The geomorphic significance of rock glaciers: estimates of rock glacier debris volumes and headwall recession rates in West Greenland. Geomorphology 35: 41-67.

Ikeda, A. & N. Matsuoka (2002): Degradation of talus-derived rock glaciers in the Upper Engadin, Swiss Alps. Permafrost and Periglacial Processes 13: 145-161.

Ikeda, A., Matsuoka, N. & A. Kääb (2003): A rapidly moving small rock glacier at the lower limit of the mountain permafrost belt in the Swiss Alps. In: Proceedings of the 8th International Conference on Permafrost, Zürich, Balkema, 1: 455-460.

Imhof, M. (1996): PERM – ein Programm für die automatisierte Kartierung von Permafrost in den Schweizer Alpen. In: Simulation der Permafrostverbreitung in den Alpen mit geographischen Informationssystemen. Arbeitsbericht NFP 31, vdf Hochschulverlag AG, ETH Zürich: 25-33.

Imhof, M., Pierrehumbert, G., Haeberli, W. & H. Kienholz (2000): Permafrost investigation in the Schilthorn Massif, Bernese Alps, Switzerland. Permafrost and Periglacial Processes 11: 189-206.

IPCC (2001a): Climate Change 2001 – The Scientific Basis. Intergovernmental Panel on Climate Change. Third Assessment Report of Working Group I.

IPCC (2001b): Climate Change 2001 – Impacts, Adaption and Vulnerability. Intergovernmental Panel on Climate Change. Third Assessment Report of Working Group II.

Isaksen, K., Ødegard, R. S., Eiken, T. & J. L. Sollid (2000): Composition, flow and development of two tongue-shaped rock glaciers in the permafrost of Svalbard. Permafrost and Periglacial Processes 11: 241 – 257.

Isaksen, K., Holmlund, P., Sollid, J. L. & C. Harris (2001): Three deep alpine-permafrost boreholes in Svalbard and Scandinavia. Permafrost and Periglacial Processes 12, 1: 13-25.

Jäckli, H. (1957): Gegenwartsgeologie des bündnerischen Rheingebietes. Beiträge zur Geologie der Schweiz, Geotechnische Serie Bern, 36: 126.

Jakob, M. (1995): Dendrochronology to measure average movement rates of gelifluction lobes. Dendrochronologia 13: 141-146.

Johnson, P. G. (1983): Rock glaciers. A case for a change in nomenclature. Geografiska Annaler A 65, 1-2: 27-34.

Johnson, P. G. (1992): Micro-relief on a rock glacier, Dalton Range, Yukon, Canada. Permafrost and Periglacial Processes 3: 41-47.

Kääb, A. (1996): Photogrammetrische Analyse zur Früherkennung gletscher- und permafrostbedingter Naturgefahren im Hochgebirge. Mitteilungen der VAW/ETH Zürich 145: 181.

Kääb, A. (1997): Oberflächenkinematik ausgewählter Blockgletscher des Oberengadins. Beiträge aus der Gebirgs-Geomorphologie. Mitteilung der VAW-ETH Zürich 158: 121-140.

Kääb, A. (2000): Photogrammetry for early recognition of high mountain hazards: new techniques and applications. Physics and Chemistry of the Earth, Part B, 25, 9: 765-770.

Kääb, A. (2002): Monitoring high-mountain terrain deformation from repeated air- and spaceborne optical data: examples using digital aerial imagery and ASTER data. Journal of Photogrammetry & Remote Sensing 57: 39-52.

Kääb, A. (2004): Mountain glaciers and permafrost creep. Research perspectives from earth observation technologies and geoinformatics. Habilitation thesis. Department of Geography, University of Zürich.

Kääb, A. & R. Frauenfelder (2001): Temporal variations of mountain permafrost creep. First European Permafrost Conference, Rome: 56.

Kääb, A. & M. Funk (1999): Modelling mass balance using photogrammetric and geophysical data: a pilot study at Griesgletscher, Swiss Alps. Journal of Glaciology 45, 151: 575-583.

Kääb, A. & W. Haeberli (1996): Früherkennung und Analyse glazialer Naturgefahren im Gebiet Gruben, Wallis, Schweizer Alpen. Internationales Symposium Interpraevent 1996, 4: 113-122.

Kääb, A. & M. Vollmer (2000): Surface geometry, thickness changes and flow fields on creeping mountain permafrost: automatic extraction by digital image analysis. Permafrost and Periglacial Processes 11, 4: 315-326.

Kääb, A. & M. Weber (2004): Development of transverse ridges on rock glaciers: field measurements and laboratory experiments. Permafrost and Periglacial Processes 15: 379-391.

Kääb, A., Haeberli, W. & G. H. Gudmundsson (1997): Analysing the creep of mountain permafrost using high precision aerial photogrammetry: 25 years of monitoring Gruben

rock glacier, Swiss Alps. Permafrost and Periglacial Processes 8, 409-426.

Kääb, A., Gudmundsson, G. H. & M. Hoelzle (1998): Surface deformation of creeping mountain permafrost. Photogrammetric investigations on rock glacier Murtèl, Swiss Alps. Proceedings of the 7th International Conference on Permafrost, Yellowknife, Canada. Collection Nordicana, 57: 531-537.

Kääb, A., Isaksen, K., Eiken, T. & H. Farbrot (2002): Geometry and dynamics of two lobe-shaped rock glaciers in the permafrost of Svalbard. Norsk Geografisk Tidsskrift – Norwegian Journal of Geography 56: 152-160.

Kääb, A., Kaufmann, V., Ladstädter, R. & T. Eiken (2003): Rock glacier dynamics: implications from high-resolution measurements of surface velocity fields. In: Proceedings of the 8th International Conference on Permafrost, Zürich, Balkema, 1: 501-506.

Kahmen, H. (1997): Vermessungskunde. Berlin, New York: 732.

Karte, J. (1979): Räumliche Abgrenzung und regionale Differenzierung des Periglaziärs. Ferdinand Schöningh, Paderborn: 211.

Kaufmann, V. (1996): Geomorphometric monitoring of active rock glaciers in the austrian alps. 4th International Symposium on High Mountain Remote Sensing Cartography.

Kaufmann, V. & R. Heiland (1998): Zur Morphometrie des Dösener Blockgletschers (Nationalpark Hohe Tauern, Österreich). Wiener Schriften zur Geographie und Kartographie 11: 102-114.

Kaufmann, V. & R. Ladstädter (2000): Spatio-temporal analysis of the dynamic behaviour of the Hochebenkar rock glaciers (Oetztal Alps, Austria) by means of digital photogrammetric methods. 6th International Symposium on High Mountain Remote Sensing Cartography 2000. Ethiopia, Kenya, Tanzania.

Kaufmann, V. & R. Ladstädter (2002): Monitoring of active rock glaciers by means of digital photogrammetry. ISPRS Commission III, Symposium "Photogrammetric Computer Vision". Austria, Graz.

Kaufmann, V. & R. Ladstädter (2003): Quantitative analysis of rock glacier creep by means of digital photogrammetry using multi-temporal aerial photographs: two case studies in the Austrian Alps. In: Proceedings of the 8th International Conference on Permafrost, Zürich, Balkema, 1: 525-530.

Keller, F. (1992): Automated mapping of mountain permafrost using the program PERMAKART within the Geographical Information System ARC/INFO. Permafrost and Periglacial Processes 3: 133-138.

Keller, F. (1994): Interaktionen zwischen Schnee und Permafrost. Mitteilungen der VAW/ETH Zürich 127: 145.

Kenyi, L. W. & V. Kaufmann (2003a): Measuring rock glacier surface deformation using SAR interferometry. In: Proceedings of the 8th International Conference on Permafrost, Zürich, Balkema, 1: 537-541.

Kenyi, L. W. & V. Kaufmann (2003b): Estimation of rock glacier deformation using SAR interferometry data. IEEE Transactions on Geoscience and Remote Sensing. 41, 6: 1512 – 1515.

Kerschner, H. (1985): Quantitative palaeoclimatic inferences from lateglacial snowline, timberline and rock glacier data, Tyrolean Alps, Austria. Zeitschrift für Gletscherkunde und Glazialgeologie 21, 363-369.

King, L. (1983): High mountain permafrost in Scandinavia. 4th International Conference on Permafrost, Fairbanks, Alaska. National Academic Press, Washington: 612-617.

King, L. (1996): Dauerfrostboden im Gebiet Zermatt – Gornergrat – Stockhorn: Verbreitung und permafrostbezogene Erschliessungsarbeiten. Zeitschrift für Geomorphologie N. F. 104: 73-93.

Kirkbride, M. & V. Brazier (1995): On the sensitivity of Holocene talus-derived rock glaciers to climate change in the Ben Ohau Range, New Zealand. Journal of Quaternary Science 10, 4: 353-365.

Kneisel, C. (2004): New insights into mountain permafrost occurrence and characteristics in glacier forefields at high altitude through the application of 2D resistivity imaging. Permafrost and Periglacial Processes 15: 221-227.

Kneisel, C., Lehmkuhl, F., Winkler, S., Tressel, E. & H. Schröder (1998): Legende für geomorphologische Kartierungen in Hochgebirgen (GMK Hochgebirge). Trierer Geographische Studien 18.

Konecny, G. (1984): Photogrammetrie. Berlin, New York: 392.

Koning, D. M. & D. J. Smith (1999): Movement of King´s Throne rock glacier, Mount Rae Area, Canadian Rocky Mountains. Permafrost and Periglacial Processes 10: 151 – 162.

Konrad, S. K., Humphrey, N. F., Steig, E. J., Clark, D. H., Potter, N. & W. T. Pfeffer (1999): Rock glacier dynamics and paleoclimatic implications. Geology 27, 12: 1131-1134.

Kozlowski, T. T. (1979): Tree Growth and Environmental Stress. University of Washington Press, Seattle, WA: 192.

Krainer, K. & W. Mostler (2000): Reichenkar rock glacier: a glacier derived debris-ice system in the Western Stubai Alps, Austria. Permafrost and Periglacial Processes 11, 3: 267-275.

Krainer, K. & W. Mostler (2002): Hydrology of active rock glaciers: examples from the Austrian Alps. Arctic, Antarctic, and Alpine Research 34, 2: 142-149.

Kraus, K. (1996): Photogrammetrie. Band 2 Verfeinerte Methoden und Anwendungen. Dümmler, Bonn: 488.

Kraus, K. (1997): Photogrammetrie. Band 1 Grundlagen und Standardverfahren. Dümmler, Bonn: 394.

Krummenacher, B., Budmiger, K., Mihajlovic, D. & B. Blank (1998): Periglaziale Prozesse und Formen im Furggentälti, Gemmipass. Mitteilungen des Eidgenössisches Institut für Schnee- und Lawinenforschung, Davos: 245.

Kugler, H. (1974): Das Georelief und seine kartographische Modellierung. Dissertation B, Martin-Luther-Universität Halle.

Labhart, T. P. (1998): Geologie der Schweiz. Thun: 211.

Lachenbruch, A. H. & B. V. Marshall (1986): Changing climate: geothermal evidence from permafrost in the Alaskan Arctic. Science 234: 689-696.

Lambiel, C. & R. Delaloye (2004): Contribution of real-time kinematic GPS in the study of creeping mountain permafrost: examples from the Western Swiss Alps. Permafrost and Periglacial Processes 15: 229-241.

Lambiel, C., Delaloye, R., Baron, L. & R. Monnet (2003): Measuring rock glacier surface velocities with real time kinematics GPS (Mont Gelé area, western Swiss Alps). In: Haeberli, W. & D. Brandová: Abstracts of the 8th International Conference on Permafrost: 89-90.

Lang, A., Moya, J., Corominas, J., Schrott, L. & R. Dikau (1999): Classic and new dating methods for assessing the temporal occurrence of mass movements. Geomorphology 30: 33-52.

Lautensach, H. (1952): Der geographische Formenwandel. Studien zur Landschaftssystematik. Coll. Geogr., 3, Bonn.

Lindorf, H. (1994): Eco-anatomical wood features of species from a very dry tropical forest. IAWA Journal 15: 361-376.

Luetschg, M., Stoeckli, V., Lehning, M., Haeberli, W. & W. Ammann (2004): Temperatures in two boreholes at Flüela Pass, Eastern Swiss Alps: The effect of snow redistribution on

permafrost distribution patterns in high mountain areas. Permafrost and Periglacial Processes 15: 283-297.

Martin, H. E. & W. B. Whalley (1987): Rock glaciers. Part 1: rock glacier morphology: classification and distribution. Progress in Physical Geography 11: 260-282.

Matsuoka, N. & O. Humlum (2003): Monitoring Periglacial Processes: New methodology and technology. Permafrost and Periglacial Processes 14: 299-303.

Messerli, B. & J. D. Ives (eds.) (1997): Mountains of the world: a Global Priority. Parthenon, London: 495.

Messerli, B. & M. Zurbuchen (1968): Blockgletscher im Weissmies und Aletsch und ihre photogrammetrische Kartierung. Die Alpen 3: 1-13.

Mittaz, C. (1998): Energiebilanz über alpinem Permafrost. In: Beiträge aus der Gebirgsgeomorphologie. Jahresversammlung 1997 der Schweizerischen Geomorphologischen Gesellschaft der SANW. Mitteilungen der VAW/ETH Zürich 158: 152-167.

Mittaz, C., Imhof, M., Hoelzle, M. & W. Haeberli (2002): Snowmelt evolution mapping using an energy balance approach over an alpine terrain. Arctic, Antarctic, and Alpine Research, 34, 3: 274-281.

Neukum, G. (1999): The airborne HRSC-A: Performance results and application potential. In: Fritsch, D. & Spiller, R. (eds.): Photogrammetric Week `99. Wichmann, Heidelberg: 83-88.

Nötzli, J., Hoelzle, M. & W. Haeberli (2003): Mountain permafrost and recent Alpine rock fall events: a GIS-based approach. In: Proceedings of the 8th International Conference on Permafrost, Zürich, Balkema, 2: 827-832.

Nyenhuis, M. (2001): Analyse der regionalen Permafrostverbreitung im Turtmanntal, Wallis, Schweiz. Diploma thesis (unpublished), Department of Geography, University of Bonn.

Nyenhuis, M. (2005): Permafrost und Sedimenthaushalt in einem alpinen Geosystem. PhD thesis, Department of Geography, University of Bonn (in press).

Nyenhuis, M., Hoelzle, M. & R. Dikau (in press): Rock glacier mapping and permafrost distribution modelling in the Turtmanntal, Valais, Switzerland. Zeitschrift für Geomorphologie, N. F.

Ødegard, R. S., Isaksen, K., Eiken, T. & J. L. Sollid (2003): Terrain analyses and surface velocity measurements of the Hiorthfjellet rock glacier, Svalbard. Permafrost and Periglacial Processes 14: 359-365.

Osterkamp, T. E. (1983): Response of Alaskan permafrost to climate. In: Proceedings of the 4th International Conference on Permafrost, Fairbanks, Alaska, USA: 145-152.

Osterkamp, T. E. & V. E. Romanovsky (1999): Evidence for warming and thawing of discontinuous permafrost in Alaska. Permafrost and Periglacial Processes 10, 1: 17-37.

Otto, J. - C. (2001): Das geomorphologische System des Turtmanntales. Formen, Substrat, Prozesse. Diploma thesis (unpublished), Department of Geography, University of Bonn.

Otto, J. - C. & R. Dikau (2004): Geomorphologic system analysis of a high mountain valley in the Swiss Alps. Zeitschrift für Geomorphologie N. F. 48, 3: 323-341.

Outcalt, S. I. & J. B. Benedict (1965): Photo-interpretation of two types of rock glaciers in the Colorado Front Range, U.S.A. Journal of Glaciology 5: 849-856.

Owens, P.N. & O. Slaymaker (eds.) (2004): Mountain geomorphology. Arnold, London: 313.

Ozenda, P. (1988): Die Vegetation der Alpen im europäischen Gebirgsraum. Stuttgart, New York.

Passarge, S. (1921): Die Landschaft. Verlag von Quelle & Meyers.

Paterson, W. S. B. (1994): The physics of glaciers. Butterworth-Heinemann, Oxford: 481.

Penck, A. (1894): Morphologie der Erdoberfläche. Engelhorn, Stuttgart.

Pfeffer, G. (2000): Untersuchungen zur Permafrostverbreitung mit geophysikalischen Methoden im Turtmanntal / Wallis. Diploma thesis (unpublished), Department of Geography, University of Bonn.

Pillewizer, W. (1957): Untersuchungen an Blockströmen der Ötztaler Alpen. Abhandlungen des Geographischen Institutes der Freie Universität Berlin 5: 37-50.

Potter, N. (1972): Ice-cored rock glacier, Galena Creek, northern Absaroka Mountains, Wyoming. Geological Society of America Bulletin 83: 3025-3057.

Potter Jr., N., Steig, E. J., Clark, D. H., Speece, M. A., Clark, G. M. & A. B. Updike (1998): Galena Creek rock glacier revisited - new observations on an old controversy. Geografiska Annaler 80A, 3-4: 251-265.

Rasemann, S. (2004): Geomorphometrische Struktur eines mesoskaligen alpinen Geosystems. Bonner Geographische Abhandlungen 111: 240.

Rathjens, C. (1982): Geographie des Hochgebirges: 1 Der Naturraum. Teubner, Stuttgart: 210.

Roer, I. (2001): Bioindikation von Blockgletschersystemen in einem hochalpinen Tal (Turtmanntal, Wallis, Schweiz). Diploma thesis (unpublished), Department of Geography, University of Bonn: 114.

Roer, I. (2003): Rock glacier kinematics in the Turtmanntal, Valais, Switzerland – observational concept, first results and research perspectives. In: Proceedings of the 8th International Conference on Permafrost, Zürich, Balkema, 2: 971-975.

Roer, I., Kääb, A. & R. Dikau (2005): Rockglacier kinematics derived from small-scale aerial photography and digital airborne pushbroom imagery. Zeitschrift für Geomorphologie N. F. 49, 1: 73-87.

Roer, I., Kääb, A. & R. Dikau (in press): Rockglacier acceleration in the Turtmann valley (Swiss Alps) – probable controls. Norwegian Journal of Geography.

Sartori, M. (1990): L´unité du Barrhorn (zone pennique, Valais, Suisse). Memoires de Géologie Thesis, Lausanne.

Schneider, B. (2001): Fluctuations of air temperature as a reason for short-term velocity changes at the rock glacier Äusseres Hochebenkar (Ötztal Alps, Tyrol)? First European Permafrost Conference, Rome: 62-63.

Schneider, B. & H. Schneider (2001): Zur 60jährigen Messreihe der kurzfristigen Geschwindigkeitsschwankungen am Blockgletscher im Äusseren Hochebenkar, Ötztaler Alpen, Tirol. Zeitschrift für Gletscherkunde und Glazialgeologie 37, 1: 1-33.

Schrott, L. (1994): Die Solarstrahlung als steuernder Faktor im Geosystem der subtropischen semiariden Hochanden (Agua Negra, San Juan, Argentinien). Heidelberger Geographische Arbeiten 94: 199.

Schweingruber, F. H. (1983): Der Jahrring. Standort, Methodik, Zeit und Klima in der Dendrochronologie. Haupt, Bern: 234.

Schweingruber, F. H. (1990): Mikroskopische Holzanatomie. 3rd edition. Eidgenössische Forschungsanstalt für Wald, Schnee und Landschaft, Birmensdorf: 226.

Schweingruber, F. H. (1996): Tree Rings and Environment. Dendroecology. Haupt, Bern: 609.

Schweingruber, F. H., Eckstein, D., Serre-Bachet, F. & O. U. Bräker (1990): Identification, presentation and interpretation of event years and pointer years in dendrochronology. Dendrochronologia 8: 9-38.

Seppi, R., Baroni, C. & A. Carton (2003): Rock glacier inventory of the Adamello Presanella massif (Central Alps, Italy). In: Haeberli, W. & D. Brandová: Abstracts of the 8th International Conference on Permafrost: 145-146.

Shroder, J. F. (1978): Dendrogeomorphological analysis of mass movement on Table Cliffs Plateau, Utah. Quaternary Research 9: 168-185.

Slaymaker, O. & T. Spencer (1998): Physical geography and global environmental change. Longman, New York: 292.

Smith, M. W. & D. W. Riseborough (2002): Climate and the limits of permafrost: a zonal analysis. Permafrost and Periglacial Processes 13: 1-15.

Sollid, J. L. & L. Sørbel (1992): Short communication: rock glaciers in Svalbard and Norway. Permafrost and Periglacial Processes 3: 215-220.

Stocker-Mittaz, C., Hoelzle, M. & W. Haeberli (2002): Modelling alpine permafrost distribution based on energy-balance data: a first step. Permafrost and Periglacial Processes 13, 4: 271-282.

Stokes, M. A. & T. L. Smiley (1968): An introduction to tree-ring dating. University of Chicago Press, Chicago: 73.

Strahler, A. N. (1952): Dynamic basis of geomorphology. Bulletin of the Geological Society of America 63: 923-937.

Strozzi, T., Kääb, A. & R. Frauenfelder (2004): Detecting and quantifying mountain permafrost creep from *in situ* inventory, space-borne radar interferometry and airborne digital photogrammetry. International Journal of Remote Sensing 25, 15: 2919-2931.

Tatenhove, F. van & R. Dikau (1990): Past and present permafrost distribution in the Turtmanntal, Wallis, Swiss Alps. Artic and Alpine Research 22, 3: 302-316.

Thorn, C. E. (1992): Periglacial Geomorphology: What, Where, When? In: Dixon, J. C. & A. D. Abrahams (eds.): Periglacial Geomorphology, Proceedings of the 22nd Ann. Binghampton Symp. in Geomorphology. Wiley & Sons, Chichester: 1-30.

Thorn, C. E. (2003): Making the most of new instrumentation. Permafrost and Periglacial Processes 14: 411-419.

Thornes, J. B. (1979): Processes and interrelationships, rates and changes. In: Embleton, C. & J. B. Thornes (eds.): Process in geomorphology. Arnold, London: 378-387.

Torge, W. (2001): Geodesy. De Gryter, Berlin: 416.

Troll, C. (1941): Studien zur vergleichenden Geographie der Hochgebirge der Erde. Ber. Ges. d. Freunde u. Förderer d. Univ. Bonn: 49-96.

Troll, C. (1966): Über das Wissen der Hochgebirgsnatur. Erdkundl. Wissen 11: 127-151.

Troll, C. (1973): High mountain belts between the polar caps and the equator: their definition and lower limit. Arctic and Alpine Research, 5, 3: A19-A27.

Vietoris, L. (1972): Über die Blockgletscher des Äusseren Hochebenkars. Zeitschrift für Gletscherkunde und Glazialgeologie 8: 169-188.

Vollmer, M. (1999): Kriechen alpinen Permafrostes: Grundlagen zur digitalen photogrammetrischen Bewegungsmessung. Diploma thesis (unpublished), Department of Geography, University of Zürich.

Vonder Mühll, D. (1993): Geophysikalische Untersuchungen im Permafrost des Oberengadins. Mitteilungen der VAW/ETH Zürich 122: 222.

Vonder Mühll, D. & W. Haeberli (1990): Thermal characteristics of the permafrost within an active rock glacier (Murtèl/Corvatsch, Grisons, Swiss Alps). Journal of Glaciology 36: 151-158.

Vonder Mühll, D., Hauck, C., Gubler, H., McDonald, R. & N. Russill (2001): New geophysical methods of investigating the nature and distribution of mountain permafrost with special reference to radiometry techniques. Permafrost and Periglacial Processes 12, 1: 27-38.

Wagner, S. (1992): Creep of alpine permafrost from borehole deformation at Murtèl rock glacier, Grison (Swiss Alps). Permafrost and Periglacial Processes 3: 157-162.

Wahrhaftig, C. & A. Cox (1959): Rock glaciers in the Alaska Range. Geol. Soc. Am. Bull. 70: 383-436.

Werner, P. (1994): Die Natur im Wallis: Die Flora. Martigny: 259.

Whalley, W. B. (1974): The origin of rock glaciers. Journal of Glaciology 13: 323-324.

Whalley, W. B. & F. Azizi (1994): Rheological models of active rock glaciers: Evaluation, critique and a possible test. Permafrost and Periglacial Processes 5: 37-51.

Whalley, W. B. & H. E. Martin (1992): Rock glaciers: II models and mechanisms. Progress in Physical Geography 16, 2: 127-186.

Whalley, W. B., Palmer, C., Hamilton, S. & J. E. Gordon (1994): Ice exposures in rock glaciers. Journal of Glaciology 40: 427-429.

White, S. E. (1981): Alpine mass movement forms (noncatastrophic): classification, description, and significance. Arctic and Alpine Research 13, 2: 127 – 137.

Wolman, M. G. & J. P. Miller (1960): Magnitude and frequency of forces in geomorphic processes. Journal of Geology 68: 54-74.

Zeiske, K. (2000): Surveying made easy. Leica Geosystems AG, Heerbrugg, Switzerland: 35.

Zick, W. (1996): Bewegungsmessungen 1965-1994 am Blockgletscher Macun I (Unterengadin / Schweiz) - neue Ergebnisse. Zeitschrift für Geomorphologie N. F. Suppl.-Bd. 104: 59-71.

Zoltai, S. C. (1975): Tree ring record of soil movements on permafrost. Arctic and Alpine Research 7, 4: 331-340.

MAPS:

Topographischer Atlas der Schweiz (1:50.000), Siegfriedkarte (TA 500 St. Niklaus)

WEBPAGES:

http://www.geo.unizh.ch/~kaeaeb/e&mhtml/kinbed.html (last visited 13.12.2004)

http://www.utl.ch/geotest.html (last visited 30.11.2004)

http://www.scilands.de (last visited 30.11.2004)

APPENDIX 1A

PUBLISHED DATA ON HORIZONTAL VELOCITIES				
Region/Location	**Horizontal velocity [m*a^{-1}]** (mean, if not indicated)	**Measuring period**	**Method**	**Reference**
Europe				
Austria				
Austria, Kaunsertal, Ölgruben-Rg	0.04-0.55	1938-1939	terrestrial photogrammetry	Pillewizer (1957)
Austria, Kaunsertal, Ölgruben-Rg	0.35-0.75	1938-1953	terrestrial photogrammetry	Pillewizer (1957)
Austria, Ötztal, Äusseres Hochebenkar	0.75	1938-1953	terrestrial photogrammetry	Pillewizer (1957)
Austria, Ötztal, Äusseres Hochebenkar (profile 3)	0.85 (max)	1953-1955	terrestrial photogrammetry	Pillewizer (1957)
Austria, Ötztal, Äusseres Hochebenkar (profile 3)	0.84 (max)	1954-1955	terrestrial geodetic survey (line of rocks)	Vietoris, in Pillewizer (1957)
Austria, Ötztal, Äusseres Hochebenkar (profile 2)	1.53 (max)	1953-1955	terrestrial photogrammetry	Pillewizer (1957)
Austria, Ötztal, Äusseres Hochebenkar (profile 2, rock 3)	1.61	1951-1952	terrestrial geodetic survey (line of rocks)	Vietoris, in Pillewizer (1957)
Austria, Ötztal, Äusseres Hochebenkar (profile 2, rock 3)	1.84	1952-1953	terrestrial geodetic survey (line of rocks)	Vietoris, in Pillewizer (1957)
Austria, Ötztal, Äusseres Hochebenkar (profile 1)	3.57 (max)	1953-1955	terrestrial photogrammetry	Pillewizer (1957)
Austria, Ötztal, Äusseres Hochebenkar (profile 1)	3.3 (max)	1955-1956	terrestrial geodetic survey (line of rocks)	Vietoris, in Pillewizer (1957)

Austria, Ötztal, Inneres Hochebenkar	1.1	1953-1955	terrestrial photogrammetry	Pillewizer (1957)
Austria, Ötztal, Äusseres Hochebenkar, profile 1	3.35 (max)	1954-1962	line of rocks, terrestrial geodetic survey	Vietoris (1972)
Austria, Ötztal, Äusseres Hochebenkar, profile 2	0.95, 1.48 (max)	1951-1970	line of rocks, terrestrial geodetic survey	Vietoris (1972)
Austria, Ötztal, Äusseres Hochebenkar, profile 3	0.75 (max)	1954-1970	line of rocks, terrestrial geodetic survey	Vietoris (1972)
Austria, Ötztal, Hochebenkar-Rg, profile 2540	3.57	1952/1953	photogrammetry	Kaufmann (1996)
Austria, Ötztal, Hochebenkar-Rg, profile 2540	0.32	1985-1990	terrestrial geodetic survey	Kaufmann (1996)
Austria, Ötztal, Hochebenkar-Rg, profile 2540	0.57	1990-1995	terrestrial geodetic survey	Kaufmann (1996)
Austria, Ötztal, Hochebenkar-Rg, profile 2630	1.80	1952/1953	photogrammetry	Kaufmann (1996)
Austria, Ötztal, Hochebenkar-Rg, profile 2630	0.49	1985-1990	terrestrial geodetic survey	Kaufmann (1996)
Austria, Ötztal, Hochebenkar-Rg, profile 2630	0.65	1990-1995	terrestrial geodetic survey	Kaufmann (1996)
Austria, Ötztal, Hochebenkar-Rg, profile 2680	0.75	1952/1953	photogrammetry	Kaufmann (1996)
Austria, Ötztal, Hochebenkar-Rg, profile 2680	0.36	1985-1990	terrestrial geodetic survey	Kaufmann (1996)
Austria, Ötztal, Hochebenkar-Rg, profile 2680	0.48	1990-1995	terrestrial geodetic survey	Kaufmann (1996)
Austria, Ötztal, Hochebenkar-Rg	1.25 (max)	1977-1986	terrestrial photogrammetry	Kaufmann (1996)
Austria, Dösen Tal, Dösen-Rg, region A (front)	0.18	1954-1993	photogrammetry + terrestrial geodetic survey	Kaufmann (1996)

Austria, Dösen Tal, Dösen-Rg, region B	0.21	1954-1993	photogrammetry + terrestrial geodetic survey	Kaufmann (1996)
Austria, Dösen Tal, Dösen-Rg, region C (rootzone)	0.17	1954-1993	photogrammetry + terrestrial geodetic survey	Kaufmann (1996)
Austria, Ötztal, Ölgruben-Rg	0.5	1923-1924	?	Finsterwalder (1928), in Kaufmann (1996)
Austria, Stubaier Alpen, Inneres Reichenkar	2.0 (mean), 6.94 (max.)	1997-1998	differential GPS	Chesi et al. (1999); Krainer & Mostler (2000)
Austria, Stubaier Alpen, Inneres Reichenkar	0.64	1954-1990	comparison of aerial photographs (front advance)	Chesi et al. (1999); Krainer & Mostler (2000)
Austria, Ötztal, Äusseres Hochebenkar-Rg	1.8 (max)	1953 - 1969	digital photogrammetry	Kaufmann & Ladstädter (2000)
Austria, Ötztal, Äusseres Hochebenkar-Rg	1.1 (max)	1969 - 1979	digital photogrammetry	Kaufmann & Ladstädter (2000)
Austria, Ötztal, Äusseres Hochebenkar-Rg	„slight decrease“	- 1990	digital photogrammetry	Kaufmann & Ladstädter (2000)
Austria, Ötztal, Äusseres Hochebenkar-Rg	1.1 (max)	1990 - 1997	digital photogrammetry	Kaufmann & Ladstädter (2000)
Austria, Ötztal, Inneres Hochebenkar-Rg	0.55 (max)	1953-1969	digital photogrammetry	Kaufmann & Ladstädter (2000)
Austria, Ötztal, Inneres Hochebenkar-Rg	0.3 (mean)	1969 - 1979	digital photogrammetry	Kaufmann & Ladstädter (2000)
Austria, Ötztal, Äusseres Hochebenkar-Rg	> 0.8 (max)	1981-1990	digital photogrammetry	Kaufmann & Ladstädter (2002)
Austria, Ötztal, Äusseres Hochebenkar-Rg	1.31 (max)	1953-1997	digital photogrammetry	Kaufmann & Ladstädter (2003)
Austria, Ötztal, Inneres Hochebenkar-Rg	0.55 (max)	1953-1969	digital photogrammetry	Kaufmann & Ladstädter (2002)
Austria, Ötztal, Inneres Hochebenkar-Rg	0.35 (max)	1953-1997	digital photogrammetry	Kaufmann & Ladstädter (2003)

Austria, Hohe Tauern National Park, Hinteres Langtalkar	0.9 (max)	1969-1991	digital photogrammetry	Kaufmann & Ladstädter (2002)
Austria, Hohe Tauern National Park, Hinteres Langtalkar	1.8 (max)	1991-1997	digital photogrammetry	Kaufmann & Ladstädter (2002)
Austria, Hohe Tauern National Park, Hinteres Langtalkar	1.5 (max)	1999-2000	terrestrial geodetic survey	Kaufmann & Ladstädter (2003)
Austria, Hohe Tauern National Park, Hinteres Langtalkar	2.8 (max)	1997-1998	digital photogrammetry	Kaufmann & Ladstädter (2003)
Austria, Dösen valley, Dösen-Rg	0.006/35 days (mean), 0.018/35 days (max)	1992 (35 days)	D-InSAR	Kenyi & Kaufmann (2003a, 2003b)
Austria, Ötztal, Äusseres Hochebenkar	3.9 (mean), 6.6 (max) (1950s, 1960s); 1.5 (mean), 2.0 (max) (1990s)	1938-1999	(terrestrial-photogrammetric profiles (1938-1951)); terrestrial geodetic survey	Schneider (2001)
Austria, Ötztal, Äusseres Hochebenkar	3.9	1954-1962	terrestrial geodetic survey	Schneider & Schneider (2001)
Austria, Ötztal, Äusseres Hochebenkar (alongside)	0.54/0.51	1997-1998/1998-1999	terrestrial geodetic survey	Schneider & Schneider (2001)
Austria, Ötztal, Äusseres Hochebenkar (across)	0.53(line 0), 1.06 (line 1), 1.02 (line 2), 0.75 (line 3)	1997-1998	terrestrial geodetic survey	Schneider & Schneider (2001)
Austria, Ötztal, Äusseres Hochebenkar (across)	0.54(line 0), 1.1 (line 1), 1.16 (line 2), 0.84 (line 3)	1998-1999	terrestrial geodetic survey	Schneider & Schneider (2001)
Austria, Ötztal, Äusseres Hochebenkar (across)	0.53 (line 1), 0.67 (line 2), 0.49 (line 3)	1981-1999	terrestrial geodetic survey	Schneider & Schneider (2001)
France				
France, Haute-Ubaye, Marinet	0.1-0.3	?	terrestrial geodetic survey	Evin et al. (1990)
France, Haute Ubaye, Haut-Vallon du Loup, Petit Loup	0.16	1948-1979	photogrammetry	Evin & Assier (1983)
France, Haute Ubaye, Haut-Vallon du Loup, Loup principal	0.19	1948-1979	photogrammetry	Evin & Assier (1983)

France, Haute Ubaye, Haut-Vallon du Loup, Asti	0.08	1948-1979	photogrammetry	Evin & Assier (1983)
France, French Alps, Laurichard	0.25 (line A), 0.6-0.9 (line B, C)	1979-1984	terrestrial geodetic survey	Francou & Reynaud (1992)
France, French Alps, Laurichard	0.56	1983-1991	terrestrial geodetic survey	Francou & Reynaud (1992)
Iceland				
North Iceland, Nautadalur	0.025	?	?	Martin & Whalley (1987), in Whalley & Martin (1992)
Italy				
Italy, Adamello Presanella Group A37, Genova valley	0.05 (min) – 0.21 (max)	1 year	terrestrial geodetic survey	Seppi et al. (2003)
Italy, Adamello Presanella G42, Amola valley	0.02 (min) – 0.16 (max)	1 year	terrestrial geodetic survey	Seppi et al. (2003)
Norway				
Norway, Svalbard, NW coast, Kongsfjord area	0.03-0.1	1986-1990	?	Sollid & Sørbel (1992)
Norway, Svalbard, Hiorthfjellet	0.083 (min) – 0.095 (max)	1994 – 1998	terrestrial geodetic survey	Isaksen et al. (2000)
Norway, Svalbard, Birkafjellet	0.041 – 0.056	1995 - 1997	terrestrial geodetic survey	Isaksen et al. (2000)
Norway, Svalbard, Nordenskiöldkysten-Rg	0.0 – 0.01	1969 - 1990	digital photogrammetry	Kääb et al. (2002)
Norway, Svalbard, Brøggerbreen-Rg	0.04 (max)	1971 – 1995	digital photogrammetry	Kääb et al. (2002)
Norway, Svalbard, Hiorthfjellet-Rg	0.095 – 0.108	1994 - 2002	terrestrial geodetic survey	Ødegard et al. (2003)

Norway, Svalbard, Prins Karls Forland, Nr. 12 + 15	0.02-0.04	1996-2000	terrestrial geodetic survey + differential GPS	Berthling et al. (2003)
Switzerland				
Grisons				
Switzerland, Grisons, Val Sassa	1.3-2.0	1918-1919	painted line of rocks	Chaix (1923)
Switzerland, Grisons, Val Sassa	1.05-1.37	1919-1921	painted line of rocks	Chaix (1923)
Switzerland, Grisons, Val dell' Acqua	1.55	1918-1919	painted line of rocks	Chaix (1923)
Switzerland, Grisons, Val dell' Acqua	1.35	1919-1921	painted line of rocks	Chaix (1923)
Switzerland, Grisons, Val Sassa	1.36	1921-1942	painted line of rocks	Chaix (1943)
Switzerland, Grisons, Val dell' Acqua	1.58	1921-1942	painted line of rocks	Chaix (1943)
Switzerland, Grisons, Macun I	0.16	1965-1967	terrestrial geodetic survey	Barsch 1969
Switzerland, Grisons, Val Sassa	1.05-3.95 (cumulative)	1952-1959	terrestrial geodetic survey	Eugster (1973)
Switzerland, Grisons, Val Sassa	0.8-2.8 (cumulative)	1954-1959	terrestrial geodetic survey	Eugster (1973)
Switzerland, Grisons, Val Sassa	0.47-0.52	?	?	Girsperger (1973), in Whalley & Martin (1992)
Switzerland, Grisons, Murtèl	0.07	1932-1955	photogrammetry	Barsch & Hell (1975)
Switzerland, Grisons, Murtèl	0.03	1955-1971	photogrammetry	Barsch & Hell (1975)

Switzerland, Grisons, Murtèl	0.04	1971-1973	terrestrial geodetic survey	Barsch & Hell (1975)
Switzerland, Grisons, Muragl	0.21	1972-1973	terrestrial geodetic survey	Barsch & Hell (1975)
Switzerland, Grisons, Albana Rg	0.05	1932-1952	photogrammetry	Pröhl (1977), in Barsch (1996)
Switzerland, Grisons, Albana West Rg	0.1	1932-1952	photogrammetry	Pröhl (1977), in Barsch (1996)
Switzerland, Grisons, Val da l'Acqua	0.46; 0.5-1 (50-100m above snout); 1.5-2 (200-300m above snout)	1921-1979	?	Jäckli (1978), in Barsch (1992)
Switzerland, Grisons, Val da l'Acqua	0.4-0.45	1920-1980	?	Jäckli (1978), in Barsch (1996)
Switzerland, Grisons, Macun I	0.14	1967-1988	terrestrial geodetic survey	Barsch & Zick (1991)
Switzerland, Grisons, Macun I	0.27 (max)	1965-1994	terrestrial geodetic survey	Zick (1996)
Switzerland, Grisons, Murtèl	0.15 (max)	1987, 1988, 1991, 1995, 1996	photogrammetry	Kääb (1996); Kääb (1997); Kääb et al. (1998)
Switzerland, Grisons, Muragl	0.5 (max)	1981, 1985, 1990, 1994, 1998, 1999	photogrammetry	Kääb (1997); Kääb (2002)
Switzerland, Grisons, Schafberg	0.08 (max)	1971-1991	photogrammetry	Kääb (1997)
Switzerland, Grisons, Murtèl	0.05 – 0.15	1987-1996	digital photogrammetry	Kääb et al. (1998)
Switzerland, Grisons, Pontresina-Schafberg, BH1	0.02 – 0.04	1990–1997	borehole deformation (point information!)	Hoelzle et al. (1998)
Switzerland, Grisons, Pontresina-Schafberg, BH2	0.01		borehole deformation (point information!)	Hoelzle et al. (1998
Switzerland, Grisons, Pontresina-Schafberg	0.02 – 0.03	1971 – 1991	photogrammetry	Hoelzle et al. (1998

Switzerland, Grisons, Muragl	0.5 (max)	1981–1994	photogrammetry	Kääb & Vollmer (2000)
Switzerland, Grisons, Suvretta	2.0 (max)	1992, 1997	photogrammetry	Kääb (2000)
Switzerland, Grisons, Suvretta	2.0 (max)	1992-1997	digital photogrammetry	Kääb & Frauenfelder (2001); Frauenfelder et al. (2004)
Switzerland, Grisons, Murtèl-Corvatsch	0.07	1987-1995	borehole deformation (point information!)	Arenson et al. (2002)
Switzerland, Grisons, Pontresina-Schafberg1	0.03	1991-2000	borehole deformation (point information!)	Arenson et al. (2002)
Switzerland, Grisons, Pontresina-Schafberg2	0.02	1994-1999	borehole deformation (point information!)	Arenson et al. (2002)
Switzerland, Grisons, Muragl3	0.3	1999-2000	borehole deformation (point information!)	Arenson et al. (2002)
Switzerland, Grisons, Muragl4	0.15	1999-2000	borehole deformation (point information!)	Arenson et al. (2002)
Switzerland, Grisons, Büz North (upper)	0.5-0.8	1998-1999	terrestrial geodetic survey	Ikeda et al. (2003)
Switzerland, Grisons, Büz North (upper)	0.6-0.96	1999-2000	terrestrial geodetic survey	Ikeda et al. (2003)
Switzerland, Grisons, Büz North (upper)	1.1-1.45	2000-2001	terrestrial geodetic survey	Ikeda et al. (2003)
Switzerland, Grisons, Büz North (lower)	0.02-0.2	1998-1999	terrestrial geodetic survey	Ikeda et al. (2003)
Switzerland, Grisons, Gianda Grischa	0.4-0.5 (average), 0.8 (max)	1971-1998	digital photogrammetry	Frauenfelder et al. (2004)
Switzerland, Grisons, Suvretta	0.06-1.6	1971-1998	digital photogrammetry	Frauenfelder et al. (2004)
Switzerland, Grisons, Munteratsch	0-0.1	1971-1998	digital photogrammetry	Frauenfelder et al. (2004)

Switzerland, Grisons, Albana	0.05-0.19	1971-1998	digital photogrammetry	Frauenfelder et al. (2004)
Valais				
Switzerland, Valais, Weissmies	0.7 (max)	1958-1964	photogrammetry	Messerli & Zurbuchen (1968)
Switzerland, Valais, Grosses Gufer	0.75 (max)	1950-1962	photogrammetry	Messerli & Zurbuchen (1968)
Switzerland, Valais, Gruben	0.63	1979-1982	terrestrial geodetic survey	Haeberli (1985)
Switzerland, Valais, Gruben	1.0 (max)	1970-1995	photogrammetry	Kääb 1996; Kääb et al. (1997)
Switzerland, Valais, Furggentälti	0.5	1960-1974	photogrammetry	Krummenacher et al. (1998)
Switzerland, Valais, Furggentälti	0.8	1974-1985	photogrammetry	Krummenacher et al. (1998)
Switzerland, Valais, Furggentälti	0.7	1985-1992	photogrammetry	Krummenacher et al. (1998)
Switzerland, Valais, Furggentälti	1.35	1994-1996	terrestrial geodetic survey	Krummenacher et al. (1998)
Switzerland, Valais, Turtmann valley	0.65 (max)	1975-1993	digital photogrammetry	Elverfeldt (2002)
Switzerland, Valais, Turtmann valley, HuHH1	0.84 (max)	10.9.2001-30.8.2002	terrestrial geodetic survey	Roer (2003)
Switzerland, Valais, Mont Gelé rock glaciers	0.05 (min) - 1.25 (max)	2000–2001	differential GPS	Lambiel et al. (2003)
Switzerland, Valais, Yettes Condjà, rgB	1.35 (max)	2000-2003	differential GPS	Lambiel & Delaloye (2004)
Switzerland, Valais, Yettes Condjà, rgC	0.35 (max)	2000-2003	differential GPS	Lambiel & Delaloye (2004)

Switzerland. Valais, Réchy, Becs-de-Bosson Rg, L1	>0.05	2001-2003	differential GPS	Lambiel & Delaloye (2004)
Switzerland. Valais, Réchy, Becs-de-Bosson Rg, L2	1.2 (max)	2001-2003	differential GPS	Lambiel & Delaloye (2004)
Switzerland, Valais, Gruben	2.0 (max)	1975-1999	photogrammetry	Strozzi et al. (2004)
Switzerland, Valais, Gruben	?	1995 (1 day) + 1998 (35 days)	D-InSAR	Strozzi et al. (2004)
Switzerland, Valais, Rothorn	0.3 (max)	1975-1999	photogrammetry	Strozzi et al. (2004)
Switzerland, Valais, Rothorn	0.5 (max)	1996 (88 days) + 1999 (70 days)	D-InSAR	Strozzi et al. (2004)
Switzerland, Valais, Jegi	0.5 (max)	1975-1999	photogrammetry	Strozzi et al. (2004)
Switzerland, Valais, Jegi	0.5 (max)	1996 (88 days) + 1998 (35 days)	D-InSAR	Strozzi et al. (2004)
Switzerland, Valais, Mattwald	0.22 (max)	1975-1999	photogrammetry	Strozzi et al. (2004)
Switzerland, Valais, Mattwald	0.5 (max)	1996 (88 days) + 1998 (35 days)	D-InSAR	Strozzi et al. (2004)
Switzerland, Valais, Findletälli	0.3-0.6 (average), 1.2 (max)	1975-1999	digital photogrammetry	Frauenfelder et al. (2004)
Comparisons (Ch, Ö, Svalbard)	-	-	different methods	Kääb et al. (2003)
Asia				
Middle Asia, Zailijskiy Alatau, Gorodetskiy Rg	1.1	1923-1977	?	Gorbunov (1983)
West China, Kunlun Shan, Rg1	0.02-0.03	?	?	Cui (1983), in Whalley & Martin (1992)

Nepal, Khumbu Himalaya, Lingten Rg	0.1-0.2	-	calculated via length and mean age	Barsch & Jakob (1998)
Nepal, Khumbu Himalaya, Kongma Rg	0.1-0.2	-	calculated via length and mean age	Barsch & Jakob (1998)
Nepal, Khumbu Himalaya, Dugla Rg	0.04-0.085	-	calculated via length and mean age	Barsch & Jakob (1998)
Nepal, Khumbu Himalaya, Nuptse Rg	0.1-0.2	-	calculated via length and mean age	Barsch & Jakob (1998)
North America				
USA, Alaska Range, Clear Creek Rg (upper line)	0.4-0.73	1949-1952	painted line of rocks	Wahrhaftig & Cox (1959)
USA, Alaska Range, Clear Creek Rg (upper line)	0.4-0.61	1952-1957	painted line of rocks	Wahrhaftig & Cox (1959)
USA, Alaska Range, Clear Creek Rg (lower line)	0.52-0.76	1949-1952	painted line of rocks	Wahrhaftig & Cox (1959)
USA, Alaska Range, Clear Creek Rg (lower line)	0.49-0.7	1952-1957	painted line of rocks	Wahrhaftig & Cox (1959)
USA, Colorado, Front Range, Arapaho Rg	0.09-0.19	?	terrestrial photogrammetry	Outcalt & Benedict (1965)
USA, Galena Creek Rg ML A	0.01 (min) – 0.45 (max)	1966 - 1995	terrestrial geodetic survey	Potter et al. (1998)
USA, Galena Creek Rg ML B	0.04 (min) – 0.80 (max)	1964 - 1995	terrestrial geodetic survey	Potter et al. (1998)
USA, Galena Creek Rg ML C	0.03 (min) – 0.14 (max)	1963 - 1995	terrestrial geodetic survey	Potter et al. (1998)
USA, Colorado, Front Range, Arapaho Rg	0.06	1961-1966	?	White (1971), in Barsch (1996)
USA, Colorado, Front Range, Taylor Rg	0.066	?	?	White (1971), in Whalley & Martin (1992)

USA, Colorado, Front Range, Fair Rg	0.097	?	?	White (1971), in Whalley & Martin (1992)
USA, Colorado Front Range, Cascade Creek Valley	0.1	?	?	White (1981)
Canada, Front Range, King's Throne Rg	0.056	1988 - 1996	terrestrial geodetic survey	Koning & Smith (1999)
USA, Alaska, Wrangell Mountains, Fireweed Rg	3.8 (max)	1994-1996	?	Elconin & LaChapelle (1997)
USA, Alaska, Brooks Range, Jaeger Rg	0.4	1978-1983	?	Calkin et al. (1987), in Barsch (1996)
USA, Alaska, Brooks Range, Pika Rg	0.1	1978-1983	?	Calkin et al. (1987), in Barsch (1996)
Canada, N.W.T., Tungsten Rg (central part)	2.5	1963-1980	?	Jackson & McDonald (1980), in Barsch (1996)
South America				
Argentina, Mendoza, Plomo River	100	1963-1973	terrestrial photogrammetry	Corte (1976), in Corte (1987)
New Zealand				
New Zealand, Ben Ohau Range, Ferintosh Creek	0.14 (max)	1989 - 1994	?	Brazier et al. (1998)

Rg= Rockglacier
? = no details

If not specified:
photogrammetry = aerial photogrammetry
terrestrial geodetic survey = survey using theodolite or total station
GPS = Global Positioning System
D-InSAR = Differential SAR (Synthetic Aperture Radar)-Interferometry

APPENDIX 1B

PUBLISHED DATA ON VERTICAL CHANGES				
Region/Location	**Vertical change [m*a^{-1}]**	**Measuring period**	**Method**	**Reference**
Europe				
Austria				
Austria, Kaunsertal, Ölgruben-Rg	+ 0.19-0.23	1922-	terrestrial photogrammetry	Pillewizer (1957), in Barsch (1996)
Austria, Ötztal, Äusseres Hochebenkar	0.17	1936-1953	terrestrial photogrammetry	Pillewizer (1957), in Barsch 1996
Austria, Ötztal, Äusseres Hochebenkar	0.18	1953-1997	photogrammetry	Kaufmann & Ladstädter (2000)
Norway				
Norway, Svalbard, Nordenskiöldkysten-Rg	0.0	1969 - 1990	digital photogrammetry	Kääb et al. (2002)
Norway, Svalbard, Brøggerbreen-Rg	<0.01	1971 – 1995	digital photogrammetry	Kääb et al. (2002)
Switzerland				
Switzerland, Grisons, Murtèl	-0.06	1932-1955	photogrammetry	Barsch & Hell (1975)
Switzerland, Grisons, Murtèl	+0.02	1955-1971	photogrammetry	Barsch & Hell (1975)
Switzerland, Grisons, Murtèl	-0.02	1971-1973	terrestrial geodetic survey	Barsch & Hell (1975)

Switzerland, Grisons, Muragl	-0.1	1972-1973	terrestrial geodetic survey	Barsch & Hell (1975)
Switzerland, Grisons, Pontresina-Schafberg	<0.02	1971-1991	photogrammetry	Kääb (1997)
Switzerland, Grisons, Murtèl	-0.04	1987-1996	photogrammetry	Kääb (1997)
Switzerland, Grisons, Pontresina-Schafberg	0.005-0.015	1990-1997	borehole deformation (point information!)	Hoelzle et al. (1998)
Switzerland, Valais, Weissmies	-0.3	1958-1964	photogrammetry	Messerli & Zurbuchen (1968)
Switzerland, Valais, Grosses Gufer	-0.08 (max)	1950-1962	photogrammetry	Messerli & Zurbuchen (1968)
Switzerland, Valais, Gruben Rg	-0.05	1970-1995	photogrammetry	Kääb (1996); Kääb et al. (1997)
Switzerland, Valais, Yettes Condjà, rgB	-0.32	2000-2001	differential GPS	Lambiel & Delaloye (2004)
Switzerland, Valais, Yettes Condjà, rgC	-0.1	2000-2001	differential GPS	Lambiel & Delaloye (2004)
North America				
USA, Alaska, Brooks Range, Jaeger Rg	- 0.11	1978-1983	?	Calkin et al. (1987), in Barsch (1996)
USA, Alaska, Brooks Range, Pika Rg	- 0.1	1978-1983	?	Calkin et al. (1987), in Barsch (1996)
Canada, Front Range, King's Throne Rg	-0.025	1988 - 1996	terrestrial geodetic survey	Koning & Smith (1999)

APPENDIX 1C

PUBLISHED DATA ON FRONT ADVANCE				
Region/Location	**Front advance [m*a^{-1}]**	**Measuring period**	**Method**	**Reference**
Europe				
Austria				
Austria, Ötztal, Äusseres Hochebenkar	3-4	1936-1953	terrestrial photogrammetry	Pillewizer (1957)
Austria, Ötztal, Äusseres Hochebenkar	2.4-2.7	1936-1997	terrestrial geodetic survey	Schneider & Schneider (2001)
Austria, Ötztal, Äusseres Hochebenkar	1.1	1977-1997	terrestrial geodetic survey	Schneider & Schneider (2001)
Austria, Ötztal, Äusseres Hochebenkar	5.0	1953-1969	terrestrial geodetic survey	Schneider & Schneider (2001)
Denmark				
Greenland, Disko Island, Mellemfjord	0.1	?	?	Humlum (1996)
France				
France, French Alps, Laurichard	0.3	1983-1991	terrestrial geodetic survey	Francou & Reynaud (1992)
Norway				
Norway, Svalbard, Hiorthfjellet-Rg	0.03	1994 - 2002	terrestrial geodetic survey + photogrammetry	Ødegard et al. (2003)

Switzerland				
Switzerland, Grisons, Val Sassa	0.39	1921-1942	painted line of rocks	Chaix (1943)
Switzerland, Grisons, Val dell' Acqua	0.43	1921-1942	painted line of rocks	Chaix (1943)
Switzerland, Valais, Furggentälti	0.4	1960-1995	photogrammetry	Krummenacher et al. (1998)
Switzerland, Grisons, Murtèl	0.01	1987-1996	photogrammetry	Kääb (1997)
Switzerland, Grisons, Muragl	0.05	1981-1994	photogrammetry	Kääb (1997)
Switzerland, Valais, Gruben	0.15	1970-1995	photogrammetry	Kääb (1996)
Asia				
Middle Asia, Zailijskiy Alatau, Gorodetskiy Rg	0.4-0.9 0.9 0.7	1923-1946 1946-1960 1960-1977	?	Titkov (1979), in Gorbunov (1983)
North America				
Canada, Alberta, Banff National Park	0.3-0.6	?	?	Osborn (1975), in Koning & Smith (1999)
Canada, Front Range, King's Throne Rg	0.016	1988 - 1996	terrestrial geodetic survey	Koning & Smith (1999)
USA, Alaska Range, Clear Creek Rg	0.48 (mean)	1949-1957	painted line of rocks	Wahrhaftig & Cox (1959)
USA, Colorado Front Range	0.05-0.2	?	?	White (1971, 1987), in Burger et al. (1999)
USA, Alaska, Brooks Range	0.1/0.4	?	?	Calkin et al. (1987), in Burger et al. (1999)

Appendix 2

Rockglacier activity compiled from geomorphic mapping, digital photogrammetry, terrestrial geodetic survey and dendrogeomorphology:

Nr.	Rock-glacier	State of activity (**geomorphic mapping**)	State of activity (**digital photogrammetry**)	State of activity (**terrestrial geodetic survey**)	State of activity (**dendrogeomorphology**)
1	pibw	active	active	-	-
2	Pipp1	active	active	-	-
3	Pipp2	inactive	inactive	-	-
4	Pipp3	active	active	-	-
5	Pipp4	inactive	inactive	-	-
6	Brho1	active	active	-	-
7	Brho2	active	active	-	-
8	Brle	active	active	-	-
9	Hugg1	relict	-	-	-
10	Hugg2	relict	-	-	-
11	Hufh	active	active	-	-
12	Hujp	active	active	-	-
13	Hurh1	active	inactive	-	-
14	Hurh2	inactive	inactive	-	-
15	Huhh1	active	active	active	-
16	Huhh2	inactive	partly active	-	-
17	Huhh3	active	active	active	active
18	Huhh4	relict	-	-	-
19	Hupr	inactive	-	-	-
20	Grueo0	relict	-	-	-
21	Grueo1	active	active	-	?
22	Grueo2	active	active	-	-

23	Grueo3	inactive	inactive	-	-
24	Grueo4	active	active	-	-
25	Grueo5	active	inactive	-	-
26	Grueo6	active	active	-	-
27	Grueo7	active	active	-	-
28	Grueo8	active	inactive	-	-
29	Grueo9	relict	-	-	-
30	Niggel0	relict	-	-	-
31	Niggel1	active	active	-	-
32	Niggel2	active	active	-	-
33	Niggel3a	inactive	inactive	-	-
34	Niggel3b	inactive	inactive	-	-
35	Niggel4	active	inactive	-	-
36	Niggel5	inactive	inactive	-	-
37	Niggel6	active	inactive	-	-
38	Niggel7	relict	-	-	-
39	Niggel8	relict	-	-	-
40	Chu1	active	active	-	-
41	Chu2	inactive	inactive	-	-
42	Chu3	inactive	inactive	-	-
43	Chu4	inactive	inactive	-	-
44	Chu5	relict	-	-	-
45	Chu6	inactive	-	-	-

Appendix 3

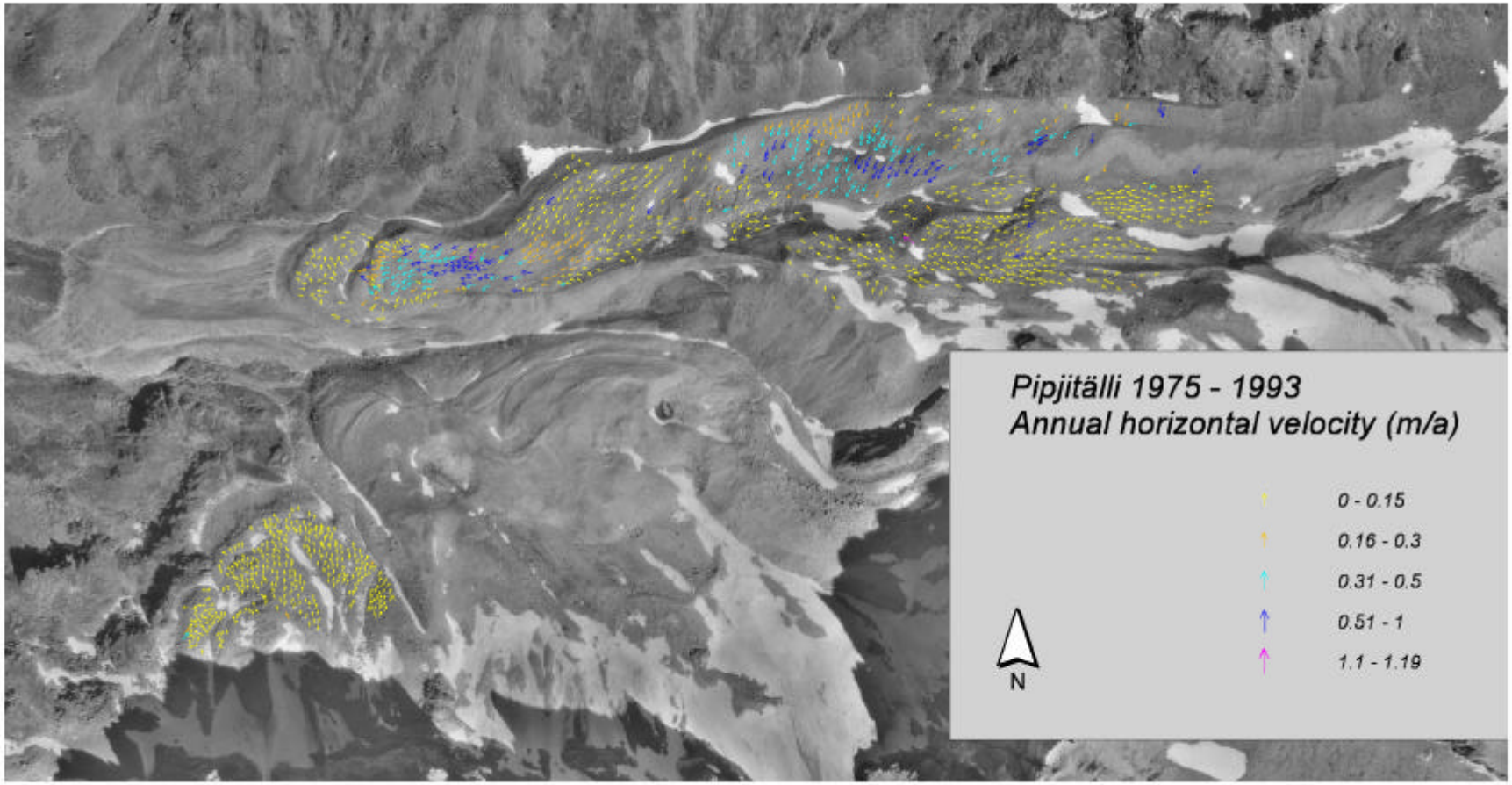
Pipjitälli 1975 - 1993
Annual horizontal velocity (m/a)
0 - 0.15
0.16 - 0.3
0.31 - 0.5
0.51 - 1
1.1 - 1.19
N

Appendix 3

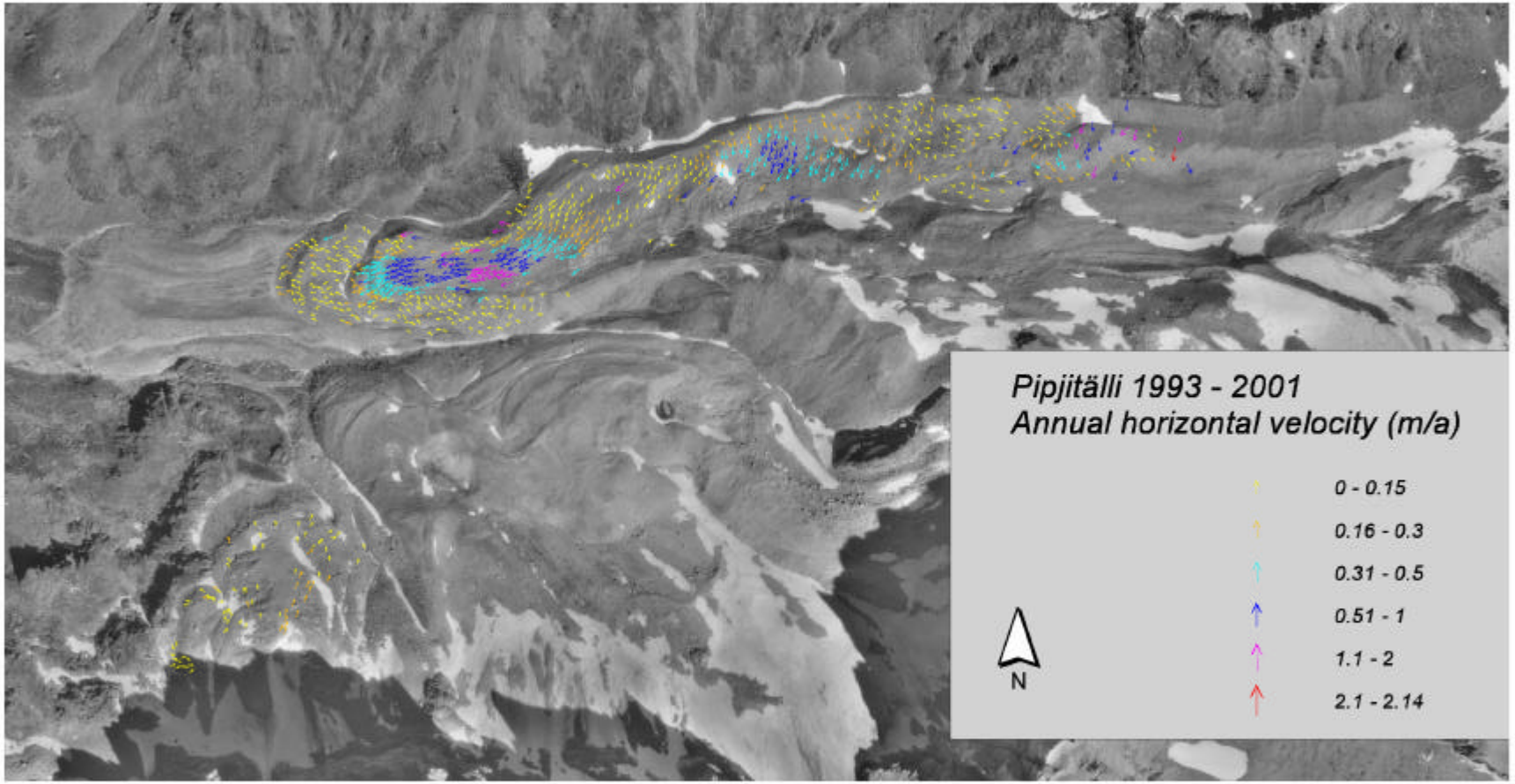
Pipjitälli 1993 - 2001
Annual horizontal velocity (m/a)
0 - 0.15
0.16 - 0.3
0.31 - 0.5
0.51 - 1
1.1 - 2
2.1 - 2.14
N

Appendix 3

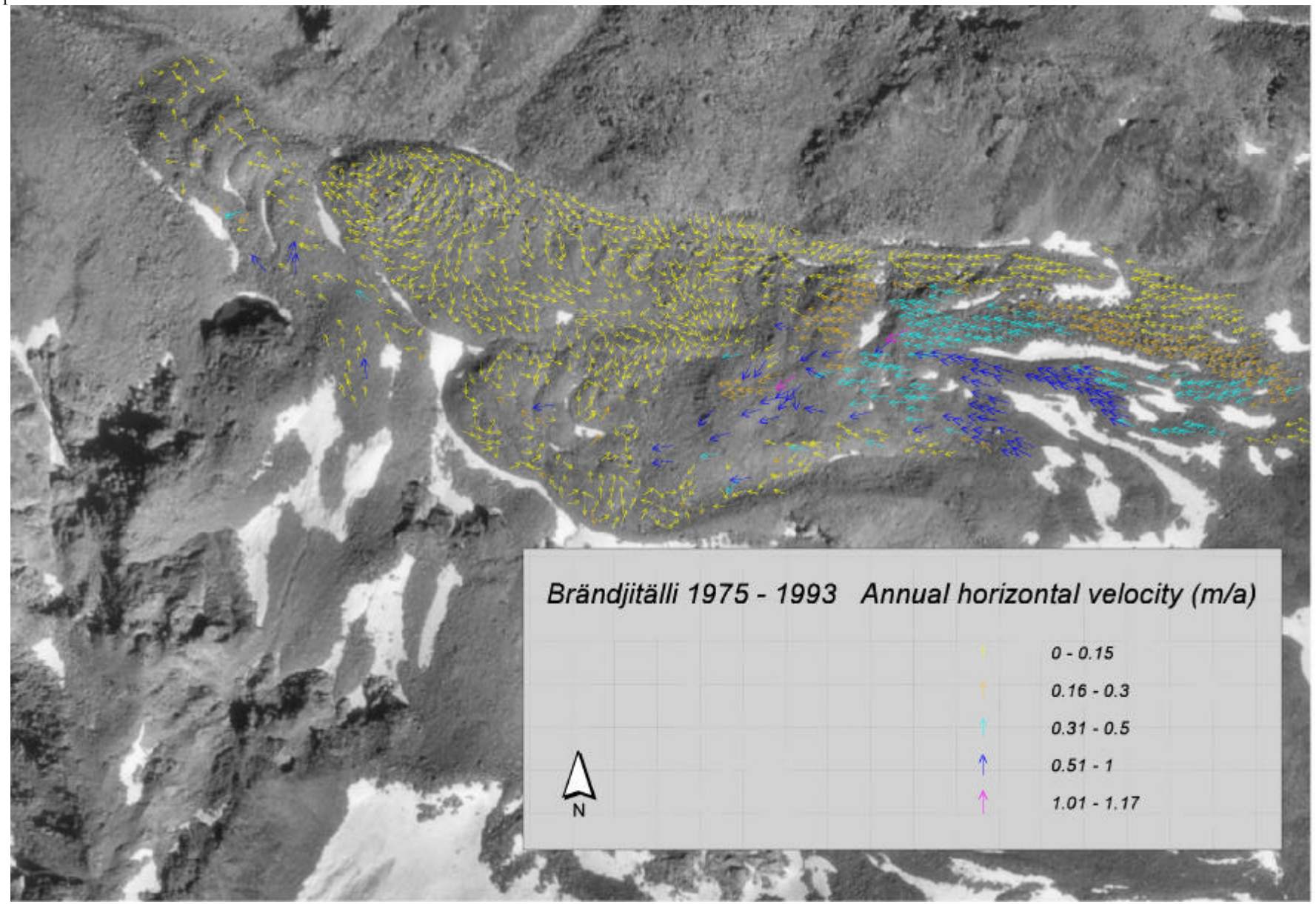
Brändjitälli 1975 - 1993 Annual horizontal velocity (m/a)
0 - 0.15
0.16 - 0.3
0.31 - 0.5
0.51 - 1
1.01 - 1.17
N

Appendix 3

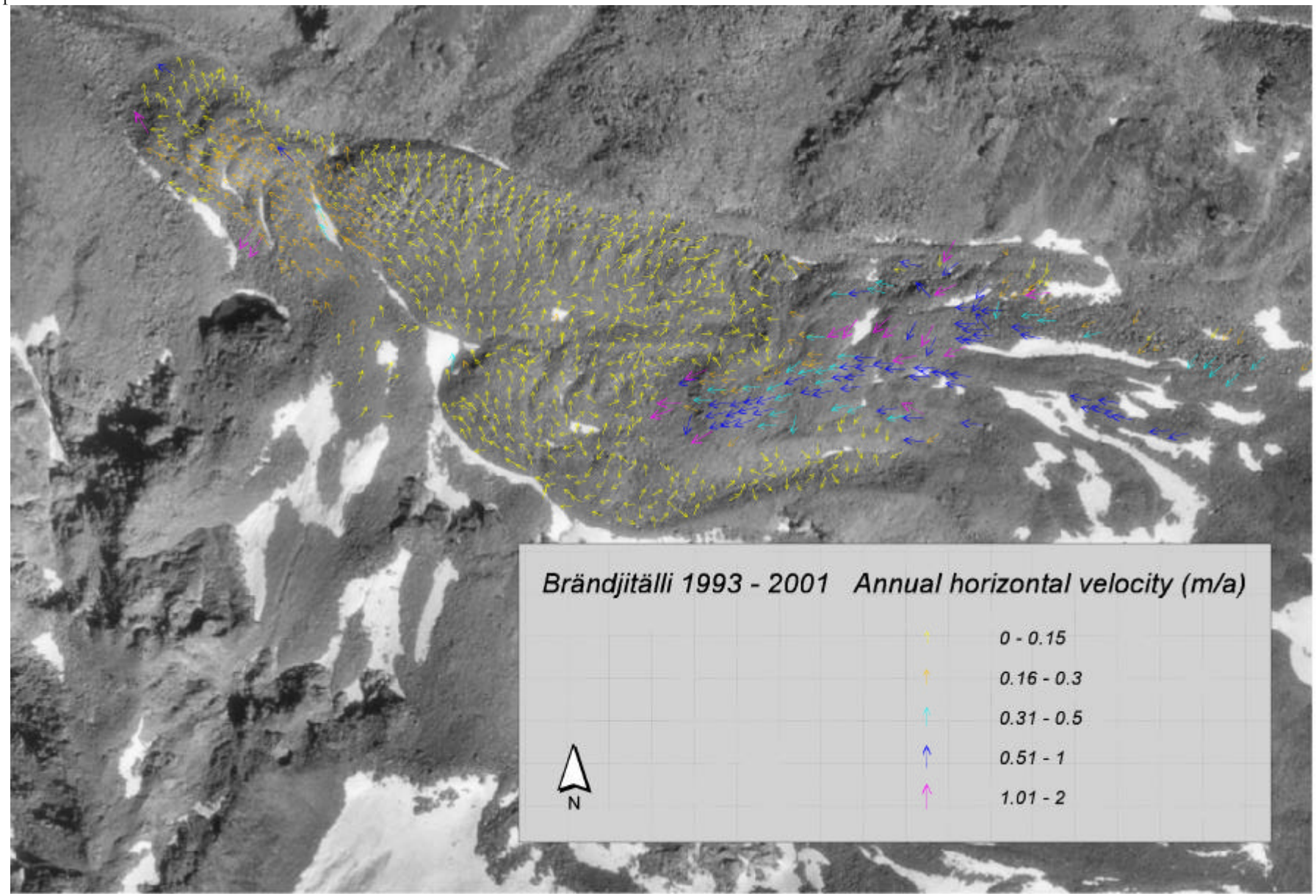
Brändjitälli 1993 - 2001 Annual horizontal velocity (m/a)
0 - 0.15
0.16 - 0.3
0.31 - 0.5
0.51 - 1
1.01 - 2
N

Appendix 3

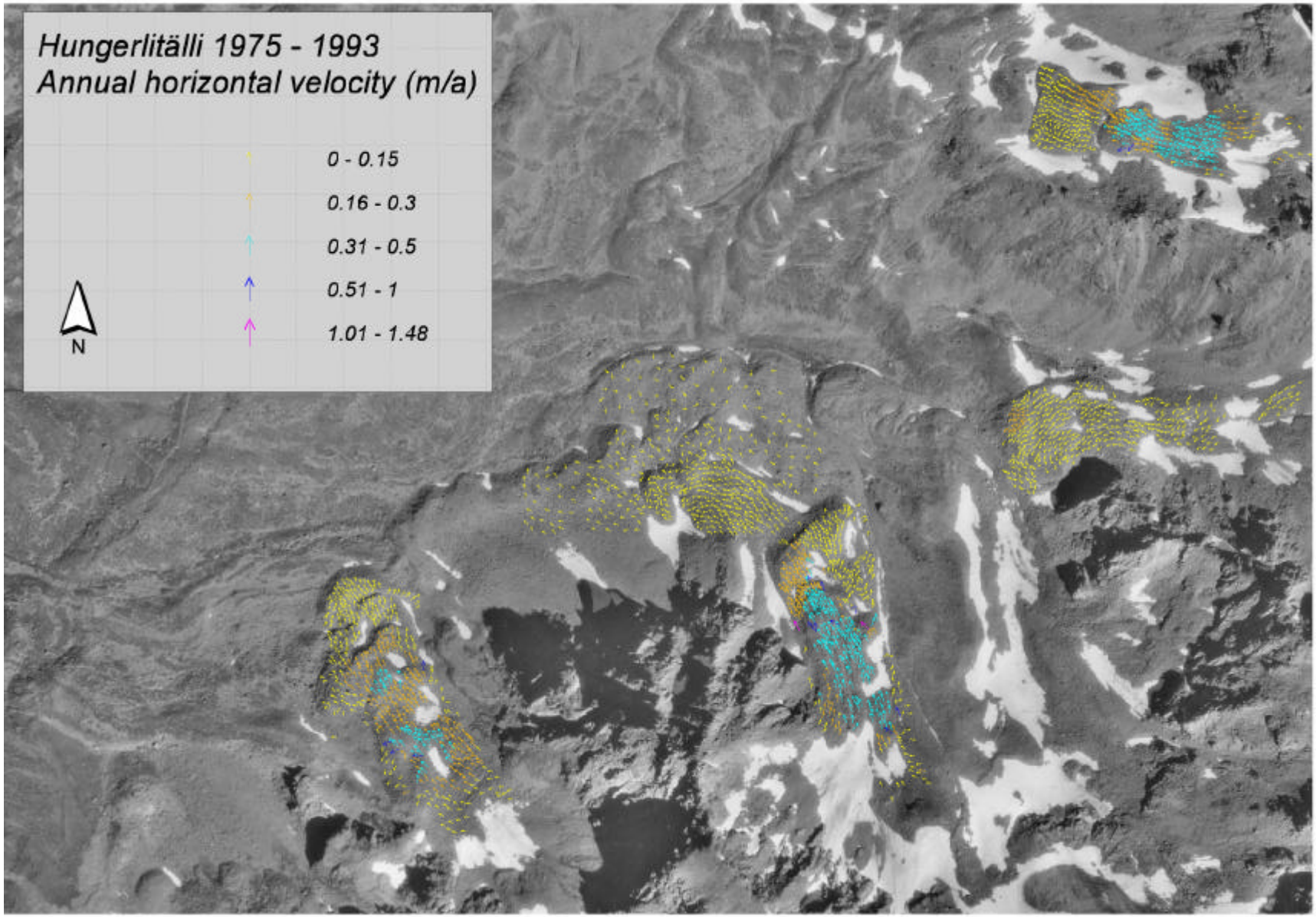
Hungerlitälli 1975 - 1993
Annual horizontal velocity (m/a)
0 - 0.15
0.16 - 0.3
0.31 - 0.5
0.51 - 1
1.01 - 1.48
N

Appendix 3

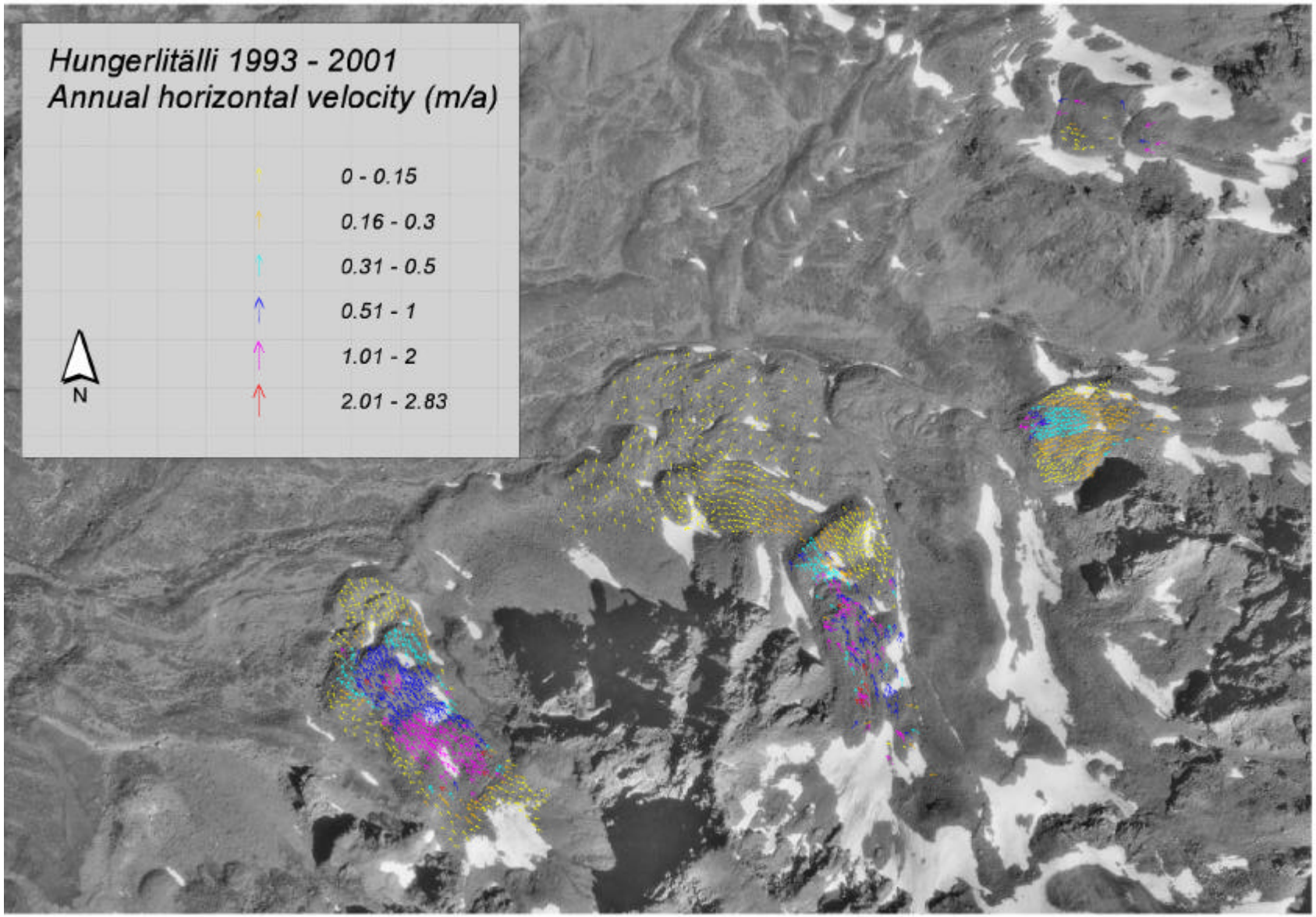
Hungerlitälli 1993 - 2001
Annual horizontal velocity (m/a)
0 - 0.15
0.16 - 0.3
0.31 - 0.5
0.51 - 1
1.01 - 2
2.01 - 2.83
N

Appendix 3

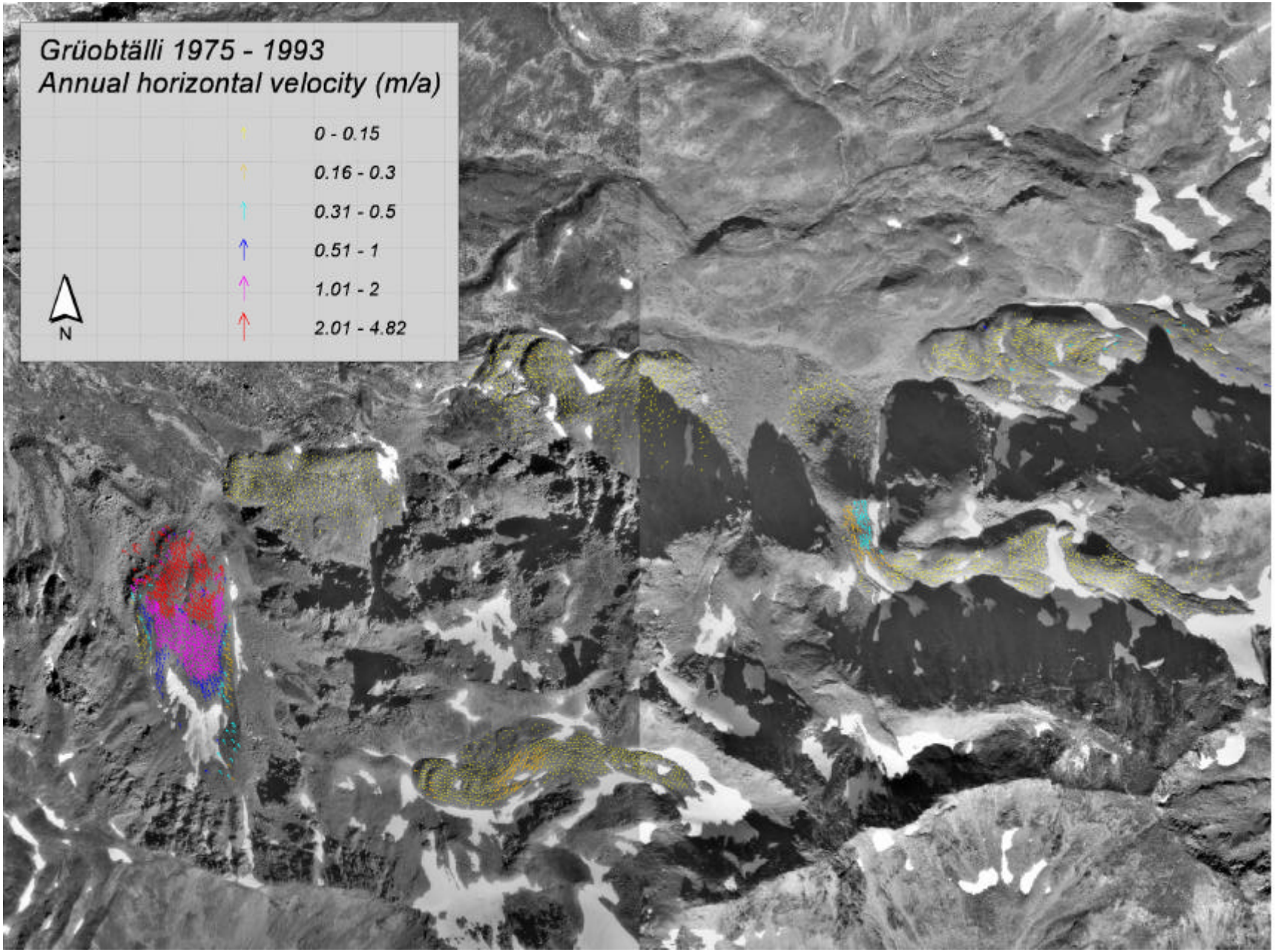
Grüobtälli 1975 - 1993
Annual horizontal velocity (m/a)
0 - 0.15
0.16 - 0.3
0.31 - 0.5
0.51 - 1
1.01 - 2
2.01 - 4.82
N

Appendix 3

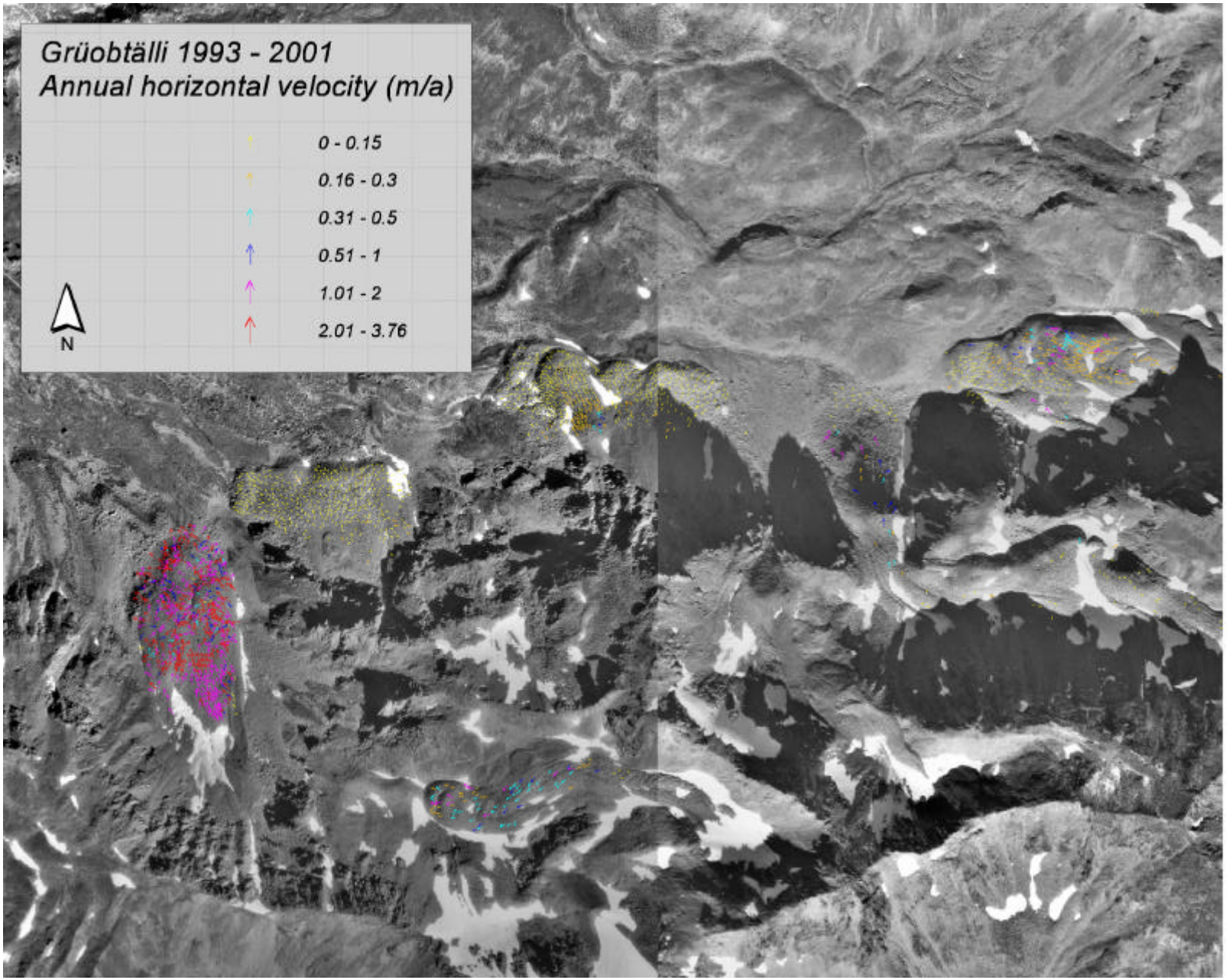
Grüobtälli 1993 - 2001
Annual horizontal velocity (m/a)
0 - 0.15
0.16 - 0.3
0.31 - 0.5
0.51 - 1
1.01 - 2
2.01 - 3.76
N